University of Quebec at Chicoutimi

A THESIS SUBMITTED IN PARTIAL FULFILMENT OF

THE REQUIREMENTS FOR THE DEGREE

OF

DOCTOR OF PHYLOSOPHY

by

Xianai Huang

STUDY ON THE DEGRADATION MECHANISM OF HEAT-TREATED WOOD BY UV LIGHT

September 2012

Université du Québec à Chicoutimi

THÈSE PRÉSENTÉE COMME EXIGENCE PARTIELLE

DU

DOCTORAT EN INGÉNIERIE

par

Xianai Huang

ÉTUDE SUR LE MÉCANISME DE DÉGRADATION PAR LA LUMIÈRE UV DU BOIS TRAITÉ THERMIQUEMENT

September 2012

Abstract

Heat-treated wood is a wood product thermally treated at high temperatures in the range of 180°C and 240°C for its preservation without using any additional chemicals. Heat treatment modifies wood both chemically and physically. Amorphous polysaccharide content (hemicelluloses) decreases, condensation and demethoxylation of lignin take place, and certain extractives are removed. Consequently, heat-treated wood possesses new physical properties such as reduced hygroscopy, improved dimensional stability, better resistance to degradation by insects and micro-organisms, and attractive darker color. These new beneficial and attractive properties make heat-treated wood popular for indoor as well as outdoor applications.

However, similar to untreated wood, heat-treated wood is also susceptible to degradation due to environmental conditions. Weathering results in poor aesthetics for heat-treated wood because of the discoloration and surface checking when exposed to UV radiation. However, investigations on the wettability changes, chemical changes, and microscopic changes of heat-treated wood after exposure to artificial weathering are very limited; and there is no publication available in the literature on the degradation taking place due to the weathering of heat-treated North American jack pine, aspen, and birch used in this study.

This work was undertaken to study the weathering degradation mechanisms of the three North American regional species (jack pine (*Pinus banksiana*), aspen (*Populus tremuloides*), and birch (*Betula papyrifera*)) heat-treated under different conditions to

understand the chemical and physical changes taking place and to compare these changes with those of untreated controlled samples when they are exposed to artificial weathering with and without water spray for various periods. Several techniques and tools were used such as color measurement, contact angle test for wettability analysis, Fourier transforms infrared spectroscopy (FTIR) and X-ray photoelectron spectroscopy (XPS) for chemical analysis, florescence microscopy (FM), and scanning electron spectroscopy (SEM) for microscopic structural analysis. These provide a great deal of insight into the degradation process.

The results show that color changes occurring during weathering of heat-treated woods are due to the increasing lignin condensation and decreasing extractives content on wood surfaces caused by heat treatment. Changes in wettability during weathering of heat-treated wood are induced by the combination of surface structural and chemical modifications. Lignin in heat-treated woods is more sensitive to weathering than other components. It is proposed that the weathering mechanism of heat-treated woods consists of the degradation of lignin matrix and extractives, which lightens the wood color. As a result, the color difference between the color of heat-treated wood before weathering and the color of the same wood during weathering increases with exposure time. Then, the leaching of other polymers present on wood surface takes place, consequently, the color returns back to its initial state and the color difference declines.

Résumé

Le traitement thermique du bois est une méthode qui consiste à chauffer le bois aux hautes températures entre 180°C et 240°C sans l'utilisation de produits chimiques additionnels, conduisant aux modifications physique et chimique des composés du bois. La teneur des polysaccharides amorphes diminue (hémicelluloses), les réactions de condensation et de déméthoxylation de la lignine ont lieu et certains extractibles du bois sont dégradés. Ceci confère au bois traité thermiquement de nouvelles propriétés physiques telles que la réduction de l'hygroscopicité, l'amélioration de la stabilité dimensionnelle, une meilleure résistance à la dégradation par les micro-organismes et les insectes ainsi qu'une couleur du bois plus foncée. Ces nouvelles propriétés avantageuses et attrayantes rendent le bois traité thermiquement populaire pour des applications extérieures et intérieures.

Toutefois, le bois traité thermiquement, tout comme le bois non traité, est susceptible à la dégradation due aux facteurs environnementaux. L'exposition du bois traité thermiquement au rayonnement UV provoque une décoloration à la surface du bois. Cependant, les études sur la mouillabilité, les changements chimiques et microscopiques du bois thermiquement modifié après exposition au vieillissement accéléré sont très limitées. De plus, il n'y a aucune publication disponible dans la littérature sur l'altération du pin, du peuplier faux tremble et du bouleau blanc nord-américain traités thermiquement qui sont utilisés dans cette étude.

Ce projet a pour but d'étudier les mécanismes de dégradation suite à l'altération de trois espèces de bois traité thermiquement des régions nord-américaines sous différentes conditions, pour comprendre les changements physiques et chimiques qui surviennent en

comparaison aux échantillons témoins, non traités quand ils sont exposés au vieillissement accéléré avec et sans d'eau pour différentes périodes. Plusieurs techniques et outils ont été utilisés tels que la colorimétrie, la mesure de l'angle de contact pour l'analyse de la mouillabilité, la spectroscopie infrarouge (FTIR) et la spectroscopie photoélectron (XPS) pour l'analyse chimique, et la spectroscopie électronique à balayage (MEB) pour l'analyse structurelle et microscopique. Ces analyses et tests permettent de fournir les éléments pour une meilleure compréhension du processus de dégradation.

Les résultats obtenus montrent que les changements de couleurs survenus pendant les tests de vieillissement accélérés du bois traité thermiquement étaient dus à l'augmentation de la condensation de la lignine et à la diminution de la teneur des extractibles à la surface du bois causées par le traitement thermique. Les changements de mouillabilité pendant la dégradation du bois traité thermiquement sont induits par la combinaison des changements structurels à la surface du bois et des modifications chimiques. La lignine du bois traité thermiquement est plus sensible aux tests de vieillissement que les autres composés. Le mécanisme de dégradation du bois traité thermiquement pourrait être dû à l'altération de la lignine et des extractibles, ce qui éclaircit la couleur du bois.

La différence entre la couleur du bois traité thermiquement avant les tests de vieillissement et la couleur de la même essence de bois pendant le vieillissement augmente. Puis, le lessivage des autres polymères présents à la surface du bois prend place, par conséquent, la couleur reprend son état initial induisant ainsi une baisse dans la différence de couleur.

Acknowledgements

Many people have helped and supported me though the course of this thesis to whom I am indebted. In particular I wish to express my sincere gratitude and appreciation to the following people:

First and foremost, I am extremely grateful to, with a deep sense of gratitude and indebtedness, Prof. Duygu Kocaefe, director of my thesis project, for her valuable suggestions and encouragement. Working with Prof. Kocaefe has been a great pleasure. Her originality, experience and contributions in the field of wood chemistry have absolutely nourished the value of this thesis. An extremely busy professional, Prof. Kocaefe has always been available and kind in need. It is an honor for me to earn my graduation under her direction.

I would like to acknowledge my co-director, Prof. Yasar Kocaefe, for his supervision, continuous guidance, suggestions, scientific and technical advice and constant encouragement. Particularly, I must thank him for his patience and tolerance with my tasks of aging calculation. His truly scientific intuition exceptionally inspired and helped me grow as a student and a researcher.

I would like to express my thanks to my co-director, Prof. André Pichette, for offering me the opportunity to work at Laboratoire d'analyse et de séparation des essences végétales (LASEVE) for wood chemical components analysis and there I had the chance to know many researchers and students who helped me a lot.

I am very grateful to Prof. Yaman Boluk in every possible way that I had the opportunity to work closely with him at Alberta Research Center for chemical analysis. I have enjoyed the way he and his colleagues, Dr. Zhao Liyan and Dr.Zhu Jesse, trained me on the procedure of wood chemical component determination and utilization of the FTIR instrument as well as his collaboration during the time when I was at Alberta. I thank Prof. Boluk also for accepting to be members of the doctoral examination and supervision committees and hope to keep up our collaboration in the future.

I gratefully thank Dr. Carl Tremblay and Prof. Vakhtang Mshvildadze for being members of the doctoral examination and supervision committee and for their valuable comments and questions during my seminars.

I would like to express my thanks to Prof. Ramdane Younsi and Prof. Sandor Poncsak for their time and critical scientific suggestions on two reports. I would like to extend my thanks to Mr. Rénald Delisle, Mr. Jacques Allaire, and Mr. Jean Paquette, technicians at GRTB, for their technical support. I have had fruitful scientific and non-scientific conversations with my colleagues and my friends, Sudeshna Saha, Serge Thierry Lekounougou, and Noura Oumarou. I thank them for their scientific comments on my

project and their encouragements. I have enjoyed working with them and the happy moments we had together which cheered me up and stirred the work.

I would like to express my deepest gratitude to Prof. Zhan Zhang, Centre universitaire de recherche sur l'aluminium (CURAL), UQAC, for SEM measurements.

I would like to thank also the scientific staff, Mr. Dimitre Karpuzov and Mr. Shihong Xu, for helping me with the utilization of experimental facilities (XPS) at Alberta University and for their hospitality.

I would like to express my gratitude to Ms. Liyan Zhao, Alberta Research Center, Canada, for her kindness in performing FTIR measurements of a large number of samples, in spite of their busy research load.

I gratefully thank Prof. Cornélia Krause, who gave me the chance to work at the biology laboratory of UQAC on the florescent image analysis. It is my great pleasure to convey my hearty thanks to Ms. Sonia Pedneauit, research assistant, and Tommy Larouche, undergraduate student, for their solutions to technical problems in preparing of FSM samples.

To Ms.Caroline Potvin and Ms. Helene Gagnon, laboratory assistant of the Chemistry Department, UQAC, I would like to express my thanks for finding time and allowing me to independently use the UV-Vis spectrophotometer and for critical scientific comments on chemical procedures with friendliness and kindness.

It would like to convey my thanks to the Department of Applied Sciences (DSA) and UQAC administration for their support. To Ms. Chantale Dumas, secretary of DSA, without you, this list is incomplete. I would like to take the opportunity to thank the DSA and the PAIR program for partially supporting my participation at three international conferences at Hamilton, Canada, Montreal, Canada and Madison, USA.

It is a pleasure to express my gratitude wholeheartedly to Prof. Kocaefe's family for their warm welcome and kind hospitality in Chicoutimi. My dearest friends, Jing Lai, Peng Shen, Jie Qing who never let me feel alone at Chicoutimi. Thanks to Prof. Grant X.Cheng and his family, for a variety of social activities and for making me feel like part of their family. Thanks to Youmei and Linlin as well as their families who always encouraged me and who were there for me and my family when we were in need.

And I will never forget that this thesis would not have been possible without the recommendation of my respected Master supervisor Prof. Zhang Qisheng, Nanjing Forestry University, China. I would like to express my thanks to him and Dr. Cheng Liheng, scientist, Alberta Research Center, for his recommendation so that I had the opportunity to pursue my PhD in the group of GRTB at UQAC.

Guanzhong Huang, my father, and Donglan Lu, my mother back in China, deserve a special mention for their immense spiritual support and encouragement for the completion

of my thesis. Thanks to Ying Lu, my sister, and Leirong Huang my little brother, for taking care of the family when I was absent and struggled for my PhD.

This thesis would not have been completed without you, my devoted partner, Kun. This wouldn't have happened if it was not for his scientific suggestions as well as my family life, his encouragement, his sacrifice, his confidence in me, his affection, and his love. There are no words to thank him. Thanks to his family for their support and to have let me meet you and be your partner.

To my lovely beautiful princess Amy, now 2 years old...The best part of my life. I have no words and only kisses to thank her. Since she was 4 months old, she has sacrificed a lot and has missed moments every child in those years of age deserves with his or her mom that could have been the most important for her. Sometimes weekends, sometimes evenings... I love you my little baby Amy.

I would like to thank all the sponsors of this research project, namely, Fonds de recherche du Québec- Nature et les technologies (FRQNT), Développement Économique Canada (DEC), Ministère du Développement Économique, de l'Innovation et de l'Exportation (MDEIE), Conférence Régionale des Élus du Saguenay-Lac-St-Jean (CRÉ), University of Quebec at Chicoutimi (UQAC), Fondation of the University of Quebec at Chicoutimi (FUQAC), FP Innovations and our industrial partners (PCI Industries, Ohlin Termo Tech, Industries ISA, Kisis Technologies) for their financial contributions and valuable collaboration.

Finally, I would like to thank everybody who played a role in successful completion of this thesis and I apologize that I could not thank them personally one by one.

List of publications

Refereed Journal Papers:

1. **X. Huang**, D. Kocaefe, Y. Kocaefe, Y. Boluk, A. Pichette (2012) A spectrocolorimetric and chemical study on color modification of heat-treated wood during artificial weathering. Applied Surface Science. 258 (14) , pp. 5360-5369, http://dx.doi.org/10.1016/j.apsusc.2012.02.005
2. **X. Huang**, D. Kocaefe, Y. Kocaefe, Y. Boluk, A. Pichette (2011) Changes in Wettability of Heat-Treated Wood due to Artificial Weathering. Wood Science and Technology. 2012. pp. 1-23 Article in Press
3. **X. Huang**, D. Kocaefe, Y. Kocaefe, Y. Boluk, A. Pichette (2011) Study of the degradation mechanisms of heat-treated jack pine (*Pinus banksiana*) under artificial sunlight irradiation. Polymer Degradation and Stability. (accepted) March 15, 2012
4. **X. Huang**, D. Kocaefe, Y. Boluk, Y. Kocaefe, A. Pichette (2011) Effect of Surface Preparation on the Wettability of Heat-Treated Jack Pine Wood Surface by Different Liquids. Holz als Roh- und Werkstoff. 2012, pp. 1-7 Article in Press DOI: 10.1007/s00107-012-0605-z
5. **X. Huang**, D. Kocaefe, Y. Boluk, C. Krause (2012) Structural analysis of heat- treated birch (*Betula papyrifera*) surface due to artificial weathering. Applied Surface Science. (Accepted) April, 2012

6. D. Kocaefe, **X. Huang**, Y. Boluk, Y. Kocaefe (2012) Quantitative characterization of chemical degradation of heat-treated wood surfaces during artificial weathering using XPS. Surface and Interface Analysis. (Accepted) June, 2012
7. D. Kocaefe, **X. Huang**, Y. Boluk, Y. Kocaefe (2012) Study on weathering behavior of jack pine heat-treated under different conditions. Journal of Energy and Power Engineering. (Accepted) November, 2012
8. R. Younsi, D. Kocaefe, S. Poncsak, **X. Huang**, S. Saha, (2010) A High Thermal Treatment of Wood: A Basic Theory and Numerical Modeling, International Journal of Energy, Environment and Economics. (In press)

Book Chapters:

9. R. Younsi, D. Kocaefe, S. Poncsak, **X. Huang**, S. Saha (2010) A High Thermal Treatment of Wood: A Basic Theory and Numerical Modeling in 'Heat Treatment: Theory, Techniques and Applications', pp 201-223, Novapublishers. ISBN: 978-1-61324-684-9.

Conference Papers:

10. D. Kocaefe, **X. Huang**, Y. Boluk, Y. Kocaefe (2012). Comparison of weathering behavior of jack pine heat-treated under different conditions. 9th International Conference on Heat Transfer, Fluid Mechanics and Thermodynamics, 16-18 July 2012, Malta
11. **Xian Ai Huang,** Duygu Kocaefe, Yasar Kocaefe, Yaman Boluk, André Pichette (2013) Impact du vieillissement sur la microstructure surfacique et la mouillabilité du tremble

(*Populus tremuloides*) traité thermiquement. 81er Congrès de L'ACFAS, May 6-10, 2013, Université Laval, Quebec, Canada

12. **Xian Ai Huang**, Duygu Kocaefe, Yasar Kocaefe, Yaman Boluk, André Pichette (2013) Étude sur la modification de la couleur et de la composition de la surface du tremble (*Populus tremuloides*) torréfié pendant le vieillissement. 81er Congrès de L'ACFAS, May 6-10, 2013, Université Laval, Quebec, Canada
13. **X. Huang**, D. Kocaefe, Y. Boluk, Y. Kocaefe, A. Pichette (2010). Study on the Discoloration Mechanism of Heat-Treated Wood by Weathering. FPS 64th International Convention, June 20-22, 2010, Madison, Wisconsin, USA
14. **X. Huang**, D.Kocaefe, Y.Boluk, Y. Kocaefe, A. Pichette(2009). Effect of Surface Conditions on the Wetting of Heat-Treated Jack Pine. 8th World Congress of Chemical Engineering, Augest 23-27, 2009, Montreal, Quebec, Canada.
15. **X. Huang**, D. Kocaefe, Y. Boluk, Y. Kocaefe, A. Pichette (2009). Changes in the Surface Microstructure and Wettability of Untreated and Heat-Treated Jack Pine due to Weathering. Surface Canada 2009, 21st Canadian Conference on Surfaces, 02-05 June 2009, McMaster University, Hamilton, Ontario
16. **X. Huang**, D. Kocaefe, Y. Boluk, Y. Kocaefe, A. Pichette (2009). Modification in Surface Composition of Untreated and Heat-Treated Jack Pine during Weathering. Surface Canada 2009, 21st Canadian Conference on Surfaces, 02-05 June 2009, McMaster University, Hamilton, Ontario
17. S.Saha, D. Kocaefe, **X.huang**,Y. Boluk, A. Pichette (2009). Characterizing Surface Thermodynamic Properties of Coated and Hear-Treated Wood. Surface Canada 2009,

21st Canadian Conference on Surfaces, 02-05 June 2009, McMaster University, Hamilton, Ontario

Editorial Contribution

18. D. Kocaefe, **X. Huang (2012)** Heating Up The Benefits. Furniture Design And Manufacturing Asia. pp 28-31

http://flipbook.digiflip.com/FDM2012/July/flipviewerxpress.html

Table of contents

List of symbols and abbreviations

θ	Contact angle of water on any surface (°)
γ_{SV}	Interfacial tension between solid and vapor (mNm^{-1})
γ_{SL}	Interfacial tension between solid and liquid (mNm^{-1})
γ_{SL}	Interfacial tension between liquid and vapor (mNm^{-1})
γ_S	Solid surface free energy in vacuum (mNm^{-1})
π_e	Equilibrium spreading pressure of adsorbed vapor of the liquid on solid
K	Absorption coefficients
S	Scattering coefficients
$R_{\lambda(sample)}$	Sample reflectance
$R_{\lambda(standard)}$	Reflectance of Whatman cellulose paper (no.42)
L*	Lightness intensity
a*	Chromatic coordinates on the green/red axis
b*	chromatic coordinates on the blue/yellow axis
ΔL*	difference in the lightness
Δa*	difference in chromaticity coordinates on the green/red axis
Δb*	difference in chromaticity coordinates on the blue/yellow axis
t	denotes those after exposure of t h.
ΔE	Total color difference.
A	Area (m^2)
A_t	Cross-sectional areal (m^2)
C_1	First radiation (3.742×10^8 W·μm^4/m^2)
C_2	Second radiation (1.439×10^4 W·μm^4/m^2)
F_{ij}	View factor
h	Convection heat transfer coefficient (W/m^2·K)
k	Thermal conductivity (W/m·K)

q	Heat transfer rate (W)
T	Temperature (K)
ρ	Mass density (kg/ m^3)
μ	Viscosity (kg/s · m)
ε	emissivity
σ	Stefan-Boltzmann constant (5.670×10^{-8} $W/m^2\cdot K^4$)
λ	wavelength (μm)

SEM	Scanning electron spectroscopy
XPS	X-ray photoelectron spectroscopy
FTIR	Fourier transforms infrared spectroscopy
UV	Ultraviolet light
SUSIM	Solar UV Spectral Irradiance Monitor
LT	Longitudinal tangential surface of wood
LR	Longitudinal radial surface of wood

AAR	Accelerated Aging Rate
AATD	Accelerated Aging Time Duration
DRTA	Desired Real Time Aging
AAT	Accelerated Aging Temperature
AT	Ambient Temperature
Q10	Accelerated Aging Factor

List of tables

List of figures

CHAPTER 1

INTRODUCTION

1.1. Background

1.1.1 Heat treatment of wood

Wood is commonly used as engineering and structural material because of its versatile and attractive properties such as mechanical strength, low density, low thermal expansion, and aesthetic appeal [1]. Heat-treated wood is a relatively new product treated at high temperatures in the range of 180 and 220°C. The product resulting from this treatment is a natural wood without any chemical addition. Heat treatment modifies wood both chemically and physically. Chemical changes occurring due to heat treatment at high temperatures are the decrease in amorphous polysaccharide content (hemicelluloses), condensation and demethoxylation of lignin, and the removal of certain extractives [1-3]. Consequently, heat-treated wood possesses new physical properties such as reduced hygroscopy, improved dimensional stability, better resistance to degradation by insects and micro-organisms, and, attractive darker color. These new versatile and attractive properties make heat-treated wood popular for outdoor applications. But this technique also brings about some disadvantages, such as increased fragility and cost.

1.1.2 Weathering of wood

Growth of the wood products industry has been accompanied by a significant expansion in the use of wood in outdoor applications. However, untreated wood, similar to other biological materials, is susceptible to environmental degradation. Wood undergoes

degradation induced by weathering factors such as solar radiation ((UV), visible, and infrared light), moisture (dew, rain, snow, and humidity), temperature and oxygen [4]. Among these factors, UV radiation which is a part of solar radiation is known to be mainly responsible for initiating a variety of chemical changes and discoloration of wood surfaces [1, 4]. Wood, a composite made up of cellulose, hemicelluloses, lignin, and extractives, is capable of absorbing all wavelengths of electromagnetic radiation which initiates photo-degradation [5]. The color of untreated wood exposed to outdoor conditions changes very rapidly. First, it becomes yellow or brown, followed by the graying [4, 6]. Wood color changes during weathering due to the photo-degradation of lignin and wood extractives [4]. α-carbonyl, biphenyl and ring-conjugated double bond structures in lignin can absorb UV light and react with oxygen to form chromophoric groups as carbonyl (C=O) and carboxyl (-COOH) groups [5, 7]. Absorption of UV light results in the breakage of weak chemical bonds which may lead to fading and cracking of wood [8].

1.2. Statement of the problem

One of the advantages of the heat treatment of wood at high temperatures is the darker color of the final product (appearance). However, similar to untreated wood, heat-treated wood is also susceptible to environmental degradation. Studies have also shown that weathering results in poor aesthetics for heat-treated wood because of the discoloration and surface checking when exposed to UV radiation [2, 9-12]. Several reports are available on the study of color and dimensional stability after natural and accelerated weathering of heat-treated wood [1, 11, 13-20]. Most of the previous studies on weathering of heat-treated wood are limited to the description of discoloration. A complete understanding of the

mechanisms involved in the weathering process would allow the development of new treatments and finishes that could greatly enhance the durability of heat-treated wood and provide greater protection against degradation due to weathering. However, many aspects of the weathering of heat-treated wood are not completely understood. Investigations on the wettability changes, chemical changes and microscopic changes of heat-treated wood after exposure to artificial sunlight irradiation are very limited, and there is no publication available in the literature on the degradation taking place due to the weathering of heat-treated North American species samples used in this study.

1.3. Objectives

The global objective of this project is to study the mechanisms of degradation of three heat-treated North American regional species of wood (jack pine (*Pinus banksiana*), aspen (*Populus tremuloides*), and birch (*Betula papyrifera*)) to understand the chemical and physical changes taking place, and to identify the stages of these changes when the heat-treated wood is exposed to artificial weathering for various periods. As explained above, this project will focus on the study of the degradation mechanism due to the weathering. The specific objectives are:

1) to study the wettability of heat-treated wood in three directions (on axial, radial, and tangential surfaces) before and after weathering since wettability affects significantly the deposition of paint or coating on wood surfaces;

2) to observe the color changes of heat-treated wood exposed to artificial weathering (accelerated aging) for different periods;

3) to investigate the microscopic changes taking place on heat-treated wood surfaces in order to study the breakdown of wood structure caused by weathering;

4) to analyze the surface characteristics of heat-treated wood after weathering using different chemical analysis methods in order to understand the mechanism of degradation of heat-treated wood due to chemical changes;

5) to investigate the modifications in wood components (lignin, cellulose, hemicelluloses and extractives) in order to study the chemical change mechanism during weathering;

6) to study the correlation between color change, microscopic structural change, and chemical change of heat-treated wood as well as the effect of weathering conditions on color changes of sample surfaces;

7) to investigate the influence of different weathering factors such as simulated sunlight and moisture (water spray) on the degradation of heat-treated wood surfaces;

8) to compare the mechanisms of degradation for heat-treated and untreated wood;

9) to compare the degradation mechanisms of heat-treated surfaces of different wood species.

1.4. Scope of the work

In order to attain this research goal, several techniques and tools for the study of heat-treated wood surfaces were used such as color measurement, contact angle test for wettability analysis, Fourier transforms infrared spectroscopy (FTIR) and X-ray photoelectron spectroscopy (XPS) for chemical analysis as well as fluorescence

microscopy and scanning electron spectroscopy (SEM) for microscopic structural analysis. These provide a great deal of insight into the degradation process for both heat-treated and untreated wood exposed to artificial weathering. These techniques allow in-depth study on the impact of heat treatment and the modification of wood surface by weathering.

The results of this project will contribute to the solution of discoloration problem and the improvement of product quality; consequently, it will help the manufacturers and the customers. This will help the region maintain its leadership in this area by providing a better quality product than their competitors and will enable the industries of the region to have access to new markets.

CHAPTER 2

LITTERATURE SURVEY

This section summarizes the reported studies on the physical and chemical changes occurring in untreated wood during weathering, the physical and chemical differences between heat-treated wood and untreated wood, and the methods for investigating the degradation mechanism of heat-treated wood due to weathering.

2.1. Heat treatment of wood Heat treatment is one of the processes used to modify the properties of wood [21]. Wood boards were heat-treated in a prototype furnace. The wood was in contact with hot and inert combustion gases (nitrogen, water vapor and carbon dioxide) during the treatment. The presence of humidity is important, which acts as a screen gas and protects the wood from oxidation [22]. Water was evaporated and injected into the gas to simulate the presence of humidity. Operating parameters such as maximum treatment temperature, maintenance time at this temperature, heating rate and gas humidity are also have significant effect on wood quality [22].

Heat-treated wood possesses many new properties such as better resistance to biodegradation, better dimensional stability, and more attractive color. One of the important advantages of the high temperature heat-treatment of wood is the modification of its color. This is important for the utilization of wood for decorative purposes as a value-added product. In the last decade, extensive studies contributed to the development of wood heat treatment methods suitable for industrial applications and investigated the changes in wood properties during heat treatment [23-31].

2.1.1. Color changes due to heat treatment

A number of studies on the change of wood color due to heat-treatment are reported in the literature. It was reported that the temperature and the duration of heat treatment significantly affected the color of wood samples, and the effect of temperature was much more marked than the other factors [28, 32]. The luminance index of wood color parameter was more sensitive to treatment condition, and it decreased with increasing temperature and time. This kind of variation tendency was the same for all wood samples, but the extent of variation differed substantially among different wood species. The color parameter, especially the total color difference, can be used as a prediction of wood strength [33]. High temperature drying process caused darkening on the surfaces of alder and beech veneers. The total color change value increased linearly with increasing exposure time [34].

2.1.2. Micro-structural changes of wood during heat treatment

A few researchers have studied the microstructural properties of heat-treated wood by means of SEM. Boonstra et al. (2006) found that the heat treatment did have an effect on the anatomical structure of wood although this depended on the wood species considered and on the treatment method and conditions used. Softwood species with narrow annual rings and an abrupt transition from earlywood into latewood were sensitive to tangential cracks in the latewood section. Radial cracks occurred mainly in impermeable wood species such as Norway spruce, caused by large stresses in the wood structure during treatment. Sapwood of treated pine species revealed some damage to parenchyma cells in the rays and epithelial cells around resin canals whereas this phenomenon has not been noticed in the heartwood section [35]. However, it was found that the anatomical structure

of wood was only slightly affected during heat treatment [36]. Vessels, fibers, parenchyma, and rays were still intact after heat treatment. The main difference between the untreated and heat-treated wood was the presence of important quantities of extractives deposited in the vessels, which normally disappear after the thermal treatment [36].

2.1.3. Wettability change during heat treatment

The hydrophobic character of wood is often mentioned, but not well-investigated [37]. In fact, the heat-treated wood becomes rather hydrophobic, which could cause problems during varnish or paint deposition. The wettability of four different European heat-treated wood species (pine, spruce, beech, and poplar) was studied by [38], and a decrease in wettability with the heat treatment was reported which is in good agreement with the results of Hakkou and his colleagues [39]. According to Hakkou et al., the plasticization of lignin leading to reorganization of the lignocellulosic polymeric components of wood seems to be the more probable explanation for the changes in wettability. His results showed that high temperatures generally used for wood heat-treatment are not needed to modify its hydrophilic properties which can be readily modified at lower temperatures. It was reported that the number of OH-groups decreased as well during heat treatment, which can play an important role in the more hydrophobic behavior of heat-treated wood [28].

2.2. Weathering tests of wood

Weathering is the general term used to define the slow degradation of materials exposed to the weather. The degradation mechanism depends on the type of material, but the cause is a combination of factors found in nature: moisture, sunlight, temperature, chemicals, abrasion by windblown materials, and biological attack [40] . Wood is a naturally durable material that has long been recognized for its versatile and attractive engineering and structural properties [41]. The wood and wood-based products are popular for use as shelter [40]. In recent years, the use of wood in outdoor applications is significantly expanded [42]. However, like other biological materials, wood is susceptible to environmental degradation [40, 42]. If wood products are to achieve a long service life, it is necessary to understand the weathering process and then develop wood treatments to retard this degradation. However, wood products are generally put on the market with a comprehensive account of its physical and mechanical properties, and there is seldom sufficient data as to how long a wood product will fulfill its function satisfactorily outdoors before it needs repair or replacement [43]. As natural outdoor exposure tests are expensive and time consuming, it is difficult to understand the whole natural weathering process.

For a comprehensive view of wood weathering, a number of studies on the general features of natural outdoor weathering, the accelerated natural weathering tests and the artificial weathering of untreated wood are available [4, 41, 42, 44-47].

2.2.1. Natural outdoor weathering

The deleterious effect of wood weathering has been ascribed to a complex set of reactions induced by a number of factors [48]. The weathering factors related to changes in the wood surface are as follows: solar radiation (ultraviolet (UV), visible, and infrared light), moisture (dew, rain, snow, ice, and humidity), temperature, air gas, biological attack and other factors [4]. Of these factors, it is generally accepted that only a relatively narrow band of the electromagnetic spectrum of sunlight, i.e., ultraviolet light (UV) is responsible for the primary photochemical process in the weathering or oxidative degradation of wood [42]. The following section describes the two most important factors of weathering on the degradation of wood surface exposed outdoor: sunlight and moisture.

2.2.1.1. Sunlight

The radiation comprises distinct ranges that affect weathering: UV radiation, visible light, and infrared radiation. The UV and visible solar radiation that reaches the earth's surface is limited to the range between 295-800 nm. Wavelengths from 800 to about 3000 nm are infrared radiation (see Figure 2.1). The photon energy from the sun that reaches the earth's surface is inversely proportional to the wavelength of the radiation [40].

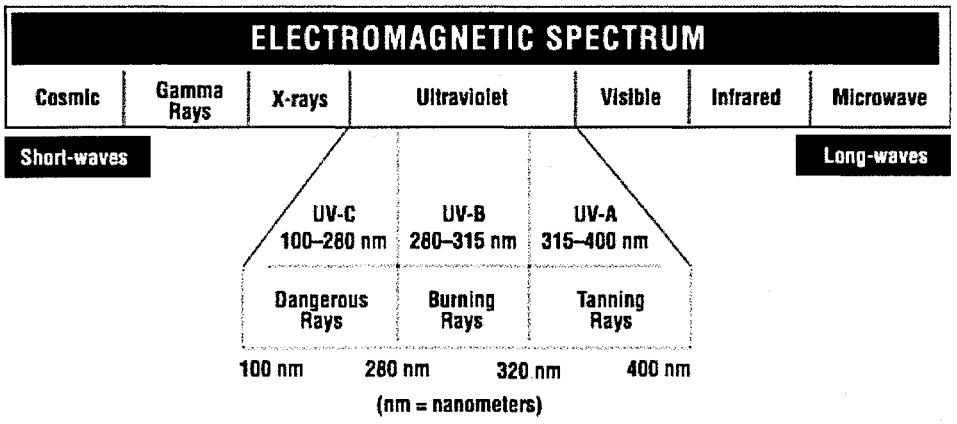

Figure 2. 1 Schematic of the electromagnetic spectrum[5]

a) UV radiation

Ultraviolet (UV) radiation is the electromagnetic radiation just like visible light, radar signals, and radio broadcast signals (see Figure 2.1). UV radiation has shorter wavelengths (higher frequencies) compared to visible light but have longer wavelengths (lower frequencies) compared to X-rays. The sun emits UV radiation in the UVA, UVB, and UVC bands, but because of absorption in the atmosphere's ozone layer, 99% of the UV radiation that reaches the Earth's surface is UVA. Some of the UVB and UVC light are responsible for the effect of the ozone layer [49]. As it can be seen from Figure 2.2 of the spectral irradiance ($W/m^2 \cdot nm$) as a function of wavelength [50], although the energy of photons at 200 nm is quite high, the spectral irradiance is quite low. As the wavelength increases to 400 nm, the energy of photons decreases, but the spectral irradiance increases [49].

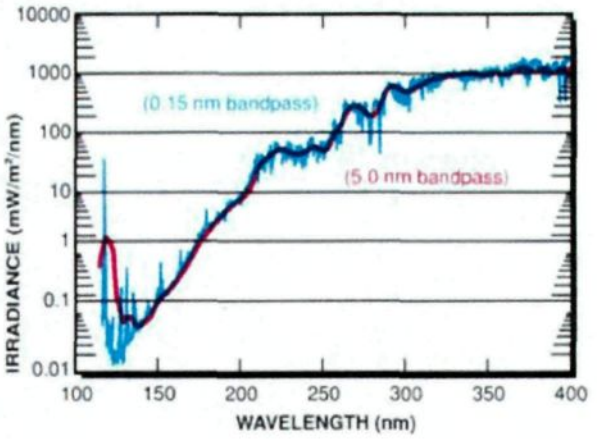

Figure 2. 2 The Solar UV Spectral Irradiance Monitor (SUSIM) measured solar UV output in the wavelength band from 120 to 400 nm

The importance of photo-oxidation in the breakdown of many polymeric materials located outdoors and the major role of UV radiation has long been recognized. Although this region of the solar spectrum contains less than 5% of solar energy, in general, only this range of wavelength has sufficient energy to break the bonds in polymers [43]. Sufficient energy to disrupt a chemical bond must be absorbed by some chemical moiety in the system in order for a photochemical reaction to occur. The bond dissociation energies and corresponding wavelengths having the necessary energy for breaking these bonds for several chemical moieties were studied [51] and are listed in Table 2.1. It can be seen from this table that the bond dissociation energies for many of the carbon-oxygen moieties commonly found in lignin fall within the UV radiation range of 295-400 nm [49].

Table 2. 1 Bond dissociation energies and radiation wavelengths [51]

Bond	Bond Dissociation Energy (Kcal/mol)	Wavelength (nm)
C-C(Aromatic)	124	231
C-H(Aromatic)	103	278
C-H(Methane)	102	280
O-H(Methanol)	100	286
C-O(Ethanol)	92	311
C-O(Methanol)	89	321
CH_3COO-C(Methyl ester)	86	333
C-C(Ethane)	84	340
C-Cl(Eethyl ether)	82	349
C-$COCH_3$(Acetone)	79	362
C-O(Methyl ether)	76	376
CH_3-SH(Thiol)	73	391
C-B_r(Methyl bromide)	67	427
N-N(Hydrazine)	57	502
C-I(Methyl iodide)	53	540

b) Visible light

It is not only the UV portion of the solar spectrum which is responsible for the breakdown of wood surface [4]. Miller and Derbyshire [4, 52] showed that visible light may also contribute to the breakdown of wood during weathering. A loss in strength was associated with the light-induced depolymerization of lignin and all cell constituents as well as with the subsequent breakdown of wood microstructure [53].

2.2.1.2. Moisture (rain, ice , snow)

The properties of wood are such that rain or dew falling on untreated wood is quickly absorbed by the surface layer through capillary action, followed by adsorption within the wood cell walls; consequently, the moisture content of wood increases and the wood swells

[54]. The moisture content difference between the surface and the interior results in the development of stresses in the wood as it swells and shrinks. The stress is greater with the steeper gradient and usually the greatest near the surface of the wood. Warping and face checking may occur and contribute further to the unbalanced stresses[55].

The effect of water on wood exposed outdoors was studied by Banks and Evans [56] who exposed thin radial sections of scotch pine and lime to deionized water over the temperature range 25-65°C. Losses in wet tensile strength and toughness occurred rapidly at temperatures higher than 50°C. Banks and Evans suggested that these phenomena were due purely to physicochemical processes and that the losses in strength may contribute significantly to detachment of paints and other finishes from wood surfaces.

Anderson and his co-workers studied wood weathering under three different conditions: light-only artificial weathering, water-only artificial weathering, and full artificial weathering (light and water). They found from FTIR spectra that full artificial weathering affected wood quite differently than the effects of either light or water alone. Weathering with light alone has a less effect, whereas weathering with water alone has no effect on the wood surfaces. And the effect of combination of light and water is more significant than their individual effects during the weathering process [57].

2.2.2. Accelerated artificial weathering

There is a constant need to get information on how a wood product will weather in advance of a real natural weathering exposure. In order to meet this requirement, accelerated artificial weathering tests are widely used for wood material certification. They attempt to simulate the primary weathering agents, such as solar radiation, temperature, and

humidity [43]. Particularly, a variety of light sources were used to simulate sunlight and to create the damage caused by sunlight. There are several UV light sources being used in practical artificial weathering tests, including carbon arc lamps, mercury arc lamps, metal-halide arc lamps, fluorescent UV lamps, xenon arc lamps (commonly used as sunlight simulators), deuterium arc lamps, and tungsten-halogen incandescent lamps. The light from a mercury lamp is predominantly at discrete wavelengths while all of others are with more continuous emission spectra [58]. The process of passing an electric current through a gas to produce UV radiation is the mechanism whereby UV radiation is produced artificially.

a) To simulate sunlight, the oldest known generator is the enclosed carbon arc lamp. It was widely used and for many applications, particularly in the paints field [43] . However, it is deficient at the low wavelength end of the spectrum compared with tropical noon day sun [43], and it has certain inconveniences and lack of flexibility for weathering wood.

b) The use of a metal-halide source with a Schott WG345 filter is appropriate for studies on biological effects due to UV-A region [59].

c) Mercury-vapor lamps, although not useful for establishing correlations, are useful for basic studies of spectral lines.

d) Another light source which is growing in use is fluorescent lamp, which is cheap and has low power. Fluorescent UV test equipment has a limited primary emission in the UV portion of the spectrum of 300 to 400nm (see Figure 2.3(b)) and does not reproduce sunlight; only its damaging effects are considered [60].

e) At present, filtered xenon lamps are used widely because of their great similarity to sunlight. The xenon-lamp tests simulate the whole spectrum of the sunlight including ultraviolet, visible, and infrared light (see Figure 2.3 (a).

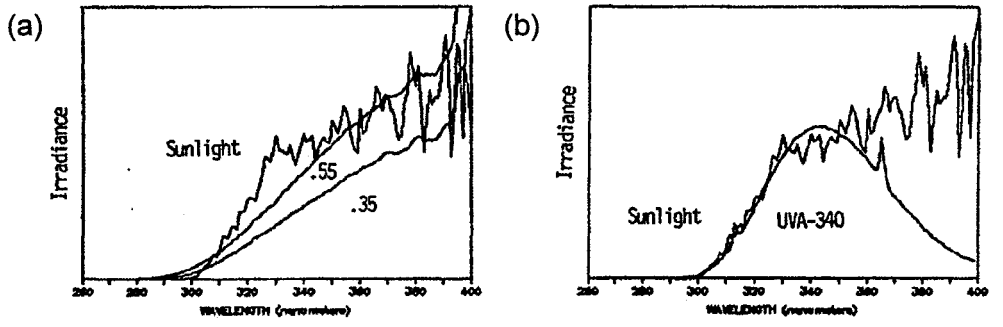

Figure 2. 3 (a) Sunlight vs. xenon arc lamp and (b) Sunlight vs. florescent lamp (UVA-340)

Many experimental studies in wood weathering were based on either optically filtered xenon arc lamps or fluorescent lamps [13, 46, 61-63]. Atlas Weatherometer and Q-panel QUV weathering tester (UVA-340 lamps) or Q-sun weathering tester (Xenon-lamp) (Q-panel company, USA) are popular in the study of polymer weathering tests.

2.2.3. Artificial weathering versus natural weathering

The use of artificial sources is advantageous since it is independent of geographical location and seasonal variations; however, it is often difficult to compare the results obtained in different laboratories due to 'slight' differences in the physical characteristics of the UV sources used. In addition, natural aging is a very complex phenomenon, and a good light source is not a sufficient condition for establishing reliable correlations through experiments [49]. The correlation and the acceleration factor must be considered when an accelerated weathering for wood products is carried out. The acceleration factor for any

sample will vary depending not only on the accelerated aging test, but on the geographical, seasonal and environmental conditions of outdoor exposure [59]. It is not possible to establish a single acceleration factor for extrapolating test results to predict lifetimes under natural weathering conditions for a variety of materials. Generally, the greater the acceleration is, the poorer the correlation is [60].

2.3. Property changes of untreated wood during weathering

This section summarizes the reported studies on the physical and chemical changes occurring in untreated wood during weathering, the physical and chemical differences of heat-treated wood with untreated wood, and the methods for investigating the degradation mechanism of heat-treated wood due to weathering. Various deleterious effect of wood weathering, such as color changes, micro-structural changes, and chemical changes will be discussed here in detail; and the weathering factors responsible for changes on the wood surface will be described.

2.3.1. Color changes of untreated wood during weathering

Wood is an excellent material for different commercial uses due to its attractive color and grain. The wood color characteristics depend on the chemical components of wood that interact with light. Hence, wood changes color when it is exposed to solar irradiation. Extensive studies and observations have shown that most wood species of commercial importance are prone to discoloration with age. Discoloration occurs both outdoors and indoors [64]. Wood surface discoloration varies with environmental conditions such as solar radiation (ultraviolet, visible, and infrared light), moisture (dew, rain, snow, and

humidity), temperature, oxygen, air pollutants, etc. [65]. Exposed to light, dark woods become light and light woods become dark; eventually, all woods become gray [4].

a) Discoloration behavior of various woods under light irradiation

The effects of light on the color of wood surface are mainly to fade or to darken and to change the tone of the color. Discoloration of wood is classified into five patterns during 100 h exposure to light irradiation: darkening, darkening-fading, darkening-fading-darkening, fading, and fading-darkening. Wood with a light color darkens more. Many softwoods continue to darken with light irradiation, and many tropical woods discolor as a result of mixture of darkening and fading [66]. Of the 100 wood species studied by Minemura and Umehara (1979), 10% has a higher value of whiteness after 100 h of light exposure compared to the color change observed for non-irradiated wood.

b) Wavelengths participating in discoloration

The rate of discoloration is usually related to the wavelengths of light [19, 67]. When 75 species of wood were exposed to light, 62% of the woods discolored with UV light and 28% of the wood discolored with visible light [64, 68]. The wavelength range for lightening or bleaching is considered to be 390-580nm; light with a wavelength of less than 390nm darkens wood and greater than 580nm causes no discoloration [64, 69]. The UV light is one the most effective environmental factors which cause severe discoloration on wood surfaces [64, 70-72].

c) Wood compounds related to discoloration

Almost all of the affected materials have a guaiacyl ring structure and an oxygenation structure at the neighboring α-position on the aromatic ring [73]. The α-carbonyl

conjugated C=C double bond and phenolic hydroxyl groups are the principal chromophoric groups in wood [64, 68].

In several species of wood, It was reported that the UV radiation penetrates only 75 μm below the surface, whereas visible light penetrates 200 μm [53]. Therefore, the change of color is limited to the surface. Color changes result from the modification of the outer layer of wood surface [34, 53, 67].

Change in the color of wood is also affected by other factors such as temperature, water, and atmosphere in contact with wood. In addition, exposure to light can cause deterioration of wood which could result in a rougher surface.

2.3.2. Micro-structural changes of untreated wood during weathering

The weathering of wood causes wood surface roughening and cracking; and it damages the microstructure. Wood exposed to outdoor weathering undergoes checking and surface erosion due principally to the effects of solar radiation and stresses imposed by cyclic wetting, temperature changes, environmental pollutants, and certain micro-organisms [74]. Several publications describe the closely related observations of microscopic changes on artificial weathering (UV irradiation) of wood surfaces [75-77]. Changes on the wood surfaces were very similar to those found for natural outdoor weathering [78]. These studies generally have been made on untreated wood and often with Radiata pine or southern yellow pine. A number of researchers have examined the effect of weathering on the physical structure of wood [8, 74, 79-84]. Microscopic studies showed characteristic ridges on the S3 wall layer, wall checking, ray and pit degradation, and middle lamella breakdown.

Borgin and his co-workers [84] investigated wood samples varying in age from 900 to 4400 years with SEM and found the weakest parts of the structure, and therefore the most susceptible to failure, are the middle lamella S1 region and the interfibrillar matrix. Parts of the wall exhibit fissures, cracks, and loss of adhesion, not found in recent wood. In spite of the breakdown of certain elements at ultra-structural (submicron structural) level, the samples had retained almost their normal macroscopic appearance and properties. As long as the main reinforcing structural elements, the microfibrils, remain intact, the major properties of wood do not apparently undergo drastic changes [84]. Four hardwoods (red oak, white oak, yellow-poplar, and sweet gum) were exposed to outdoor weathering and to artificial UV light with wavelengths of $\lambda > 220$ nm and $\lambda > 254$ nm by Hon and his colleagues [81] and then they studied these using SEM. The results showed that all wood species exhibit surface deterioration after an exposure of 30 days to sunlight or 500 hours to UV light. Loss of middle lamella, separation of procumbent cells, and damage of pit structures were observed on transverse sections for all species [85]. Kuo and Hu [77] exposed red pine sapwood to UV light for 3 to 40 days. The effect of UV irradiation on ultra-structural changes of cell walls was studied by SEM. The study of transverse sections showed that during the initial stages of UV irradiation, lignin in cell corners and in the compound middle lamellae was preferentially degraded and also the radial middle lamellae sustained a greater rate of UV degradation than the tangential middle lamellae. Occurrence of massive cell as a result of cell wall thinning was not observed until surfaces were exposed to UV light for more than 10 days [77]. Owen [86] analyzed the wood surface under a variety of artificial weathering conditions using SEM. He found that the effect of

light on the weathering process was quite rapid, and SEM data showed that water has a deleterious effect on the physical characteristics of the surface. After 2400 h of light and water exposure, many of the pit structures coalesced, creating deep crevasses in the wood. SEM micrograph of samples weathered with only water for 300 h indicated that the pit borders were left largely intact but some structural damage could be observed. The effect of weathering on Scots pine and Norway spruce treated with unpigmented commercial primers was studied by Paajanen [87]. Structural changes occurring in radial longitudinal surfaces during weathering over a period of 24 weeks were examined using a reflected light microscope and a scanning electron microscope. Micro-checks were aligned parallel to microfibrils of the cell wall or parallel or the axis of the tracheids and occurred first in latewood. The first larger checks appeared in thin-walled earlywood tracheids near thick-walled latewood tracheids. After 12 weeks of exposure, delamination of the secondary wall occurred. After 24 weeks, there were some visible macroscopic checks on the surfaces and very little separation of individual cells occurred. There were no notable differences in checking and surface erosion between pine and spruce. Blue stain colonization was found first in the cracks between tracheids, and it was more common on pine than on spruce. The priming of wood did not prevent but retarded structural changes occurring in the underlying wood. The higher the level of the solid contents in the primers were, the more likely the occurrence of structural changes was retarded [87].

Evans [88] studied with SEM the benzoylated wood exposed to natural weathering, which provided strong evidence for the stabilization of lignin as a result of benzoylation. Benzoylation of high weight gain, however, caused extensive swelling of the wood cell

wall and large losses in the tensile strength of the veneers [88]. Pandey [89] studied the weathering characteristics of modified rubberwood by SEM and FTIR. Scanning electron microscopy of untreated wood surfaces exposed for 125 and 360 days showed the formation of ridges in the S3 cell-wall layer adjacent to the lumen, together with wall checking and pit degradation. Stain hyphae and spores were also observed colonizing on wood cell lumens [89]. Schmalzl and Evens [90] studied radiata pine veneers treated with a range of titanium, zirconium, and manganese compounds and exposed to natural weathering. He found that, after weathering, untreated veneers showed microchecking of bordered pit apertures. The titanates appeared to restrict microchecking during weathering in areas where surface deposits were retained on veneer surfaces. SEM observations also suggested that veneers treated with the manganese compounds were less heavily degraded than the untreated controls.

In conclusion, microscopic studies show that, after weathering, the microstructure of wood surfaces changes. Weathering affects the width of tracheids and results in checking, distortion and erosion on tracheids, separation of cells, middle lamella layer breakdown, roughening of cell wall surface, checks of pit, "pilling" of the surface, delamination of cell wall, cracks of early and latewood boundary, erosion and damage of pit border, fungus in tracheids and rays.

2.3.3. Wettability changes of untreated wood during weathering

2.3.3.1. Theory of surface wettability

a) Young's equation

When a drop of liquid on a solid surface comes to equilibrium state, it exhibits a finite contact angle θ with the solid [91]. Young's equation for the classical case of the three-phase line of contact between a smooth, rigid solid phase, S, a liquid, L, and its vapor, V, express the relationship between the equilibrium contact angle, θ, and the interfacial tensions as given below [92] :

$$\gamma_{LV}\cos\theta = \gamma_{SV} - \gamma_{SL} \tag{2.1}$$

where: γ_{SV}: interfacial tension between solid and vapor (also called solid surface free energy), γ_{SL}: interfacial tension between solid and liquid (also called solid/liquid interfacial free energy), γ_{LV}: interfacial tension between liquid and vapor (also called liquid surface free energy or surface tension), θ: contact angle.

The values of γ_{SV}, γ_{SL}, γ_{LV} differ depending on the type of solid, gas, and liquid. Wettability criteria are:

If $\gamma_{SV} < \gamma_{SL}, \cos\theta < 0, \theta > 90°$, the liquid cannot wet the solid. The bigger the contact angle is, the worse the wettability is.

If $\gamma_{LV} > \gamma_{SV} - \gamma_{SL} > 0, 0 < \cos\theta < 1, \theta < 90°$, the liquid can wet the solid. The smaller the contact angle is, the better the wettability is, and the larger the solid surface free energy is.

If $\gamma_{LV} = \gamma_{SV} - \gamma_{SL}, \cos\theta = 1, \theta = 0°$, the liquid completely wets the solid.

Although the Young's equation has given the thermodynamic definition of the interfacial tensions, the value γ_{LV} cannot be obtained experimentally with Equation (2.1). Considering the micro-mechanism of spreading, Equation (1) can be modified as [92],

$$\gamma_{LV}\cos\theta = \gamma_S - \pi_e - \gamma_{SL} \qquad (2.2)$$

where : γ_S : the solid surface free energy in vacuum

π_e : the equilibrium spreading pressure of the adsorbed vapor of the liquid on solid.

2.3.3.2. Wettability changes

The wetting properties of wood such as contact angle, surface free energy, and interfacial work of adhesion depend on many factors: wood species, different treatments, sapwood or heartwood, previous history such as exposure to water, light, weathering or biological attacks, cleanliness, method of drying, grain orientation, and aging of exposed surface [93, 94]. Freshness of the wood surface is one of the most critical factors for the extended durability of painted wood and only a fresh high-energy surface guarantees optimum adhesion conditions [95]. The loss of coating ability and glueability with increasing age of a wood surface is a phenomenon that has attracted the interest of several researchers [95-99]. They came to the conclusion that the aging effect is essentially due to migration of wood extractives to the exterior surfaces after the surface preparation and that the wettability of wood surfaces decreases with aging of the surface [100].

Surface aging of wood has been shown to drastically reduce its wettability and, in turn, the quality and the strength of the glue bond. Such effects rapidly occur in the first

hours of exposure and continue to be magnified with time, but at a decreasing rate [92]. A decrease in the total surface free energy with surface age is reported by Gindl et al. [100]. Kalnins and Feist [94] suggested that weathering of wood increases the wettability by: 1) reducing or removing the water-repellent effect of extractives; 2) degrading the hydrophobic lignin component of wood; and 3) allowing cellulose to become more abundant on the surface. It is likely that major differences exist between species of wood.

Kishino and Nakano [45, 101] investigated the changes in wettability of tropical woods for outdoor purposes during artificial weathering up to 600 h. On the whole, the wettability of specimens decreased upon exposure up to 20 h; above that, it increased. They found that the changes in wettability during artificial weathering differed depending on wood species. The IR spectra and stereoscopic micrographs indicated that the differences in wettability between species were likely due to the structural changes on the surface during artificial weathering and the increase in wettability was due to chemical changes.

Nguyen and Johns [93] studied the effects of aging and extraction on the polar components and dispersion components of the surface free energy on redwood and Douglas-fir. They found that loss of surface free energy with aging appears to be related to environmental factors rather than to wood properties.

The feasibility of UV light exposure for the activation of surface using radial and tangential surfaces of two wood species, spruce and teak, was assessed by Ginld et al. [100]. In their study, they reported that, with UV radiation exposure, the measured contact angle of distilled water decreased significantly but there was no clear difference between the two wood species. At a specific wavelength of UV light, the surface free energy,

especially the base component of wood, increases significantly, i.e., it improves the adhesion properties of wood. It was also mentioned that UV irradiation provides cleaning of the wood surface, opening of the pits, changes in surface morphology, and to a certain extent alteration of surface chemical composition. Also, the impact of UV light exposure was similar for both radial and tangential surfaces.

2.3.4. Chemical changes during weathering

The wood contains 40-50% cellulose which is a homopolymer of high molecular weight, 20-30% hemicelluloses (heteropolymers of the pentoses and hexoses with low molecular weight), 15-20% lignin which is a cross-linked polymer of phenyl units (C_6H_5), and a small quantity of extractives. UV/visible lights cause chemical modifications of these compounds leading to a discoloration of the wood. Indeed, these chemical modifications change the quantity and nature of the components responsible for the original wood color (chromophores). Lignin absorbs light below 500 nm while the extractives such as tannins, flavonoids, and stilbenes absorb light over 500 nm [102]. Lignin is responsible for the absorption of 80-95% of UV radiation; the complex sugars absorb 5-20% while extractives absorb about 2% [103].

Lignin is composed of many aromatic rings and other chemicals that absorb UV strongly (between 200-400 nm), which causes degradation. The degradation of lignin occurs via several stages. The chemical species generated by the absorption of UV radiation are phenoxy radicals which initiate a series of chemical reactions that lead to degradation processes [104].

The degradation of cellulose under UV radiation occurs after the degradation of lignin. The presence of lignin retards the photolytic degradation of cellulose because lignin is a good UV absorber [104]. During the degradation of cellulose, the lower wavelength UV causes the formation of hydrolysable functions while the longer wavelength UV produces peroxide groups in the presence of oxygen. Therefore, exposure to UV for a short period gives wood a darker color. If wood is exposed to UV light over a long period of time, the color becomes lighter. Since the discoloration of wood is due to hydrolysis of cellulose, it also coincides with the weakening of mechanical properties. The degradation of cellulose follows a first order kinetics. During degradation, there are two types of products. The free radicals of alkoxy, hydroxymethyl, formyl as well as carbon monoxide and hydrogen are produced [105, 106].

Study of Hon (1984) on the surface of wood exposed to outdoor weathering and UV irradiation showed that ESCA provides valuable information and insight into the manifestation of weathering and photo-oxidation. XPS studies of four hardwoods, which were exposed to outdoor weathering and artificial ultraviolet (UV) light, revealed a high oxygen content on the wood surfaces indicating severe oxidation of wood. The generation of new chromophoric groups and the loss of lignin on the oxidized surface were demonstrated experimentally by infrared studies [85]. Toth et al. (1993) used XPS to study Norway spruce pulp samples before and after irradiation with artificial light. They found that the O/C atom ratio increases and significant changes are apparent in the C1s spectra but not in the O1s spectra. The XPS spectra of irradiated wood and lignin showed that photo-oxidation had occurred in both extracted wood, untreated lignin, and acetylated

samples[107]. UV weathering performance of polyvinyl chloride (PVC) containing different concentrations of wood powder was studied by Matuana and Kamdem (2002) based on the assessment of XPS data and other test results. Gindl et al. (2004) determined the effects of aging on the surface chemistry, wettability, and surface free energy in accordance with the acid-base theory using contact angle measurements and x-ray photoelectron spectroscopy. Changes in surface chemistry of wood fiber-thermoplastic surfaces weathered under a xenon arc-type accelerated weathering apparatus were studied using spectroscopic techniques. XPS was used to verify the occurrence of surface oxidation [108]. Stark and Matuana (2007) used XPS to investigate the chemical composition changes of wood flour-filled high-density polyethylene (HDPE) composites aged in a xenon-arc weathering apparatus. Salaita et al. (2008) examined the weathering behavior of southern yellow pine (SYP) wood samples pretreated in different solutions using XPS and other types of physical characterization. XPS O/C ratios increase due to the oxidation of the surface during weathering. Exposure to UV light results in bond breakage and reaction with oxygen in the presence of air to form organic functional groups. This oxide containing surface layer can protect the underlying wood from deterioration if it is insoluble in water and remains on the surface.

In summary, the change in the color of wood due to the effect of light can be attributed to the formation of quinones, quinine methides, and biphenyls that come from the degradation of lignin or groups that contain oxygen such as α-carbonyl groups and carboxylic, and hydroperoxide due to the degradation of cellulose [105, 106].

All the results given above are obtained for untreated wood during weathering or heat-treated wood before weathering. There is almost no study on the impact of weathering of heat-treated wood, especially for species in Quebec.

CHAPTER 3

EXPERIMENTAL

In this chapter, the techniques used for synthesizing and characterizing the heat-treated wood surfaces will be discussed along with the experimental procedures used.

3.1. Heat treatment

The following three species, one softwood and two hardwood, which are commonly used for outdoor applications in North America, were studied: jack pine (*Pinus banksiana*), aspen (*Populus tremuloides*), and birch (*Betula papyrifera*). Wood boards of approximately 6500 × 200 × 30 mm were heat-treated in a prototype furnace of University of Quebec at Chicoutimi (UQAC), Quebec, Canada. The natural gas was used to heat the furnace. Thus, the wood was in contact with hot and inert combustion gases (nitrogen, water vapor and carbon dioxide) during the treatment. Water was evaporated and injected into the gas to simulate the presence of humidity. Table 3.1 shows the conditions used during the heat treatment. During each tests, four wood boards were heated gradually until a predetermined maximum temperature. When this temperature was reached, it was maintained for a period (which is called holding time in the Table 3.1) in order to homogenize the temperature distribution within the wood as much as possible. The heating rate in Table 3.1 is an average value. The woods were then cooled down with direct water spray.

Then, they were subjected to artificial weathering. Untreated wood boards, kiln dried with the final moisture content of about 12%, were also exposed to artificial weathering

along with specimens heat-treated at high temperatures for comparison purposes. Specimens were arbitrarily selected for a complete statistical randomization. They were stored in a room at 20°C and 40% relative humidity (RH) until they were exposed to the artificial weathering and the characterization tests described below.

Table 3. 1 Conditions of heat treatment

(LT: longitudinal tangential surface, LR: longitudinal radial surface)

Sample	Species	Surface	Max Temp (°C)	Heating Rate (°C/h)	Holding Time [1] (h)	Humidity
1	Jack pine	LT	Untreated	-	-	-
2	Jack pine	LR	Untreated	-	-	-
3	Jack pine	LT	190	15	1	Yes
4	Jack pine	LR	190	15	1	Yes
5	Jack pine	LT	200	15	1	Yes
6	Jack pine	LR	200	15	1	Yes
7	Jack pine	LT	210	15	1	Yes
8	Jack pine	LR	210	15	1	Yes
9*	Jack pine	LT	210	-	-	-
10 *	Jack pine	LR	210	-	-	-
11	Aspen	LT	Untreated	-	-	-
12	Aspen	LR	Untreated	-	-	-
13	Aspen	LT	200	15	1	Yes
14	Aspen	LR	200	15	1	Yes
15	Aspen	LT	210	15	1	Yes
16	Aspen	LR	210	15	1	Yes
17	Aspen	LT	220	15	1	Yes
18	Aspen	LR	220	15	1	Yes
19	Birch	LT	Untreated	-	-	-
20	Birch	LR	Untreated	-	-	-
21	Birch	LT	195	15	1	Yes
22	Birch	LR	195	15	1	Yes
23	Birch	LT	205	15	1	Yes
24	Birch	LR	205	15	1	Yes
25	Birch	LT	215	15	1	Yes
26	Birch	LR	215	15	1	Yes

* The wood samples 9 and 10 were obtained from ISA Industries, Normandin, Quebec. The heat-treatment was carried out using Finish ThermoWood technology at the maximum temperature of 210°C, other information on heat treatment is not available. The other samples were heat-treated in the UQAC prototype furnace.

[1] The holding time is the time at the end of process at the maximal temperature.

3.2. Artificial weathering tests

Specimens of 70 × 65 (on longitudinal surfaces) ×20 mm (in thickness) were cut from sapwood of heat-treated and untreated wood, and then planed to have smooth surfaces. The prepared specimens of 70 × 65 × 20 mm were used in artificial weathering tests. The tests were carried out on both longitudinal tangential surface (LT) and longitudinal radial surface (LR) of the wood samples.

3.2.1. With water spray

Artificial weathering tests were conducted at the Laval University in collaboration with FPInnovation. The samples were exposed to UV light using two commercial chambers, Atlas Material Testing Technology LLC (USA) Ci65/Ci65A Xenon Weather-Ometer and Q-Sun Xenon test chamber (Xe-1-B) (see Figure 3.1) . A controlled irradiance water-cooled xenon arc with a CIRA inner filter and a Soda outer filter was used as the source of radiation to simulate sunlight. Tests were performed according to Cycle 1 of Standard ASTM G155: 102 min Xenon light, 18 min light and water spray (air temperature and humidity are not controlled) without dark cycle to simulate rain during natural weathering. The black panel temperature was set to 63±3°C and the irradiance level was 0.35W/m^2 at 340 nm. Heat-treated samples and untreated control samples of each species were exposed to UV light. The irradiation was interrupted after 72, 672, and 1512 hours of exposure and samples for each set of experimental conditions were taken out for evaluation of surface properties.

Figure 3. 1 Q-Sun Xenon test chamber (Xe-1-B)

3.2.2. Without water spray (artificial sunlight irradiation tests)

Artificial sunlight irradiation exposure test was conducted at South Florida Test Service, Accelerated Weathering Laboratory, using an Atlas Ci65/Ci65A Xenon Weather-Ometer. This device used a controlled irradiance water-cooled xenon arc with a CIRA inner filter and a Soda outer filter as the source of radiation to simulate sunlight. Tests were performed according to the standard ASTM G 147-02. The program cycle was continuous xenon light without dark cycle to simulate the natural sunlight radiation. There was no water spray, but the relative humidity was kept constant at 50±5%. The humidity was controlled by injecting water to air in another chamber besides the main chamber. This prevented the direct water spray to the wood sample surfaces (see Figure 3.1). The black panel temperature was 63±3°C and the irradiance level was 0.55W/m^2 at 340 nm. The longitudinal tangential (LT) and longitudinal radial (LR) surfaces of heat-treated samples

and untreated control samples were exposed to the light source. The irradiation was interrupted after 72, 168, 336, 672, 1008, and 1500 hours of exposure, and samples from each set of samples (untreated or heat-treated under different experimental conditions) were taken out at the end of each weathering time for the evaluation of surface properties. They were stored in the room at 20°C and 40% relative humidity until they were subjected to the characterization tests described below.

Many methods are available for characterizing the physical and chemical properties of various material surfaces, but only a few have been particularly useful for the analysis of wood during weathering. The determination of color, the fluorescence microscopy, SEM, XPS, and FTIR, the techniques mostly used in the study of wood properties, as well as the contact angle analysis on sample surface, were used in this study.

3.3. Color determination

Color is of considerable importance in wood species which are used for decorative purposes. The study of the distribution sphere of wood color showed that all the a* and b* were in positive sphere of chromaticness, and L* values ranged from 20 to 85 [109]. The L* represents the lightness intensity ranging from 0 to 100 where 0 represents black and 100 represents white. The a* value describes the chromatic coordinates on the green/red axis, ranging from -127 (pure green) to +127 (pure red). The b* value represents the position on the blue/yellow axis, ranging from -127 (pure blue) to +127 (pure yellow).

The surface color of specimens exposed to artificial weathering for different periods was measured using a reflectance spectrophotometer (Datacolor, CHECK TM) with a

measuring head which has a diameter of 10 mm (shown in Figure 3.2). Equipment calibration was carried out with standards provided by the supplier.

Figure 3. 2 Datacolor, CHECK TM

The color system L*a*b*(1976) according to the CIELab (Commission Internationale d'Eclairage) standard [110] was used to determinate color modifications. The system is characterized by three parameters, L*, a*, and b*. A three-dimensional coordinate is assigned in the CIEL*a*b* color space (see Figure 3.3).

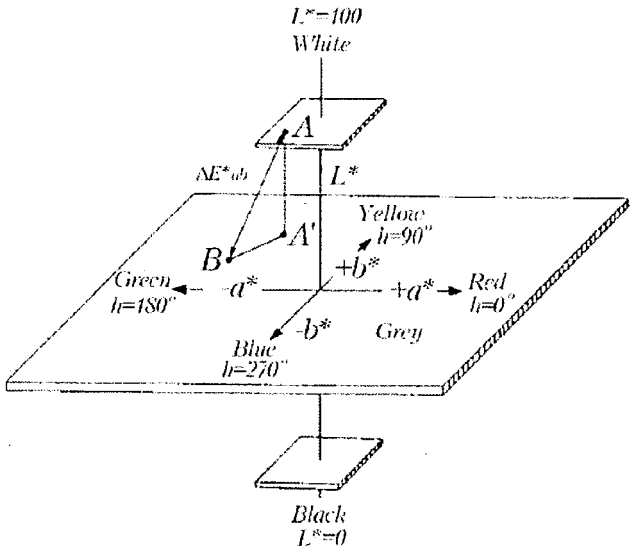

Figure 3. 3 CIEL*a*b* System [33]

The difference in the lightness (ΔL*) and the chromaticity coordinates (Δa* and Δb*) for the specimens before and after exposure to artificial sunlight irradiation were calculated according to following equations based on a D65 light source for simulating the daylight:

$$\Delta L = L_t^* - L_0^* \tag{3.1}$$

$$\Delta a = a_t^* - a_0^* \tag{3.2}$$

$$\Delta b = b_t^* - b_0^* \tag{3.3}$$

where the subscript "0" represents the values before the artificial sunlight irradiation, and "t" denotes those after an exposure of "t" hours.

The total color difference (ΔE) was calculated as a function of the artificial sunlight weathering time according to the equation given below.

$$\Delta E = (\Delta L^{*2} + a^{*2} + b^{*2})^{\frac{1}{2}} \tag{3.4}$$

The spectrum is the mean value of nine measurements taken at different positions on wood surface. The Kulbelka-Munk (K-M) equation defines a relationship between the sample spectral reflectance (in %) and its absorption and scattering characteristics. The K-M spectra were calculated according to the K-M equation given below[111]:

$$F(r_\lambda) = \frac{K}{S} = \frac{(1-r_\lambda)^2}{2r_\lambda} \tag{3.5}$$

where K and S are the absorption and scattering coefficients, respectively. r_λ can be obtained by equation below:

$$r_\lambda = \frac{R_{\lambda(sample)}}{R_{\lambda(standard)}} \tag{3.6}$$

where $R_{\lambda(sample)}$ is the reflectance of the sample and $R_{\lambda(standard)}$ represents the reflectance of a Whatman cellulose paper (no. 42) with a defined porosity [112].

3.4. Surface wettability tests

3.4.1. Wood surface preparation

Both heat-treated and untreated wood samples were prepared by sawing to approximate dimensions of 200mm in length in the longitudinal direction, 20mm in thickness in the tangential direction and 20mm in height in the radial direction. The specimens were divided into five groups, and each group was prepared using a different method: sawing (group 1), planing (group 2), and sanding with a sandpaper of 100-grit (group 3), 150-grit (group 4), and 180-grit (group 5). The equipment used for the wood preparation was an ordinary woodworking machine. Each machining process began with

sawing followed (in the last four groups) by planing. Then, the specimens were sanded with different grit sandpapers (in the last three groups). Wood dust was removed from the specimens with a brush after each machining process.

3.4.2. Contact angle tests

Wetting experiments were performed using three polar probe liquids. The physical properties and surface tensions of these liquids are shown in Table 3.2. Formamide (Methanamide) and ethylene glycol (ethane-1,2-diol) were used to study the acidic and basic characteristics of the wood surface, respectively. Both liquids were purchased from Sigma-Aldrich. Distilled water was used in the experiments with water.

Table 3. 2 Physical Properties of Probe Liquids

Name	Water (WT)	Ethylene glycol (EL)	Formamide (FM)
Molecular formula	H_2O	$C_2H_4(OH)_2$	$HCONH_2$
Surface tension[1] ($mN\ m^{-1}$)	72.75	47.7	58.2
Probes	bi-functional	acidic	basic
Molar mass ($g\ mol^{-1}$)	18.0153	62.068	45.04
Density ($g\ m^{-3}$)	0.998	1.1132	1.133
Viscosity[2] (mPa·s)	1.0050	14 (>99%)	3.764

[1,2]: The surface tensions and viscosities are measured at 20°C.

Wetting parameters obtained with water were significantly well-correlated with coating adhesion [113, 114]. Surface wettability experiments were performed using distilled water. Contact angle tests can characterize the thermodynamic properties (surface energy and

acid-base characteristics) of heat-treated wood surface [40]. Measurement of contact angle was performed at ambient condition of 20°C and 40% RH. The contact angles between water and latewood specimen surfaces were determined using a sessile-drop system, First Ten Angstroms FTA200 (Figure 3.4), equipped with a CCD camera and an image analysis software. The system uses video image processing which makes the faster determination of dynamic contact angles possible compared to the conventional contact angle goniometry. The initial period after trigger was 0.033s and the post-trigger period multiplier was set to 1.1. A drop of test liquid with a volume of 15μl was dosed automatically by an auto-syringe and picked up by the specimen (20 × 20 × 70 mm) placed on a movable sample table. Measurements of contact angle were carried out by the sessile-drop profile method with a view across to the grain. The wetting process parallel to the grain was investigated. Six to twelve tests were performed for each set of experimental conditions. The contact angles between each droplet and specimen surface were measured both on the left side and the right side of the droplet, and the mean contact angles were automatically calculated. Images of the drop in contact with the substrate were continuously captured at full video speed. The dynamic contact angle data were used to assess the wood surface wettability.

Figure 3. 4 First Ten Angstroms (FTA200)

3.5. Microscopies

3.5.1. Fluorescence microscopy (light microscopy)

The fluorescence microscope is an optical microscope used to study the properties of organic or inorganic substances using the phenomena of fluorescence in addition to reflection and absorption. It is widely used in the study of wood anatomy.

In this study, structural properties of untreated and heat-treated jack pine, aspen and birch before and after weathering were investigated. Sections cut transversely through wood at a thickness of 7-20 μm were examined and photographed with Nikon eclipse E600 Microscope (see Figure. 3.5). Some sections were also stained with 0.05% aqueous toluidine blue prior to examination with the photomicroscope. The light microscopy was also used on sections that had been stained with 1% aqueous osmium tetroxide (OsO_4) for

10–30 min at room temperature. Sections for the scanning electron microscopy (SEM) were cut from the same blocks that had been used to produce sections for light microscopy. Enlargements of 4x, 10x, 40x, 50x (objective), were used.

Figure 3. 5 Nikon eclipse E600 Microscope

3.5.2. Scanning electron microscopy (SEM)

Since the commercial introduction of the scanning electron microscope in 1965, wood anatomists have keenly described the structure of wood with a clarity frequently lacking in micrographs obtained by other means [88]. The SEM was used quite early for the assessment of wood anatomy [115]. The value of SEM for the determination of the anatomical features of wood is now well established, especially as the representation of two or even three cut planes is possible. The great depth of field and the relatively easy specimen preparation required make it an ideal instrument for the investigation of the surface features of wood [116].

Scanning electron microscopy (SEM) analysis was used to study the microscopic structural changes in heat-treated wood occurring during artificial weathering. Small wood blocks measuring 20 ×20 mm on the weathered tangential face were cut from heat-treated and untreated boards after artificial sunlight irradiation of different times (0, 336, 672 and 1512 hours). For subsurface cell degradation analysis, same blocks measuring 20 ×10 mm on the transverse and radial faces were used. The specimens were immersed in water for 30 minutes and then cut with a razor blade mounted onto a microtome by carefully cutting one of the end-grain surfaces and one radial surface. A new razor blade was used for each final cut. Another method is to split wood samples. However, these surfaces are rough and they usually do not allow the observation of the cell lumen. The specimens were washed in distilled water to remove the bleaching agent, then air-dried at room temperature for more than two nights, and desiccated with phosphorus pentoxide for 10 days. Finally, all blocks were sputter-coated with a palladium/gold layer (20 nm) by SC7640 Auto/Manual High Resoultion Sputter Coater (see Figure 3.6) and then mounted onto standard aluminum stubs using electrically conducting paste. It is necessary to apply palladium/gold layer on the wood surface in order to strengthen the electrical conductivity of sample, since a specimen surface is required to be electrically conductive for SEM examination. The samples were scanned using a Jeol scanning electron microscope (JSM 6480LV) with magnification up to 300000× at 10kV of accelerating voltage (see Figure 3.7). The distance between the sample and the electron microscope head was 20-25mm with a spot size of 35. The specimen temperature was approximately 20°C and the column vacuum was $6.66*10^4$ Pa. Digital images were transferred to a personal computer and saved as image files. To improve

image quality, resolution, contrast and brightness were corrected digitally on the computer. Electron micrographs of the UV irradiated longitudinal tangential surface were taken for different weathering times. SEM micrographs of longitudinal radial surfaces were also taken to observe the cell damage from radial direction.

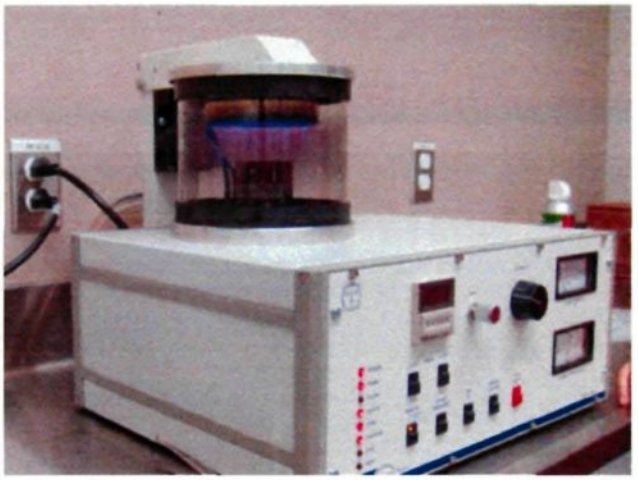

Figure 3. 6 SC7640 Auto/Manual High Resoultion Sputter Coater

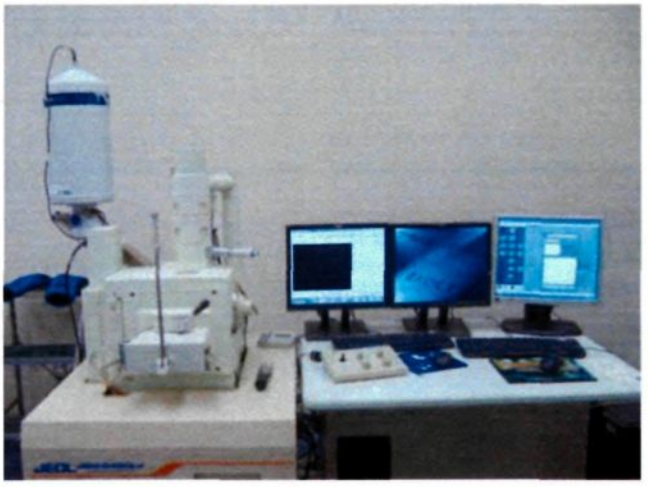

Figure 3. 7 Jeol scanning electron microscope (JSM 6480LV)

3.6. Analysis of surface chemical characteristics

3.6.1. FTIR spectroscopy analysis

Infrared spectroscopy is a highly useful tool for obtaining rapid information on the structure of wood constituents and chemical changes taking place in wood due to various treatments. The Fourier transform infrared (FTIR) spectrometer has been used for wood surface characterization to estimate the carbohydrate contents in wood and lignocellulosic materials [44, 46, 61, 117-124]. The transmission and diffuse reflectance infrared (DRIFT) spectra has an advantage over other methods because it is a quick, easy, and nondestructive method; and thus the structure of the wood is maintained when the spectra are measured directly from solid wood surfaces.

The effect of weathering on cellulose crystallinity and the chemical compositions of both cellulose and lignin on wood surfaces were studied using Fourier transform infrared spectroscopy. The air-dried specimens (10×20×20 mm) were examined using Jasco FT/IR 4200 (Figure 3.8) equipped with a diamond micro-ATR crystal. IR spectra were recorded in the wave number range of 550–4000cm^{-1}at 4 cm^{-1} resolution for 20 scans prior to the Fourier transformation. As stated in introduction that the weathering degradation take place up to a depth of 75 μm to 900 μm. The sampling depth of infrared radiation was 0.2–5μm depending on the wave number at the micro-ATR crystal incident angle of 47°. This ensured that the recorded IR spectra of wood surfaces were sufficiently surface-sensitive. Thus, changes in IR spectral features were solely caused by changes in surface chemistry during weathering duration, and there was no change in bulk chemistry of the interior part of the wood specimen. The aperture diameter was 7.1mm. All spectra were analyzed using

the Jasco spectra manager software. The IR spectra for each treatment and artificial weathering time were transformed into absorbance spectra. All relative intensity ratios were normalized relative to the peak of the band at 2900 cm^{-1} which is C-H stretching in methyl and methylene groups [45]. In FTIR, it is very important to use a spectral band that does not change during the treatment process if quantitative analysis is to be performed. And it is difficult to identify a reference spectral band that remains completely invariable throughout the whole treatment. The band of 2900 cm^{-1} is one of the bands that change less than C-OH, C-OC, R-COO-R or Ar-OCH_3 bonds during the treatment. This band was assumed to be invariable during the experiment. In reality, it does not remain fully unchanged because it is present in volatile components, such as hydrocarbons, fatty acids, steroids, lactones, furans terpenes, etc. These volatiles leave the wood surface and are partially replaced by those migrating toward surface from the interior of wood during treatment [28]. Nevertheless, the chosen band is one of the bands that change least during the treatment. The quantitative FTIR values that are used here serve only for qualitative comparison in the discussion of the results.

Figure 3. 8 Jasco FT/IR 4200

3.6.2. XPS spectroscopy analysis

X-ray photoelectron spectroscopy (XPS), also known as Electron Spectroscopy for Chemical Analysis (ESCA), is the most widely used surface analysis technique because of its relative simplicity in use and data interpretation. The elemental identity, chemical state, and quantity of an element can be determined by XPS. This method analyzes the surface to a depth of about 1-20 nm and provides information about the chemical states (bonding and oxidation), surface composition as well as the location of atom types within the samples [125]. It has been used previously to investigate the changes after the chemical treatment of numerous lignocellulosic materials, and in particular, of polymers with functionally modified surfaces [81, 125, 126]. As for the study of surface chemistry of complex organic materials, XPS has been widely used for the investigation of the surface chemical composition in the field of pulp and paper [126-129]. Similarly, many studies have been

reported on XPS analysis of wood to investigate the differences among various species of wood subjected to different mechanical treatments and the changes in the surface chemistry following different wood treatment processes. Many researchers used XPS in order to investigate the chemical characteristics of wood [63, 81, 85, 100, 107, 108, 130-133] and correlated the results with wetting measurements [63, 97, 100, 130, 134-139]. However, investigations of chemical changes in heat-treated wood by X-ray photoelectron spectroscopy (XPS) are quite rare.

Small wood chips (approximately 10 mm × 10 mm of exposed surface and 1mm in thickness) were cut with a cutter blade from heat-treated and untreated wood surfaces of three species before and after artificial weathering at different times. All preparations were carried out avoiding all contact with bare hands, and the samples were immediately placed in vacuum plastic bags. The XPS measurements were performed with AXIS Ultra XPS spectrometer (Kratos Analytical) at the Alberta Centre for Surface Engineering and Science (ACSES) (See Figure.3.9), University of Alberta. The base pressure in the analytical chamber was lower than 2 x 10^{-8} Pa. Monochromated Al Kα (hν = 1486.6 eV) source was used at a power of 210 W. The resolution function of the instrument for the source in hybrid lens mode was 0.55 eV for Ag 3d and 0.70 eV for Au 4f peaks. The photoelectron exit was along the normal of the sample surface. The analysis spot was 400×700 μm. Charge neutralizer was used to compensate for sample charging during the analysis. The survey scans spanned from 1100 to 0 eV binding energy, they were collected at analyzer pass energy (PE) of 160 eV and a step of 0.35 eV. For the high-resolution spectra, the pass-energy of 20 eV with a step of 0.1 eV was used. CASA software was utilized for data

processing. A linear background was subtracted from each peak. Then the peak area was evaluated and scaled to the instrument sensitivity factors. The composition was calculated from the survey spectra with the sum of all peaks after scaling equal to 100 %. The spectra fitting and component analysis were performed using the high-resolution spectra. The number of components and their binding-energy positions (shown in Table 3.3 below) were taken from Inari *et al.* and Ahmed *et al.* [127, 140]. No specific chemical group is assigned to the O_3 peak, since this peak is difficult to fit and unstable. The peak widths (FWHM) of the fitted components were determined in the range of 1.1-1.5 eV for C1s and 1.4-1.8 eV for O1s.

Table 3. 3 Classification of carbon and oxygen peak components for wood materials

Group	Chemical shifts / peak position (eV)	Carbon or oxygen bond to
Carbon		
C_1	284.6	C-C , C-H (Carbon atoms bonded only with carbon or hydrogen atoms)
C_2	284.6+1.5±0.2	C-O (Carbon atoms bonded with one oxygen atom)
C_3	284.6+3.0 ±0.2	C=O , O-C-O (Carbon atoms bonded to a carbonyl or two non-carbonyl oxygen atoms)
C_4	284.6+4.1±0.2	O-C=O (Carbon atoms bonded to one carbonyl and one non-carbonyl oxygen atoms)
Oxygen		
O_1	531.4±0.4	O-C=O
O_2	531.4+1.9±0.4	C-O-,C=O,C-O-C, O-C=O
O_3	531.4+3.0±0.4	

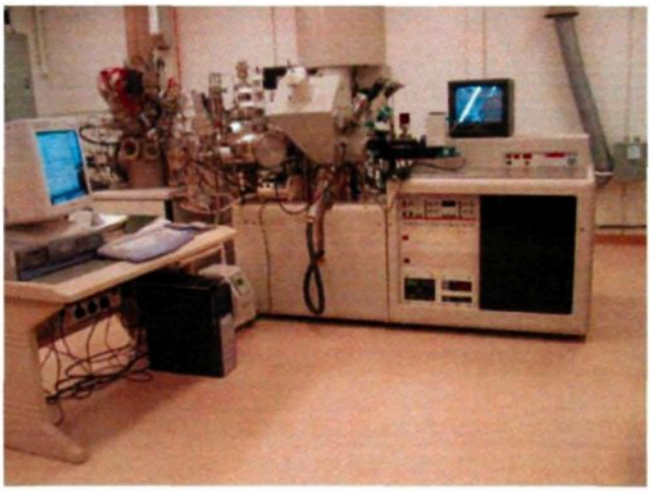

Figure 3. 9 AXIS Ultra XPS spectrometer

3.7. Chemical component analysis

This study involves the isolation, determination and characterization of the constituents and components (extractives, lignin, pentosan, and holocellulose) of the untreated and heat-treated wood before and after weathering for 1512 hours. Table 3.4 summarizes the analysis that was used for all three species, and Figure 3.10 shows the scheme for the chemical analysis of various wood samples. The space available for weathering was limited in the aging chamber. Therefore, a priority was given to heat-treated samples although some untreated samples were also exposed to weathering for comparison purposes. Since it takes sufficient quantity of sample for the chemical component analysis and just around 75 μm thickness on the sample surface after weathering can be used, there was not enough sample to carry out this analysis of untreated wood.

Table 3. 4 Summary of analysis

Sample	Before weathering		After weathering	
	Untreated wood	Heat-treated wood	Untreated wood	Heat-treated wood
Jack pine	Extr/L/P/ Hol	Extr/L/P/ Hol	-	Extr/L/P/ Hol
Aspen	Extr/L/P/ Hol	Extr/L/P/ Hol	-	Extr/L/P/ Hol
Birch	Extr/L/P/ Hol	Extr/L/P/ Hol	-	Extr/L/P/ Hol

Extr: Analysis of extractive; L: Analysis of lignin; P: Pentosan; Hol: Analysis of holocellulose

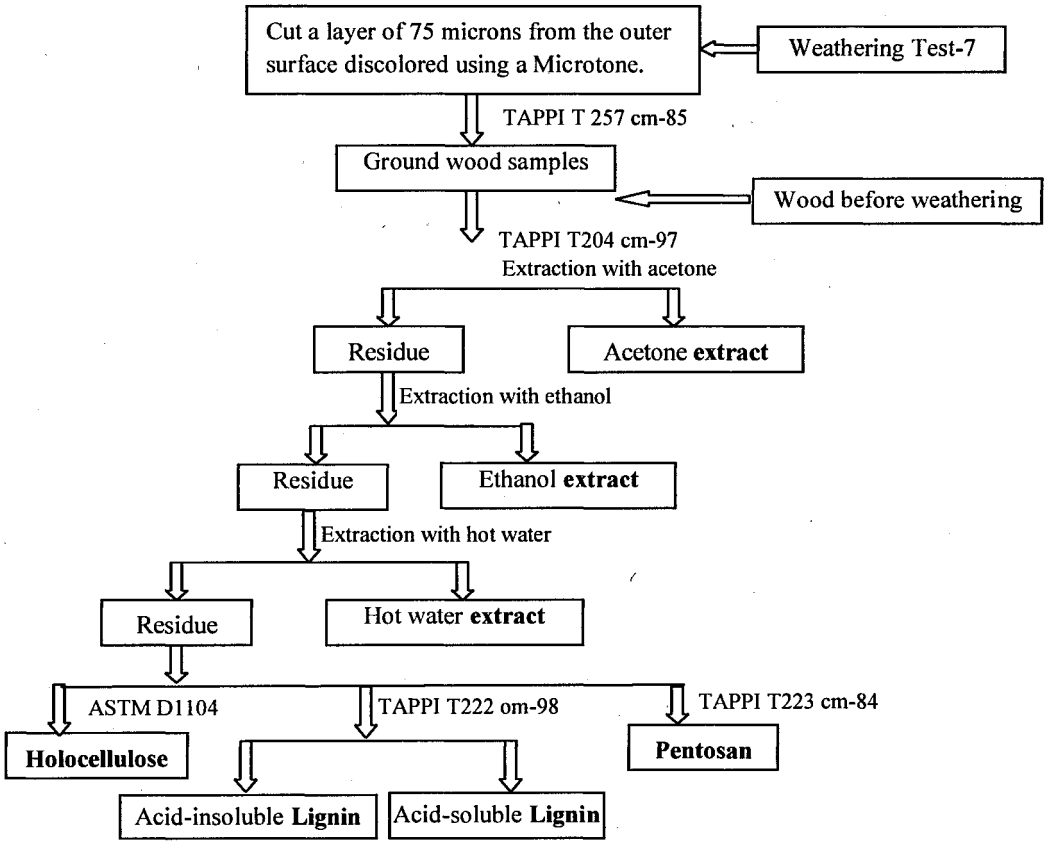

Figure 3. 10 Scheme for the chemical analysis of wood samples

3.7.1. Preparation of samples

The untreated (kiln-dried) three wood species were heat treated, jack pine and aspen at 210°C and birch at 215°C before weathering. These temperatures were chosen based on the results of heat treatment parameter optimization studies. In this study, wood samples were collected from two or three different wood boards. Using a microtone, layers of approximately 75-micron in thickness were cut from the wood surfaces which were discolored by weathering after 1512 h. The samples of different experimental sets were ground and classified according to the procedure given in TAPPI Standard T257- os-76 (TAPPI, 1997) and used as obtained for moisture content (TAPPI 211om-93) determination.

3.7.2. Analysis of extractives

According to TAPPI standard, the extractives of wood samples should be extracted with the solvent mixture of ethanol and benzene. As benzene is known to be extremely hazardous to health, it is replaced with acetone. The extractives are extracted sequentially with acetone and 95% ethanol using extraction methods given in TAPPI Standard (T204 cm-97). Extractive-free wood samples were obtained according to TAPPI standard sample preparation procedure (TAPPI Standard T 12 os-75). The wood sample powder is extracted sequentially with acetone, 95% ethanol, and water before the determination of acid insoluble lignin content as well as pentosan and holocellulose contents.

3.7.3. Determination of Klason Lignin content

The method of TAPPI Standard T222 om-98 is applied to separate and determine acid insoluble lignin content in extractive-free wood samples.

3.7.4. Determination of pentosan content

The procedure given in TAPPI Standard T223 cm-84 is used to determine the changes in pentosan content.

3.7.5. Determination of holocellulose content

The holocellulose is defined as the fraction of carbohydrate (cellulose plus hemicelluloses) in wood which is insoluble in water. The holocellulose was obtained by adding 2.5 g of extractive-free sample in a 250-ml Erlenmeyer flask to which 80 ml of hot distilled water, 0.5 ml of acetic acid, and 1 g of 80% sodium chlorite were added. A 25-ml Erlenmeyer flask was inverted in the neck of the reaction flask. The mixture was heated in a water bath at 70°C. After 60 minutes, 0.5 ml of acetic acid and 1 g of sodium chlorite were added. After each succeeding hour, fresh portions of 0.5 ml acetic acid and 1 g sodium chlorite were added and mixed. Addition of 0.5 ml acetic acid and 1 g of sodium chlorite was repeated more than four times until the wood sample was completely separated from lignin. After chloriting for 6 to 8 h, the samples were left without further addition of acetic acid and sodium chlorite in the water bath for overnight. At the end of 24 hours of reaction, the holocellulose was cooled and filtered on a tarred fritted dics glass thimble until the yellow color (the color of holocellulose is white) and the odor of chlorine dioxide was removed, washed with acetone, vacuum oven dried at 105°C for 24 hours, and then placed in a desiccator for an hour and weighed.

CHAPTER 4

RESULTS AND DISCUSSION

In this chapter, all the results of this project are presented and discussed. The section 4.1 details the modifications of wood properties that occur during the heat-treatment process. Afterwards, the surface chemical characterization, color changes, microscopic structural changes, and the wetting characteristics of the three heat-treated wood surfaces due to artificial weathering with water spray are presented in Sections 4.2, 4.3, 4.4, and 4.5, respectively. In Section 4.6, the investigation of degradation behavior of heat-treated wood under artificial sunlight irradiation without water spray is discussed. In the final section, the calculation of solar heat gains on wood surfaces under outdoor conditions and in indoor artificial weathering tests is presented.

4.1. Modifications of wood properties due to heat treatment

4.1.1. Color changes

Heat treatment of wood is an effective method to improve the dimensional stability and the durability against biodegradation.

a) Color changes due to different temperatures of heat treatment reported using CIE-L*a*b* system

The curves of Figure 4.1 were plotted in order to verify the existence of a relationship between the chromatic variations occurring during heat treatment at different temperatures and the total color differences (ΔE) for three species using the CIE-L*a*b* system. Decrease in a* values indicates the tendency of wood surface to become greener while their

increase shows a tendency to become more red. The rate of change of a*values represents the rate of wood color change. All three species show a tendency to become reddish during heat treatment. There is a proportional increase in a* values with increasing heat treatment temperatures for jack pine. The values of a* reach their maximum at 205°C for birch and at 210°C for aspen. Afterwards, they decrease if the heat treatment temperature is further increased to 215°C for birch and 220°C for aspen (Figure 4.1 (a)). Decrease in b*values indicates the tendency of wood surface to become bluer while increase of b*values shows a tendency to become yellower. Values of b* for aspen and birch decrease with increasing heat treatment temperature, although it can be observed that color co-ordinates b* increase after the heat treatment at temperatures lower than 200°C characterizing a tendency to become yellowish (Figure 4.1 (b)).

As indicated by the modifications in L* values, lightening and darkening of wood surface can be observed. Figure 4.1 (c) shows L* plotted as a function of temperature during heat treatment for the three species. L* is the most sensitive and visualized parameter for the wood surface quality during heat treatment. L*values decrease due to heat treatment for the three investigated wood species, which means that the samples lost lightness. The lightness variation can be separated into two regions. During the heat treatment at lower temperatures (less than 200°C), a slow decrease in the lightness indicates that the wood becomes darker. The variation becomes more significant when the heat treatment temperature exceeds 200°C for all species. A previous study also reported the darkening of wood surface due to heat treatment as a function of the heat treatment temperatures and the type of wood species [33]. Hemicelluloses of heat-treated wood first

degrade and consequently the lignin contents of heat-treated wood increase proportionally. Thus, changes in lightness of wood during heat treatment are mainly due to the hemicellulose degradation, and wood color becomes darker starting from the beginning of heat treatment. The degradation of hemicelluloses intensifies with increasing heat treatment temperature.

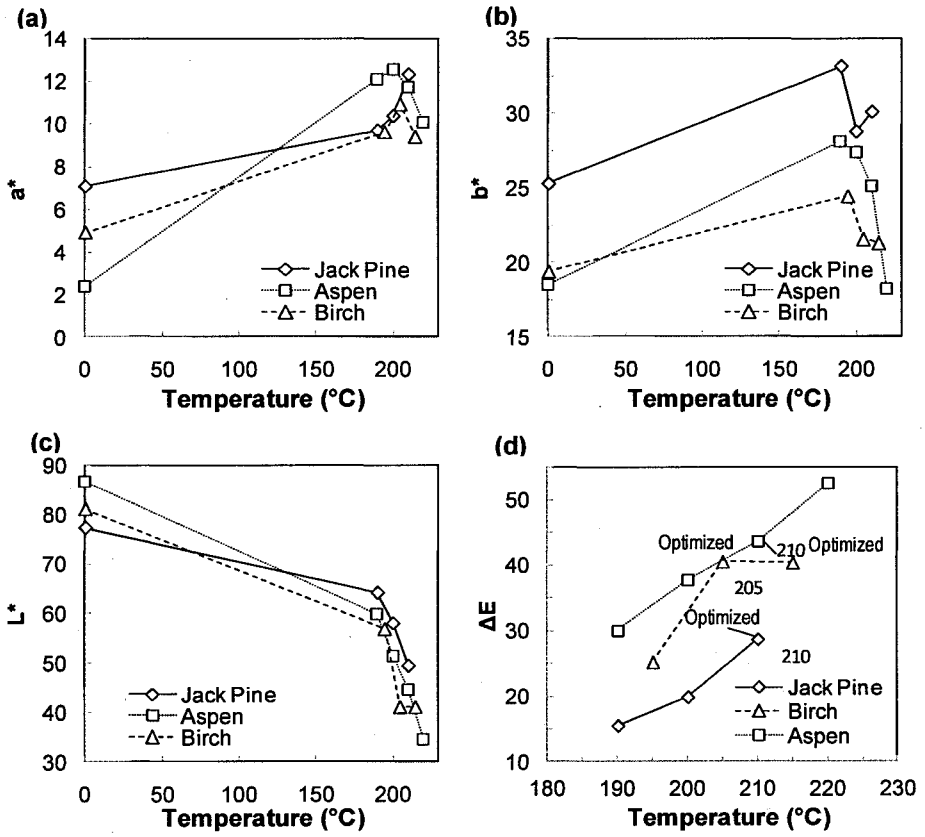

Figure 4. 1 Color changes on tangential surfaces of wood heat-treated at different temperatures presented using CIE-L*a*b* system: (a) red/green coordinate (a*), (b) yellow/blue coordinate (b*), (c) lightness coordinate (L*), (d) total color difference (ΔE)

Total color differences (ΔE) of wood surfaces of three species heat-treated at different temperatures are shown in Figure 4.1 (d). With increasing heat treatment temperature, the total color differences (ΔE) of heat-treated jack pine and aspen increase almost at the same rate. The ΔE of birch increases significantly from 200°C to 205°C while it changes slightly from 205°C to 215°C. The temperature 205°C was chosen as the optimized heat treatment temperature for birch wood while 210°C was chosen for jack pine and aspen wood according to the physical and mechanical properties. After heat treatment, the color changes of aspen wood are found to be the highest among the three species and those of jack pine are the lowest. These results indicate that the color of hardwood (aspen and birch) changed more significantly than the color of softwood (jack pine) during the heat treatment process. This is well correlated with the chemical analysis results of holocellulose contents in section 4.5 (see Table 4.5). Among the species studied, the color of jack pine changes the least; and it has the lowest content of holocellulose, which is more sensitive to degradation during heat treatment.

b) Influence of humidity during heat treatment

Figure 4.2 (a, b, c) shows the color differences of aspen and birch wood heat-treated with and without humidity. No testing was done for jack pine.

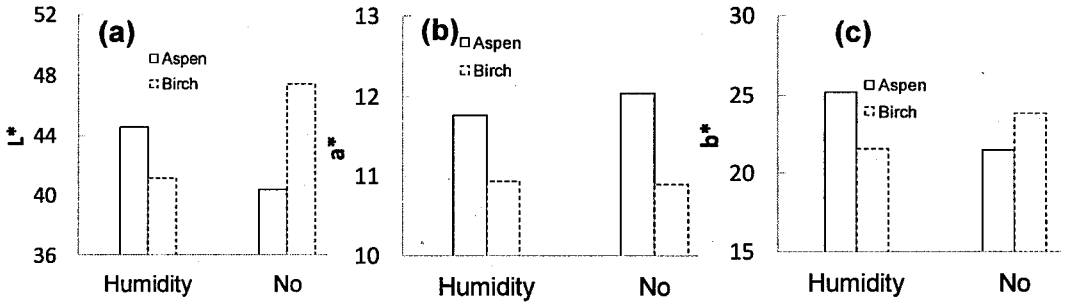

Figure 4. 2 Color differences of aspen and birch wood surfaces after heat treatment with and without humidity: (a) lightness coordinate (L*), (b) yellow/blue coordinate (a*), (c) red/green coordinate (b*)

According to differences of L* values between heat treatment with and without humidity (shown in Figure 4.2 (a)), the tendencies observed for aspen and birch wood are different in the absence and presence of humidity. The lightness of aspen heat-treated using humid gas is higher while that of birch is lower than that of the cases when a dry gas is used during the heat treatment. Similar to L*value, b*value displays the same trends for aspen and birch wood regarding the influence of humidity during heat treatment (Figure 4.2 (c)). However, the yellow/blue values (a*) of both aspen and birch woods mainly stay the same regardless of the humidity (Figure 4.2 (b)). From the above results, it is not possible to identify a clear trend for the color change of wood due to the presence of humidity in gas during heat treatment. The influence of humidity control during heat treatment on color changes was studied only on aspen wood.

4.1.2. Wettability analysis

4.1.2.1. Influence of heat treatment conditions in wettability of wood surfaces

Wood is a porous material so there are many different-size cells and vacant spaces through which liquid can penetrate and spread. The phenomena taking place during the wetting of wood by liquid (the contact angle formation, spreading, and penetration) are reported in literature [141]. The wetting of jack pine, aspen, and birch wood, heat-treated under different conditions, by water and the wetting of the untreated samples of the same species were investigated. The results are presented below.

a) Effect of heat treatment temperature

The mean values of dynamic contact angles as well as initial contact angles for all samples heat-treated at different temperatures are presented in Figures 4.3 to 4.6.

Figure 4.3 shows the results of the dynamic contact angle of water on jack pine surface heat-treated at temperatures of 190°C, 200°C, and 210°C and that of the untreated control sample. As it can be seen from Figure 4.3, the contact angles of all heat-treated jack pine wood are higher (less wettable) than those of untreated wood at all times and decrease at a slower rate with increasing time. This shows that wood becomes more wettable as the time increases and this change is slower for the heat-treated wood compared to that of untreated wood. The results indicate that heat treatment has significant effect on the wetting of jack pine wood. It decreases the water absorption of jack pine. As the heat treatment temperature increases from 190°C to 210°C, the contact angles increase significantly. The results show that the wettability of jack pine wood decreases with increasing heat treatment temperature. The changes in wettability as a function of different heat treatment

temperatures are not linear. The differences in contact angles between 190°C and 200°C are not as significant as those between 200°C and 210°C.

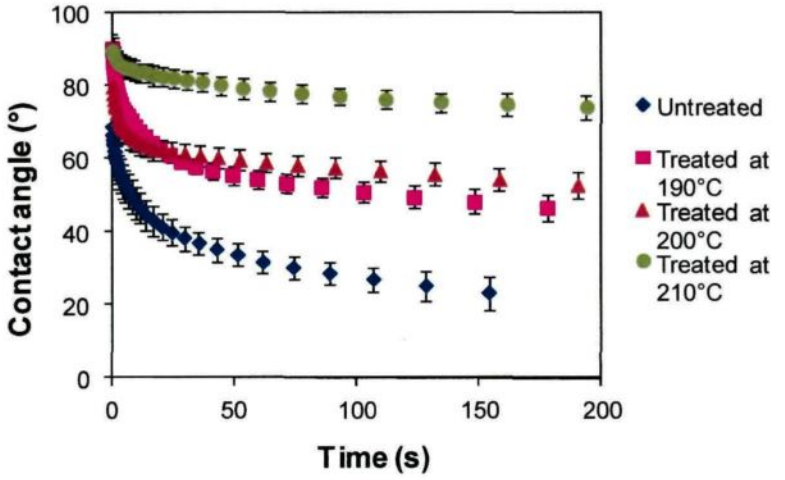

Figure 4. 3 Dynamic contact angle of water on jack pine surface heat-treated at different temperatures and on untreated control samples

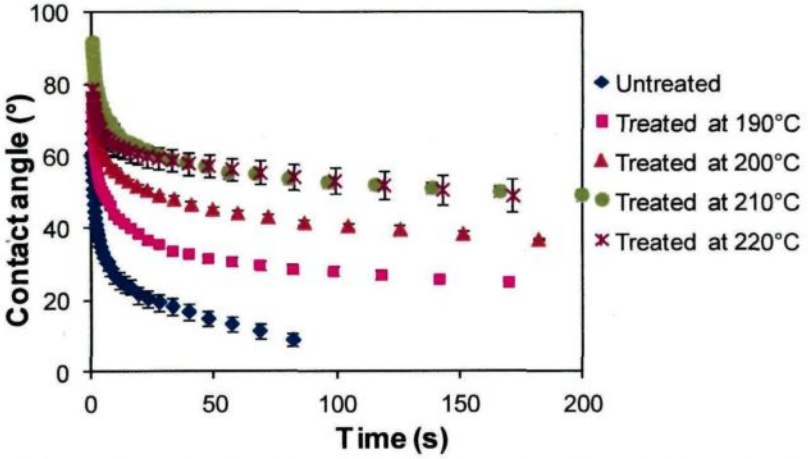

Figure 4. 4 Dynamic contact angle of water on aspen surface heat-treated at different temperatures and on untreated control samples

The results of the dynamic contact angle of water on aspen surface heat-treated at temperatures of 190°C, 200°C, 210°C, and 220°C and that of the untreated control sample are shown in Figure 4.4. Similar to jack pine wood, the contact angles of all heat-treated aspen wood are higher than those of untreated wood at all times and decrease at a slower rate with increasing time. As the heat treatment temperature increases from 190°C to 210°C, the contact angles increase significantly. This indicates the wettability of aspen wood by water decreases due to heat treatment with increasing heat treatment temperature. However, the change in contact angle with heat treatment temperature, consequently, water absorption does not follow the same trend as jack pine. The contact angles of aspen heat-treated at 210°C are almost the same as those treated at 220°C. This means that there is no need to increase the heat treatment temperature higher than 210°C to decrease the water absorption and to increase dimensional stability of aspen wood.

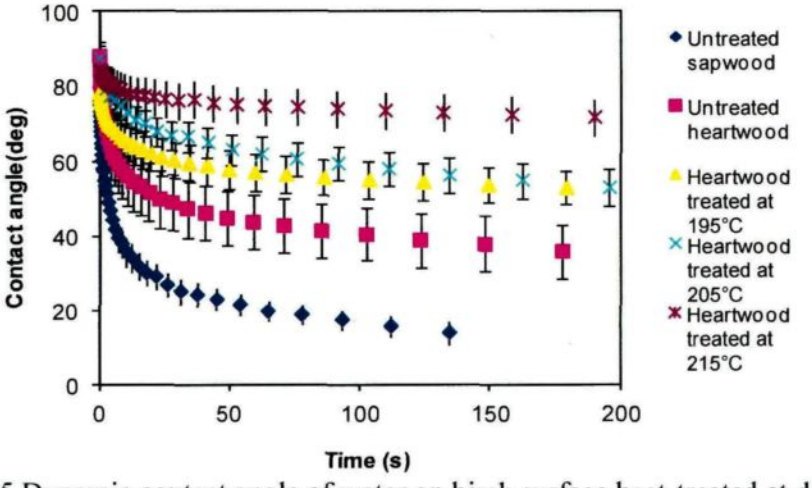

Figure 4. 5 Dynamic contact angle of water on birch surface heat-treated at different temperatures and on untreated control sample

The dynamic contact angles of water on birch sapwood surface heat-treated at three different temperatures (195°C, 205°C, and 215°C) and untreated sapwood and heartwood samples are shown in Figure 4.5. Similar to jack pine and aspen wood, the contact angles of all heat-treated birch wood are higher than those of untreated wood both for sapwood and heartwood at all times. With increasing heat treatment temperature up to 215°C, the contact angles increase and they decrease slowly with increasing time. This indicates that the water wettability of birch wood decreases more with increasing heat treatment temperature. The contact angles of heartwood are higher than sapwood at all times. This might be explained by the presence of more extractives in heartwood than sapwood which can increase the wood hydrophobic property.

The initial contact angle gives information on the contact angle formation and thus can be used to calculate the surface tension. Figure 4.6 (a, b, c) shows the initial contact angles of water on untreated and heat-treated three wood species at different temperatures. All initial contact angles of heat treated jack pine and aspen wood are higher than those of untreated wood while that of birch heartwood are almost the same with that of the birch heat-treated at 205°C. This indicates that the extractives of birch wood have the same effect on wood wettability as that of the heat treatment temperature since heartwood is rich in extractives. For jack pine and aspen wood, heat-treatment at 210°C results in the highest initial contact angles for these species while the birch wood heat-treated at 205°C has the highest initial contact angle among those of the heat-treated samples.

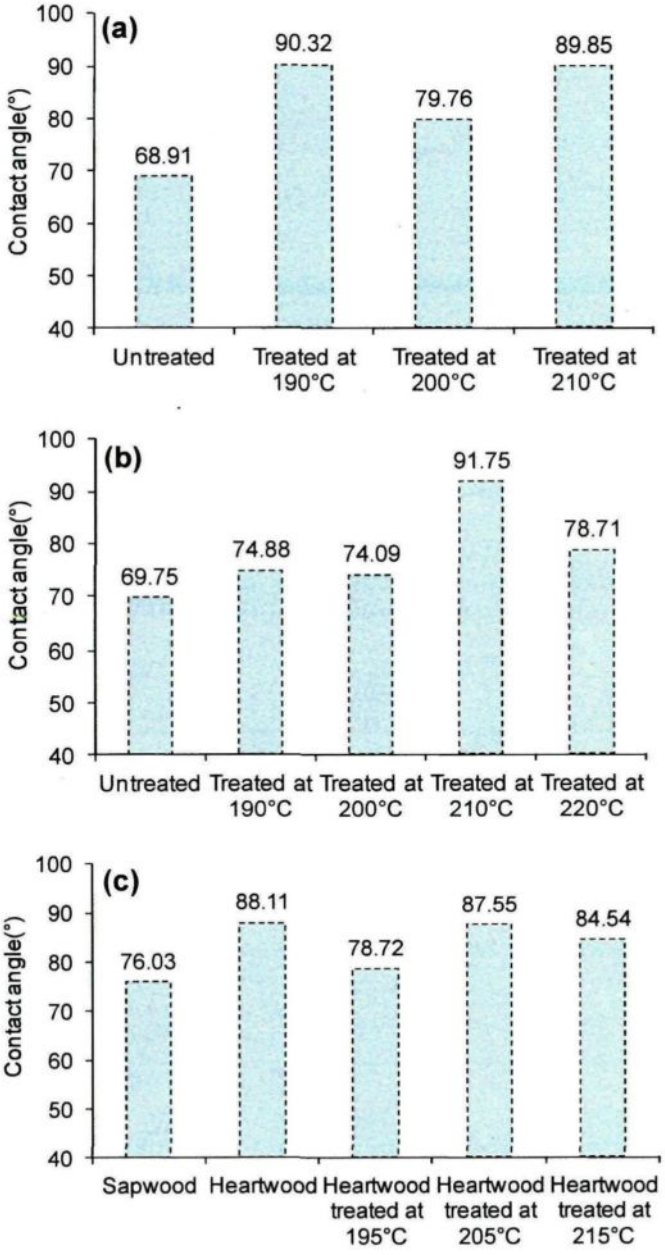

Figure 4. 6 Initial contact angle of water on surfaces of three different species heat-treated at different temperatures and on controled untreated samples: (a) jack pine, (b) aspen (c) birch

b) Effect of humidity

The dynamic contact angles of water on aspen and birch wood surfaces heat-treated with and without humidity are shown in Figure 4.7. The contact angles of all heat-treated birch wood are higher than those of heat-treated aspen wood at all times. The initial contact angles of wood heat-treated in the presence of humidity are higher and decrease faster with increasing time than those treated without humidity for both aspen and birch wood. After about 10s, all the contact angles of birch treated with and without humidity are higher than those of aspen. This indicates that the wettability of heat-treated birch wood is smaller than that of aspen mainly due to the differences in their densities and different porosity effect. After 50s, the contact angles of aspen heat-treated with and without humidity approaches each other while those for birch heat-treated without humidity become higher than those for birch treated with humidity.

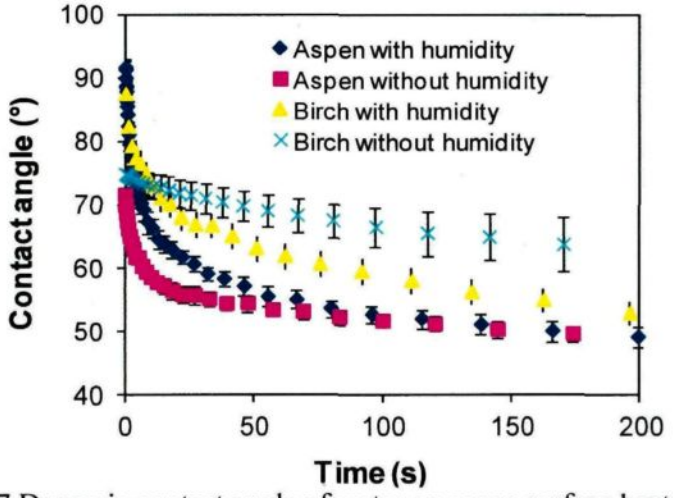

Figure 4. 7 Dynamic contact angle of water on aspen surface heat-treated with and without humidity

4.1.2.2. Influence of surface preparation on the wettability of heat-treated wood surface by different liquids

The dynamic wetting of heat-treated jack pine by three different probe liquids (see Table 3.2) on wood surfaces prepared by sanding (with three different sandpapers), planing, and sawing was studied (see Section 3.4). Their wetting characteristics were compared with those of the untreated jack pine.

The wettability was quantitatively evaluated using a dynamic wetting model which makes it possible to describe and quantify the spreading and penetration ability of liquids on wood surfaces [142]. The model can be expressed as:

$$\theta = \frac{\theta_i \theta_e}{\theta_i + (\theta_e - \theta_i)\exp(K(\frac{\theta_e}{\theta_e - \theta_i})t)} \tag{4.1}$$

where: θ_i is the initial contact angle, θ_e is the equilibrium contact angle (here the angle is measured 40s after the drop deposit on the surface), K is the penetration and spreading rate constant, and t is the absorption time. K-value represents how fast the liquid spreads and penetrates into the porous structure of wood. By knowing the K-value, spreading and penetration for a given liquid-solid system can be quantified. Higher K-value indicates that the contact angle reaches equilibrium more rapidly and the liquid penetrates and spreads faster (increased wetting). K-value of a particular liquid-solid system can be determined by curve-fitting the experimental data to Equation (4.1) using a nonlinear method. If the measured apparent equilibrium contact angle is zero, a contact angle of 0.01 must be used in Equation (4.1) in order to solve for the K-value [142].

Table 4. 1 Contact angles and K-values on heat-treated and untreated jack pine surfaces for different machining processes and probe liquids.

Heat Treat	Probe Liquid	Machining process	Contact angles		Decrease Percent (%)	K-value		R^2 model fit
			θ_i (°)	θ_e (°)		Mean (1/s)	CV	
Heat-treated	WT	100	84.15(2.16)	50.65(1.206)	39.80	0.055(0.005)	25.811	0.936
		150	108.17(2.55)	77.66(5.06)	28.20	0.025(0.003)	33.947	0.920
		180	88.78(3.61)	52.10(1.09)	41.31	0.069(0.005)	24.587	0.978
		P	106.99(2.14)	85.22(2.17)	20.35	0.026(0.003)	30.813	0.959
		S	117.50(2.54)	83.89(3.44)	28.61	0.021(0.003)	43.102	0.972
	ET	100	55.83(1.47)	4.22(0.57)	92.43	0.991(0.198)	52.764	0.909
		150	48.64(1.15)	4.46(1.23)	90.83	0.878(0.191)	48.562	0.933
		180	49.11(2.87)	4.87(0.89)	90.08	0.780(0.114)	35.819	0.928
		P	78.37(1.97)	27.73(2.84)	64.62	0.206(0.040)	47.337	0.970
		S	80.59(1.27)	3.91(1.24)	95.14	0.574(0.056)	27.672	0.956
	FM	100	48.71(1.91)	0.01(0)	99.98	2.670(0.257)	23.621	0.945
		150	25.78(3.00)	0.01(0)	99.96	10.755(1.115)	27.440	0.970
		180	60.58(2.03)	0.01(0)	99.98	3.254(0.466)	35.085	0.935
		P	87.88(2.78)	28.78(2.92)	67.24	0.135(0.020)	36.220	0.949
		S	78.22(1.82)	0.01(0.00)	99.99	1.872(0.145)	24.450	0.926
Untreated	WT	100	83.33(2.66)	20.78(6.44)	75.06	0.186(0.028)	48.999	0.961
		150	75.55(1.37)	5.19(1.36)	93.13	0.417(0.043)	32.826	0.955
		180	70.03(2.14)	26.76(3.57)	61.78	0.112(0.015)	31.876	0.942
		P	96.53(2.71)	73.02(1.67)	24.36	0.029(0.003)	22.304	0.973
		S	86.25(1.53)	39.15(4.17)	54.60	0.075(0.008)	34.440	0.927
	ET	100	53.11(3.46)	2.92(0.31)	94.50	1.009(0.096)	25.407	0.967
		150	48.63(2.34)	4.57(0.27)	90.60	0.560(0.038)	16.451	0.959
		180	41.46(3.94)	2.75(0.38)	93.35	0.620(0.050)	19.861	0.974
		P	57.11(1.75)	7.42(1.30)	87.00	0.452(0.067)	36.064	0.965
		S	62.49(1.45)	0.01(0.001)	99.99	0.913(0.103)	29.854	0.988
	FM	100	48.18(2.52)	0.01(0)	99.98	5.224(0.367)	18.994	0.955
		150	51.54(4.36)	0.01(0)	99.98	6.117(0.939)	35.612	0.970
		180	58.01(1.70)	0.01(0)	99.98	6.827(0.916)	57.558	0.953
		P	64.95(1.81)	0.01(0)	99.98	0.893(0.123)	37.571	0.950
		S	48.32(2.54)	0.01(0)	99.98	10.552(0.796)	24.877	0.961

WT= Water; ET= Ethylene glycol; FM=Formamide; P= Planed; S=Sawn; 100, 150, 180 are samples sanded with 100, 150, 180 grit paper, respectively; data in parentheses are asymptotic standard errors; CV: coefficient of variation; θ_i: Initial contact angle; θ_e: equilibrium contact angle (measured at 40s, choose 0.01 if the value is 0); K : the penetration and spreading constant; R^2: correlation coefficient for K value.

The mean values of contact angles as well as the spreading and penetration constants (K-values) for all samples and their correlation coefficients (R^2) were calculated using the code SAS 9.1. The results are presented in Table 4.1. R^2 values of the wetting model are over 0.92 for all of the wood surfaces examined. R^2 is a measure of the fit quality, and its value indicates that the wetting data fits the cited model well. Table 4.2 shows the results of the three-way analysis of variance for the initial contact angles, equilibrium contact angles (measured at 40 s), and K-values based on different surface preparations, type of liquid, and whether the wood was heat-treated or not. From the results shown in Table 4.2, the P-values for all three parameters (presence of heat treatment, surface preparation, and type of probe liquid) are all less than 0.0001 for K-values and both initial and equilibrium contact angles. This indicates that these three factors have significant effect on the wetting of jack pine. The contact angle as a function of time and K-values for the different wood surfaces and three probe liquids are shown in Figures 4.8, 4.9, and 4.10. The results are discussed in more detail below.

Table 4. 2 Three-way analysis of variance for the initial contact angles, equilibrium contact angles, and K-values of jack pine for different surface preparations, different liquids, and heat treatment

Effect of variance	Degrees of Freedom	F-value*			P* > F		
		θ_i	θ_e	K-value	θ_i	θ_e	K-value
Heat treatment	1	156.7	261.7	20.05	<0.0001	<0.0001	<0.0001
Liquid	2	677.2	1089.6	372.45	<0.0001	<0.0001	<0.0001
Machining	4	109.7	73.8	35.04	<0.0001	<0.0001	<0.0001
Treatment× Liquid	2	17.6	120.3	16.24	<0.0001	<0.0001	<0.0001
Liquid×Machining	8	17.2	18.7	29.47	<0.0001	<0.0001	<0.0001
Treatment×Machining	4	30.1	8.0	21.09	<0.0001	<0.0001	<0.0001
Treatment×Liquid×Machining	8	16.9	21.5	20.75	<0.0001	<0.0001	<0.0001

*F-value is a statistical indicator and is equal to the variance of the group means / the mean within group variances. P (the measurement of distance between individual distributions) is the probability of obtaining a result at least as extreme as the one that was actually observed, given that the null hypothesis is true. As F-value goes up, P goes down, i.e., more confidence in the difference between two means.

a) Effect of heat treatment on dynamic wetting

As can be seen from Table 4.1, the mean values of initial and equilibrium contact angles of three liquids on heat-treated wood prepared by different methods are higher than those of untreated wood, respectively, while mean K-values and percent decrease in contact angle show opposite trends with the exception of formimade on wood surface sanded by 150-grit sandpaper. Nearly all the results show that the wettability of wood by three liquids decreases with heat treatment. It can be seen from Table 4.2 that heat treatment has a significant effect (P-value<0.0001) on all the three parameters (θ_i,θ_e, K-value) of the

wetting. The degradation of hemicelluloses of wood during heat treatment results in the reduction of OH bonds and O-acetyl group, and the subsequent cross-link formation between the wood fibres makes wood more hydrophobic [143]. According to Rowell et al. and Hakkou et al. [38, 144], the changes in lignin and cellulose during heat treatment also contribute to the reduction in water absorption. As it can be seen from Figure 4.8, the contact angles formed by water on heat-treated jack pine surface are higher than those of untreated wood produced by same machining process for all times with an exception of surface produced by 150-grit . This shows that the heat treatment decreases the wettability of wood by water, which is in accordance with the results of previous studies [143]. As it can be seen from Figure 4.9, both heat-treated and untreated wood surfaces prepared by planing has the largest contact angles with ethylene glycol (less wetting), followed by sawn surface and finally by sanded surface. The differences in contact angles of the heat-treated wood surfaces prepared using different methods are more significant than those of untreated wood. In general, similar trends are observed for formimade (Figure 4.10). Consequently, heat treatment affects most the wetting of planed surface by formimade, followed by those of sawn and sanded surfaces. This agrees with the results shown in Table 4.2 that indicate a strong effect of heat treatment and different machining methods on the initial contact angle (30.1°) and the equilibrium angle (8.0°).

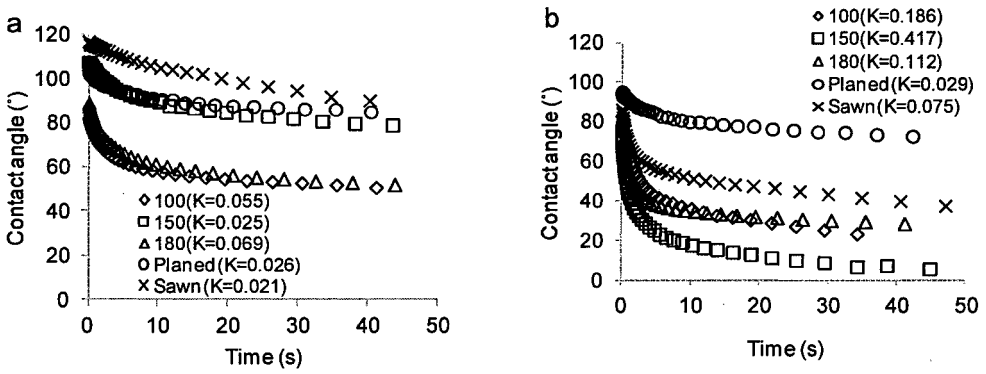

Figure 4. 8 Dynamic contact angle of water on (a) heat-treated and (b) untreated jack pine surfaces using prepared different machining methods

b) Effect of surface preparation on wetting

From the comparison of the results presented in Figures 4.8 to 4.10, it is clear that sanding with different sandpapers (100-grit, 150-grit, and 180-grit) decreases the contact angles of both heat-treated and untreated wood for all three liquids used compared to surface prepared by sawing or planing. The contact angles of planed surfaces are generally the highest and their rate of decrease is the lowest compared to all other surfaces produced by sanding or sawing for almost all the cases studied with the exception of heat-treated wood vs. water. In addition, it can be seen from Table 4.1 that lower initial contact angles and higher K-values for all three liquids especially for water are observed for the wetting on the sanded surfaces compared to the other two preparations. It indicates that the sanding process increases the wettability of heat-treated jack pine as well as untreated wood. This result is in agreement with the previous studies on untreated wood [145]. Sanding produces surfaces free of visible defects and makes surfaces uniformly absorbent for coating [146, 147]. Stehr [148] explained that sanding creates more damage and roughness on the surface

structure, and consequently, increases the surface area. This facilitates the movement of the liquid due to capillary forces. Figure 4.8 (a) shows that there is no significant difference between heat-treated wood surface produced by planing and sanding by 150-grit paper while the contact angles of water on planed surface are much higher than those of sawn surface at all times for untreated wood (shown in Figure 4.8 (b)). It is clear from Figure 4.8 and Table 4.1 that there is no significant difference between the wettability of the heat-treated wood surfaces sanded with 180-grit and 100-grit paper by water. Under these conditions the surfaces are more wettable compared to those sanded with 150-grit paper. However, untreated wood surface sanded with 150-grit paper has the best wettability by water, which agrees well with the observations of Sinn and his co-workers [136]. This might be due to the destruction of cell wall structure more when sanding with 150-grit paper which increases wood wettability.

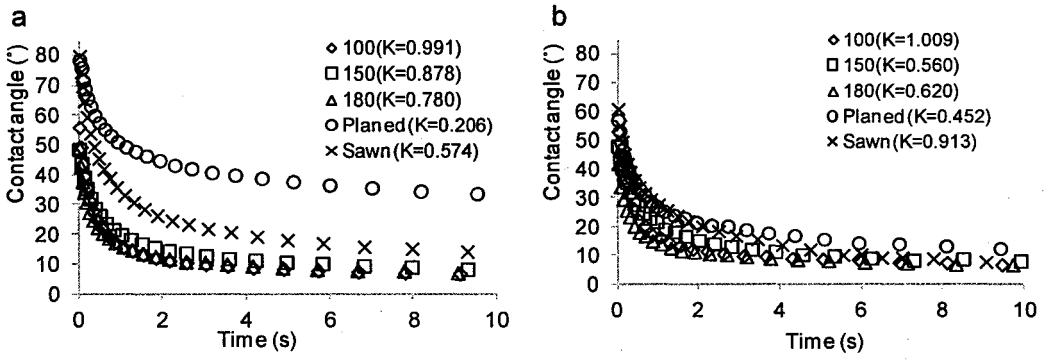

Figure 4. 9 Dynamic contact angle of ethylene glycol on (a) heat-treated and (b) untreated jack pine surfaces prepared using different machining methods

c) Effect of liquid type

Spreading and penetration of liquids are also strongly related to the acidic-basic nature and the viscosity of probe liquid. From the results of the variance analysis shown in Table 4.2, P-values for different probe liquids are all less than 0.0001 for all the three parameters (initial contact angle, equilibrium contact angle, and K-value) indicating that the liquid type has a significant effect on the wettability of wood. Comparing the mean values of contact angles as a function of time for three different probe liquids on heat-treated wood surfaces (Figure 4.8 (a), Figure 4.9 (a) and Figure 4.10 (a)), it is clear that all the samples are wetted most by formamide. This also can be seen from Table 4.1. Formamide which is basic has the highest K-values compared with those of water and ethylene glycol. Stehr et al. [148] demonstrated that formamide is a strong hydrogen-bonding liquid which radically reduces the interfacial free energy at the liquid-solid interface through acid base interactions, therefore, increases the spreading and penetration rate. Mantanis and Young [149] explained that wood surfaces have a very strong acidic character so that the strongest interactions occur with basic liquids while much weaker interactions occur with acidic liquids. Accordingly, stronger interactions with formamide results in an increase in spreading and penetration rate. This probably is the reason for higher wetting rates observed with formamide compared with those of water and ethylene glycol. It is also interesting to note that the K-values of ethylene glycol and water (<1, see Table 4.1) are relatively closer and smaller compared to those of formamide (>1). Ethylene glycol has also the highest viscosity which reduces the rate of wetting.

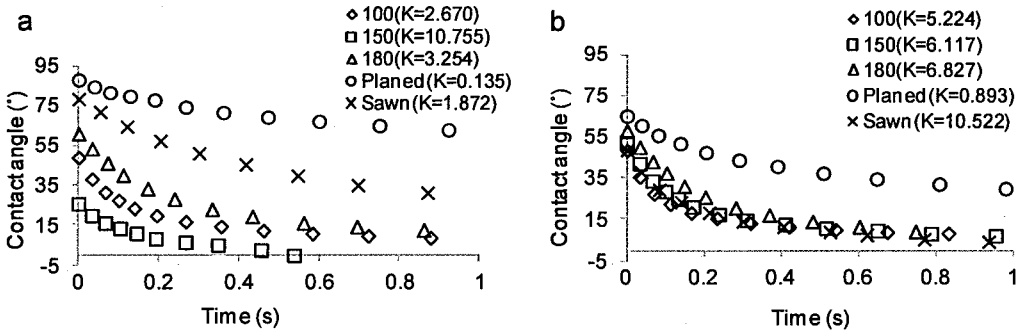

Figure 4. 10 Dynamic contact angle of formamide on (a) heat-treated and (b) untreated jack pine surfaces prepared using different machining methods

4.1.3. Analysis of fluorescence microscope images

Analysis of fluorescence microscope images of aspen heat-treated at different temperatures reveals the effect of heat treatment on the anatomical structure of hardwood.

With this analysis, the cell lumen area, cell lumen length and the cell width can be calculated (Figure 4.11). The cell lumen area and the cell lumen length increase with increasing heat treatment temperature while the cell width displays the opposite trend.

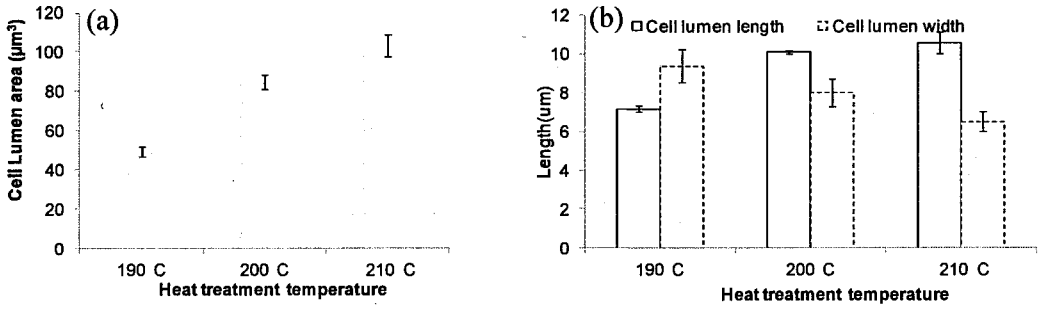

Figure 4. 11 Cell sizes of aspen heat-treated at different temperatures: (a) Cell lumen area, (b) Cell lumen length and cell width

Figure 4.12 shows the cell number distribution as a function of cell lumen area. The numbers of cells with smaller cell lumen area decrease and those of greater cells lumen area increase with increasing heat treatment temperature. This implies that the heat treatment causes the cell wall to become thinner and cell lumen area to become larger.

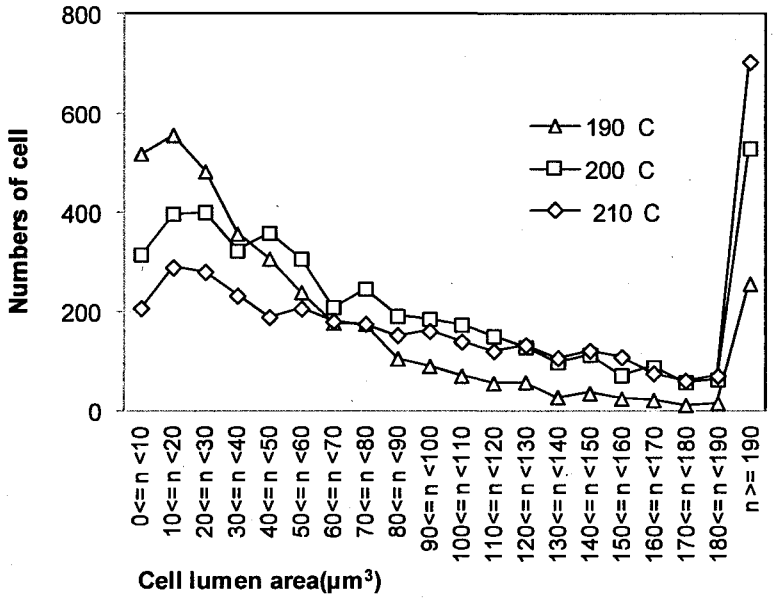

Figure 4. 12 Numbers of cells as a function of different cell lumen area for aspen heat-treated at different temperatures (n is the cell lumen area)

The ratios of cell wall length/lumen length decrease with increasing heat treatment temperature in both radial and tangential directions (Figure 4.13). The rate of decrease in radial direction is clearly larger than that in tangential direction. This might be due to the fact that the heat treatment decomposes wood cell wall more in radial direction; therefore, the cell width becomes thinner at a faster rate.

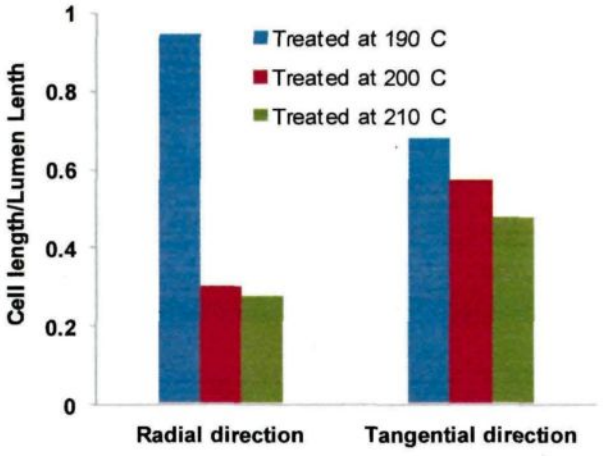

Figure 4. 13 Ratio of cell wall length/lumen length of aspen heat-treated at different temperatures

4.1.4. Analysis of SEM

Figure 4.14 shows the SEM images on transverse surfaces of heat-treated and untreated jack pine. Comparing Figure 4.14 (a, c) and (b, d), it can be seen that the cracks on middle lamella and thinning of cell wall take place after thermal treatment for both latewood and earlywood. Heat-treated jack pine wood looks more brittle than untreated wood. However, structural changes due to heat treatment are not significant and it is very likely that plasticization of cell wall material occurs only to a very limited degree during heat treatment. It is substantiated with the result of Kollmann and Sachs who found comparable features in spruce after thermal treatment between 190°C and 240°C [35].

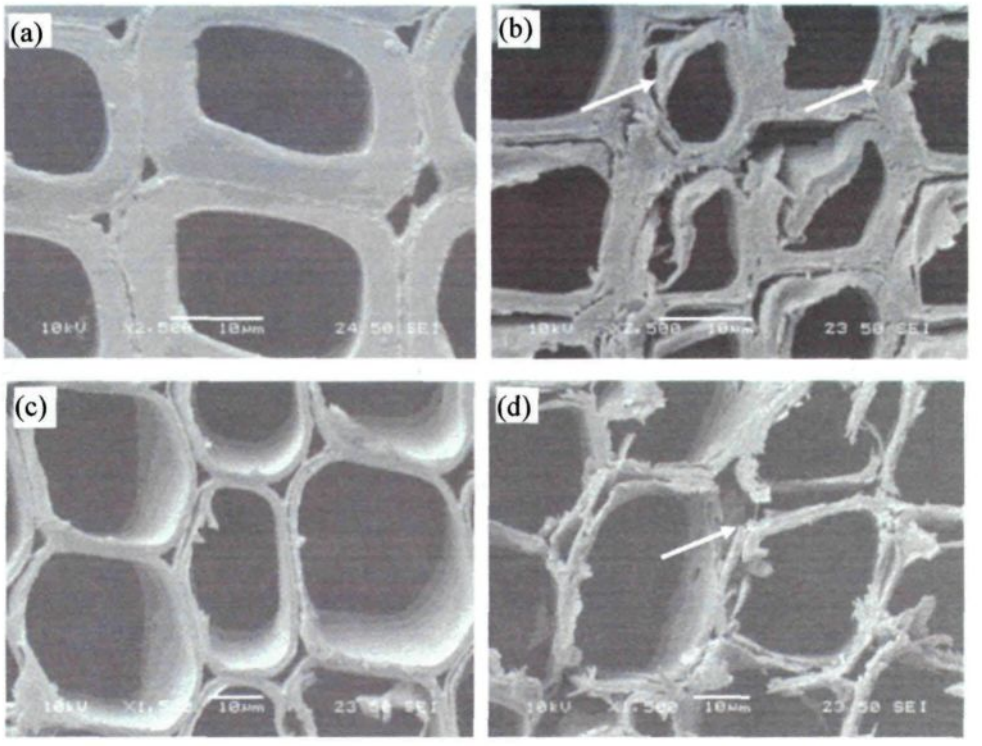

Figure 4. 14 SEM images on transverse surfaces of heat-treated and untreated jack pine: (a): untreated jack pine, latewood; (b): heat-treated jack pine, latewood; (c): untreated jack pine, earlywood; (d): heat-treated jack pine, earlywood

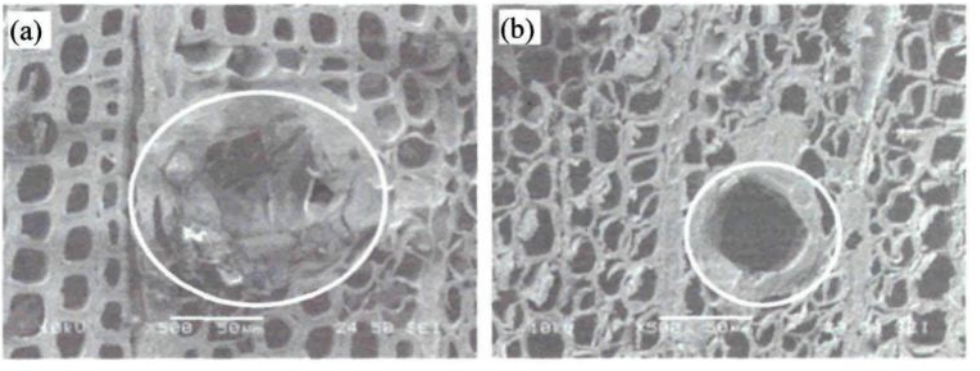

Figure 4. 15 SEM images of resin channel of heat-treated and untreated jack pine: (a): untreated jack pine, latewood; (b): heat-treated jack pine, latewood

Analysis of Figure 4.15 (a) and (b) indicates that the anatomical structure of jack pine was only slightly changed during heat treatment. Fibers and tracheids around the resin channel are still obvious after heat treatment. The main differences were the presence of important quantities of extractives deposited in the resin channels, which disappeared after heat treatment (see Figure 4.15 (b)). These results are in agreement with the previous research [140].

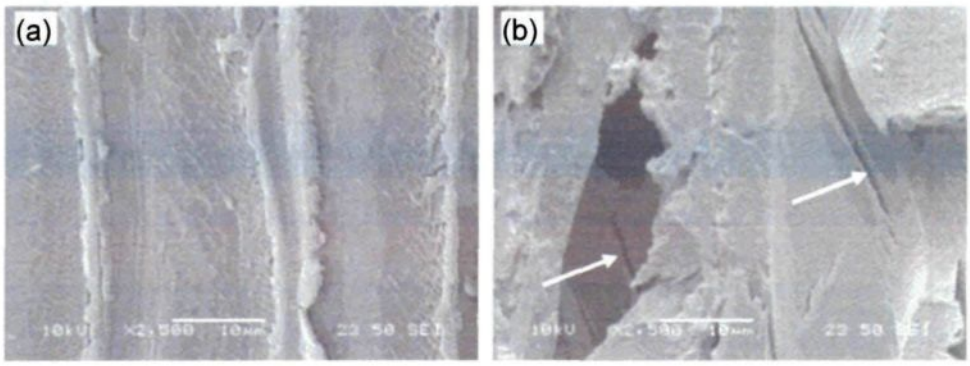

Figure 4. 16 SEM images of cell wall of heat-treated and untreated jack pine radial surface: (a): untreated jack pine, latewood; (b): heat-treated jack pine, latewood

Micro-cracks are visible on cell wall of jack pine wood after heat treatment (Figure 4.16 (b)). This result is in agreement with that observed on transverse surface (Figure 4.14 (a)). These checks appear to be a result of stress caused by differential shrinkage due to heat treatment. The increasing water pressure due to the increasing temperature can also play a role in the formation of checks during heat treatment. SEM microscopic analysis of jack pine wood before and after heat treatment is presented in Figure 4.16. SEM microscopic analysis indicates that the anatomical structure of wood is only affected during heat treatment. Fibers and rays are still obvious after the heat treatment. The main

differences are presence of important quantities of extractives deposited in the resins channels, which disappear after thermal treatment. This results is in agreement with the previous research [36].

Similar to jack pine wood, the presence of cracks on middle lamella, thinning cell wall width, delamination of cells as well as plasticization of aspen wood take place after heat treatment for both latewood and earlywood (Figure 4.17 (b and d)) compared to untreated aspen (Figure 4.17 (a and c)). Compared to jack pine wood, aspen wood displays less structural changes due to heat treatment. Comparing Figure 4.17 (e), (f) and (g), it can be seen that the thinning of cell wall on middle lamella takes place on birch transverse surface after heat treatment at both 195°C and 215°C. Nevertheless, it seems that there is no cracking. Heat-treated birch wood looks more brittle than its untreated counterpart. However, structural changes due to heat treatment are not obvious, and it is likely that plasticization of cell wall material occurs only to a limited degree during heat treatment. This is in agreement with the results of Kollmann and Sachs who found comparable features in spruce after heat treatment between 190°C and 240°C [35]. Compared to the sample heat-treated at 195°C, the sample heat-treated at 215°C displays more significant structural changes due to heat treatment as seen in Figure 4.17 (g), showing more thinning of the cell wall width.

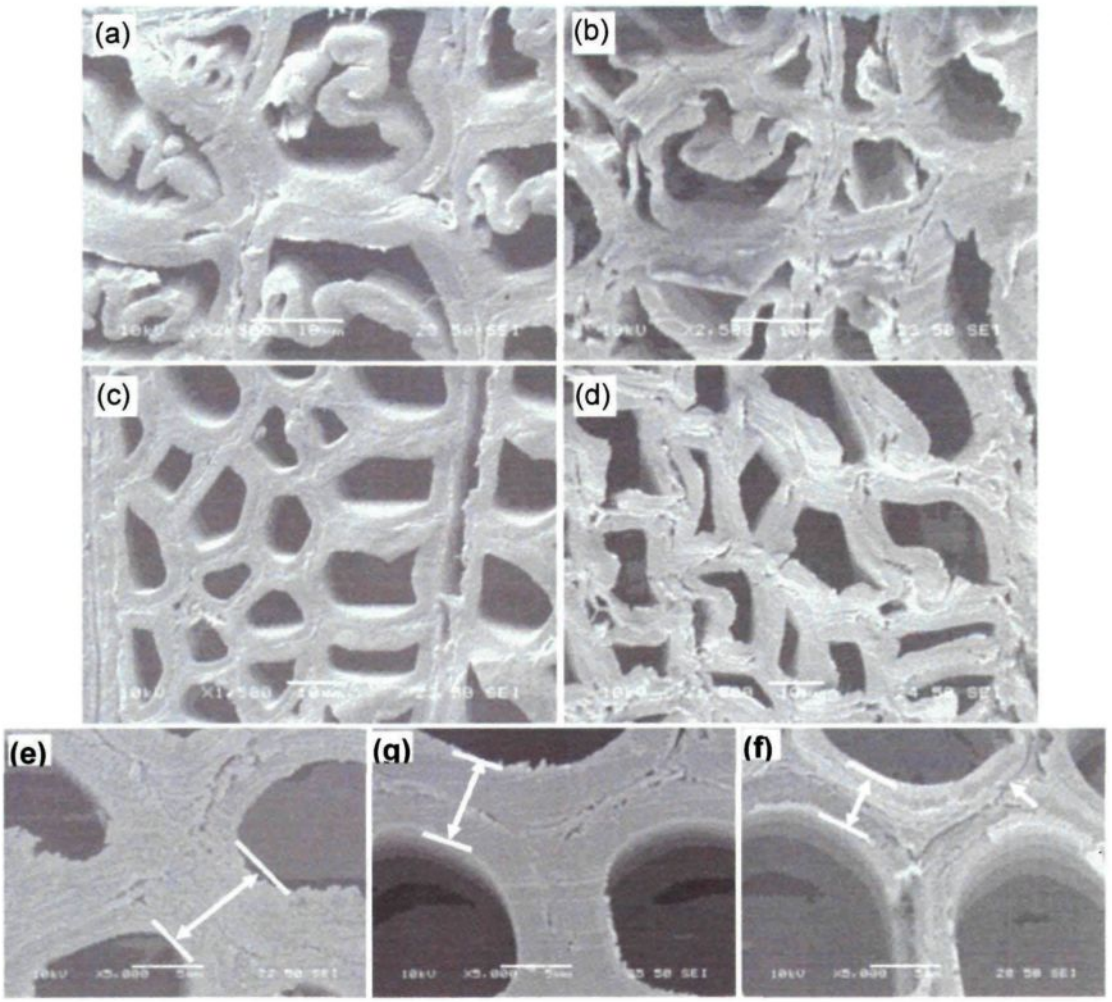

Figure 4. 17 SEM images on transverse surface of heat-treated and untreated aspen and birch: (a) untreated aspen, latewood; (b) heat-treated aspen at 210°C, latewood; (c) untreated aspen, earlywood; (d) heat-treated aspen at 210°C, earlywood; (e) untreated birch before weathering; (f) heat-treated birch at 195°C before weathering; (g) heat-treated birch at 215°C before weathering

4.1.5. Chemical composition analysis

For a good understanding of the influence of heat treatment on wood chemical components, the chemical composition analyses of aspen wood before and after heat treatment under different conditions, such as temperature, heat rate, holding time and humidity, were carried out in this study. Sufficient information on the heat treatment conditions was available for aspen; therefore, aspen was chosen to investigate the changes in chemical composition during heat treatment under different conditions. Table 4.3 presents the data for heat-treated and untreated woods of the current study as well as the literature data. The differences between the reported data and those of this study for untreated aspen sample are most probably due to the differences in wood compositions and the utilization of different analysis methods.

The extractives cover a wide range of chemical compounds though their amount is small compared to other chemical components in wood. The amount is markedly influenced by seasonal growth rate, wood species as well as the method of drying of the wood. Different solvents remove different combinations. Acetone, ethanol, and hot water extractive contents decrease with increasing heat treatment temperature when the other parameters are kept the same. This indicates that the extractives in wood are removed during the heat treatment, and higher temperatures have greater influence. The acetone extractive contents of all heat-treated aspen samples are less than that of untreated wood (3.51%). However, the ethanol extractive contents of some heat-treated wood samples are higher than that of untreated wood in this study (1.36%), but all of them are lower than the

data from the literature (3.8%). This result might be due to the experimental error during the extractive determination for the untreated aspen.

Generally, untreated wood contains around 20% to 30% lignin. The lignin percent of aspen wood increases after heat treatment, and this increase is more pronounced when the heat treatment temperature is increased. It might be due to smaller influence of heat treatment on the lignin content than on other wood components. Decrease especially in hemicellulose percentage causes an increase in lignin percentage. Actual quantity does not change.

Hardwood hemicellulose consists mainly of pentosans, and its content in hardwoods is about 19 to 25% (TAPPI stantard1984). It can be seen from Table 4.3 that the pentosan contents of aspen decrease after heat treatment for all heat treatment conditions. Increasing the heat treatment temperature and holding time as well as the lack of humidity can intensify the degradation of pentosan while the effect of heating rate is comparatively less.

Holocellulose is the term used for the product obtained after the removal of lignin form wood[150]. The holocellulose content of aspen slightly decreases with the heat treatment temperature up to 210°C, but it decreases significantly to 57.97% when the treatment temperature is increased to 220°C.

From these results, it can also be observed that the higher heating rate during heat treatment reduces all the extractive contents. However, the contents of lignin, pentosan, and holocellulose do not vary significantly with the change in the heating rates (15°C/h or 10°C/h) during heat treatment. Comparison of the variations in lignin, pentosan, and holocellulose contents indicates that pantosan is the most sensitive component of aspen

wood to humidity and holding time during the heat treatment process. The results of the chemical component data are in agreement with those of the mechanical properties which were studied in a previous research [28]. Considering the impact on the mechanical properties of heat-treated aspen wood [28], the following heat treatment conditions seem to give the best results: heat treatment temperature of 210°C, heating rate of 15°C/h, one-hour holding time, and the presence of humidity.

Table 4.3 Chemical composition analysis of aspen woods

Temp (°C)	Heating rate (°C/h)	Holding time (h)	Humidity	Extract			Lignin %	Pentosan %	Holocellulose %	Reference
				Acetone %	Ethanol %	Hot Water %				
0	-	-	-	-	3.8	-	18.1	17.2	-	[151]
0	-	-	-	3.51	1.36	4.82	19.04	17.94	72.70	Present study
190	15	1	yes	3.23	1.88	4.37	20.34	14.48	71.54	Present study
200	15	1	yes	2.98	1.75	2.89	22.59	14.04	71.08	Present study
210	15	1	yes	2.04	1.27	2.73	22.71	13.99	70.79	Present study
220	15	1	yes	2.02	1.20	2.46	31.13	6.67	57.97	Present study
210	15	1	no	2.16	1.56	2.29	37.98	3.35	63.83	Present study
210	15	**3**	yes	2.17	1.26	2.85	51.38	8.65	62.34	Present study
210	**10**	1	yes	3.19	1.54	3.17	22.10	14.49	71.13	Present study

4.1.6. Conclusions

1) Color of hardwood changes more significantly than that of softwood due to heat treatment. After heat treatment, the color changes of aspen wood are the highest among the three species and those of jack pine are the lowest. It was not possible to clearly identify a trend of color change due to the presence of humidity during heat treatment.

2) Wettability by water of three wood species decreases due to heat treatment with increasing heat treatment temperature. Changes in water absorption with increasing temperatures are not linear. All initial contact angles of heat-treated jack pine and aspen wood are higher than those of untreated wood. Extractives of birch wood decrease the wood wettability similar to increasing heat treatment temperature.

3) The dynamic wetting of heat-treated wood indicates that the heat-treated wood is wetted less and absorbs less amount of liquid compared to the untreated wood due to the degradation of wood components (hemicelluloses, lignin, and cellulose) during heat treatment. Sanding increases the wettability of heat-treated jack pine surfaces by different liquids. The wetting by water is faster on sanded wood surfaces compared to those prepared by other machining methods for both heat-treated and untreated samples. The heat-treated wood becomes most hydrophobic when wood surfaces are sanded by 180-grit paper compared to those prepared by other machining process. Heat-treated wood surfaces also have a very strong acidic character similar to that of untreated wood. Therefore, a basic liquid has higher spreading and penetration rates (K-value) than an acidic liquid for both heat-treated and untreated wood surfaces.

4) Humidity of heat treatment increases initial contact angles, and the rate of change in contact angle decreases with time for both aspen and birch wood. Wettability of heat treated birch wood is higher than that of aspen mainly due to their different densities.

5) Heat treatment decomposes wood cell wall more in radial direction compared to tangential direction, and then the cell width thins faster in this direction. After heat treatment, cracks on middle lamella form and the thinning of cell wall takes place for both late and early jack pine wood. Heat-treated wood appears more brittle. Plasticization of cell wall material occurs only to a very limited degree during heat treatment. Fibers and rays are still obvious after heat treatment. Extractives deposited in the resin channels disappear after heat treatment. Caused by differential shrinkage due to heat treatment, micro-cracks are visible on cell wall on transverse and tangential surfaces. Compared to jack pine wood, aspen wood displays less structural changes due to heat treatment.

6) Heat treatment decomposes hemicelluloses of wood. It has less influence on lignin content than on hemicelluloses. Acetone extractive contents of heat-treated aspen are lower than those of their untreated counterparts. However, ethanol extractive contents of heat-treated aspen are higher than that of untreated wood, which is in agreement with the previous study [152]. This might be due to the degradation of some extractives and the formation of other extractives during heat treatment.

4.2. Chemical modification of heat-treated wood surfaces during artificial weathering

4.2.1. General

As it was stated in chapter 2, two investigation methods suited for characterizing the changes in chemical composition of a wood surface are X-ray photoelectron spectroscopy (XPS) and Fourier transform infrared spectroscopy (FTIR). The XPS technique covers the subsurface to a depth of about 10 nm, providing information on the chemical states, surface chemical composition as well as the location of atoms types of the samples [81, 125]. It has been previously used to analyze the changes of wood surface after different treatments [153, 154] and to differentiate between softwood and hardwood [138]. Its application to the surface analysis of heat-treated wood without exposure to weathering [126] as well as weathered untreated wood [81] have been reported. To our knowledge, however, XPS investigations on weathered heat-treated wood surfaces are rare, and there is no comparative study on the chemical composition modifications induced by artificial weathering of the untreated and heat-treated species which is of interest in the current work. In this study, the changes in surface chemistry of heat-treated North American jack pine (*Pinus banksiana*), aspen (*Populus tremuloides*), and birch (*Betula papyrifera*) occurring during artificial weathering were investigated using XPS spectroscopy. In addition, the XPS characterization of changes in surface chemical composition was also used in order to study the effect of heat treatment conditions. Furthermore, a quantitative study on the acid-base properties of heat-treated wood during artificial weathering using XPS technique is currently lacking in the literature. The acid-base properties of wood have a significant

influence on the behavior of wood surface in contact with any liquid [138]. Determination of these properties provides a sound foundation for the development of coatings and the improvement of adhesion properties of heat-treated wood surface. According to Fawkes [155], the acid-base properties can be quantitatively characterized by XPS. The Holmes-Farley and Whitesides [156] divided the interfaces into three regions, and they emphasized that XPS technique penetrates the subsurface to a about 10 nm depth and offers an opportunity to analyze the specific groups in the second region near the surface together with those in the outermost layer [156], in other words, to detect both the surface and the subsurface modifications. Therefore, XPS was also used during this study for the characterization of acid-base properties in the subsurface of heat-treated woods exposed to artificial weathering. The FTIR technique was used to identify the functional groups present at the surface of heat-treated wood samples. By following the peaks assigned to wood components, it was possible to identify the differences in surface characteristics based on heat treatment conditions and following the loss of wood components after artificial weathering.

It should be mentioned that although both XPS and FTIR are techniques used to determine surface chemistry, each technique has strengths and weakness. The penetration depth of XPS is less than that of FTIR. The depth of penetration of FTIR into the sample at the contact position depends on wave number, angle of incidence, and refractive index. Thus, XPS is more of a surface sensitive technique than FTIR. In addition, the wood surface may get oxidized as shown by XPS, while the oxygenated functional groups of surface layer are shown to be decreasing by FTIR. FTIR was able to characterize the

crystallinity of cellulose as well as the loss of lignin during weathering from the wood surface, which was consistent with the chemical components analysis results after weathering. Furthermore, there is no published study available on the chemical analysis of main heat-treated wood components after weathering.

4.2.2. Characterization using X-ray photoelectron spectroscopy

4.2.2.1. XPS survey spectra

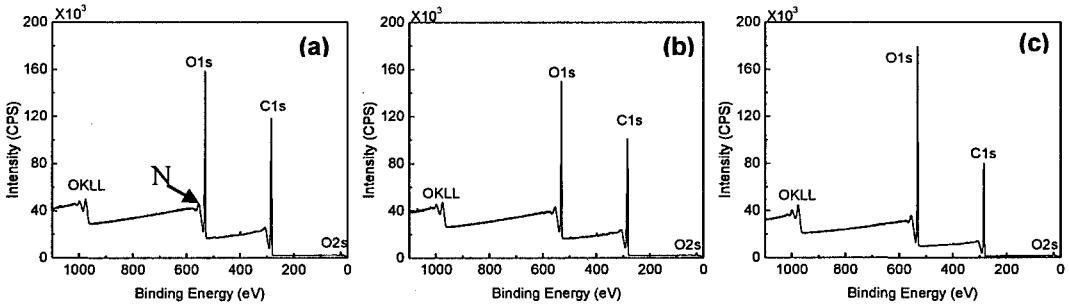

Figure 4. 18 XPS survey spectra of untreated and heat-treated birch wood before and after weathering for 1512 h: (a) untreated before weathering, (b) heat-treated at 215°C before weathering, (c) heat-treated at 215°C and weathered for 1512 h

The typical XPS survey spectra of untreated birch wood sample before artificial weathering and heat-treated birch wood samples before and after artificial weathering for 1512 h are shown in Figure 4.18 (a-c), respectively. The survey spectra for heat-treated and untreated jack pine and aspen exhibit similar findings. Results of birch were chosen for analysis. Both spectra of untreated (see Figure 4.18 (a)) and heat-treated samples (see Figure 4.18 (b)) reveal the presence of carbon, oxygen, and small amounts of nitrogen as expected. It can be seen from the comparison of the survey spectra of heat-treated samples before and after weathering that the carbon C1s peak decreases and the oxygen O1s peak

increases as a result of weathering. In this analysis, the focus was on the resolution of the C1s peak and O1s peak since these were the two elements found to be present in noticeable amount. Other elements gave lower peaks indicating that they have very low concentrations at the surface of the samples investigated in this study.

4.2.2.2. O/C ratios

It has been previously reported that the degradation of cellulosic materials and polymers can be detected by a change in the O/C atomic ratio [140]. The O/C atomic ratio is almost always used in quantitative analysis when XPS is used to characterize wood surfaces [138]. O/C ratio can be calculated by using the total areas of peaks of different components and their respective photoemission cross-sections. The evolutions of oxygen to carbon (O/C) ratio for the three wood species studied during heat treatment and weathering are shown in Figure 4.19 (a) and (b), respectively.

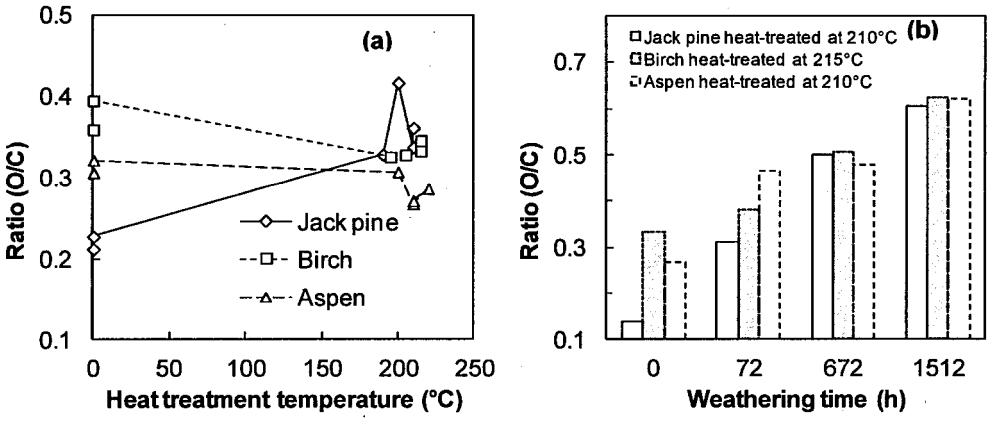

Figure 4. 19 O/C ratio evolution of three wood species during (a) heat treatment and (b) weathering

In principle, the O/C ratio of cellulose, which has the gross formula ($C_6H_{10}O_5$), is calculated as 0.83. Hemicellulose, which is mainly represented by glucuronoxylans, has an

O/C of approximately 0.8. The contribution of lignin is more complex and therefore more difficult to calculate. The theoretical value of O/C for lignin is around 0.33 [81, 140]. Therefore, a high oxygen-to-carbon atomic ratio reflects high cellulose and hemicellulose contents while a low O/C ratio suggests the presence of more lignin on wood surfaces. Figure 4.19 (a) shows that O/C ratios reduce slightly after heat treatment for both birch and aspen samples before weathering. This is in agreement with the result of the study by Nguila and Petrissans [140], which reported that O/C ratio decreased from 0.55 to 0.44 after the high temperature heat treatment of beech wood. Sernek [135] also showed that wood drying at high temperatures between 160°C and 180°C decreased the O/C ratio of wood. This decrease in O/C ratio due to heat treatment suggests that the lignin content increases whereas the hemicelluloses content decreases on the birch and aspen sample surfaces. This finding agrees with previous studies of chemical component analysis on heat-treated woods [157]. Dehydration of polymers (cellulose and hemicelluloses) initially present in wood leads to the formation of volatile by-products and the increase in lignin proportion. This explains the decrease in O/C ratio of birch and aspen wood after heat treatment. However, the O/C ratios of all heat-treated jack pine samples are higher than those of untreated samples in this study. It has been reported that the high carbon content in wood samples is also an indication of the presence of extractives on the wood surface [158]. Untreated jack pine wood is rich in carbon-rich extractives (about 6%) of waxes, fats and terpenes and lignin guaiacyl units [137]. This can be confirmed by the lower oxygen to carbon ratio (high carbon content) of untreated jack pine compared to those of other two species (see the initial O/C ratios in Figure 4.19 (a)).The increase in O/C ratio of jack pine

samples is probably due to the partial removal of the abundant carbon-rich extractives in jack pine during high temperature heat treatment.

Figure 4.19 (a) and (b) indicate that the changes provoked in wood composition by weathering are more important compared to those induced by heat treatment on wood surface. As it was stated previously, the O/C ratio gives a direct measurement of the surface oxygen content, and high O/C ratio indicates high carbohydrate contents while low O/C ratio reflects higher lignin content on wood surface. Figure 4.19 (b) shows that O/C ratio increases with increasing weathering time for three heat-treated species. This means that weathering reduces lignin content, consequently, the carbohydrates content increases on all heat-treated wood surfaces during the weathering within the range studied. O/C ratios of sample surfaces of all three species after weathering for 1512 h are much higher than O/C value of lignin (0.33) and relatively close to the ESCA experimental value of 0.62 of cellulose [81, 140]. This implies that weathering resulted in wood surfaces richer in cellulose and poorer in lignin. Higher oxygen contents of weathered wood surfaces also suggest that there is oxidation reaction occurring during weathering [81]. When considering the changes in the O/C ratio during weathering, heat-treated jack pine is modified most, followed by heat-treated aspen and birch. This indicates an influence of the type of wood species on the surface modification due to weathering. Lignin content of softwood (jack pine) is higher than that of hardwood (birch and aspen) which is supported by the comparison of O/C ratios shown in Figure 4.19 (b). Lignin is the most sensitive component due to the oxidation reaction during weathering. Thus, the results showed that weathering degraded heat-treated jack pine surfaces more than the surfaces of other two species;

however, the three heat-treated species studied exhibit similar O/C ratios after a weathering period of more than 672 h. Although the O/C ratios of cellulose calculated theoretically (0.83) and found experimentally (0.62) are quiet different, they both are significantly larger than that of lignin.

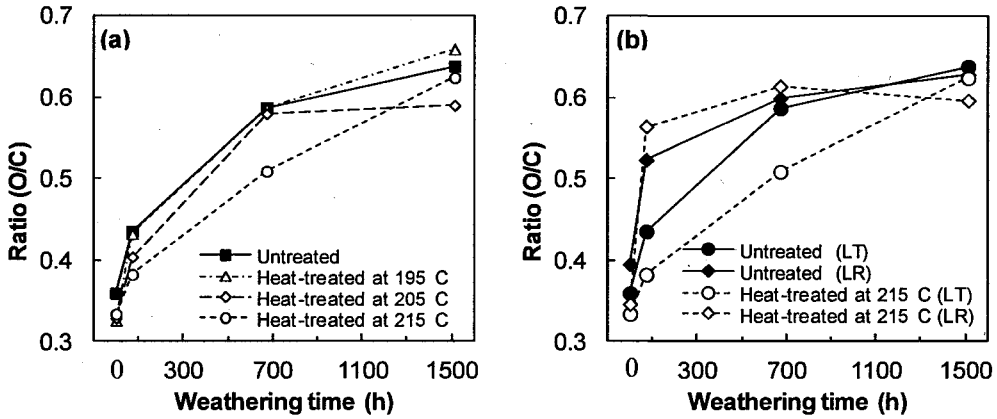

Figure 4. 20 O/C ratio of heat-treated birch during weathering: (a) effect of different heat treatment temperatures, (b) effect of direction (LT represents longitudinal tangential surface, LR represents longitudinal radial surface)

Figure 4.20 shows the effect of treatment temperature and wood direction on O/C ratio for untreated and heat-treated birch wood during artificial weathering. The O/C ratios are higher for untreated birch than for the corresponding heat-treated samples at different temperatures during weathering with the exception of untreated sample after 1512 h of weathering. This sample has slightly lower O/C ratio than that of the sample heat-treated at 195°C (see Figure 4.20 (a)). This suggests that the lignin content of the birch surface increases whereas the hemicelluloses content decreases after heat treatment nearly at all weathering times. Decrease in the O/C ratio with the decreasing the heat treatment

temperature indicates that, as the heat treatment temperature increases, the degradation of hemicelluloses increases; and this tendency is also maintained during weathering.

Chemical properties of wood are known to be a function of direction. A study on tangential surfaces (LT) and radial surfaces (LR) of the three heat-treated woods was conducted to study if the O/C ratio is affected by direction during weathering (see Figure 4.20 (b), Table 4.4, and Table 4.5). The O/C ratios are found to be slightly higher on radial surfaces compared to that on tangential surfaces. This suggests the presence of higher lignin content on tangential surface for both heat-treated and untreated birch samples (see Figure 4.20 (b)). The difference between different directions is less before weathering comparing to those after weathering of 336 h and 672 h for heat-treated birch. The O/C ratios increase more on radial surfaces than on tangential surfaces for both untreated and heat-treated birch during weathering. Likewise, the heat-treated jack pine and aspen show a trend similar to that of birch (see O/C ratio in Table 4.4 and Table 4.5). This is most likely linked to presence of different structures on surfaces at different directions. The radial ray cells present cross surfaces on longitudinal tangential surface which reduces the area exposed to artificial irradiation and oxygen, consequently, reducing the odds of oxidation reaction more significantly in this direction compared to radial surfaces during the weathering process. The O/C radio differences provoked by different wood directions are larger than those caused by the heat-treatment temperature at the same corresponding weathering times.

Table 4. 4 Summary of XPS spectral parameters of heat-treated jack pine

Heat treatment condition	Surface	Weathering time (h)	O/C	Component (%)				Component (%)		
				C_1	C_2	C_3	C_4	O_1	O_2	O_3
Untreated	LT	0	0.21	63.92	27.15	5.43	3.5	0.78	99.22	-
		72	0.39	35.91	43.4	9.71	8.77	0.77	83.53	15.7
		672	0.59	19.79	49.2	15.32	15.68	0.87	79.34	19.79
		1512	0.55	25.06	49.62	17.36	7.96	1.43	82.84	15.72
Untreated	LR	0	0.23	69.25	22.63	5.34	2.79	-	100	-
		72	0.44	38.82	38.2	15.36	5.14	1.47	95.09	3.44
		672	0.58	23.85	47.81	19.2	7.13	2.5	86.26	11.23
		1512	0.52	29.13	46.9	13.08	10.89	1.96	81.77	16.27
Heat-treated at 190°C	LT	0	0.13	81.41	13.91	0.95	3.73	-	55.68	44.32
		72	0.33	47.64	37.69	3.34	11.33	-	88.97	11.03
		672	0.57	25.98	55.6	15.02	3.39	1.47	93.74	4.78
		1512	0.60	25.28	56.77	14.41	3.54	1.54	96.38	2.09
Heat-treated at 200°C	LT	0	0.42	45.36	42.97	6.79	4.88	3.07	96.93	-
		72	0.43	43.29	41.18	9.05	6.48	1.73	95.75	2.52
		672	0.56	27.87	53	16.11	3.02	1.74	95.74	2.53
		1512	0.60	22.09	58.78	15.99	3.14	1.53	96.13	2.34
Heat-treated at 210°C	LT	0	0.14	76.69	19.31	0.79	3.21	-	97.1	2.52
		72	0.31	56.97	32.96	4.71	5.36	0.38	96.51	3.49
		672	0.50	22.74	58.11	15.79	3.35	1.02	96.17	2.81
		1512	0.61	26.96	52.83	14.4	5.81	0.97	94.19	4.84
Heat-treated at 210°C	LR	0	0.36	52.33	37.02	6.84	3.8	2.62	97.38	-
		72	0.52	33.86	49.06	10.48	6.59	1.04	96.54	2.42
		672	0.62	22.93	58.25	15.49	3.33	1.68	96.2	2.12
		1512	0.62	20.8	59.01	16.53	3.66	1.31	95.21	3.48

Table 4. 5 Summary of XPS spectral parameters of heat-treated aspen

Heat-treatment condition	Surface	Weathering time (h)	O/C	Component (%)				Component (%)		
				C_1	C_2	C_3	C_4	O_1	O_2	O_3
Untreated	LT	0	0.31	48.33	40.54	3.91	7.22	0.83	99.17	-
		72	0.36	44.27	37.34	8.33	7.36	-	80.84	19.16
		672	0.55	22.49	48.75	19.67	6.84	0.9	74.04	25.05
		1512	0.62	16.71	49.66	23.31	9.58	1.15	69.67	29.19
Untreated	LR	0	0.32	53.19	36.6	5.15	5.06	1.01	98.99	-
		72	0.37	43.63	37.49	10.4	8.48	1.93	85.48	12.59
		672	0.57	24.73	53.19	13.91	8.16	1.73	88.18	10.08
		1512	0.60	14.86	37.25	42.78	5.11	0.98	77.91	21.11
Heat-treated at 200°C	LT	0	0.38	49.75	37.42	8.37	4.46	6.34	91.86	1.8
		72	0.50	34.71	47.58	11.98	5.74	2.27	91.68	6.06
		672	0.60	19.46	52.18	15.67	12.69	3.3	72.31	24.39
		1512	0.59	17.74	51.23	23.6	6.58	2.03	87.16	10.81
Heat-treated at 210°C	LT	0	0.27	61.44	28.91	3.68	5.98	-	88.4	11.6
		72	0.47	43.75	37.32	9.09	9.84	0.98	70.03	28.99
		672	0.48	37.32	43.83	8.7	10.15	2.11	91.58	6.31
		1512	0.62	19.54	51.39	19.05	10.03	1.32	90.93	7.75
Heat-treated at 220°C	LT	0	0.39	39.83	39.01	14.12	7.05	3.39	85.07	11.54
		72	0.54	27.9	50.13	8.33	13.64	2.04	86.88	11.09
		672	0.58	20.74	52.48	14.95	11.83	2.11	70.64	27.25
		1512	0.63	13.34	45.97	25.31	13.02	1.43	71.55	24.99
Heat-treated at 210°C	LR	0	0.37	48.66	40.12	6.43	4.79	1.6	95.75	2.66
		72	0.46	45.11	33.94	12.43	8.52	0.96	99.04	-
		672	0.55	29.4	39.86	14.67	16.05	1.68	82.16	16.17
		1512	0.75	19.18	50	25.8	4.09	2.37	93.05	4.58

4.2.2.3. C1s peaks

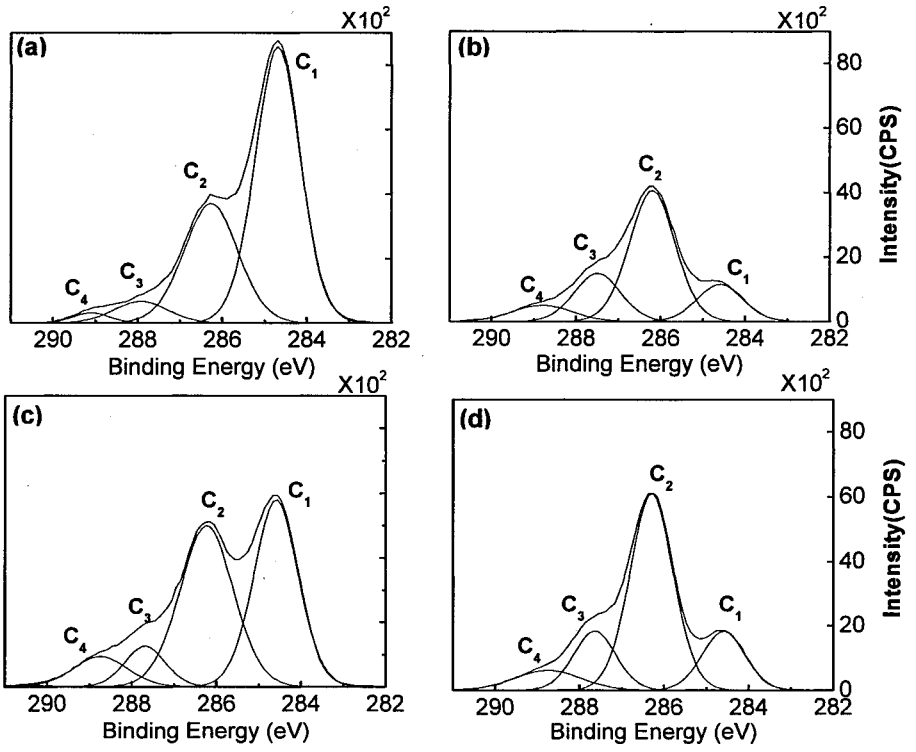

Figure 4. 21 C1s spectra of untreated and heat-treated birch wood before and after weathering for 1512 h: (a) untreated before weathering, (b) untreated after weathering for 1512 h, (c) heat-treated before weathering, (d) heat-treated after weathering for 1512 h.

To evaluate the chemical structures of the surface of heat-treated wood, high-resolution XPS spectra of C1s and O1s levels were processed. Other elements have very low concentrations at the surface of heat-treated and untreated wood samples of this study which is in agreement with the results of Shen et al. [138]. All of the Cls spectra were found to consist of components related to carbon-containing functional groups. The high-resolution of C1s was fitted with their decomposition into four components according to the

literature [125, 127, 138, 140, 158]. The fitted peaks are shown in Figure 4.21 after curve fitting. The four peaks in deconvoluted high resolution XPS spectrum of the C1s peaks are expressed as C_1-C_4 and these carbon bands correspond to C-C and/or C-H(C_1), C-O(C_2), C=O or/and O-C-O(C_3) and O=C-O(C_4), respectively, as shown in Table 3.3. The chemical shifts and binding energies of C1s peaks found in this study are in good agreement with the literature values for woody materials [138]. The high-resolution of the XPS spectra of C1s of untreated and heat-treated birch samples before and after artificial weathering for 1512 h were detected and shown in Figure 4.21. Careful analysis of the line shapes and intensities of each component at weathered surfaces show that the heat-treated birch surface exhibits similar XPS patterns to that of untreated sample surface after weathering for 1512 h (see Figure 4.21 (b) and (d)). However, the XPS patterns changed considerably due to weathering for both untreated and heat-treated birch surfaces. The contribution of C_1 and C_2 peaks are more important than C_3 and C_4 peaks for samples before weathering indicating that they have higher concentrations at both heat-treated and untreated sample surfaces before weathering. These two peaks are modified by the weathering process. The detailed analysis of the C1s region for heat-treated and untreated samples showed that the most important contributions for surfaces before weathering come from the C_1 class (see Figure 4.21 (a) and (c)), while the most important contributions for weathered surfaces come from the C_2 class (see Figure 4.21 (b) and (d)). C_1 peak corresponds to carbon linked to carbon (C–C) groups present in lignin, hemicelluloses and extractives such as the fatty acids and hydrogen (C-H) groups of lignin and extractives, and C_2 peak component corresponds to OCH groups of lignin and C–O–C linkages of extractives and polysaccharides of wood

[140]. As can be seen from the comparison of the C1s spectra of untreated and heat-treated samples before and after weathering (see Figure 4.21), C_1 and C_2 peaks changed most significantly for birch due to weathering. It appears that the C_1 class is most abundant in wood before weathering while the weathered surfaces are rich in C_2 class for both heat-treated and untreated birch samples. It is important to investigate the changes of C_1 and C_2 contributions during weathering for samples heat-treated at different temperatures to study the effect of treatment temperature on chemical elemental composition of heat-treated wood surface.

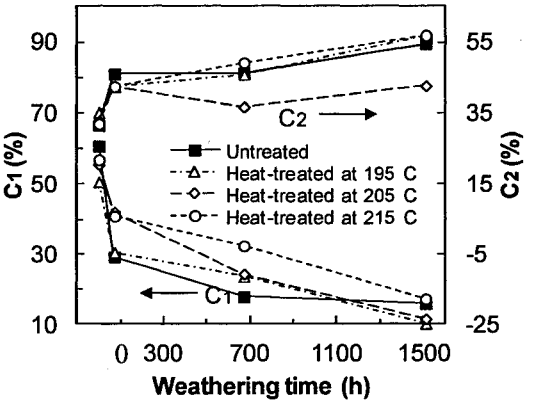

Figure 4. 22 Effect of heat treatment temperature on the C_1 and C_2 fractional areas of heat-treated and untreated birch during weathering

Figure 4.22 shows the variation in peak area contributions of C_1 and C_2 components as a function of weathering time for untreated and heat-treated birch samples at three different temperatures. Since cellulose have a much higher contribution from C_2 than lignin, the contribution of the C_1 for cellulose can be neglected [127]. Therefore, C_1 is associated with the presence of lignin and extractives on wood surface and C_2 is considered

to originate mainly from cellulose and hemicelluloses. The C_1 contributions decrease whereas the C_2 contributions increase with increasing weathering time during weathering for all birch samples. Almost the same trend as C_2 can be observed for C_3 contribution indicating the percent contribution of the O-C-O linkages in cellulose and hemicelluloses and to a less extent that of carbonyl groups (C=O) increase during weathering. This proves again that the weathered surfaces are poor in lignin and comparatively rich in cellulose and hemicelluloses. The C_4 peak representing a carbon atom linked to a carbonyl and noncarbonayl oxygen is insignificant in all birch samples (only about 5%). This might be explained by the presence of possibly low content of carboxylic groups on the sample surfaces before and after weathering. The results show that the effect of heat treatment on the C1s spectra of birch wood surface is less significant than that of weathering. C_1 contribution decreases slightly after heat treatment (see Figure 4.22), and C_2 contribution seems to increase slightly. However, the difference in C_1 contribution between heat-treated and untreated samples increase up to the weathering time of 672 h and then decreases slightly at 1512 h. C_1 contributions of heat-treated birch surfaces change less compared to that of untreated sample implying that the weathering has less influence on the lignin component of heat-treated wood surface. The trends in the variation of C_2 contributions on heat-treated sample surfaces are similar to those of untreated ones except for samples heat-treated at 205°C exhibit the lowest changes. This suggests that the cellulose and hemicelluloses contents of birch sample heat-treated at 205°C are degraded by weathering less than those untreated and other heat-treated birch samples in this study. The high-resolutions of the C1s spectra of heat-treated jack pine and aspen samples show similar

changes. The summary of XPS spectral parameters of heat-treated jack pine and aspen samples were calculated and are shown in Table 4.4 and Table 4.5, respectively.

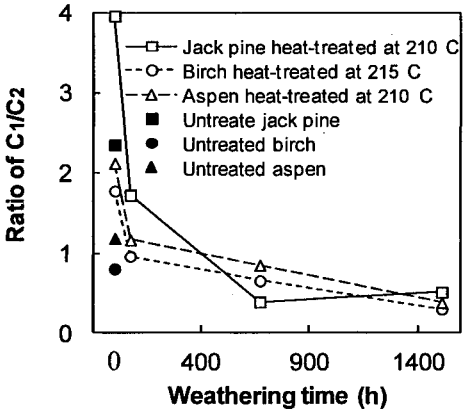

Figure 4. 23 Aromatic carbons/aliphatic carbons ratio (C_1/C_2) of heat-treated woods as a function of weathering time

According to the study of Nishimiya [159], the C_1 and C_2 peaks correspond to those of aromatic carbon and aliphatic carbon in wood, respectively. The relations between the weathering time and the aromatic carbons/aliphatic carbons ratio (C_1/C_2 or C_{aro}/C_{ali}) of three heat-treated woods are presented in Figure 4.23. These ratios are thought to be a reflection of the amount of aromatic carbons of lignin in the heat-treated wood samples. The C_{aro}/C_{ali} ratios of all three species rise after heat treatment at 210 and 215 °C. This is due to the decrease in aliphatic carbons originating from the degradation of hemicelluloses and cellulose caused by high temperature treatment and the possible formation of condensed aromatic rings which might noticeably influence the weathering resistance of the wood surface. The C_{aro}/C_{ali} ratios of all three heat-treated species are more than 1.5 before weathering and reduce sharply after weathering for 72 h, and then continue to decrease to

around 0.5 at a lower rate up to 1512 h except for heat-treated jack pine. The ratio of heat-treated jack pine samples rises slightly between 672 h and 1512 h. The decline in the C_{aro}/C_{ali} ratios during weathering is due to the degradation of aromatic rings in lignin which may noticeably influence the color and the strength of the heat-treated wood surface. Differences of aromatic carbons/aliphatic carbons ratio between different heat-treated species decline with increasing weathering time. Though differences between species still exist even after the surface develops a cellulose-rich layer with regard to chemical properties, different types of wood have similar chemical structures even after the artificial weathering for relatively long times such as 1512 h. Therefore, the differences in color and other physical properties between heat-treated species are probably no longer significant at this stage which was confirmed by color measurements, contact angle tests, and SEM analyses of the heat-treated wood in previous studies [157, 160]. The change of C_{aro}/C_{ali} ratio of heat-treated jack pine due to weathering is more significant than those of birch and aspen, which is possibly due to the difference in the guaiacyl content between softwood (jack pine) and hardwood (birch and aspen) and due to the presence of different extractives. The lignin of softwood consist of guiacyl nuclei whereas the lignin of birch and aspen is made up of a mixture of guaiacy and syringyl nuclei [161]. According to the study of Colom and his co-workers [61], the guaiacyl nuclei are more sensitive to the artificial weathering degradation process than the syringyl nuclei. In view of the literature and the study stated above, it can be said that the aromatic rings of lignin in heat-treated jack pine degrades more rapidly than those of birch and aspen. Parallel to these results, the C_{aro}/C_{ali}

ratios are found to be a function of species type to different extents depending on the weathering time for the heat-treated specimens tested in this study.

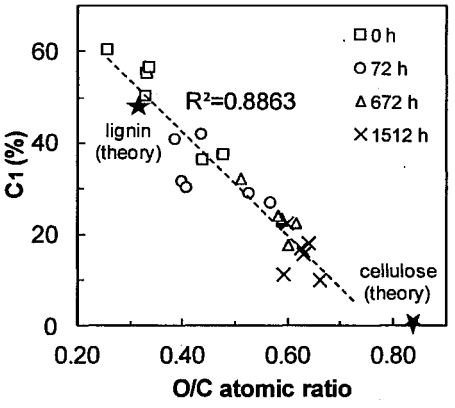

Figure 4. 24 Correlation of the O/C atomic concentration ratio with the percentage of C_1 carbon for heat-treated birch wood

The percentage of C_1 carbon for heat-treated birch wood is inversely proportional to the O/C atomic concentration ratio, as shown in Figure 4.24. Also shown are theoretical points given by Johansson et al. for wood lignin and pure cellulose, according to the chemical composition of these substances [129]. A linear correlation between the two measures can be observed, with a high correlation coefficient of 0.8863. When the percentage of C_1 versus O/C atomic concentration ratio is plotted for heat-treated jack pine and aspen, the following correlation coefficients of linear regression analysis are obtained: 0.9657 for heat-treated jack pine and 0.8787for heat-treated aspen. This indicates that the types of lignin present, although they might be chemically modified during weathering, are sufficiently similar to allow a consistent lignin determination on heat-treated samples used in this study. In addition, as the weathering exposure time increases, the points of

percentage of C_1 carbon vs. O/C ratio shift towards the theoretical value of cellulose for all three heat-treated species studied. This indicates that the lignin content of heat-treated samples declines during artificial weathering; consequently, specimens tend to exhibit abundant cellulose content after the weathering of 1512 h. The linear fit to the data of Figure 4.24 is nearly parallel to the line drawn through the theoretical values for lignin and cellulose. This indicates that the contamination levels on sample surfaces are constant for the data set and the relatively small variance of the plotted points can be attributed to random error.

4.2.2.4. O1s peaks

The electronegativity and polarizability of substituents interacting directly or indirectly with the oxygen atom result in complex shift behavior of O1s peak. In addition, the difficulty to distinguish between simple and double bonds between the oxygen and carbon atoms also leads to relatively sparse study on O1s peak of wood materials compared with the C1s peak reported in the literature [127]. It was suggested to compare the decomposition of this peak to known models [162]. For example, a binding energy of 531.6±0.4 eV was attributed to oxygen atoms between two phenolic groups or an oxygen bound to a carbon through double bond for O_1 [162]. It was proposed that this component was associated to lignin and that increase in the O_1 indicates a decrease in carbohydrates on the fiber surface and an increase in lignin and extractives[163]. It was also observed that eliminating lignin from the fiber surface by high temperature treatment decreased fractional area of O_1 and increased that of O_2 [127]. However, normally lignin relative content increases during heat treatment due to the degradation of hemicelluloses. Thus, this change

of O_1 area might be due to the evacuation of extractives during heat treatment. All oxygen atoms of cellulose are attributed to O_2 component with a binding energy of 533.2 eV by Whatman [127]. The phenolic oxygen is attributed to O_3 of a binding energy of 534.3±0.4 eV which is mainly associated with lignin in woody materials [162]. Consequently, the presence of O_3 component in XPS spectra indicates the presence of lignin on wood surface.

In this analysis, the high-resolution of O1s was fitted with their decomposition into two or three components depending on the samples. Figure 4.25 shows examples of the O1s spectra of heat-treated birch samples during weathering. These spectra show three components: O_1, O_2, and O_3. The binding energies of these three components are in an excellent agreement with those reported in the literature with the O1s spectra of woody material (shown in Table 3.3) [127, 140]. The analysis of the effect of heat treatment temperature on the O1s spectra of birch samples shows that the fractional areas of the O_1 and O_3 components increase whereas that of O_2 decreases (see Figure 4.25 (a) and (b)). This is in agreement with a previous study [127]. However, the weathering shows an opposite effect on the O1s spectra of heat-treated birch wood, decreasing fractional areas of the O_1 and O_3 components and increasing that of O_2 (see Figure 4.25 (c)). Because O_1 and O_3 are associated to lignin and O_2 to hemicelluloses (Table 3.3), it can be said that the heat treatment increases and the weathering process decreases the lignin relative content of the birch surface.

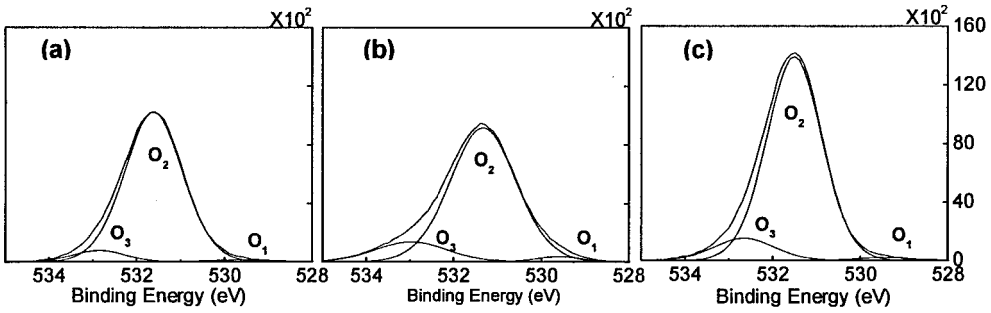

Figure 4. 25 O1s spectra of untreated and heat-treated birch wood before and after weathering for 1512 h: (a) untreated before weathering, (b) heat-treated before weathering, (c) heat-treated after weathering for 1512 h

The analysis of jack pine and aspen spectra during weathering and heat treatment shows that it is difficult to detect the O_1 or O_3 peaks for some samples (see Table 4.4 and Table 4.5). This can be attributed to the low resolution of oxygen peak decomposition. Similar to birch samples, heat treatment increases the O_1 and O_3 components and decrease O_2 component of both jack pine and aspen to various extents depending on the treatment temperature. However, the clear trends were not found for the components of O1s spectra due to weathering for untreated jack pine and aspen. Therefore, the analysis based on O1s spectra for these samples during weathering cannot be used for a typical routine analysis.

4.2.2.5. Acid-base properties

It was reported that XPS technique can be used to characterize the acid-base properties of wood surface from the occurrence of components of C1s [138]. Fowkes reported that the lower electron binding energies of XPS spectra can be considered as basic and electron-donating atoms [155]. Thus, the C_1 group is suggested to be basic according to its lowest binding energy of the four classes. C_2 is defined as acidic by the relation to OH

groups and C–O groups [126, 155]. C_3 is classed as basic in accordance with the C=O groups which is suggested to be electron donors and tend to form complex with acids [138, 155]. C_4 is judged as acidic based on the link to acetyl groups and carboxyl groups (O=C-O) [155]. In view of the literature and on the basis of Fowkes acid–base theory, the acidity can be calculated from the atomic concentrations of C_2+C_4 and the basicity from the atomic concentrations of C_1+C_3, respectively. The ratio of acidity to basicity (A/B) can then be expressed as (C_2+C_4)/(C_1+C_3) [138].

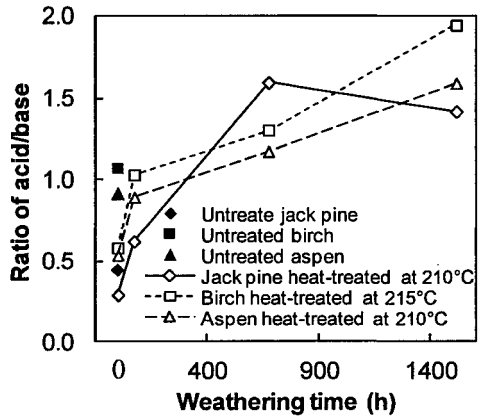

Figure 4. 26 Comparison of the ratio of acidity to basicity (A/B) of three heat-treated woods during weathering

The evolutions of acidity to basicity (A/B) ratios of the three heat-treated woods during weathering are compared in Figure 4.26. Also the values for the three untreated woods before weathering are shown in this figure. The results showed that the heat-treated woods have lower A/B values than the corresponding untreated woods for all three species. This indicates that the heat treatment causes a decrease in wood acidity for all species considered during this study. Acidity of wood is mainly due to hydrogen atoms present in

different wood components. The carboxylic acidic functions of hemicelluloses affect the acidity of wood more than the hydroxyl groups of polysaccharides which represent lower acidity [137]. Therefore, the decrease in wood acidity might be attributed to the degradation of hemicelluloses during heat treatment leading to the decrease of carboxylic acid functions mainly present in hemicelluloses. This agrees with the findings of Philipp et al.[137]. Besides, the extractives present in wood are acidic. The degradation of extractives due to heat treatment plays a role in the decrease of the acidity of wood surface after heat treatment. In addition, the jack pine has a lower A/B ratio than those of aspen and birch both for untreated and heat-treated samples. This means that total basicity of jack pine wood is stronger and its total acidity is weaker than those of aspen and birch even after heat treatment. This is probably related to the difference in lignin structure of softwood and hardwood. The basic unit of softwood lignin is guaiacyl units whilst hardwood lignin consists of a mixture of guaiacyl and syringyl units. Since jack pine belongs to softwood and the other two species are hardwood, they exhibit different acid-base properties. This is in agreement with the results of Shen et al. [138]. They reported that pine wood has lower acid/base ratio than three hardwood species (oak, beech, and yellow poplar) they investigated.

The A/B ratios increase considerably at a weathering time of 72 h but they still remain less than 1 for heat-treated jack pine and aspen and exceed 1 slightly in the case of birch. This means that all samples are basic at this weathering time. The ratios continue to rise to more than 1.5 up to 1512 h of weathering for heat-treated aspen and birch while that of jack pine rises more significantly to a maximum value of 1.6 at 672 h and then reduces

to 1.3 at 1512 h. This indicates that the heat-treated samples become more acidic as a result of weathering and the acidity increases as the weathering time increases. Three explanations might be considered to account for the increase in acidity during weathering: the first possible reason might be related to the degradation of lignin by weathering and cellulose-rich layer left on wood surface. According to Philippe et al. and De Meijer et al. [137, 164], surface free-energy electron-accepting component of cellulose (1.67) is higher than that of wood (1.1). If this is the case, the higher acidity to basicity ratios indicates higher cellulose content on wood surface after weathering. The second possible reason might be related to the cleavage of the covalent linkages between lignin and polysaccharide when lignin was depredated by weathering. There are three most frequently suggested types of the linkages: ether linkages, ester linkages, and glycosidic linkages [165]. The cleavage of these three linkages due to weathering might lead to the formation of O=C-O groups, CH_3–OH groups, and OH groups, respectively. All these acidic functional groups increase the acidity of weathered heat-treated wood surfaces. The third possible reason might be that the oxidation reaction of the polysaccharides component left on weathered wood surface after the by-products, caused by degradation of lignin, have been leached away from surface by water or moisture. The hydroxyl groups of the sugar units and the reducing end-groups of polysaccharides might be subjected to oxidative attack and convert to aldehyde, keton, and carboxyl groups [165] which are groups with acidic property. The more rapid increase in the A/B ratio of heat-treated jack pine compared to other two species (birch and aspen) up to the weathering time of 672 h might be due the higher sensitivity of guaiacyl units in softwood lignin against weathering, which was stated previously.

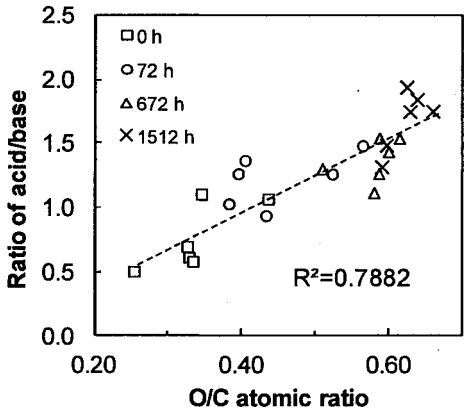

Figure 4. 27 Correlation of acidity to basicity ratio (A/B) with oxygen to carbon atomic ratio (O/C) for heat-treated birch wood during weathering

To evaluate the influence of oxygen content on the surface acid-basic properties, the ratios A/B are plotted as a function of the atomic concentration ratio (O/C) for heat-treated wood samples after weathering for different periods. Figure.4.27 shows the example of a correlation plot for heat-treated birch. A linear correlation between the atomic concentration ratio O/C and the acid/ basic ratio can be observed from this figure with a correlation coefficient of 0.7882. When a similar graph is plotted for heat-treated jack pine and aspen, the correlation coefficients of 0.9169 and 0.7857 are obtained, respectively, from the liner regression analyses. O/C ratio gives a direct measurement of the surface oxygen content, and a high oxygen content normally points to oxidation of the surface. Therefore, the results indicate that the acid/base ratio is increased proportionally as a result of oxidation caused by weathering for heat-treated species investigated in this study. This result is in conflict with the findings of Shen and his colleagues [138]. They reported that the acid/base ratio of pine wood is reduced by about 12.5% as a result of oxidation. They

came to this conclusion by using the difference between two A/B values determined by the sessile drop method and XPS. However, there are other factors which might influence the results in addition to oxidation of surface such as measuring procedure and random error. Therefore, studying a representative number of points is important. The results of the present study are based on more than 72 measurements; hence, the results are representative of the wood surfaces studied.

4.2.3. Characterization using FTIR spectroscopy

The most representative bands studied within the spectral range of 4000-550 cm^{-1} are summarized in Table 4.6. Figure 4.28 shows the FTIR spectra in the spectral region of 1800-800 cm^{-1} on heat-treated and untreated jack pine, aspen, and birch before weathering. Differences due to species and heat treatment can be clearly seen in the infrared spectra in the band shapes.

It is found that there are significant differences at 1260 cm^{-1} and 1230 cm^{-1} between hardwood (aspen and birch) and softwood (jack pine). A doublet can be detected at 1260–1230 cm^{-1} in heat-treated and untreated jack pine, while only one band at 1230 cm^{-1} can be found in the aspen and birch spectra. This is attributable to the difference in the guaiacyl content in lignin of jack pine (softwood), aspen and birch (hardwood). The lignin of softwood (jack pine) consists of guaiacyl nuclei, while those of hardwoods (aspen and birch) are components of guaiacyl and syringyl nuclei [61]. The band at 1260 cm^{-1} which represents guaiacyl ring with CO-stretching in lignin and hemicelluloses is higher in jack pine than in aspen and birch. It can be observed that the intensity of the band at 1740 cm^{-1} is slightly higher in aspen and birch than in jack pine for both heat-treated and untreated

woods. Colom et al. [61] interpreted that this is probably caused by more acetyl groups of hardwood than softwood. The intensity at 1600 and 1510 cm^{-1} of aspen and birch are similar, while in the jack pine spectra the band at 1510 cm^{-1} is stronger than at 1600 cm^{-1}, which is attributable to a stronger guaiacyl element than syringyl at 1510 cm^{-1}. This result is similar to that reported by Colom et al. [61].

Table 4. 6 Characteristic bands of IR absorption spectra in wood

Wavenumber (cm^{-1})	Functional Group	Assignment
3500-3420	-OH	Present in water and three wood polymer components [28, 45, 70]
2900	C-H, $-CH_2-$	Stretching in methyl and methylene group, Hydrocarbon chains[45, 70]
1740-1730	-COOH (C=O)	free carbonyl groups[57], Stretching of acetyl or carboxylic acid (hemicelluloses), [61, 70]
1640-1660	C=O	quinines and quinine methides[166], adsorbed water[25]
1600	C=C	Aromatic ring (lignin) [166]
1510	C=C	Aromatic ring (lignin), stronger guaiacyl element than syringyl[61, 166]
1465	C-H	Asymmetric bending in CH_3 (lignin) [61]
1426	CH_2	Aromatic skeletal vibrations (lignin) and C-H deformation in plane (cellulose) [25]
1373	C-H,	C-H bending. -CH, -CH, (carbohydrates. LCC(lignin carbohydrate complexes) bonds [25]
1335-1330	O–H	phenol group (cellulose) [25]
1316	CH2	High crystalline cellulose I (cellulose) [61]
1267-1270	CO	Guaiacyl ring with CO-stretching (lignin and hemicelluloses) [166], esters[25]
1230		Syringyl nuclei [61]
1158	C-O-C	Carbohydrate[25, 44],
1103	C-H	Guaiacyl and syringyl (lignin) [118]
1030-1050	C-O, C-H	Primary alcohol, guaiacyl(lignin)[25, 118]
896		C_1-carbon in pyranoid ring (in cellulose and hemicelluloses)[25]
813-806	C-H	Mainly vibration of mannan and C-H out of plane bending vibration in lignin (lignin) [1]

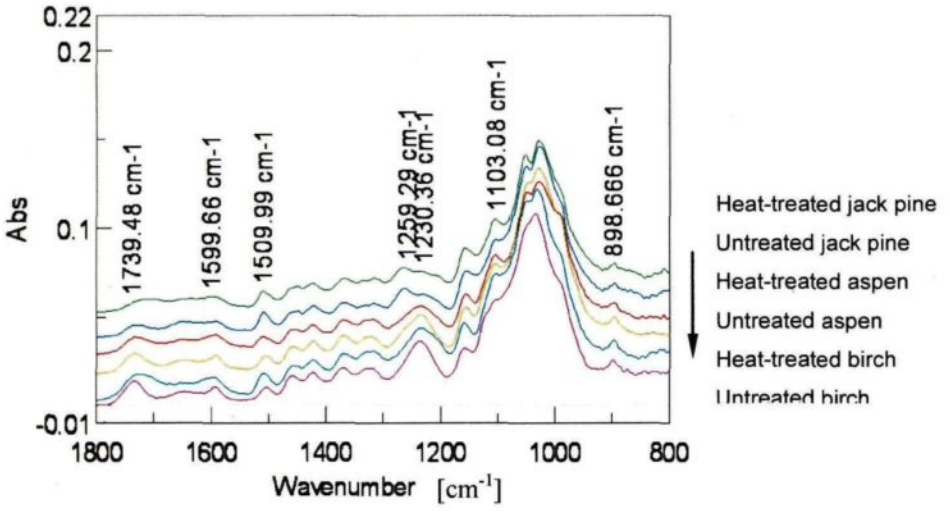

Figure 4. 28 FTIR spectra of heat-treated and untreated samples before artificial weathering

The differences in spectra of heat-treated and untreated woods have to be taken into consideration. Upon analysis of the spectra, it can be seen that the band at 1510 cm^{-1} which is assigned to lignin increases slightly after heat treatment for all species. This peak indicates splitting of the aliphatic side chains in lignin and cross-linking formation by condensation reactions of lignin, which can decrease the water absorption and consequently increase wood dimensional stability [28]. Another peak which has to be taken into consideration is the increase in C-O peak at 1103 cm^{-1} after heat treatment. This might suggest that the formation of new alcohols and esters, which can reduce the number of free hydroxyl groups, increases the hydrophobic character of wood [28, 61].

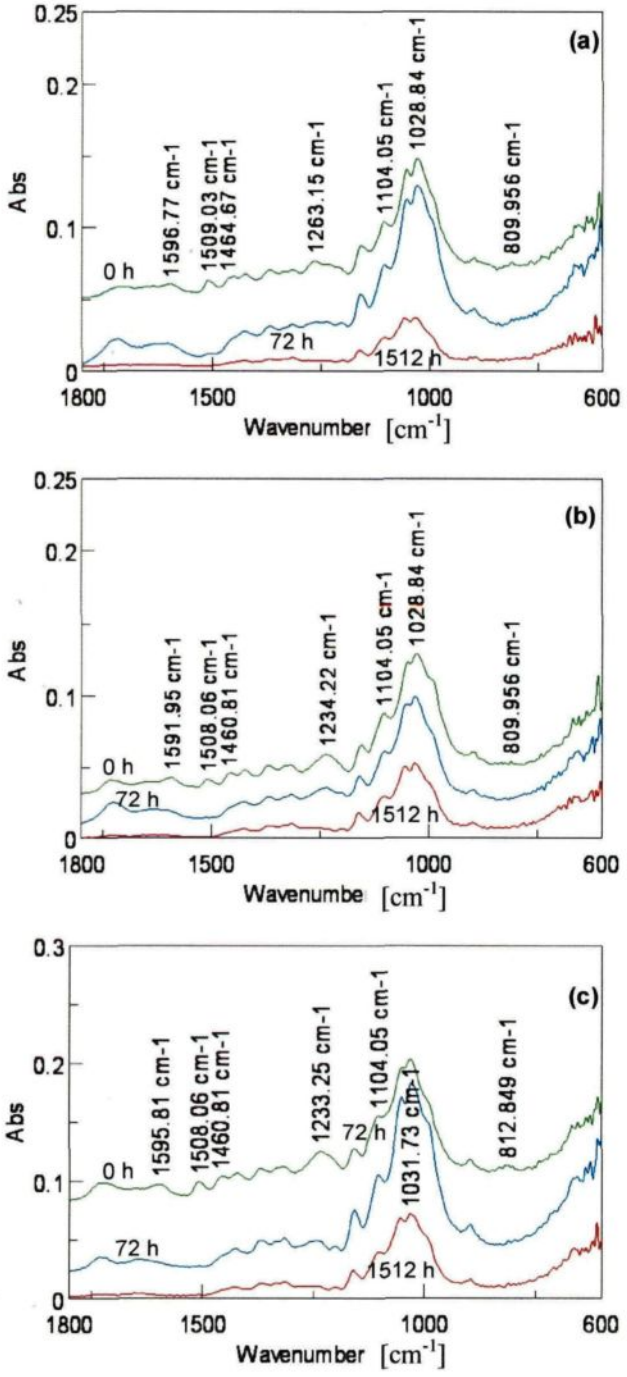

Figure 4. 29 FTIR spectra of heat-treated wood during artificial weathering: (a) jack pine, (b) aspen, (c) birch

Figures 4.29 (a-c) show the FTIR spectra in the spectral regions of heat-treated jack pine, aspen, and birch during artificial weathering, respectively. The overall IR spectrum of three heat-treated species indicate that a number of spectral features appear to be sensitive to weathering. As stated in Table 4.6, all the bands at 1600 cm^{-1}, 1510 cm^{-1}, 1465 cm^{-1}, 1263 cm^{-1}, and 1103 cm^{-1} represent lignin characteristics. As shown in Figures 4.29 (a-c), all these characteristic bands of lignin decrease significantly as a result of the weathering process for all species. It indicates that lignin is the component of heat-treated wood which is most degraded during weathering.

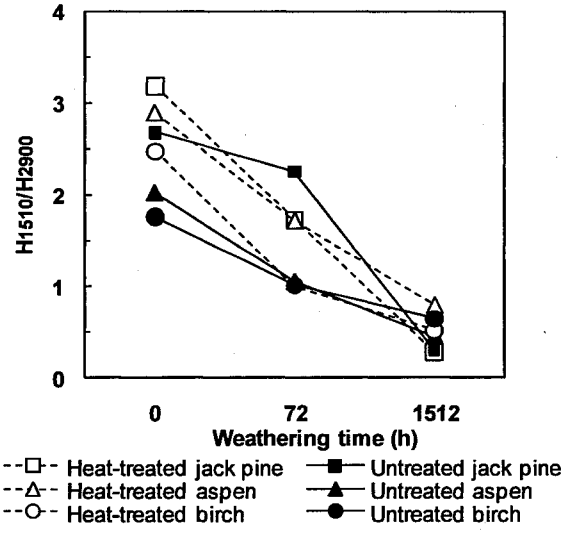

Figure 4. 30 Evolution of the lignin loss as a function of weathering time

Out of the five bands mentioned above, the evolution of lignin loss is best explained by the peak at 1510 cm^{-1} of wood samples [61]. Figure 4.30 shows the lignin loss for heat-treated and untreated wood specimens for three species after artificial weathering for different times. Before weathering, heat-treated wood surfaces show higher lignin content than those of untreated wood surfaces for the same species. After artificial weathering of

72 h, lignin in all specimens becomes degraded although a large difference can be seen in the evolution of the degradation process. It is worth noting that the difference in lignin content between heat-treated and untreated wood reduces after weathering for 1512 h. All of the cell wall polymers such as cellulose, hemicelluloses, and lignin are hydroscopic. The order of hydroscopicity is: hemicellulose > cellulose > lignin [167]. Thus, the loss of lignin means an increase in the content of other components and consequently can make the surface more hydrophilic. The same observation is reported by Kalnins and Feist [94]. They reported that the measured contact angle on weathered western red cedar dropped from 77° to 55° after four weeks of outdoor weathering. It is also reported that wettability for Sitka spruce increased when exposed to xenon arc radiation and water spray [168].

The total crystallinity index (H_{1370}/H_{2900}) is determined from the absorption ratios [169] and plotted in Figure 4.31 for both heat-treated and untreated specimens of three species. The values of the total crystallinity index refer to sum of cellulose I and cellulose II values [61]. The results indicate that crystalline cellulose becomes degraded which cause a decrease in the crystallinity of all specimens, and degradation occurs to different extents depending on species and heat treatment.

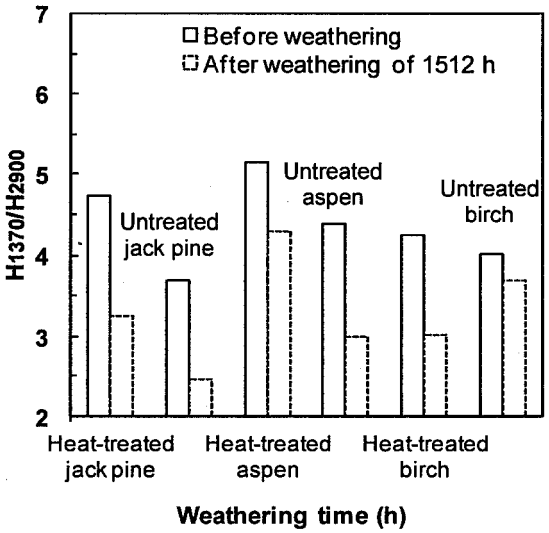

Figure 4. 31 Intensity ratios of bands at 1370 cm^{-1} (total crystallinity index) to band at 2900 cm^{-1} in FTIR spectra before (0h) and after artificial weathering and 1512 h

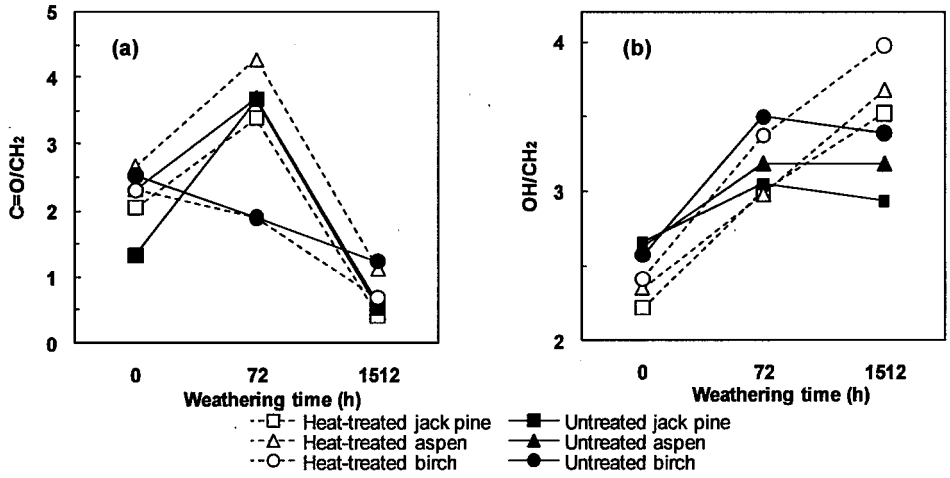

Figure 4. 32 Intensity ratios of bands at (a) 1740 cm^{-1} ($C=O/CH_2$) and (b) 3500 cm^{-1} (OH/CH_2 ratio) to band at 2900 cm^{-1} in FTIR spectra before (0h) and after artificial weathering for 72h and 1512 h

Figure 4.32 (a) and (b) shows the $C=O/CH_2$ ratio and OH/CH_2 ratio of heat-treated and untreated jack pine, aspen, and birch before weathering and after weathering for 72 h and 1512 h, respectively. With the exception of heat-treated and untreated birch, the $C=O/CH_2$ ratios of other specimens increase up to 72 h and then decrease after weathering for 1512 h (see Figure 4.32 (a)). Since the decrease in contact angle means increase in wettability, if the functional group is responsible for the increase of wettability, the tendency of the functional ratio is expected to increase with the increasing weathering time. Thus, the tendency shown in Figure 4.32 (a) suggests that, except heat-treated and untreated jack pine and aspen after the artificial weathering of 72 h, the affinities of other specimens studied during the present work for water are not attributable to the carbonyl groups. Similar result was reported in the literature [45].

4.2.4. Chemical composition analysis

For a good understanding of the mechanism of chemical changes taking place during weathering for heat-treated wood, quantitative data on the chemical components of the three wood species are invaluable. The results obtained for the main components of the investigated heat-treated woods before weathering and after weathering of 1512 h as well as for untreated woods before weathering are summarized in Table 4.7.

Wood contains a certain amount of noncellulosic carbohydrates (hemicelluloses). Softwood hemicellulose consists of both pentosans and hexosans; hardwood hemicellulose consists mainly of pentosans. Pentosan content in softwoods is about 7 to 10%, and in hardwoods about 19 to 25% (Tappi 1984). It can be seen from Table 4.7 that the pentosan contents of all the three species decrease after heat treatment. The decreased contents of

pentosan are mostly the same; however, jack pine shows much larger variation of percentage (42%) after heat treatment than aspen (22%) and birch (21%). This indicates that heat treatment decomposes the hemicelluloses of both softwood and hardwood to almost the same degree. The results show that the artificial weathering decreased pentosan contents from 5.26 % to 3.50 %, from 17.88 % to 6.62 %, and from 13.99 % to 5.48 % for jack pine, birch, and aspen, respectively.

Wood contains about 20% to 30% lignin. Determination of the lignin content of wood provides information for the evaluation of the changes the lignin undergoes during heat treatment and weathering processes. According to the study of Kocaefe and her co-workers [28], lignin undergoes some modification during thermal treatment but its absolute quantity does not change significantly. Only its relative quantity increases due to the degradation of hemicelluloses and the evacuation of extractives. Hardness, bleachability, and other wood properties such as color are also associated with the lignin content (Tappi, 1998). The lignin percent of all three woods studied increase after heat treatment (28.88% to 35.9%, 20.27 % to 26.41%, 19.04% to 22.71% for jack pine, birch, and aspen, respectively). This might be due to the smaller influence of heat treatment on the lignin content than that on the hemicelluloses. However, the lignin percent of heat-treated woods reduces considerably, after artificial weathering. The minimum lignin content of 2.5% was observed for aspen. This suggests that the weathering degrades lignin most significantly compared to other wood components for all three heat-treated woods.

The holocellulose content slightly decreases after heat treatment, but significantly increases after artificial weathering for all three species. The variation of holocellulose and

pentosan contents indicates that cellulose is the most stable component of wood during both heat treatment and weathering processes. Lignin is the most sensitive to weathering, and pentosan is the most sensitive to heat treatment.

Similar to pentosan content, extractive content slightly reduces due to heat treatment while nearly most of the extractives are degraded by weathering for all three species. The extractive content of jack pine is higher than those of birch and aspen, both for untreated and heat-treated woods before and after weathering. This can be the reason for the differences observed in the wood components analysis of three species.

Table 4. 7 Quantitative analysis of the components of studied species

	Extractive (%)		Lignin	Pentosan	Holocellulose
	Acetone	Ethanol	(%)	(%)	(%)
Untreated jack pine before weathering	5.04	1.77	28.66	9.09	60.21
Heat-treated jack pine before weathering	4.78	0.74	35.90	5.26	59.05
Heat-treated jack pine weathered for 1512 h	0.91	0.55	2.14	3.50	95.54
Untreated birch before weathering	4.42	1.72	20.27	22.77	79.05
Heat-treated birch before weathering	2.40	1.13	26.41	17.88	68.78
Heat-treated birch weathered for 1512 h	0.54	0.23	2.36	6.62	93.71
Untreated aspen before weathering	3.51	1.36	19.04	17.94	72.70
Heat-treated aspen before weathering	2.04	1.27	22.71	13.99	70.79
Heat-treated aspen weathered for 1512 h	0.29	0.30	2.50	5.48	92.13

4.2.5. Conclusions

a) The XPS spectra results show that the O/C ratio increases with weathering, indicating that the heat-treated wood surfaces are oxidized. The C1s peaks imply a decrease in the area of the C_1 (mainly from cellulose and hemicelluloses), indicating that the heat-treated wood surfaces become rich in cellulose and poor in lignin as a result of the oxidation caused by weathering. A decrease in the O1 peak originating from lignin and extractives detected in O1s peaks, therefore, the trend observed for C1s peaks is confirmed. These results suggest that lignin is more sensitive to weathering than other component in heat-treated wood surfaces. Results of acidity to basicity ratios indicate that heat treatment results in a decrease of wood acidity. This might be attributed to the degradation of hemicelluloses leading to the decrease of carboxylic acid functions mainly present in hemicelluloses. However, the acid/base ratio increases proportionally as a result of oxidation caused by weathering. The influence of weathering on chemical modification of surface was found to be more significant than that of heat treatment. The measurements performed during this study under similar conditions are reproducible indicating that the contamination levels on sample surfaces are constant and the results are reliable.

b) The FTIR spectra suggest that the OH/CH_2 ratio for heat-treated specimens is inversely proportional to the contact angle regardless of the wood species. Lignin is more sensitive to the degradation due to weathering process than other wood polymers, and the weathering degrades the hydrophobic component of lignin more than others for specimens tested in this study. Consequently, weathering allows cellulose to become more abundant on the surface. The cellulose-rich layer on wood surface causes the increase in hydroxyl

groups. The increasing amorphous cellulose transformed from crystallized cellulose due to weathering increases free hydroxyl groups, which is another reason of wettability increase.

c) Results of chemical components analysis are in agreement with those of XPS and FTIR.

4.3. Modification of color and appearance of heat-treated wood during artificial weathering

4.3.1. General

As mentioned above, heat treatment darkens the wood color. Several studies have also shown that weathering results in poor aesthetics for heat-treated wood because of the surface discoloration when exposed to natural and artificial weathering [11, 13, 18]. The tristimulus spectrocolorimetry technique has been used to quantify the color modification of heat-treated wood due to weathering. Most of the previous studies on color changes due to weathering of heat-treated wood were limited to the study of color data reported by the CIE-L*a*b* system. However, the detailed study of heat-treated wood color changes with reflectance spectra and Kubelka-Munk (K-M) spectra were unavailable in the literature; consequently, color changes of wood heat-treated by different heat treatment conditions due to weathering are not completely understood. Although several investigations were carried out to study the heat treatment effects on the mechanical properties of jack pine and birch [170-172], there is no publication available in the literature on the discoloration taking place due to the artificial weathering of the heat-treated and untreated specific wood species considered in this study. Hence, the effect of accelerated weathering on color changes of different heat-treated woods is investigated in more detail.

4.3.2. Results and discussion

4.3.2.1. Visual observation of surface appearance during artificial weathering

Figures 4.33 (a-c) present the comparison of color changes and physical changes on tangential surfaces of heat-treated jack pine, aspen, and birch during artificial weathering. It can be observed that the color of these three heat-treated woods become lighter and whiter with the increasing weathering time but at different rates. However, it is difficult to analyze the color and structural changes of the samples quantitatively from the visual appearance. A detailed analysis of color changes with reflectance spectra and Kubelka-Munk (K-M) spectra and CIE-L*a*b* system as well as the analysis of structural changes with the analysis of images obtained with florescence microscopy and SEM were carried out and presented in the following section. And visual appearances of all other samples are shown in Appendices 1-3.

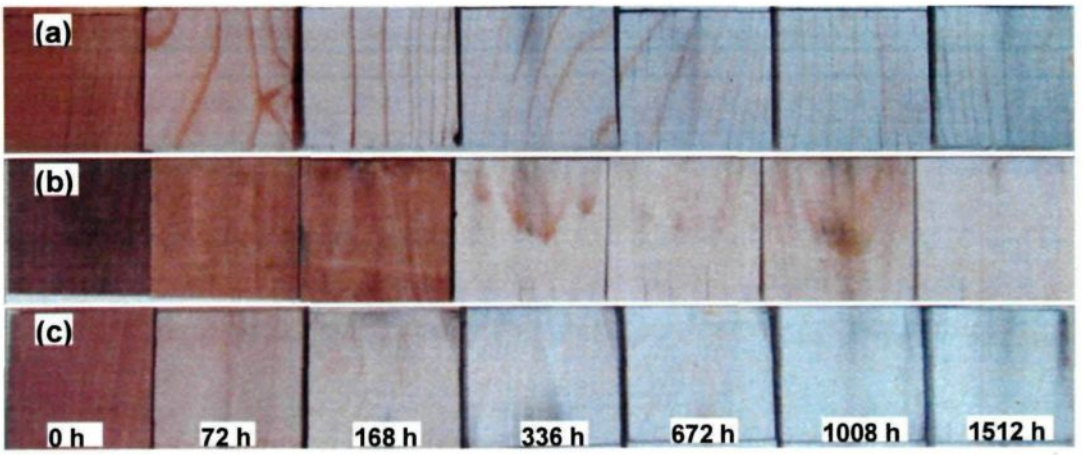

Figure 4. 33 Comparison of heat-treated surfaces of three species at different weathering times: (a) jack pine heat-treated at 210°C; (b) aspen heat-treated at 210°C; (c) birch heat-treated at 215°C

4.3.2.2. Color changes during artificial weathering

4.3.2.2.1. Color changes due to artificial weathering reported using reflectance and wavelength data

The wood reflectance spectra of untreated and heat-treated jack pine before weathering and after artificial weathering for 1512 h as obtained from the spectrocolorimeter are illustrated in Figure 4.34. The color of sample darkens due to heat treatment while colors of both untreated and heat-treated samples lighten after the weathering of 1512 h. The results show that the reflectance difference of heat-treated jack pine before and after weathering is greater than that of untreated samples. The similar trend was observed for the other two species.

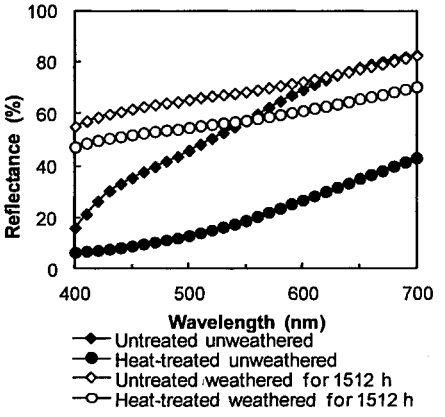

Figure 4. 34 Reflectance spectra for heat-treated and untreated jack pine before weathering and after weathering of 1512 h

It is difficult to do spectral analysis for the reflectance spectra as presented in Figure 4.34. Figure 4.35 displays the Kubelka-Munk (K-M) spectra by applying the Kubelka-

Munk (K-M) function to the reflectance spectra of Figure 4.34 and plotting the K-M spectrum. These spectra resemble absorption spectra. The K-M spectra refer to the three investigated heat-treated and untreated wood samples before weathering and after weathering for 1512 h. All investigated untreated wood species present an absorption maximum at 420 nm while heat-treated woods present an absorption maximum near 430 nm. For all three heat-treated species, a shoulder is observed for wavelengths above 600 nm after 1512 h of weathering. Visual observation of wood surface appearance shows that the heat-treated woods look darker than untreated woods for both before and after weathering. It can be observed that there is a good correlation between the K-M spectra and the visual observation. The darker heat-treated woods present absorption bands covering a larger range than lighter untreated woods in the visible region of the electromagnetic spectrum. As was stated above, hemicellulose is the component which is damaged most during heat treatment, consequently, the lignin content of heat-treated wood increases accordingly. This might explain darker color and higher absorption spectra of heat-treated woods. The results shown in Table 4.7 suggest that the K-M spectra are also well-correlated with the extractive contents for both untreated and heat-treated samples before or after weathering. The species presenting higher absorptions in the visible range are those that have larger extractive content (jack pine> birch >aspen).

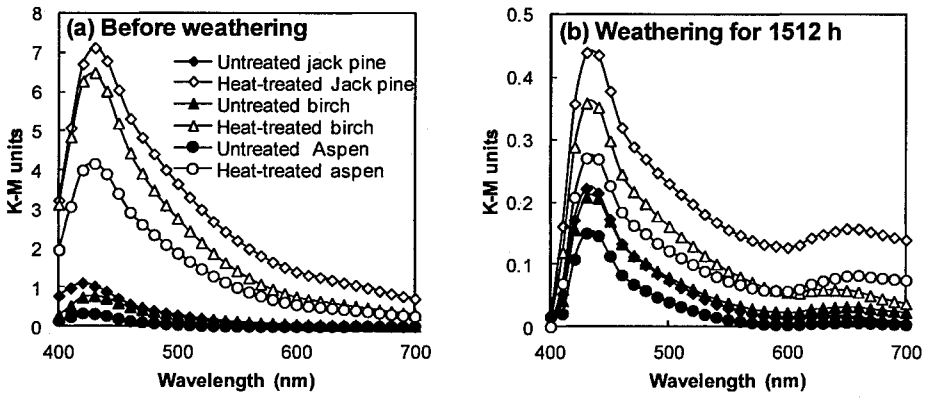

Figure 4.35 K-M spectra for the three heat-treated and untreated woods before weathering and after weathering of 1512 h: (a) before weathering; (b) after weathering for 1512 h

Figure 4.36 displays the K-M spectra of untreated and heat-treated jack pine artificially weathered for different times. The similar trend was observed for the other two species. A well-defined absorption maximum is observed at around 420 nm for untreated jack pine samples and at 430 nm for heat-treated samples during the whole duration of artificial weathering. The greatest change of K-M spectra for untreated samples occurs within the first 72 h of weathering and around the 420 nm wavelength, which corresponds to a decrease in violet shades. This indicates an increase in yellow and red colors. It is believed that the deepening of coloration is due to the formation of chromophores caused by the photo-degradation of untreated wood lignin and the migration of extractives from interior of wood substrate to wood surface due to the high temperature during accelerated weathering test. However, the K-M spectra show a decrease especially around the 420 nm between the 72 h and 168 h. This can be seen from Figure 4.34 (a) which shows a reversal of the trend seen in the first 72 h where the K-M spectra increase. At 168 h, the K-M

spectra declines at the highest rate in the 450 nm range again. This is the beginning of leaching processes by water.

The K-M spectra for heat-treated jack pine samples are illustrated in Figure 4.34 (b). The K-M spectra remain the same after weathering for 72h and decline slightly up to 168 h followed by a significant decrease at 336 h and then continue to decrease at lower rates as the weathering time increases. The difference in the K-M spectral pattern of heat-treated wood samples at the earlier stages of weathering and untreated samples might be explained by the different lignin and extractive contents of untreated and heat-treated wood. Due to degradation of hemicelluloses during the heat treatment process, the lignin concentration of heat-treated wood is higher than that of untreated wood (see Table 4.7), which results in a better resistance of heat-treated wood to photo-degradation compared to that of untreated wood. Consequently, the changes of K-M spectra of heat-treated wood samples are less than those of untreated wood when exposed to 72 h of weathearing. Furthermore, this can be confirmed by the K-M spectra of samples after weathering for 1512 h as shown in Figure 4.35 (b), where the absorption intensity of heat-treated samples are higher than those of untreated samples. This means the colors on heat-treated wood surface stay darker than those of untreated samples after photo-degradation and leaching by water during weathering. The slight change of K-M spectra during the earlier times of weathering of heat-treated wood also might be explained by the less extractive content migration from the interior of heat-treated wood towards the surface.

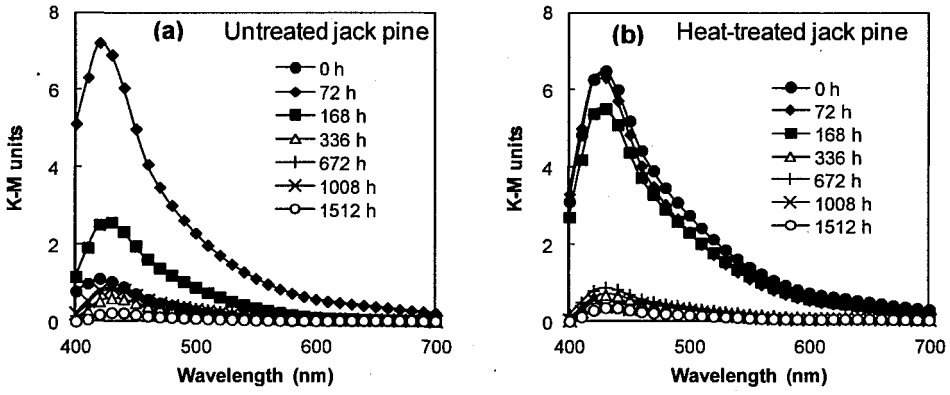

Figure 4. 36 Evolution of K-M spectra for untreated and heat-treated jack pine as a function of weathering time: (a) untreated jack pine; (b) heat-treated jack pine

As seen in Figure 4.36 (a) and (b), the intensity of the absorption bands in the K-M spectra for untreated samples increases rapidly during the initial times of weathering until it reaches the highest value after 72 h. Then, it decreases with the increasing weathering time. However, the absorption intensities of heat-treated wood decline as the weathering time increases. In order to compare and quantify the observed color changes during weathering, the time dependence of the absorption intensities were analyzed. Figure 4.37 shows the results of the variation behavior of maximum intensity for untreated and heat-treated samples. It can be observed from the results of untreated woods shown in Figure 4.37 (a) that the color change trends at the earlier times (168 h for jack pine and aspen, 72 h for birch) of weathering are different than those at later weathering times. At this stage of weathering, the major changes in the light absorption characteristics of the wood surface are observed for the jack pine. This might be due to the higher extractive and lignin contents of jack pine (see Table 4.7). The studied untreated woods show almost the same changes in the light absorption characteristics after weathering more than 168 h. The

variations in K-M spectra of heat-treated woods with weathering time are presented in Figure 4.37 (b), which are larger than those of untreated wood for the same species and at the same weathering times. It is also observed that the major changes are displayed by birch, followed by jack pine and aspen in decreasing order.

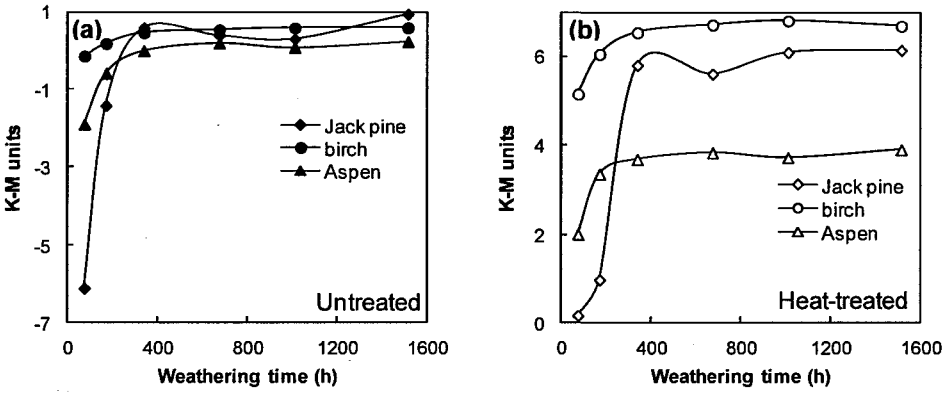

Figure 4. 37 Variation of maximum intensity in K-M different spectra of wood samples before and after weathering as measured at 420 nm for untreated woods and at 430 nm for heat-treated woods during weathering: (a) untreated wood; (b) heat-treated wood

Color modification on wood surface can also be analyzed with the CIE-L*a*b* system according to the changes of lightness L* as well as a* and b* co-ordinates that represent the color pairs red/green and yellow/ blue, respectively [110].This is a frequently used color change analysis method and has been used in other studies including the color changes of heat-treated wood during artificial weathering [11, 15, 18]. Ayadi and his co-workers [15] investigated the color changes of heat-treated ash, beech, maritime and poplar during exposure of UV light. Their study reported, using the CIE-L*a*b* system, the measurements of ΔE at different times up to 835 h. They also mentioned that untreated woods quickly darken, yellowing and reddening coloration, and the color modifications are

softened for heat-treated woods. They related the better photostability of heat-treated wood color to the increase of lignin stability by condensation and phenol content during the heat treatment. The color change results observed during artificial weathering with water spray for the three North American species heat-treated at different conditions are in good agreement with the literature.

4.3.2.2.2. Color changes due to artificial weathering reported using CIE-L*a*b* system

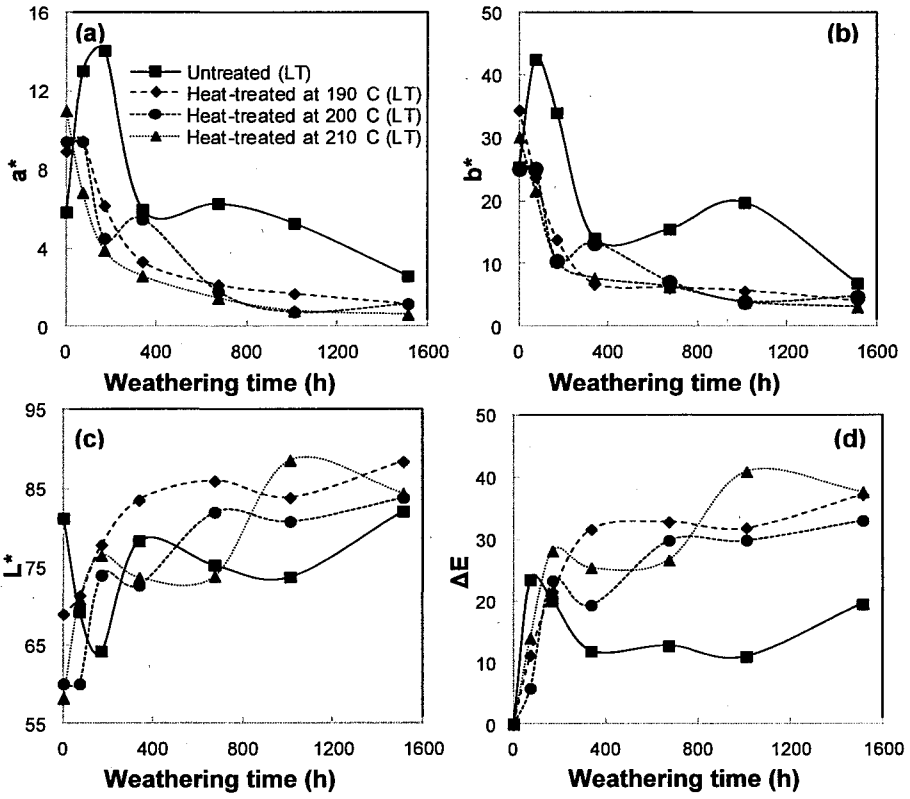

Figure 4. 38 Color changes on tangential surfaces of heat-treated jack pine during artificial weathering reported using CIE-L*a*b* system

Figure 4.38 shows the color changes of untreated and heat-treated jack pine wood on artificially weathered tangential surfaces. Figure 4.38 (a) shows red-green tint (a*values) of heat-treated and untreated jack pine wood due to weathering. The a*values of untreated samples increase to maximum after weathering of 336 h and then decrease to values similar to those of heat-treated wood samples after weathering for 1512 h. On the other hand,

a*values of woods heat-treated at 190 °C and 210 °C decline at all times of weathering. The change trends of b*values are similar to those of a*values (see Figure 4.38 (a)). The initial and final b*values after weathering of 1512 h are mostly the same on different jack pine surfaces. That indicates both that heat-treated and untreated jack pine wood display the same levels of yellow after weathering. L* value changes of untreated jack pine are irregular compared to those of heat-treated wood, which decline at the initial step of weathering up to a minimum value at 168 h, and then increase and decrease alternately. Lightness of untreated jack pine is higher than those of all heat-treated woods before weathering while the results are opposite after weathering more than 1008 h. As it can be seen from Figure 4.38 (d), the total color differences (ΔE) of heat-treated jack pine change more significantly than those of untreated wood. This is due to the difference in their initial color. The color of both untreated and heat-treated wood change to white and gray at the end of the weathering; however, the original color of heat-treated wood is darker than the original color of untreated wood.

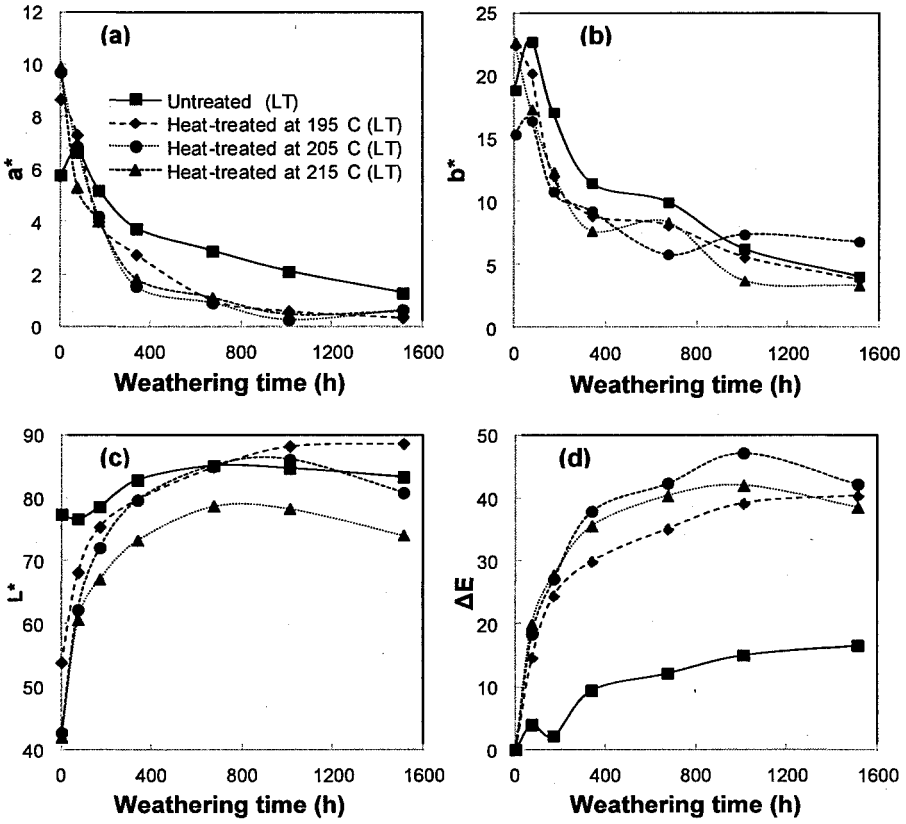

Figure 4. 39 Color changes on tangential surfaces of heat-treated birch during artificial weathering reported using CIE-L*a*b* system

The color changes of tangential surfaces of heat-treated and untreated birch wood during artificial weathering are shown in Figure 4.39. During early times of weathering, a* values of untreated wood increase (before 72 h) slightly and then decrease significantly (see Figure 4.39 (a)). a* values of all three heat-treated woods decrease rapidly to the lowest final values at 1512 h of weathering. The red-green tint levels of birch wood, heat-treated at three different temperatures, are mainly the same at all weathering times. Both heat-treated and untreated birch wood surfaces change from a slightly yellow to a blue tint after

weathering for 1512 h. L* value displays different trends for heat-treated and untreated birch wood at earlier times of weathering. L* of untreated birch wood decreases to a minimum value after weathering for 72 h followed by a slow increase and eventually levels off. That implies that untreated wood becomes darker slightly and then becomes lighter as the weathering time increases (Figure 4.39 (c)). However, the lightness of birch, heat-treated at three temperatures, increases at earlier times of weathering up to a maximum value and then changes slowly. After weathering of 1512 h, the lightness levels of wood heat-treated at 195°C are higher than those of untreated wood while those of wood heat-treated at 205°C and 215°C are lower. Trends observed for ΔE values are different for heat-treated and untreated birch wood surfaces. They don't seem to be affected by temperature. For heat-treated birch, ΔE increases significantly at the earlier times of weathering and then changes slowly. However, the ΔE values of untreated wood increase slowly and then change rapidly up to 1512 h of weathering. The total color differences of heat-treated birch are higher after weathering for 1512 h compared to that of untreated birch wood regardless of heat treatment temperature.

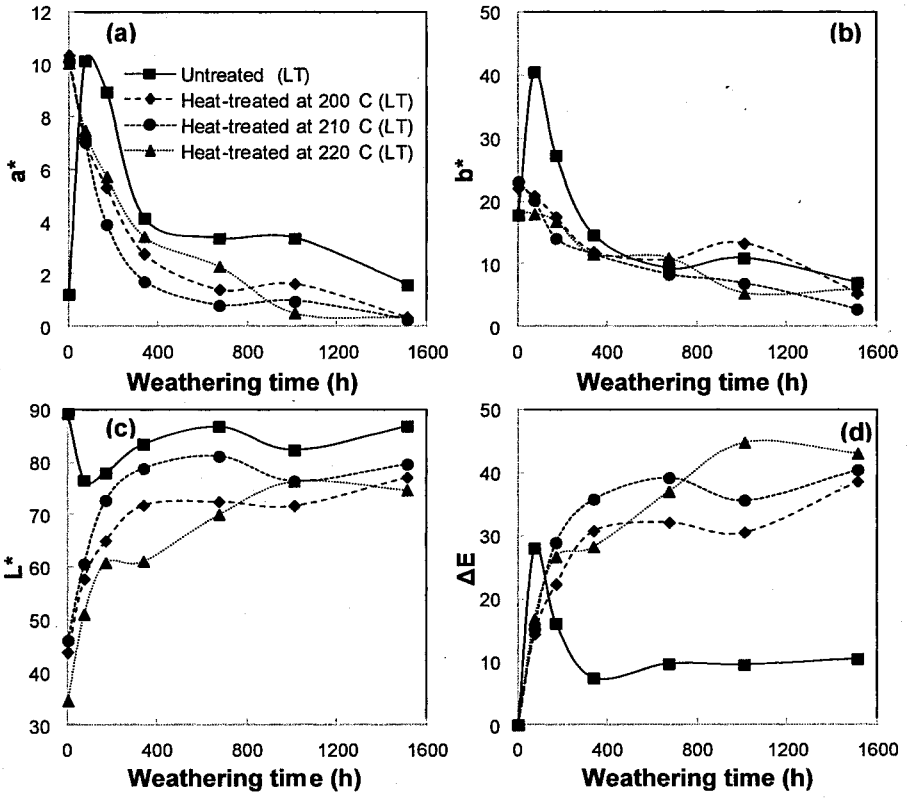

Figure 4. 40 Color changes on tangential surfaces of heat-treated aspen during artificial weathering reported using CIE-L*a*b* system

Figure 4.40 shows the color changes of tangential surfaces of untreated and heat-treated aspen at three different temperatures (200°C, 210°C, and 220°C) as a function of artificial weathering times. Figure 4.40 (a) shows a* value changes on aspen sample surfaces due to artificial weathering. During early times of weathering up to 72 h, a* values of untreated wood increase sharply and then decrease significantly at 336 h and continue to change slowly. Values of a* for aspen, heat-treated at all three different temperatures, decrease continuously throughout all weathering times. The red-green tint levels of heat-treated aspen are lower than those of untreated aspen after weathering of 1512 h. The trend

observed for the change in b* value of heat-treated and untreated aspen due to weathering is similar to that of birch. Value of b* for untreated aspen increases significantly at the beginning (72 h) up to a maximum value, then decreases first rapidly and then at slower rate after 336 h (see Figure 4.40 (b)). The trends for aspen, heat-treated at three different temperatures, are mainly the same, decreasing slowly during the entire weathering time. After weathering for 1512 h, heat-treated and untreated wood have mainly the same level of blue. Brightening and darkening of heat-treated and untreated aspen wood are observed by following the changes in L* values (shown in Figure 4.40 (c)). L* value displays different trends for heat-treated and untreated aspen wood at earlier times of weathering. L* values of untreated aspen wood decrease to a minimum after weathering for 72 h followed by a slow increase. That implies that untreated wood becomes darker and then becomes lighter as the weathering time increases. The changes in lightness trend for heat-treated aspen are different than those of untreated wood, but there does not seem to be any significant effect of heat treatment temperature (200°C, 210°C, and 220°C) on lightness. The values of lightness of heat-treated wood increase at earlier times of weathering up to a maximum value and then change slowly. After weathering of 1512 h, the lightness value of untreated aspen is higher than that of heat-treated aspen. The total color differences (ΔE) between aspen surfaces are shown in Figure 4.40 (d). Similar to jack pine and birch, the trends for the change in ΔE values are different for heat-treated and untreated aspen wood surfaces. Those of heat-treated wood surfaces are almost the same at different treatment temperatures. ΔE values of heat-treated aspen increase significantly at earlier times of weathering, and then change slowly. However, ΔE values of untreated aspen increase

significantly and then decrease rapidly up to 336 h of weathering. Afterwards, they increase again slowly up to 1512 h of weathering.

An overview of the color changes of the three woods heat-treated and subjected to artificial weathering (Figures 4.38-4.40) allows the following conclusions to be deduced:

1) It is apparent from the results of this study that weathering has a significant effect on the color of both heat-treated and untreated wood surfaces. It is also apparent from the color data analyzed using CIE-L*a*b* system that artificial weathering affects colors of heat-treated wood quite differently from those of untreated wood for the same species, especially at early weathering times (72 h). These differences found from the analysis carried out using CIE-L*a*b* system are in agreement with results of reflectance and K-M spectra presented earlier. Color parameters of untreated woods seem to initially increase and then decrease during weathering implying that more than one chemical or physical processes are occurring. Significant color changes occur in the first 72 h of weathering for all three untreated woods although the extent of the color changes varies from wood to wood. The three untreated woods become redder, yellower, and darker in the earlier times of weathering and then the color changes in an opposite direction during later times of weathering. Extractives have antioxidant properties and can limit lightening of wood color [15]. The first degradation stage of weathering is believed to be linked to the formation of chromaphoric products induced by lignin scission and migration of extractives from the interior of wood structure towards the surface. With the ongoing weathering process, chromaphoric products are leached out by water and the extractives are damaged, leaving a whiter surface which is rich in cellulose and hemicelluloses. This is confirmed by the result

of chemical analysis of wood components (see Table 4.7) and the white color of holocellulose. Chemical analysis of wood components after heat treatment at high temperatures shows a decrease in holocellulose, pentosan, and extractive contents of wood (see Table 4.7), which indicates a degradation of cellulose, hemicelluloses, and extractives for woods investigated during this study. Similar results can be found in previous studies [173, 174]. The increase in lignin and extractive contents observed after heat treatment in the samples analyzed might explain the improvement in color stability of heat-treated woods during earlier times of weathering. After the specimens have been subjected to long term artificial weathering with simulated sunlight and water spray, the final colors of heat-treated woods and untreated woods become similar.

2) Although the color change trends of heat-treated and untreated jack pine, birch, and aspen due to artificial weathering have some similar features, each wood has a uniquely different color change pattern (see Figures 4.38-4.40). It seems that during weathering processes of heat-treated woods, degradation of lignin matrix and extractives take place. This lightens the color and the color difference increases. Then, the leaching process of other polymers (such as cellulose and hemicelluloses) on wood surface occurs, consequently, the color returns to initial state and differences between initial and final colors decline. The weathering effects on different woods, heat-treated under similar conditions (210°C for jack pine and aspen, 205 °C for birch), occur much more rapidly in some species compared to others. The weathering process in heat-treated jack pine appears to be the most rapid among the three wood species studied, followed by heat-treated aspen and birch (see Figure 4.38 (d), Figure 4.39 (d), and Figure 4.40 (d)). The extent of the color

changes also varies among the species. The effect of water spray on jack pine and aspen is higher than it is on birch during weathering due to the different wood structures. The cell wall width of birch is thicker than that of other two species resulting in stronger binder strength and higher resistance to washing by water during weathering. The total color difference of heat-treated jack pine is less than those of both birch and aspen at all weathering times except at 1008 h. Jack pine is softwood and the other two wood species studied are hardwoods with somewhat comparably-structured lignin polymer component but with distinctive differences in overall composition, as noted in Table 4.7. The high lignin content of heat-treated jack pine (softwood) protects wood surface more against the weathering process compared to the lower lignin contents of other two species.

3) All the color changes on both heat-treated and untreated wood surfaces brought about by the weathering process are essentially complete approximately after 336-672 h of weathering.

4) After the specimens have been subjected to 1512 h of artificial weathering with simulated sunlight and water spray, the colors of all three heat-treated woods are found to be very similar.

5) When ΔE versus maximum absorption intensity is plotted for each heat-treated and untreated species, the following linear regression analysis and correlation coefficients are obtained: 0.807 for untreated jack pine, 0.778 for heat-treated jack pine, 0.887 for untreated birch, 0.942 for heat-treated birch, 0.986 for untreated aspen, 0.968 for heat-treated aspen. These deviations from the ideal linear correlation might be attributed to

some loss of information when a wood reflectance spectrum is transformed to color values [112, 175].

4.3.2.3. Effects of wood nonisotropicity

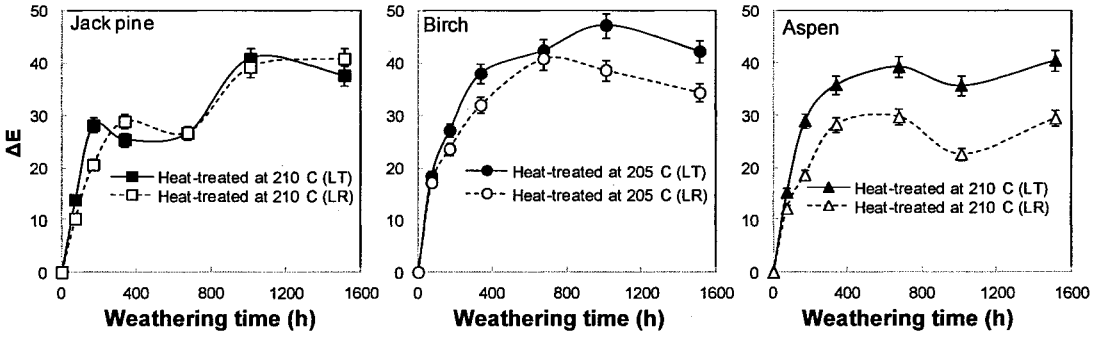

Figure 4. 41 Comparison of color differences between tangential surfaces (LT) and radial surfaces (LR) of heat-treated woods during artificial weathering

Physical and chemical properties of wood are known to be a function of direction. A study of the color change on tangential surfaces (LT) and radial surfaces (LR) of the three heat-treated wood was conducted to show if the color changes during weathering were affected by direction. The color of heat-treated jack pine is almost the same on radial and tangential surfaces at all weathering times (see Figure 4.41). However, the color changes more on tangential surfaces of heat-treated birch than on radial surfaces at all weathering times. Likewise, the heat-treated aspen shows a similar trend to birch. A statistical analysis (T-test) is used for the ΔE data companion obtained from this study. A significant difference ($P<0.05$) in ΔE data between the two different directional surfaces was found to occur at 1008 h and 1512 h of weathering for heat-treated birch and after 336 h of weathering for heat-treated aspen. This is most likely linked to presence of different

structures on different directional surfaces. The presence of radial rays causes that water moves rapidly deeper into the wood structure on tangential surfaces than radial surfaces during the weathering process. Consequently, the leaching by water induces more degradation on tangential surfaces compared to radial ones.

4.3.2.4. Heat treatment technology effects

Different heat treatment technologies are known to affect physical and chemical properties of heat-treated wood. A study on color changes of jack pine wood heat-treated using different technologies during artificial weathering was undertaken to show if the color changes were due to the heat treatment technologies. Figure 4.42 shows a comparison of total color differences (ΔE) of jack pine heat-treated with Thermo-wood technology and UQAC technology as a function of artificial weathering time. The trends for the change of ΔE values are slightly different for these two heat-treated woods. ΔE values of wood treated with UQAC technology increase significantly at earlier times of weathering and reach a maximum value (at 168 h), later decrease slightly at 336 h and then increase, reaching a maximum value at 1008 h, followed by same final value with wood treated using Thermo-wood technology after 1512 h. The trends of Thermo-wood are similar except at 1008 h. The color differences decrease rapidly at 1008 h and then increase again up to almost the same value with the UQAC-technology-treated wood after 1512 h of weathering. A different trend, observed at 1008 h, for Thermo-wood agrees with the result of the visual observation. The phenomena of color differences initially increase and then decrease during the weathering procedure implying that more than one process is taking place. The formation of chromophoric products induced by degradation of lignin in the

initial weathering and the leaching with water of these choromophoric residues result in a heat-treated wood surface which is rich in cellulose and hemicelluloses. Consequently, heat-treated wood becomes lighter gray and the color difference with that of initial heat-treated wood increases. Once the lignin matrix is damaged and the chromophoric products in the top layer of sample surfaces are leached out by water, much of the remaining lighter color polymer (such as cellulose and hemicelluloses) is believed to be removed from the surface layers by the washing action of water, too. Then, the weathering process occurs once again. This might explain the decrease of color difference during weathering. The effect on woods heat-treated by different techniques may be quite similar in the long term (1512 h) under the same weathering conditions, but the weathering effects occur much more rapidly and serious in one than another. For example, the weathering process in wood heat treated with UQAC technology appears to be more rapid but less serious than in wood heat treated with Thermo-wood technology, that the weathering process of wood heat treated with UQAC technology after 336 h is closer to that found for the wood heat treated with Thermo-wood technology at 1008 h weathering.

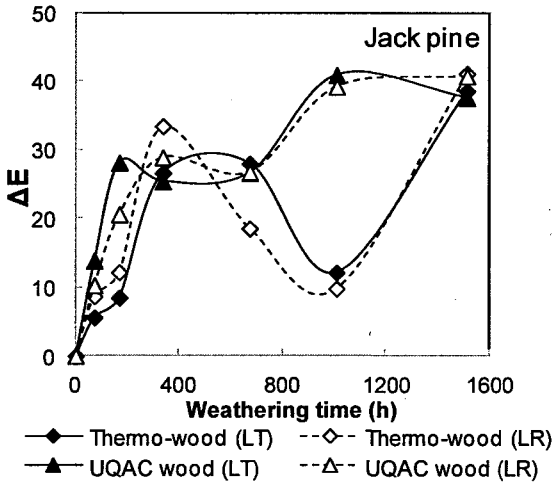

Figure 4. 42 Comparison of color difference between jack pine wood heat-treated (210 °C) by different technologies during artificial weathering

4.3.3. Conclusions

A general understanding of heat-treated wood color behavior under artificial weathering has been achieved using spectrocolorimetry. The K-M spectra of heat-treated woods during artificial weathering identified absorption bands caused by chemical modifications of the wood surface, characterizing the weathering processes. There is a major increase in yellow and red with corresponding decreases in the reflectance for all the three species during heat treatment. Heat-treated woods have better color stability during the early times of weathering, while the colors of heat-treated woods and untreated woods are very similar after the specimens have been subjected to long term artificial weathering. It is proposed that the weathering mechanism of heat-treated woods consists of the degradation of lignin matrix and extractives, which lightens the wood color and the color difference between wood surfaces before weathering and during different stages of

weathering increases. Then, the leaching process of other polymers on wood surface occurs, consequently, the color returns back to initial value and color difference decline. The rapidness and extent of the weather effects on different heat-treated woods are different. The effect of direction on color changes of heat-treated woods taking place due to weathering are different for different species.

4.4. Evaluation of microscopic structure of heat-treated wood during artificial weathering

4.4.1. General

As it was introduced in chapter 2, untreated wood exposed to the weathering undergoes checking and surface erosion due principally to the effects of weathering. Heat treatment of wood is an effective method to improve the dimensional stability and durability against biodegradation [35]. In previous studies, the chemical and color characteristics of heat-treated wood during artificial weathering have been emphasized. In this part, the study on structural changes of heat-treated woods of the three North American species is reported. The effects of artificial weathering on the anatomical structure of heat-treated woods were investigated by means of a light (fluorescence microscopy) and scanning electron microscopy (SEM) analysis.

4.4.2. Results and discussion

4.4.2.1. Analysis of fluorescence microscopy images

The transversal surfaces to the artificial weathering test were selected to examine with a fluorescence light microscope. Figures 4.43 to 4.45 present the fluorescence

microscopy images of heat-treated aspen, jack pine, and birch, and a comparison with those of untreated samples after different weathering times.

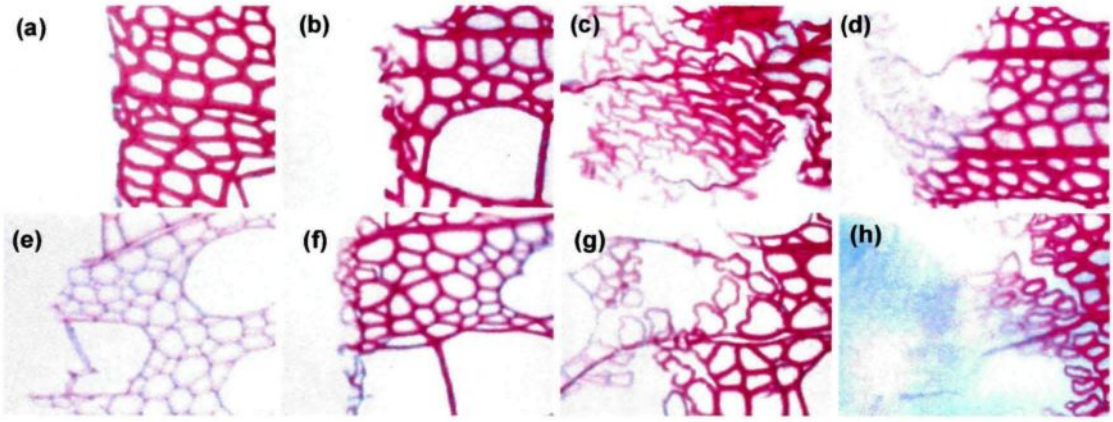

Figure 4. 43 Fluorescence microscopy images (x50) on transverse surface of heat-treated aspen (a-d) and untreated aspen (e-h) after weathering for different times:

(a, e) 0h; (b, f) 72h; (c, g) 672h; (d, h) 1512 h

The damage of one cell layer is visible after 72 h weathering for heat-treated aspen (Figure 4.43 (b)). The degradation of the cells increases and the damaged layer increases with increasing weathering time (see Figure 4.43 (a-d)). Similar to heat-treated aspen wood, the first damage of untreated aspen cells that appear on the tested surface is visible after 72 h weathering (see Figure 4.43 (f)). Developing from this damage, the separation of cells from adjoined cells takes place after 672 h of weathering (Figure 4.43 (g)). With increasing weathering time, the cell damage increases. Delamination and thinning of cells are present at the latest weathering time (Figure 4.43 (h)).

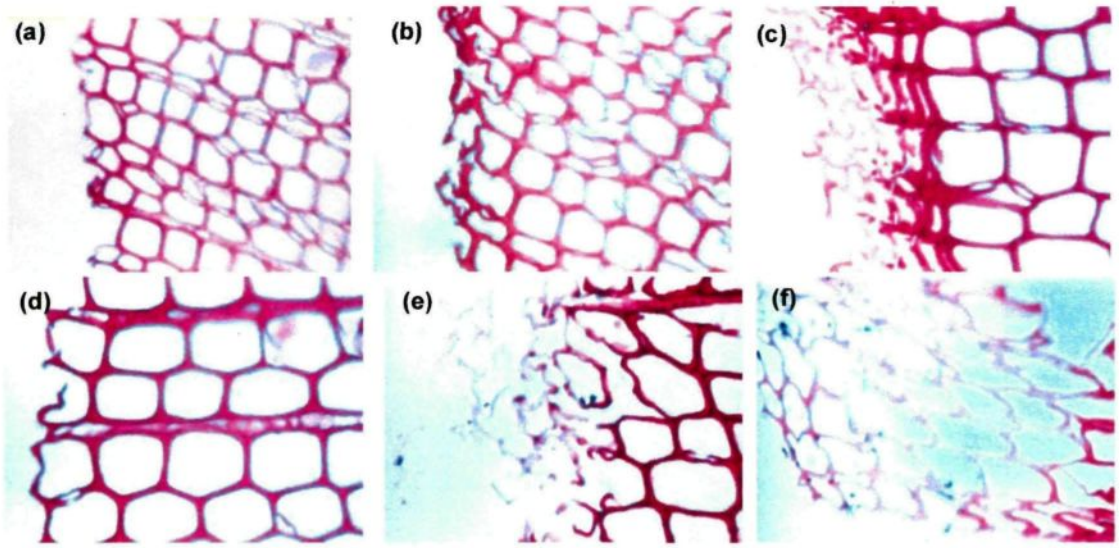

Figure 4. 44 Fluorescence microscopy images (x50) on transverse surface of heat-treated jack pine (a-c) and untreated jack pine (d-f) after weathering for different times: (a, d) 72h; (b, e) 672h; (c, f) 1512h

The damage of jack pine wood cannot be observed on the surfaces after 72 h weathering for both heat-treated and untreated wood (see Figure 4.44 (a) and Figure 4.44 (d)). The first degradation of cells appears on heat-treated jack pine wood surface at 672 h (Figure 4.44 (b)) and then increases with increasing weathering time (see Figure 4.44 (c)). The extent of damage on heat-treated jack pine wood surface is less compared to that of untreated wood surface (see Figure 4.44 (b) vs. Figure 4.44 (e), Figure 4.44 (c) vs. Figure 4.44 (f)).

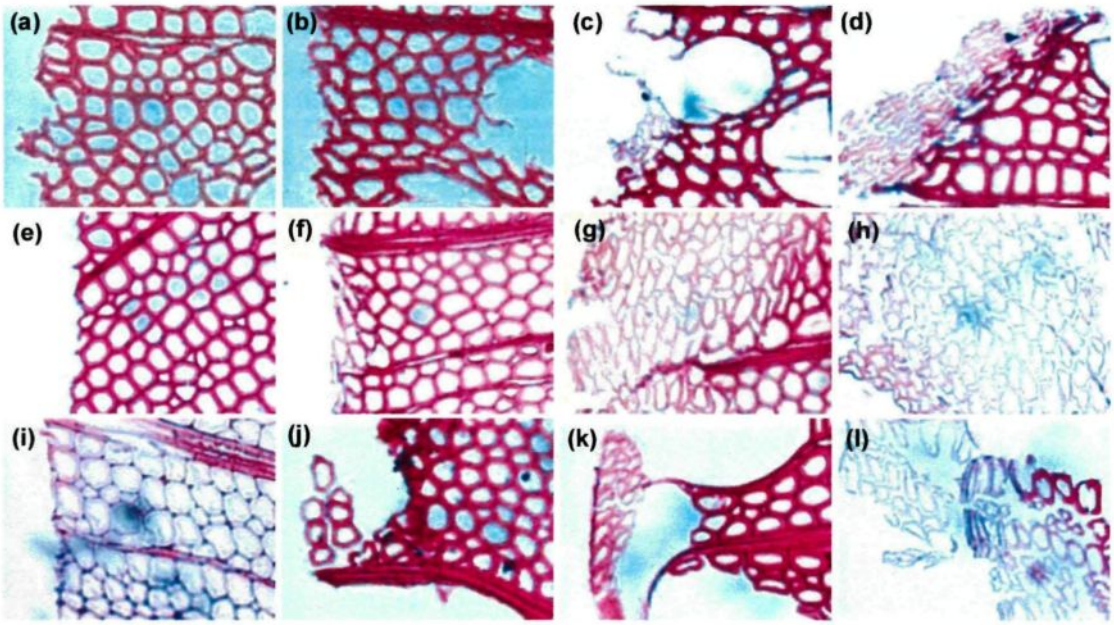

Figure 4. 45 Fluorescence microscopy images (x50) of transverse surface of birch heat-treated at 215°C (a-d), 195°C (e-h), and untreated birch (i-l) after different weathering times: (a,e,i) 0h; (b,f,j) 72h; (c,g,k) 672h; (d,h,l) 1512h

Figure 4.45 shows the fluorescence microscopy images of birch heat-treated at two different temperatures (215°C and 195°C) for different weathering times and compares them with those of non-aged wood. After 72 h of weathering, the damage of two cell layers is visible for untreated birch (Figure 4.45 (j)) while damage of one cell layer is visible for those treated at 195°C (Figure 4.45 (f)). However, for the birch wood which was heat-treated at a temperature of 215°C, the first damage of wood cells on the test surface is visible after 672 h weathering (Figure 4.45 (c)). This indicates that heat treatment increases the resistance of weathering for birch wood. The degradation of cells increases with the increasing weathering time for both heat-treated and untreated birch. Delamination and

thinning of cells appear after weathering for 672 h for untreated birch and birch heat-treated at 195°C and 215°C (Figure 4.45 (c,g,k)).

From the comparison of fluorescence microscopy images of heat-treated jack pine, aspen, and birch after aging at different times, it can be observed that the degradation increases with increasing weathering time for all three heat-treated species. The damage of jack pine wood cannot be observed on the surfaces after 72 h weathering (Figure 4.44 (a)). The first degradation of cells appears on jack pine wood surface at 672 h, then increases with increasing weathering time (Figure 4.44 (c)). The degree of damage of heat-treated jack pine wood is less compared to those of aspen and birch wood (Figure 4.43 and Figure 4.45). This indicates that heat-treated hardwood is more sensitive to weathering than heat-treated softwood, therefore, hardwood structure affected more by exposure to UV. The damage of heat-treated aspen is the most compared to those of heat-treated jack pine and birch. After weathering of 672 h, the surface of heat-treated aspen wood is totally destroyed. Delamination and thinning of cell wall take place after 672 h of weathering for heat-treated aspen (Figure 4.43 (c)) while those on jack pine and birch appear after weathering of 1512 hours (see Figure 4.44 (d) and Figure 4.45 (d), respectively).

4.4.2.2. Analysis of SEM

a) **Longitudinal surface**

Figure 4.46 shows the SEM micrographs on longitudinal tangential surface of untreated specimens before artificial weathering and heat-treated specimens before and after weathering for 1512 h. As shown in Figure 4.46 (a) and (b), (d) and (e), there is no noticeable difference on tangential surfaces of untreated and heat-treated jack pine and

aspen specimens. But in the case of birch, some micro-cracks were formed due to heat treatment even if it is less significant than those formed due to weathering. SEM analysis indicates that anatomical structure of wood is only slightly affected during heat treatment. Fibers and rays are still obvious after heat treatment. Previous section reported that the main differences were the presence of important quantities of extractives deposited in the resins channels, which disappeared after thermal treatment (see Section 4.1). This implies that the structural factors do not play an important role on wettability during heat treatment. The comparison of heat-treated wood surfaces before weathering reveals the differences in structure for all three species (see Figure 4.46 (b), (e) and (h)). The structure of jack pine (softwood) is relatively simple. The axial system is composed mostly of axial tracheids and the radial system is composed mostly of ray parenchyma cells (see Figure 4.46 (a)). The structures of aspen and birch, which are hardwoods, are much more complicated than that of jack pine (see Figure 4.46 (a)). Their axial systems are composed of vessel elements, fibers, and axial parenchyma cells in different patterns and abundance. The presence of vessel elements is the unique feature that separates hardwoods from softwoods, which are for water conduction. Fibers in hardwoods function solely as support. Similar to jack pine, the radial system of aspen and birch is composed of ray parenchyma cells, but unlike softwoods, their rays are much more diverse in size and shape. On the longitudinal tangential section, vessels appear as large cracks.

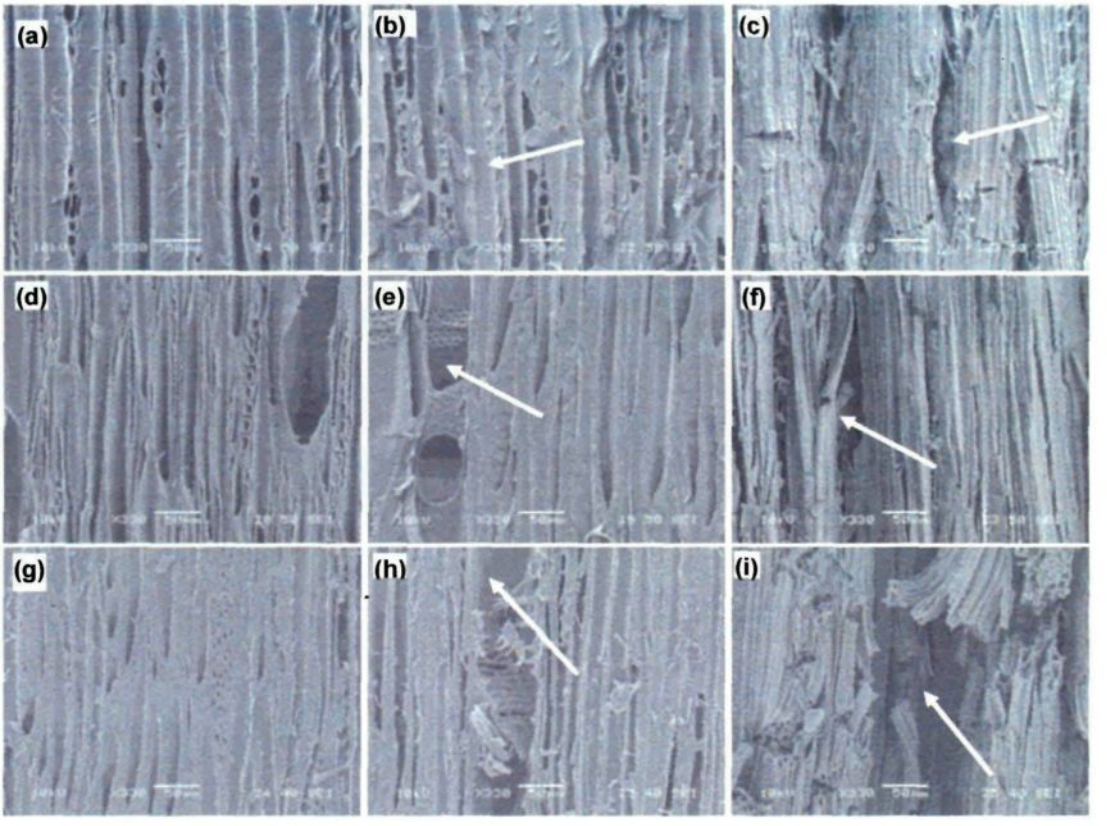

Figure 4. 46 SEM images (×330) on longitudinal tangential surfaces of specimens before and after 1512 h of artificial weathering: (a) untreated jack pine before weathering; (b) heat-treated jack pine before weathering; (c) heat-treated jack pine after weathering; (d) untreated aspen before weathering; (e) heat-treated aspen before weathering; (f) heat-treated aspen after weathering; (g) untreated birch before weathering; (h) heat-treated birch before weathering; (i) heat-treated birch after weathering

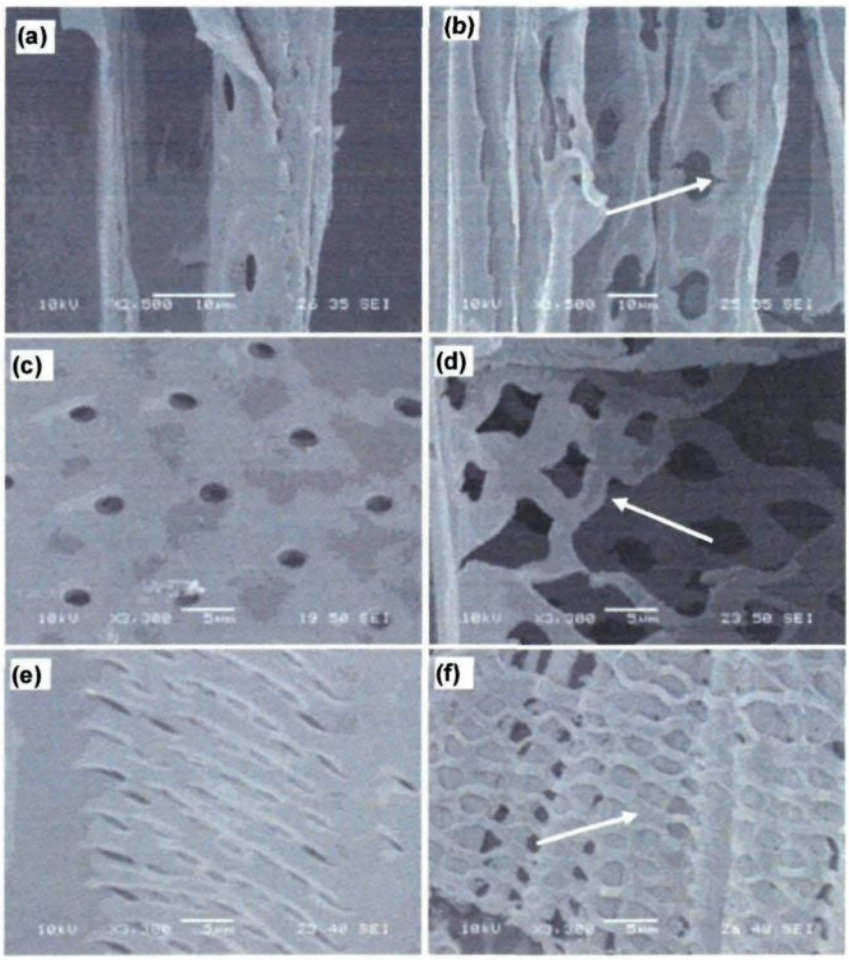

Figure 4. 47 SEM images of pits on tangential longitudinal surfaces of heat-treated wood before and after weathering of 1512 h: (a) jack pine before weathering; (b) jack pine after weathering; (c) aspen before weathering; (d) aspen after weathering; (e) birch before weathering; (f) birch after weathering

Comparison of SEM pictures in Figure 4.47 shows that there are common micro-structural changes of pits on heat-treated jack pine, aspen, and birch tangential surfaces due to weathering. Transverse cracks of pits form while no longitudinal crack across pits is observed on any of the three wood surfaces after weathering. Also, there are different

changes for different wood species. Pit cracks formed on jack pine surface are small and do not cause failure of the pits (Figure 4.47 (b)). Pit structures coalesce originating from pits on aspen surface increase, later big transverse and ruptured cracks are formed, and then deep crevasses are formed (arrow in Figure 4.47 (d)). Degradation of pits between vessel and fiber cells of heat-treated birch after weathering enlarges the area of pits but no large crevasses are observed on birch surface (Figure 4.47 (f)).

b) **Transverse surface**

Additional information on structural changes can be found in SEM micrographs on transverse surface of specimens. Figure 4.48 shows the surface micrographs on transverse surface of untreated woods before artificial weathering, heat-treated woods before and after artificial weathering for 1512 h. Comparing Figure 4.48 (a) and (b), it can be seen that the cracks on middle lamella and slight thinning of cell wall take place on jack pine transverse surface after thermal treatment. These checks appear to be a result of a stress caused by differential shrinkage due to heat treatment. Heat-treated jack pine wood looks more brittle than its untreated counterpart. However, structural changes due to heat treatment are not distinct, and it is likely that plasticization of cell wall material occurs only to a limited degree during heat treatment. This is in agreement with the result of Kollmann and Sachs who found comparable features in spruce after thermal treatment between 190°C and 240°C [35]. Compared to jack pine wood, aspen wood displays less structural changes due to heat treatment as presented in Figure 4.48 (e), showing the presence of smaller cracks on cell wall and slighter thinning of cell wall width. Similar to jack pine wood, the presence of small cracks on middle lamella, slight thinning cell wall width as well as plasticization for

birch takes place after heat treatment (Figure 4.48 (h)). Figure 4.48 (c), (f) and (i) show the microstructural changes of cell occurring after artificial weathering for 1512 h on transverse surfaces of heat-treated jack pine, aspen, and birch, respectively. The development of cracks on middles lamella and thinning of cell wall width for all of the specimens are observed (Figure 4.48); however, their magnitude which is different for different species is difficult to differentiate after the weathering of 1512 h.

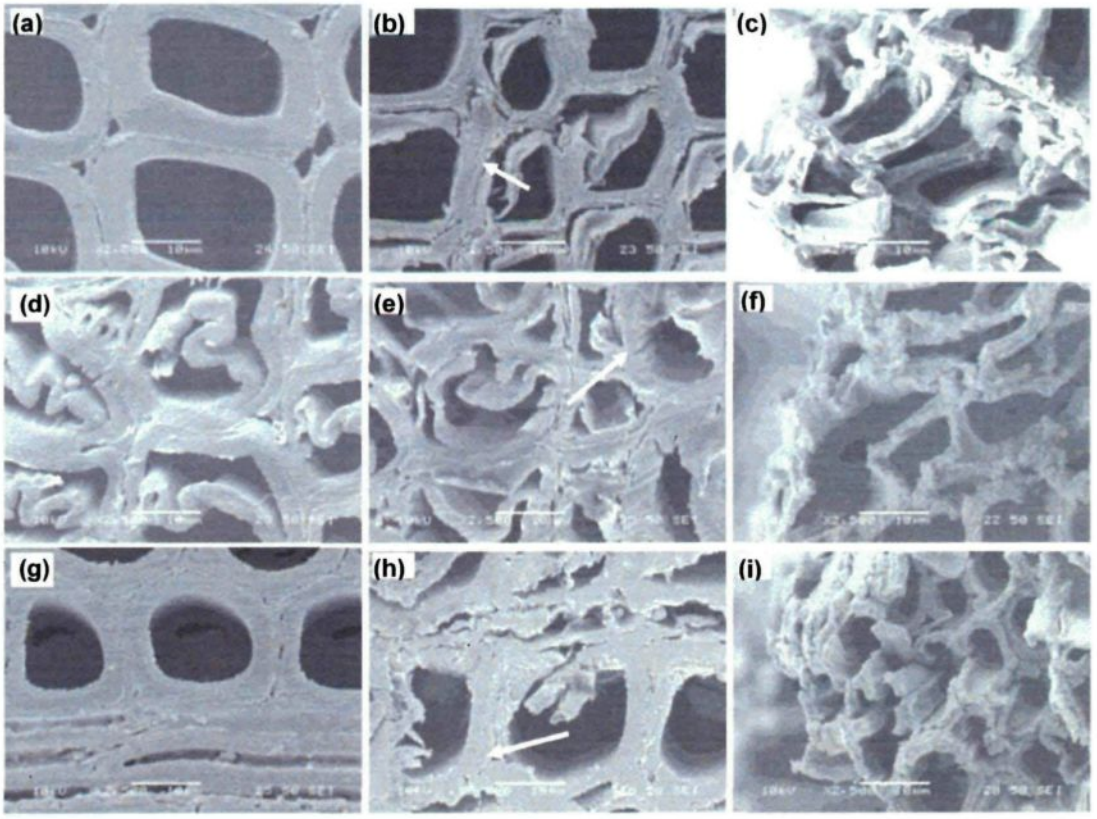

Figure 4. 48 SEM images (×2500) on transverse surface of specimens before and after 1512 h of artificial weathering: (a) untreated jack pine before weathering; (b) heat-treated jack pine before weathering; (c) heat-treated jack pine after weathering; (d) untreated aspen before weathering; (e) heat-treated aspen before weathering; (f) heat-treated aspen after weathering; (g) untreated birch before weathering; (h) heat-treated birch before weathering; (i) heat-treated birch after weathering

4.4.3. Conclusions

a) Results of fluorescence microscopy images show that the degradation increases with increasing weathering time for all three heat-treated species. Heat-treated hardwood is more sensitive to weathering than heat-treated softwood with regards to structural changes. The structure changes more and faster on untreated wood surfaces than on heat-treated wood surfaces for all three species.

b) SEM analysis indicates that degradation due to artificial weathering occurs preferentially in middle lamella of wood surface, where the lignin concentration is higher than that in the cell wall. No noticeable difference in structural change of cell wall is seen on transverse surfaces for jack pine, aspen, and birch after weathering for 1512 h. Degradation of pits appears to be different for three species after weathering. It is difficult to observe a clear difference in surface structure degradation of untreated and heat-treated wood after long term weathering.

4.5. Changes in wettability of heat-treated wood during artificial weathering

4.5.1. General

Wetting properties of wood which is one of the surface properties that is considerably practical and economically significant, give information to facilitate the understanding of chemical and physical property changes occurring during weathering. This information also gives an idea on the different adhesion or coating characteristics required in order to delay the degradation. A number of investigations were carried out on the wettability changes of wood during heat treatment. Wettability and chemical composition of four heat-treated European wood species (pine, spruce, beech, and poplar) performed at 240°C were studied

[37-39]. Effect of drying method on the surface wettability of wood strands was reported [176]. Kocaefe et al. [28] studied the effect of heat treatment on the wettability of white ash and soft maple by water. There also exists some information in the literature which discusses the changes in untreated wood wettability during weathering. The effects of aging on extracted and unextracted polar and dispersion components of the surface free energy of redwood and Douglas-fir were investigated [93]. It was suggested that loss of surface free energy with aging is related to environmental factors rather than wood itself. Wettability of Western red cedar panels exposed to outdoor weathering were studied from the standpoint of wood compositional change induced by weathering [177]. Surface aging is a significant variable affecting the wettability and adhesion of coating on wood surface [100]. The effects of ultraviolet light exposure on the wetting properties of spruce and teak wood were investigated in order to assess the viability of ultraviolet light irradiation as a surface pretreatment technique to activate surfaces for coating adhesion [178]. They proposed that UV irradiation cleaned the wood surface, consequently, the wettability and surface free energy increased significantly after a specific exposure period to UV light. Changes in wettability of tropic woods due to artificial weathering were reported [45].

As it is explained above, various studies were carried out on the wettability of untreated and heat-treated wood, and weathering of untreated wood. To our knowledge, however, the published literature on the change in heat-treated wood wettability during weathering is still lacking. The focus in this part is to investigate the evolution in wettability of the three heat-treated North American wood species during artificial weathering.

4.5.2. Results and discussion

4.5.2.1. Surface wettability changes

The dynamic wettability (contact angle vs. time) of wood samples which were exposed to artificial weathering for different times were measured. This information is useful in understanding the weathering mechanism of heat-treated wood. During this study, the effect of the weathering on the dynamic contact angle, initial contact angle, the total wetting time with water, and consequently, the wetting properties of three heat-treated woods were investigated. Furthermore, the effects of heat treatment and the type of wood species on the wettability were also studied.

Figures 4.49 presents dynamic contact angle of water as a function of time for heat-treated jack pine, aspen, and birch tangential surfaces, respectively. In these figures, the contact angle evolution with time is given for an un-weathered specimen (0 h) as well as for specimens after artificial weathering for different times (72 h, 168 h, 336h, 672 h, 1008 h, and 1512 h). As can be seen in all three figures, the weathering reduces the hydrophobic behavior of these three heat-treated woods; consequently, all the contact angles of weathered heat-treated wood are lower than those of un-weathered wood of the same species (0 h). This shows that the artificial weathering increases the wettability of wood by water. The contact angles decrease significantly after weathering of 72 h for all the three species to different extents depending on the species. As shown in Figures 4.49 (a), the contact angles of heat-treated jack pine do not seem to differ significantly after weathering for 72 h and 168 h, whereas at longer times they continue to decrease with increasing weathering times. The trends observed for both hardwood species (aspen and birch) studied

are found to be very similar (see Figures 4.49 (b) and (c)). Contact angles of heat-treated aspen and birch after weathering decrease with increasing weathering time.

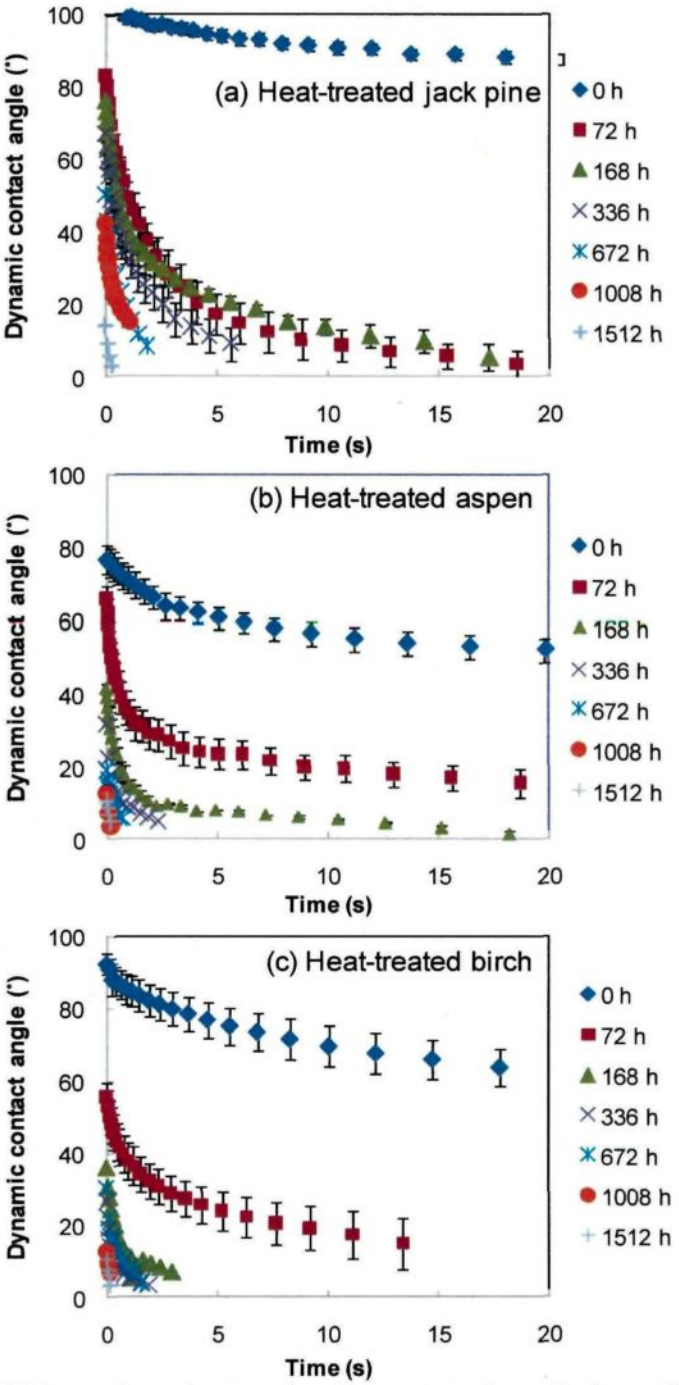

Figure 4. 49 Dynamic contact angle of heat-treated wood after artificial weathering for different times: (a) jack pine, (b) aspen, (c) birch

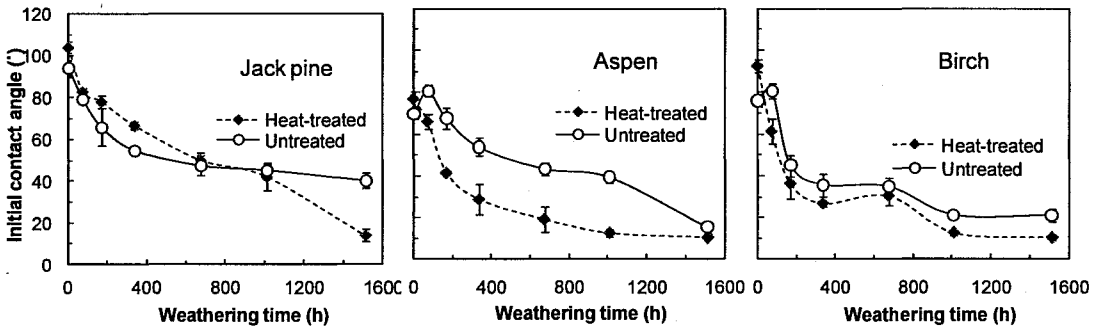

Figure 4. 50 Comparison of initial contact angles of heat-treated and untreated wood as a function of artificial weathering time for three specimens

Figures 4.50 shows the variation in initial contact angle with the weathering time for each species with and without heat treatment. The initial contact angles of all heat-treated and untreated specimens with the exception of untreated aspen and birch decrease with increasing weathering time during weathering. Those of untreated aspen and birch increase with artificial weathering time up to 72 h, above this time they again decrease. This result is similar to that reported in literature [45]. This might be due to the removal of extractives from inside towards surface of untreated samples during weathering. The initial contact angles of heat-treated specimens before artificial weathering are higher than those of untreated wood for all the three species which is in agreement with literature [37, 39, 179]. However, after artificial weathering for 1008 h, the initial contact angle of heat-treated jack pine becomes smaller than that of untreated jack pine while the same trend is observed for aspen and birch only after 72 h of weathering. This might be related to higher amount of extractives presented in untreated wood compare to those of heat-treated wood. After artificial weathering for 1512 h, the difference between the initial contact angles of untreated and heat-treated specimens is largest for jack pine. Untreated jack pine has a

contact angle of 40.3° while other specimens exhibit a contact angle of less than 20.9° for the same weathering time. The effect of heat treatment on initial contact angle after weathering for 72 h to 1008 h is the largest for aspen. These results show that the changes in wettability during artificial weathering differ with heat treatment and type of wood species.

The time required for the water drop to disappear completely (total wetting time) on all three heat-treated and untreated species before and after 1512 h of artificial weathering are presented in Table 4.8. The specimens before weathering (0 h) exhibit different total wetting times depending on the species and whether they are heat-treated or not, ranging from 235 s for untreated aspen to 3004 s for heat-treated jack pine. The total wetting time is longer for heat-treated wood compared to that of untreated wood for all three species studied. The total wetting times of all specimens after weathering of 1512 h are less than 3 s. This result suggests that weathering accelerates considerably absorption and penetration of water on both heat-treated and untreated wood surfaces; consequently, it reduces significantly total wetting time.

Table 4. 8 Total wetting time for complete surface wetting by water for three wood species before and after 1512 h of artificial weathering

Species	Heat treatment	Weathering time (h)	Total wetting time (s)	Standard Error
Jack pine	Heat-treated	0	3003.73	10.87
		1512	0.42	0.10
Jack pine	Untreated	0	1875.67	31.88
		1512	3.39	0.39
Aspen	Heat-treated	0	1730.27	503.10
		1512	0.30	0.11
Aspen	Untreated	0	235.43	17.78
		1512	0.51	0.20
Birch	Heat-treated	0	2076.61	192.28
		1512	0.30	0.07
Birch	Untreated	0	601.41	51.31
		1512	0.37	0.08

As it was stated before, weathering changes wood structural properties [75, 78, 81, 83, 85, 87, 180, 181]. The difference in wood surface structure can cause wettability differences of wood surfaces [45, 182]. Weathering induces changes not only in physical properties of a wood surface but also in its chemical properties [183, 184]. The changes in wettability during weathering can also be related to changes in the chemical properties of a wood surface [45, 100, 177]. As described in the introduction, heat treatment can cause

chemical changes such as hemicelluloses degradation on wood surface; consequently, result in a decrease in its wettability [179].

4.5.2.2. Relation between wettability and surface structural changes

Water in contact with wood surfaces is able to penetrate into the wood substance in three ways: as liquid water flow into cell lumen by capillarity; as water vapour by diffusion into cell lumen; as bound water by diffusion within the cell wall [185]. Therefore, structural differences in surfaces could exert an influence on the water entrance into wood specimens before weathering. The existence of large cracks of vessels on the surface can be observed in aspen and birch which results in lower contact angles than those of jack pine (see Figures 4.49). This result is in agreement with a previous study [45]. The structural comparison of both hardwood surfaces, aspen and birch, reveals the reason for differences in their wettability. The main cells (fibers) of aspen are thinner than those of birch, which results in a larger lumen volume and a decrease in specific gravity. Consequently, water enters the cell wall of aspen at a faster rate; therefore, aspen has smaller contact angles (less wettable and slower water penetration) than birch (shown in Figures 4.49 (b) and (c)).

Previous SEM analysis results suggests that the changes occurring due to weathering in the wettability of heat-treated woods tested in this study might be attributed to the structural changes of wood surface. Large longitudinal and horizontal cracks present on all three heat-treated species surfaces after artificial weathering for 1512 h (arrows in Figure 4.46 (c), (f), and (i)) allow easier entrance of water into cell wall, which consequently decreases contact angles (increases wood wettability). The structural differences in surfaces can also influence the contact angles of specimens after weathering. The

longitudinal cracks of heat-treated jack pine, originated from radial ray parenchyma cells during artificial weathering as shown with an arrow in Figure 4.46 (c) produce slightly higher contact angles (see Figures 4.49). In contrast, the large cracks observed on aspen and birch surfaces, originated from vessel elements due to weathering, result in lower contact angles after artificial weathering for all times (see arrows in Figure 4.46 (f), (e), and Figures 4.50). However, the contact angles of the three heat-treated woods after weathering for 1512 h are almost the same, which indicates the structural differences on different heat-treated species surfaces at this weathering stage does not have any significant effect on wettability. This might be due to the destruction of the original structure of all three wood species.

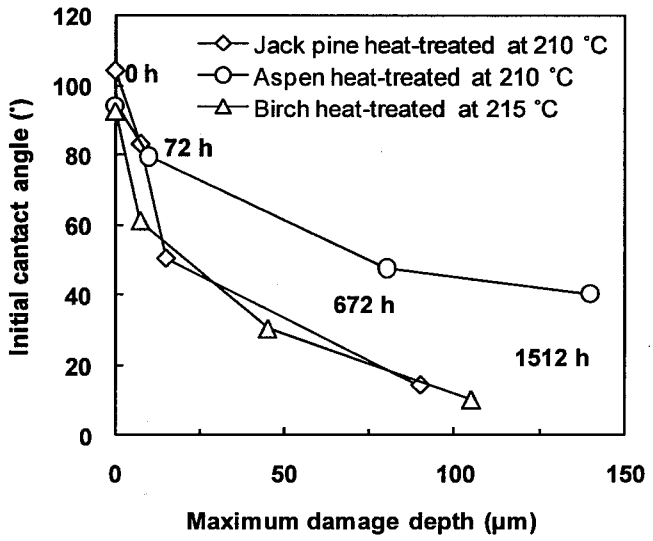

Figure 4. 51 Relationship between maximum damage depth and wettability of three heat-treated species before (0 h) and after artificial weathering for 72 h, 672 h, and 1512 h

Figure 4.51 shows the influence of maximum damage depth on the contact angles of the specimens before and after artificial weathering for 72 h, 672 h, and 1512 h. The structural changes, such as cracks on cell wall and middle lamella and the thinning of cell wall should boost wood wettability. However, as stated above, the wettability of heat-treated wood reduces due to heat treatment for all the three species. This suggests that the chemical changes of wood surfaces have more significant effect on the wettability changes than that of structural changes during heat treatment. This supports the notion described in the previous section. The differences in contact angles of different species are small after weathering for 1512 h. This can be due to the fact that the differences in microstructure between different species are no longer significant at this stage of weathering. Because the lignin concentration is higher in the middle lamella than in the cell wall, the weather degradation occurs preferentially in this area of wood surface. This is noticeable in Figure 4.48 (c), (f), and (i). The loss of lignin makes the surface more hydrophilic; that is, contact angles decrease as shown in Figures 4.49 and 4.47.

The damaged wood layer has different physical and chemical characteristics than those of wood bulk. As shown in Figure 4.51, the contact angles of the specimens clearly decrease with increasing maximum damage depth for all the heat-treated wood species and their decreasing rates differ according to species type during artificial weathering. Thus, the maximum damage depth seems to play an important role in wettability of the species during artificial weathering. After weathering for the same time, the maximum damage depth on heat-treated aspen is the highest. However, the maximum damage depth effect on the initial contact angle is more significant for heat-treated aspen than for heat-treated jack

pine and birch. This result means that the change of heat-treated wood surface structure is just one of the reasons responsible for the changes in wettability due to weathering.

4.5.2.3. Relation between wettability and surface chemical changes

The effect of wood crystallinity on the initial contact angle of heat-treated wood surfaces is shown in Figure 4.52. For all three species, the contact angle increases as the total crystallinity index increases. This indicates the loss of crystallinity as a result of weathering can, in turn, increase wood wettability. Water in contact with wood surfaces is able to penetrate into the wood substance in different ways [185]. A model called "zipper" describing the movement of water into the wood structure by forcing cell wall polymers (hemicellulose, cellulose, and lignin) apart as it moves deeper into the wood structure was proposed [186]. The hydraulic pressure makes it possible for water molecule to separate the cell wall apart. Therefore, differences in quantity and property of cell wall polymers in surfaces could exert an influence on the contact angles of specimens. The sorption of water by wood depends on the hydrophilic nature of each cell wall polymer as well as the accessibility of water to the hydroxyl groups of polymer. Most of the hydroxyl sites in the hemicelluloses and lignin are accessible to moisture. The non-crystalline portion (amorphous cellulose component) of cellulose, which is approximately 40%, and the surfaces of the crystallites are accessible to moisture, but the crystalline part (approximately 60%) is not [187, 188]. The loss of crystallinity during weathering raises the amorphous cellulose component proportion and, consequently, increases the affinity for water.

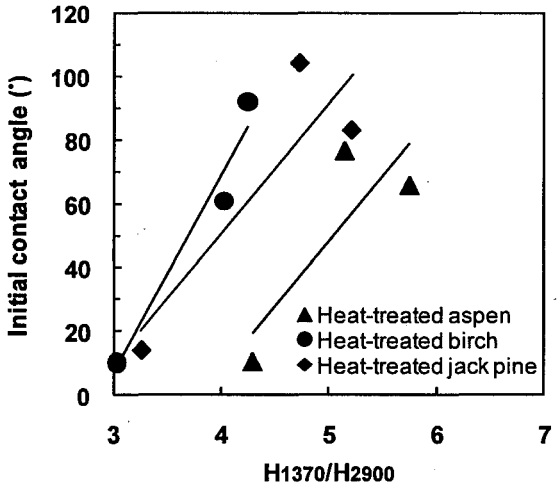

Figure 4. 52 Relationship between crystallinity (H_{1370}/H_{2900}) and contact angle of heat-treated wood surface

Wood is a hydroscopic resource. Other than structural aspect, the functional groups such as hydroxyl groups (-OH), hydrocarbon chains (-CH_2-) and carboxyl groups (-COOH) contribute to the affinity for water [45]. The hydroxyl and carboxyl groups are hydrophilic groups, while the hydrocarbon chains are hydrophobic groups. The changes of these functional groups can change the wettability of water. The bands at 3500, 2900, and 1740 cm^{-1} in Figure 4.29 refer to hydroxyl groups (-OH), hydrocarbon chains (-CH_2-) and unconjugated carbonyl groups (C=O), respectively [45, 70].

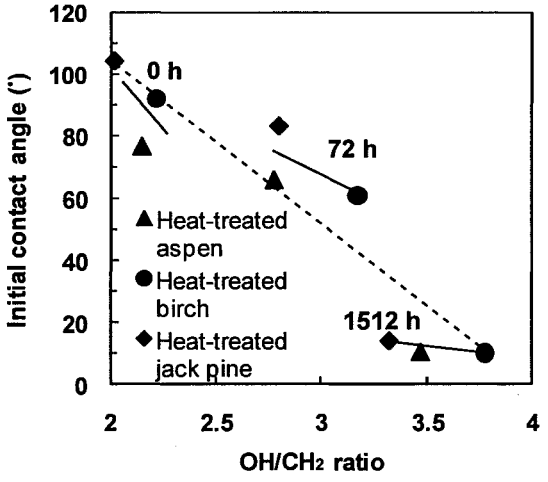

Figure 4. 53 Effect of intensity ratios of bands at 3500 cm^{-1} (OH/CH_2 ratio) to band at 2900 cm^{-1} in FTIR spectra on initial contact angles of three heat-treated woods

On the other hand, the OH/CH_2 ratios of all heat-treated woods increase as weathering time increases up to 1512 h while those of untreated woods increase relatively fast up to the weathering time of 72 h and then decrease slightly (birch, jack pine) or stay almost constant (aspen) between 72h and 1512 h as shown in Figure 4.32 (b). Before weathering, there are more hydroxyl groups on untreated wood surfaces than those of heat-treated wood for all three species; however, after weathering for 1512 h, the opposite is true. This might explain why heat-treated woods exhibit higher wettability by water than untreated woods for all specimens after the artificial weathering process, as shown in Figure 4.50. It is noteworthy to mention that the presence of extractives also has a significant effect on the water wettability of heat-treated wood surface. Kalnins and Feist [94] proposed that one reason for the wettability increase with weathering might be the reduction or removal of extractives which have the water repellent characteristics.

Extractives leave wood surface, but they are partially replaced by those migrating towards the surface from the interior of wood substance during artificial weathering exposure. Since certain extractive content has been removed during the heat treatment process, extractive content of heat- treated woods is less than that of untreated woods. Therefore, extractives replaced by those migrating towards surface from the interior part of the untreated wood are more significant than those of heat-treated wood during weathering. Thus, the quantity of extractives present on heat-treated wood surfaces is less than that of untreated wood surfaces of the same species after weathering. This decreases the hydrophobicity of heat-treated wood surfaces, and consequently decreases the contact angles (more wettable) as shown in Figures 4.50.

The OH/CH_2 ratio for each heat-treated wood species is inversely proportional to the contact angle as shown in Figure 4.53. In addition, as the weathering time increases, the contact angle vs. OH/CH_2 line shifts downwards regardless of the wood species (broken line). This indicates the OH/CH_2 ratio has more significant effect on surface contact angle than that of wood species type during artificial weathering. All specimens tend to exhibit the contact angles of less than 20° when the OH/CH_2 ratios are more than 3 after weathering of 1512 h. As described above, all characteristic IR spectra bands which represent lignin component for all three heat-treated wood species decrease during weathering. This indicates that hydrophobic lignin is degraded more than other hydrophilic wood polymers (hemicelluloses and cellulose) for the specimens tested in this study. Consequently, weathering allows cellulose to become more abundant on the surface, in other words, the wood surfaces have a cellulose-rich layer as a result of weathering. This

cellulose-rich layer causes an increase in hydroxyl groups. It was proposed that a leached and eroded cellulose-rich layer remains on the wood surface after weathering [189]. The observation of cellulose-rich layer on tropic wood surfaces after artificial weathering has been reported by Kishino and Nakano [45] . The band at 3500 cm^{-1} represents hydroxyl groups from water and three wood polymer components (lignin, cellulose, and hemicelluloses) [179]. This is confirmed by the OH/CH_2 ratios calculated by IR intensity of band at 3500 cm^{-1} to band at 2900 cm^{-1} for all specimens tested during this study, which are more than that of oven-dried filter paper (1.7) [45]. In view of the literature and the study stated above, it can be expected that the hydroxyl groups originate not only from cellulose exposed to artificial weathering, but also from other polymers (such as hemicelluloses) and the adsorbed water; and this increases wettability of heat-treated wood. It is worthed to note that part of increase in wettability on heat-treated wood surface due to weathering can be attributed to the increase of the free hydroxyl groups on surface. During this study, it is shown that the crystallinity of cellulose decreases as a function of weathering exposure. That means the cellulose component that originates from crystallized cellulose is affected, which consequently allows more amorphous cellulose content to form during the degradation process. The amorphous cellulose component exhibits additional free hydroxyl groups in the cell wall compared to crystallized cellulose, which can form more hydrogen bonds with environmental moisture and increase water absorption.

Moreover, the results shown in Figure 4.53 indicates that the heat-treated specimens tend to exhibit approximately constant initial contact angle of around 15° (see Figures 4.50) for different OH/CH_2 ratios depending on the species after artificial weathering for 1512 h.

This means that the contact angle of the specimen at this stage is independent of the parameters measured (OH/CH_2 ratios) in this study. This result agrees with the finding by Kalnins and Feist [94] stating that differences between species are probably no longer significant at this stage in regard to wettability. However, differences between species still exist even after the surface develops a cellulose-rich layer with regard to chemical properties. This result is in accordance with that found by Kishino and Nakano [45]. They reported that the wood specimens exhibit a contact angle of 0° at 10 s for different OH/CH_2 ratios after artificial weathering of 600 h depending on the species type. On the other hand, the initial contact angles for the heat-treated specimens before weathering (0 h) and after weathering for 72 h decrease as OH/CH_2 ratios increase depending on different species (Figure 4.53). This result conflicts with the statement by Kishino and Nakano [45] who found that the OH/CH_2 ratios for the specimens before weathering were approximately constant regardless of the contact angle. The influence of OH/CH_2 ratios of different species on the initial contact angle at different weathering times (such as 0 h, 72 h, and 1512 h) is different. Parallel to these results, the contact angle is found to be dependent on OH/CH_2 ratios to different extents depending on the weathering time for the heat-treated specimens tested in this study. Thus, it is probable that factors other than chemical properties, for example structural factors stated above, affect the differences in contact angles of the specimens during different weathering stages.

The presence of extractives also has a great effect on the weathering of wood for water and other liquids. Two types of extractives were discussed in wood: extractives deposited in the coarse capillary structure and extractives deposited in the cell wall

structure [190]. The extractives deposited in the cell wall structure have a great influence on the rate of swelling. As wood is exposed to weathering, the extractives are leached from the surfaces and the surface becomes less water-repellent [177]. The role of extractives in heat-treated wood during the weathering process needs to be investigated further.

4.5.3. Conclusions

a) The weathering increases the wettability of all three heat-treated woods by water. Weathering accelerates significantly absorption and penetration of water on both heat-treated and untreated wood surfaces; consequently, it reduces significantly total wetting time. Changes in wettability during artificial weathering depend on the nature of the heat treatment process and the type of wood species. From SEM and FTIR analysis, the changes in wettability during weathering are estimated to be due to the combination of structural changes in surfaces and chemical changes occurring on the wood surfaces.

b) SEM analysis indicates that the role of structural factors does not seem to be significant on the wettability change observed during heat treatment. Cracks due to weathering degradation result in easier entrance of water into the cell wall of heat-treated wood, which consequently increases wood wettability. Degradation due to weathering occurs preferentially in middle lamella of wood surface where the lignin concentration is higher than that in the cell wall. Contact angles of the specimens clearly decrease with increasing maximum damage depth for all the heat-treated wood species and their rates of decrease differ according to species type during weathering. Structural differences in different species surfaces could have an influence on the water entry into the wood before weathering. The differences in contact angles of different species after weathering for

1512 h are not significant which indicates that the differences in microstructures of different species are no longer significant at this stage of weathering.

c) The FTIR spectra results suggest that the OH/CH_2 ratio for heat-treated specimens is inversely proportional to the contact angle regardless of the wood species. Weathering allows the cellulose component to become more abundant on the surface. The cellulose-rich layer on wood surface and the increase in amorphous cellulose (transformed from the crystallized cellulose due to weathering) result in an increase of hydroxyl group, which consequently increases heat-treated wood wettability.

4.6. Degradation of heat-treated wood during artificial sunlight irradiation without water spray

4.6.1. General

In view of the literature (see Chapter 2), among the weathering factors, UV radiation which is a part of solar radiation is known to be mainly responsible for initiating a variety of chemical changes and discoloration of wood surfaces [1, 4]. Studies have also shown that artificial weathering without water spray results in poor aesthetics for untreated wood because of the discoloration and surface checking when exposed to UV radiation [2, 9-12]. Investigations on the wettability changes, chemical changes and microscopic changes of heat-treated wood after exposure to artificial sunlight irradiation are very limited, and there is no publication available in literature on the degradation taking place due to the sunlight irradiation of jack pine wood.

The investigations on the chemical and physical changes of heat-treated woods during artificial weathering with water spray to simulate the rain of natural weathering have

been previously carried out and presented in Sections 4.2 to 4.5. The objective of this section is to understand chemical and physical changes taking place, and to identify stages of these changes when the heat-treated wood is exposed to artificial sunlight irradiation without water spray for various periods. It is important to note that, in the weathering tests without water spray, air had a relative humidity of 50% even when temperature increases to the set value in the test chamber. The North American jack pine was chosen to investigate the degradation mechanisms due to sunlight irradiation without water spray. Heat-treated and untreated jack pine samples were exposed to artificially sunlight irradiation for different periods. The changes in microscopic and chemical structures and modifications taking place on heat-treated wood surfaces due to irradiation were analyzed using different analysis methods.

To avoid repetition, the changes due to artificial weathering with water spray which were analyzed and presented previously will not be discussed in detail; only some comparisons with those results will be given.

4.6.2. Testing materials and artificial sunlight irradiation(UV-VIS irradiation) tests

Jack pine (*Pinus banksiana*), commonly used for outdoor applications in North America, was studied. The wood samples were obtained from ISA Industries, Normandin, Quebec. The heat-treatment was carried out using Finish ThermoWood technology at the maximum temperature of 210°C.

Artificial sunlight weathering test was conducted at South Florida Test Service, Accelerated Weathering Laboratory (ATLAS weathering services), using an Atlas Ci65/Ci65A Xenon Weather-Ometer. There was no water spray but relative humidity was

set at 50±5%. The black panel temperature was 63 ±3 °C and irradiance level was 0.55 W/ m^2 at 340 nm. The irradiation was interrupted after 72, 168, 336, 672, 1008, and 1500 h of weathering and samples from each set of samples (untreated or heat-treated under different experimental conditions) were taken out at the end of each weathering time for evaluation of surface properties. They were stored in room temperature at 20 °C and 40% relative humidity until they were subjected to the characterization tests.

4.6.3. Results and discussion

4.6.3.1. Changes in properties of heat-treated wood during artificial sunlight irradiation

4.6.3.1.1. Visual observation

Figure 4.54 (a, b, c) shows the color changes and physical changes on radial and tangential surfaces of heat-treated jack pine and the tangential surface of untreated wood during artificial sunlight irradiation without water spray. The colors of both heat-treated and untreated jack pine become whiter with increasing weathering time. The final colors of these specimens obtained under three sets of experimental conditions are similar. The visual inspection shows that the radial surfaces of heat-treated wood are smooth and remained without cracks even after artificial sunlight irradiation of 1500 h (Figure 4.54 (a)). On the other hand, minor cracks starts to appear on the tangential surfaces of treated specimens after accelerated sunlight weathering of 672 h (shown with arrows in Figure 4.55 (b)). Visible cracks are clearly observed on the tangential surfaces of the untreated specimens after weathering of 1500 h while there is no crack appeared on radial part of sample surface during the artificial sunlight irradiation. These results indicate that the

development of cracks due to sunlight irradiation is more significant on tangential surfaces than on radial surfaces for both heat-treated and untreated jack pine. This phenomenon is probably due to the effect of rays on the swelling and shrinking stresses on radial surfaces produced under artificial sunlight irradiation. Compared to untreated specimen weathered for 1500 h (see Figure 4.54 (c)), the heat-treated boards retain their physical structure better, and it is clear that their surface is smoother and has fewer cracks as shown in Figure 4.54 (a, b). This result agrees with the previous study of Manoj and his co-workers [11]. They reported that no surface checks were observed on the weathered surfaces of oil heat-treated specimens and the percent swelling after weathering in treated specimens was less than that of untreated wood.

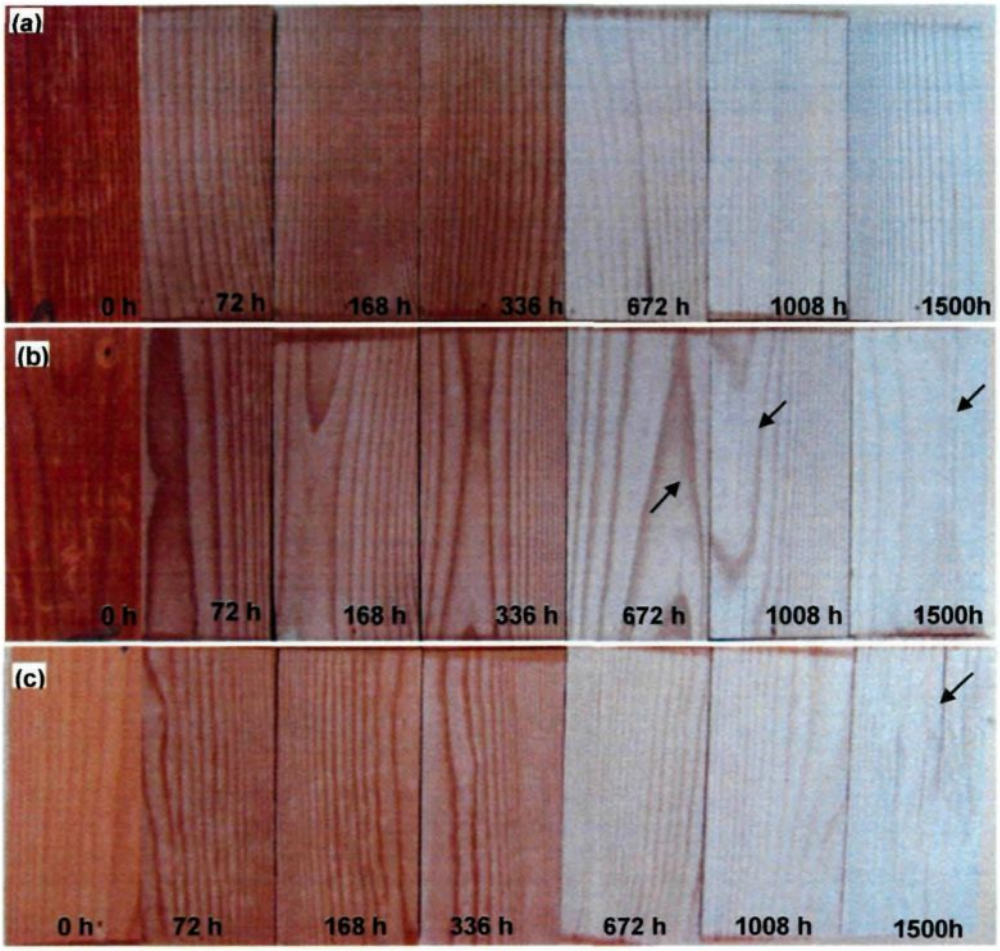

Figure 4. 54 Jack pine surfaces during artificial sunlight irradiation: (a) radial surface of wood heat-treated without water spray, (b) tangential surface of heat-treated wood, (c) tangential surface of untreated wood

4.6.3.1.2. Microscopic structural changes

During this study, the scanning electron microscope (SEM) was used to investigate the breakdown of heat-treated jack pine wood structure caused by artificial sunlight irradiation. Wood surfaces, both heat-treated and untreated, were investigated. SEM analysis of the transverse and longitudinal surfaces of heat-treated jack pine wood clearly

shows the microstructural changes occurring during sunlight irradiation (see Figures 4.55-4.58) as explained below.

a) Degradation of middle lamellar

From the comparable features on the transverse surfaces of jack pine before and after heat treatment (Figures 4.55 (a) and (b)), it can be seen that the changes of cell wall material due to heat treatment occurs only to a limited degree during heat treatment. The photo degradation took place preferentially in the middle lamella and primary wall for both heat-treated and untreated jack pine wood. This phenomenon is particularly noticeable at the corners of the middle lamella shown in the micrograph of the untreated jack pine transverse surface after an weathering of 1500 h (see Figure 4.55 (c)). Heat-treated wood transverse surface shows similar degradation (see Figure 4.55 (d)). Both untreated and heat-treated wood degraded at the middle lamella when subjected to artificial sunlight irradiation. As reported in the literature [191], the middle lamella and primary wall are mainly composed of lignin (84%) with lesser amounts of hemicelluloses (13.3%) and even some cellulose (0.7%). The severe degradation in the middle lamella after sunlight irradiation indicates that lignin is more photosensitive than other composites in wood cell wall. In addition, the heat-treated wood degraded more severely at the secondary wall than untreated wood due to artificial sunlight irradiation (see Figure 4.55 (c) and (d)). This can be explained with the degradation of hemicelluloses [9] content of the secondary cell wall which is already low in cellulose content compared to that of untreated wood due to heat treatment (see Figure 4.55 (b)); consequently, the percentage of lignin is increased. The

concentration and content of hemicellulose are higher in the secondary wall than in the middle lamella and primary wall [191].

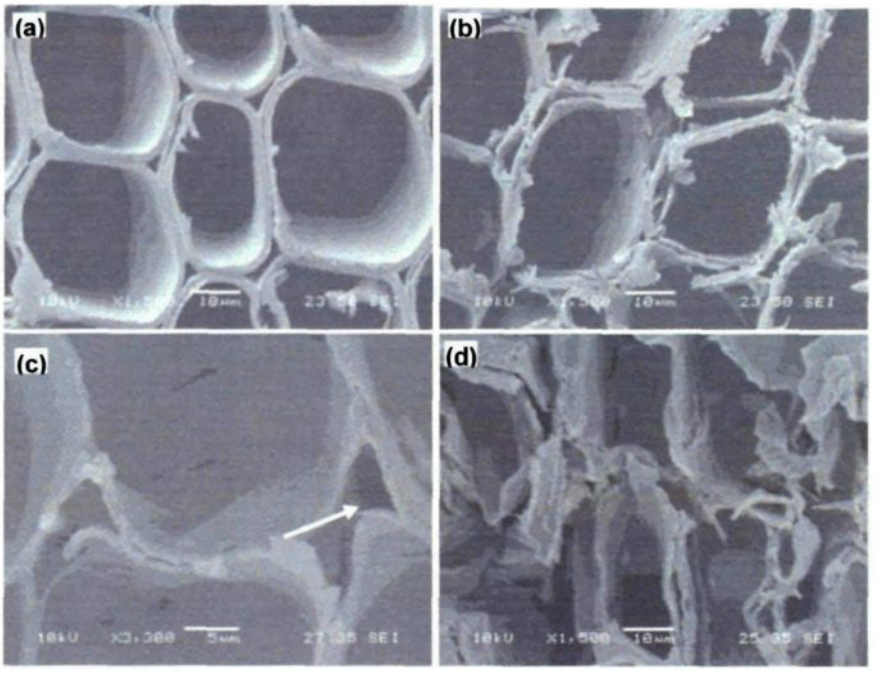

Figure 4.55 SEM images comparing the structural changes of earlywood tracheids on a transverse surface due to heat treatment without water spray and weathering to artificial sunlight irradiation for 1500 h: (a) untreated before weathering; (b) heat-treated before weathering; (c) untreated after weathering; (d) heat-treated after weathering

The artificial sunlight irradiation induces the degradation of cells around the resin channels (see the arrow in Figure 4.56 (b)), which is caused by differential dimensional changes between the ray cells of resin channels and the surrounding wood during artificial sunlight irradiation.

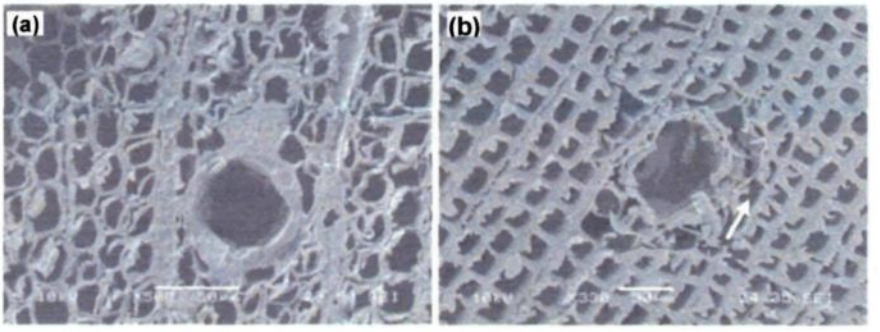

Figure 4. 56 SEM images of resin channels on transverse surfaces of jack pine heat-treated without water spray before and after artificial sunlight irradiation: (a) heat-treated before weathering; (b) heat-treated after an weathering of 336 h

b) Checking of cell wall

Micrographs of tangential surface of heat-treated wood also show the degradation of lignin during artificial sunlight irradiation (see Figures 4.57 (a-c)). After artificial sunlight irradiation for 672 h, longitudinal cracks which extend aligned with the fibril orientation and diagonal to the fiber axis of the tracheid, diagonal cracks originating from pits, and a zone of decay on the tangential surface of heat-treated wood (see Figure 4.57 (b)) are observed. The cracks developed and enlarged principally as a result of contraction in cell walls caused by the moisture during the extended irradiation exposure. It seems that the binding of cellulose microfibrils in the various cell wall layers by lignin has been degraded after artificial sunlight irradiation for 1500 h. Consequently, a separation between two adjacent cells occurred and tracheids loosened, collapsed, and became detached from the substrate of wood (see Figure 4.57 (c)).

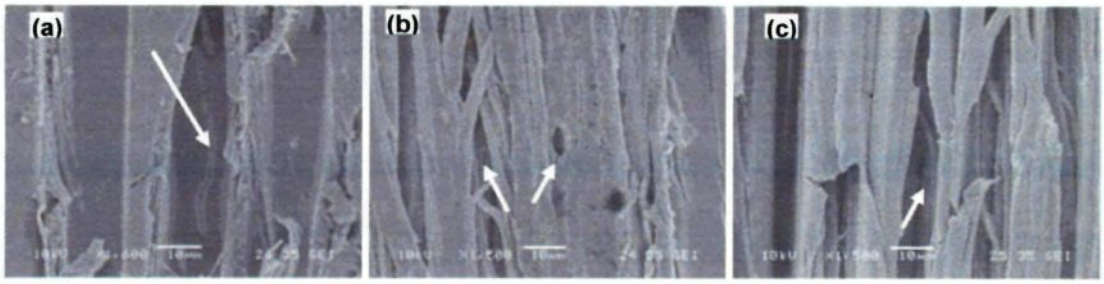

Figure 4. 57 SEM image showing micro-cracks on tracheid cell wall of a tangential surface of jack pine latewood due to heat treatment without water spray and artificial sunlight irradiation: (a) heat-treated before irradiation; (b) heat-treated after irradiation for 672 h; (c) heat-treated after irradiation for 1500 h

The checking of heat-treated jack pine wood surface during sunlight irradiation is different depending on the part and the direction of wood grain. Figure 4.58 (a) and (b) shows the SEM micrographs of radial and tangential surfaces of heat-treated jack pine irradiated for 1500 h. The comparison of both surfaces reveals the difference in cracks features on both surfaces. A large number of small longitudinal and transversal cracks are observed from the micrographs on the tangential surface. In contrast, the existence of large longitudinal cracks along the earlywood/ latewood interface can be observed on the radial surface. Larger number of cells becomes detached from the earlywood bands on the radial surface of heat-treated wood compared to those of latewood. The different degradation behaviors are observed for earlywood and latewood of heat-treated jack pine and are shown in Figure 4.58 (c) and (d). Abundant uniseriates and diagonal microchecks occurred on longitudinal tangential surface of heat-treated earlywood after irradiation for 336 h, and all ray cells had disappeared from the surfaces of weathered wood; consequently, only cavities remained (see Figure 4.58 (c)). However, no transverse cracks are observed on the

earlywood surface. In contrast, no diagonal microchecks of cell wall are observed on the surface of latewood (see Figure 4.58 (d)) even after an irradiation of 1500 h. However, large longitudinal cracks originating from the degradation of ray cells, transverse cracks caused by the break of microfibril (see big arrows in Figure 4.58 (d)), many pit structures coalesce (see small arrow), and deep crevasses in the cross field form.

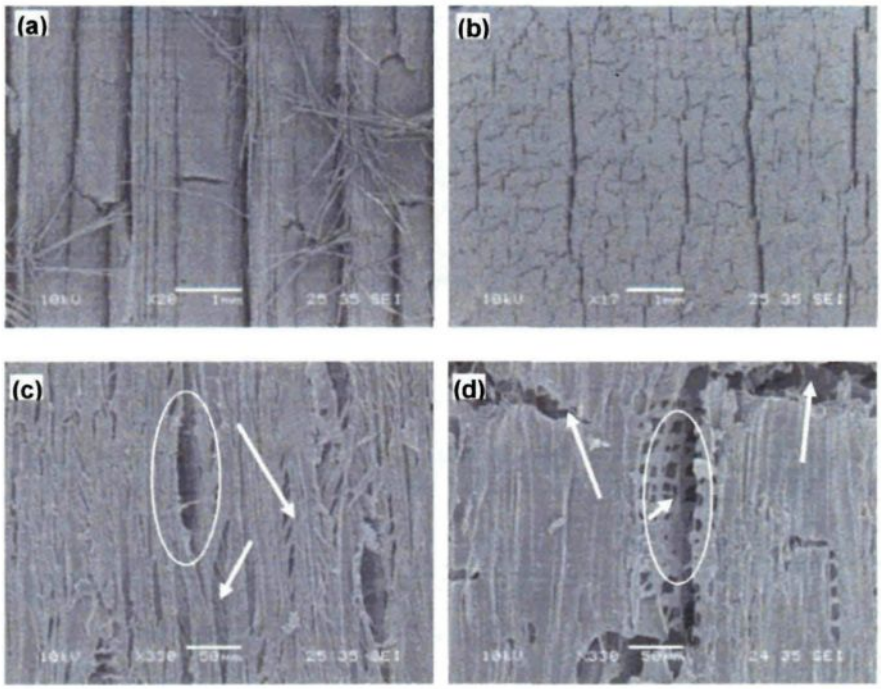

Figure 4. 58 SEM images comparing cracks on jack pine heat-treated without water spray due to artificial sunlight irradiation: (a) radial surface irradiated for 1500 h, (b) tangential surface irradiated for 1500 h; (c) earlywood irradiated for 336 h; (d) latewood irradiated for 336 h

SEM analysis indicates that the degradation of heat-treated jack pine due to artificial weathering without water spray occurs in the middle lamella between wood cells, where the lignin concentration is highest in the cell structure. Comparing with the SEM analysis

results of heat-treated wood subjected to weathering with water spray, which was presented in Section 4.4, the structural changes in the cell wall are similar for the cases with and without water spray after weathering for 1500 h.

4.6.3.2. Color changes during artificial sunlight irradiation

Figure 4.59 shows plots of the redness (a*), yellowness (b*), lightness (L*), and the total color difference (ΔE) of heat-treated and untreated jack pine as a function of artificial sunlight irradiation time.

Decrease in a* values indicates a tendency of wood surface to become greener while increase points out to a tendency to become redder. The rate of change of a*values represents the rate of wood color change. During early times of weathering, a*value of untreated wood increases significantly with artificial weathering exposure up to 72 h while those of heat-treated wood decreases significantly on both radial and tangential surfaces. Then the a*values of both heat-treated (radial and tangential surfaces) and untreated wood reaches almost the same end value with irradiation time up to 336 h. Subsequently, they decrease rapidly after irradiation for 672 h, followed by a decrease at a slower rate up to 1500 h. The red-green tint levels of heat-treated and untreated wood are mainly the same after irradiation of 672 h, 1008 h as well as 1500 h, respectively.

Decrease of b*values indicates a tendency of wood surface to become bluer while increase of b*values means a tendency to become yellower. As shown in Figure 4.59 (b), the trend observed for the b*value changes of heat-treated wood on both radial and tangential surfaces due to artificial sunlight irradiation is similar to that of a*value, decreasing significantly at the beginning, later remaining the same for certain time, and

then descending rapidly followed by a decrease at slower rate. The b* value of untreated wood stays constant with irradiation time up to 168 h, and then decreases quickly up to 672 h, next the decrease rate was reduced. After artificial sunlight irradiation for 168 h, the changes of b*value for the three wood surfaces are almost the same. The color of both heat-treated and untreated jack pine surface becomes bluer during exposure to irradiation.

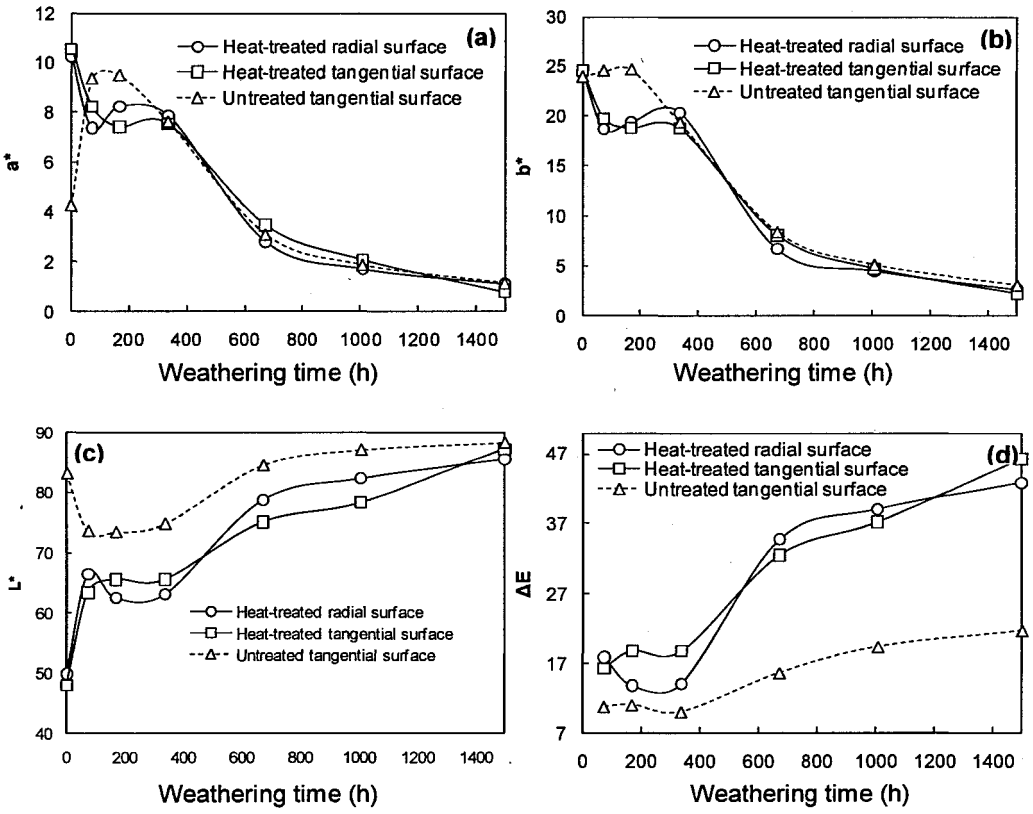

Figure 4. 59 Color changes of jack pine surface during artificial sunlight irradiation without water spray: (a) red/green coordinate (a*), (b) yellow/blue coordinate (b*), (c) lightness coordinate (L*), (d) total color difference (ΔE)

As shown by the changes in L* values, brightening and darkening of wood surface were evaluated. Figure 4.59 (c) shows L* plotted as a function of the weathering time for heat-

treated and untreated jack pine. L* is the most sensitive parameter for the wood surface quality during artificial sunlight irradiation. Similar to a*value, L*value displays different trends for heat-treated and untreated jack pine at earlier times of irradiation, whereas the trends observed for radial and tangential surfaces of heat-treated wood are similar. For untreated wood, L* decreases to a minimum value up to irradiation time of 72 h, then it increases at a different rate during extended artificial irradiation. This implies that untreated wood become darker when exposed to sunlight for 72 h and then become lighter as the irradiation time increases. It is demonstrated that the darkening of untreated wood during the first stage of artificial sunlight irradiation is mainly due to the migration of extractives to the wood surface caused by the high temperature during artificial sunlight irradiation. Several previous studies reported similar result of darkening of untreated wood surface depending on different artificial sunlight weathering times and the type of wood species [11, 17, 18, 192]. The lightening of heat-treated wood increases during the first irradiation stage of 72 h, later stayes more or less stable up to 168 h, and then increases with increasing times of weathering until the end of the test. This matches with the lightness result of untreated wood. Extractives of heat-treated wood have been degraded and removed during high temperature heat treatment. Thus, changes in lightness of heat-treated wood with increasing time of artificial sunlight irradiation are mainly due to the lignin photodegradation and become lighter starting from the beginning of irradiation. After an irradiation of 1500 h, similar to the tendencies observed for redness (a*) and yellowness (b*), the lightness levels of heat-treated and untreated wood are mainly the same. This

indicates that the final colors of untreated and heat-treated jack pine after artificial sunlight irradiation for 1500 h become alike.

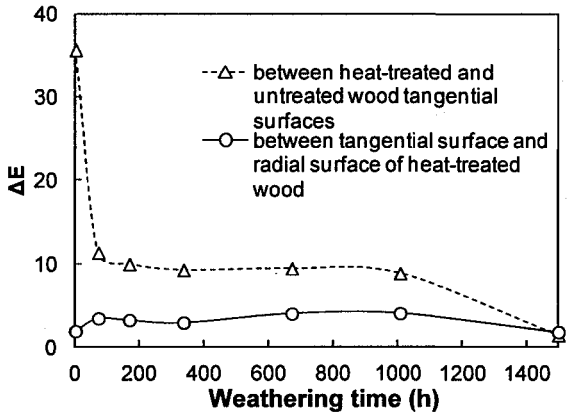

Figure 4. 60 Total color difference between different specimens at the same artificial sunlight irradiation stage

Figure 4.59 (d) presents the total color differences (ΔE) for heat-treated and untreated specimens. The colors of radial and tangential surfaces of heat-treated wood are almost the same. It can be observed that the color of heat-treated jack pine changes more significantly than that of untreated wood at all times during artificial sunlight irradiation. This result disagrees with the results of several previous investigations on the color change of heat-treated and untreated wood [1, 11, 13, 15, 17]. Ayadi and his co-workers reported that the color difference for ash, beech, maritime pine, and poplar heartwood, heat-treated under nitrogen, was less during the 835 h of UV-light weathering when compared to that of untreated wood [15]. They attributed the better resistance of heat-treated wood to light to the less attack on lignin. But they did not show the details of color tint change such as lightness; therefore, it is difficult to compare their results with the results of the present

work. It was reported that the color of heat-treated Scots pine changed less than that of untreated wood during artificial weathering [17]. Thermal modification of spruce wood was found to be effective in stabilizing color during long term artificial UV light exposure [18]. Manoj and his colleagues found that oil heat treatment can improve Radiata Pinewood color stability, and this was attributed to a protective oil layer on the wood surfaces [11]. It was also reported that color of heat-treated okan sapwood changed less compared to the color change observed for the same species before treatment [13].

Lightness is the most sensitive parameter for the wood surface quality during sunlight irradiation. The total color change depends mainly on the changes in lightness. In the view of the studies mentioned above, the lightness of untreated woods decreases and increases whiles those of heat-treated wood increases during different irradiation stages. The tendency of color change of wood during weathering experiments depends on artificial weathering conditions, type of wood species, and heat treatment techniques and conditions. It was shown that the color change trends of both heat-treated and untreated jack pine specimens used in this study are similar after 72 h resulting in relatively close final colors after irradiation for 1500 h (see Figure 4.59 (a-c)). As shown in Figure 4.60, it can be observed that the color difference between heat-treated and untreated woods at the same artificial irradiation stage reduces rapidly at the beginning of irradiation (72 h), later remains mainly the same up to 1008 h, and finally decreases to a value of 1.4 after 1500 h. According to Yoshimoto et al. [193], the above values of color difference between heat-treated and untreated samples after an artificial sunlight irradiation weathering of 1500 h, are significant and visible to the naked eye. It is possible to perceive differences of about

3.8 units of ΔE^* [17, 192]. Thus, the difference of ΔE between heat-treated and untreated wood surfaces during artificial sunlight irradiation is due to the difference in their initial colors. The color of both untreated and heat-treated specimens changes to white and gray at the end of the irradiation; however, the original color of heat-treated wood is darker than that of untreated wood before irradiation. The color of wood surface is related to the different wood composites depending on type of wood species and wood treatment methods used. The decrease in lightness and the increase in the color difference of heat-treated wood are caused by a decrease in hemicelluloses content, especially pentosan [33]. It was reported that thermal treatment at high temperature degraded cellulose, hemicelluloses[194] and extractives [195]. Kollman and Fengel reported that heat treatment caused lignin condensation[194]. Photo-discoloration of untreated wood was mainly due to chromophores formed from the photodegradation of lignin and degradation and leaching away of extractives during weathering. Extractives have antioxidant properties and can limit wood color change to light [15]. In the view of these results, the lower color stability of heat-treated jack pine was estimated to be due to increase in lignin condensation and decrease in extractives caused by heat treatment. Consequently, the heat-treated wood surface has reduced antioxidant properties attributed to lower extractive content, and its color changes more than that of untreated wood during artificial sunlight irradiation.

A comparison of the color changes of the heat-treated jack pine subjected to artificial weathering with water spray (Figure 4.38) and without water spray (Figure 4.59) indicates that:

1) Weathering has a significant effect on the color of the heat-treated wood surfaces for both cases with and without water spray. All the color changes on surfaces brought about by both weathering processes are essentially complete approximately after 672 h of weathering. After the specimens have been subjected to 1500 h of weathering, the colors due to both weathering processes are found to be similar.

2) Artificial weathering with water spray affects colors of heat-treated wood quite differently compared to those without water spray for the same species, especially at early weathering times (<372 h). The color parameters of heat-treated woods subjected to weathering with water spray seem to change significantly at the beginning and then slightly for the rest of the weathering period. However, in the case of weathering without water spray, the color of woods changes slightly even during the initial weathering period as well. The change of color takes place earlier in weathering process with water spray compared to that without water spray.

4.6.3.3. Wettability changes

During this study, the dynamic wettability of sample surfaces which were exposed to artificial sunlight radiation for different times was recorded and compared with that of non irradiated (non weathered) samples. The effect of the sunlight irradiation on dynamic contact angle with water, consequently, on the wetting properties of heat-treated jack pine was investigated. Furthermore, the effects of heat treatment on the wettability were also studied.

Figure 4.61 (a) and (b) present dynamic contact angle of wood/water system as a function of time for untreated and heat-treated jack pine tangential surfaces, respectively. In

these figures, the contact angle evolution with time is given for a non-weathered specimen (irradiation time of 0 h) as well as for specimens after artificial sunlight irradiation for 72 h and 1512 h. All the contact angles of irradiated wood are lower than those of non-irradiated wood, indicating the sunlight irradiation has impact on the hydrophobic behavior for both untreated and heat-treated jack pine woods. Contact angles of untreated and heat-treated samples after irradiation reduces with increasing irradiation time to different extents. All dynamic contact angles of heat-treated sample before irradiation are higher than those of untreated sample. On the contrary, the contact angles for heat-treated sample after irradiation for 72 h are lower considerably than those of untreated sample due to the different effect of artificial sunlight irradiation on heat-treated and untreated wood surfaces. The contact angles of untreated and heat-treated jack pine do not seem to differ significantly after irradiation for 1500 h, and water is absorbed by both woods within one second.

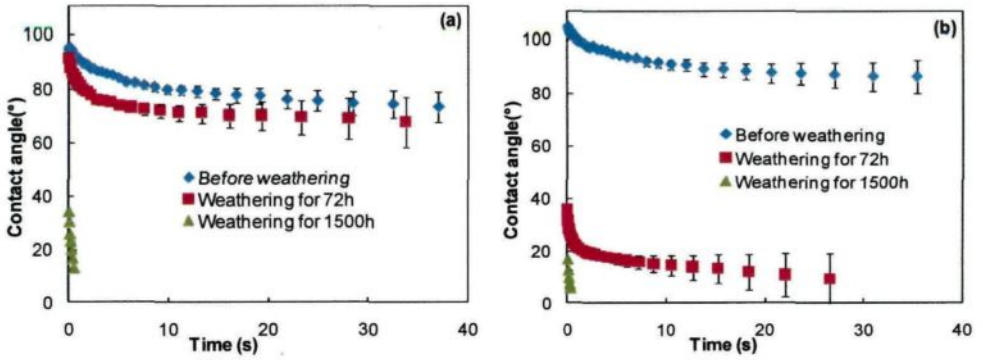

Figure 4. 61 Wettability on tangential surfaces of jack pine latewood before and after artificial sunlight irradiation for different periods: (a) untreated wood, (b) wood heat-treated without water spray

As stated previously, the difference in wood surface structure can cause wettability differences between wood surfaces [45, 182]. SEM analysis indicates that anatomical structure of samples is only slightly affected during heat treatment whereas dynamic contact angles increase significantly after heat treatment. This implies that the structural factors do not play an important role on wettability while the chemical changes of wood surfaces have more significant effect on the wettability changes during heat treatment. As it was stated before, sunlight irradiation changes the structural properties of heat-treated wood (Figure 4.55-4.59). Similar to the case of weathering with water spray, SEM analysis indicates that the changes occurring in the wettability of heat-treated samples tested might be attributed to the surface structural changes due to sunlight irradiation. Cracks formed on heat-treated sample surfaces after artificial sunlight irradiation (shown in Figure 4.57 (c), (d) and Figure 4.58) decrease the contact angles and thus increase the wettability (shown in Figure 4.61 (b)). This effect of sunlight irradiation on wettability is different for heat-treated and untreated samples after artificial sunlight irradiation weathering of 72 h. No evidence is observed that the differences in contact angles of heat-treated and untreated wood after this time is related to their structural properties. In addition, the contact angles of both heat-treated and untreated woods after irradiation for 1500 h are relatively close, which is in agreement with the results of heat-treated jack pine, birch, and aspen after weathering with water spray for 1512 h (see Section4.5). This indicates that either the structural differences on different wood surfaces do not have any significant effect on wettability or the structural changes are similar for different woods and for different weathering processes for this weathering period.

Further analysis of the structural changes found in SEM micrographs on the transverse surfaces of specimens seems to demonstrate the evolution of water wettability on heat-treated samples during artificial sunlight irradiation (see Figure 4.55). As it was stated above, the lignin concentration is highest in the middle lamella, and thus the photo-degradation occurs preferentially in this area. This is noticeable in Figure 4.55 (c) and (d). The degradation of the middle lamella results in the separation of adjoined cells, which causes easier entrance of water into wood. Furthermore, the degradation of lignin by irradiation also makes the surface more hydrophilic.

It can be observed that the wettability of all three heat-treated woods by water increased during both weathering processes with and without water spray (see Section 4.4).

4.6.3.4. Chemical changes due to irradiation without water spray

a) FTIR analysis

In this study, the results of the infrared study of heat-treated jack pine samples during artificial sunlight irradiation without water spray were presented and compared with those of untreated samples in order to investigate the mechanism details. Figure 4.62 shows the FTIR spectra between the spectral region of 1800-750 cm^{-1} on untreated jack pine before irradiation and heat-treated samples irradiated under simulated sunlight for different periods. Chemical differences brought about by heat treatment and light irradiation can be clearly seen in the infrared spectra in the band shapes.

The spectra differences between heat-treated and untreated woods have to be taken into consideration. The top two spectra in Figure 4.62 show uniquely different infrared spectra for untreated and heat-treated jack pine before irradiation, respectively, although

their infrared spectra in the studied region had some similar features. Upon analysis of the spectra, it can be seen that the relative intensity of band at 1740 cm^{-1} (which is a characteristic of non-conjugated carbonyl group stretching in xylan in hemicelluloses) decreases slightly after heat treatment whereas the relative intensity at 1510 cm^{-1} (which is assigned to lignin) is not significantly affected by heat treatment (increases slightly). This is similar to the tendencies at 1510 cm^{-1} for birch and aspen (see Section 4.2). This indicates that the degradation of hemicelluloses can consequently cause a decrease in water absorption. This can be confirmed by the lower relative intensity on heat-treated sample surface of band at 1650 cm^{-1} which may refer to adsorbed water. Another peak which has to be taken into consideration is the decrease, after heat treatment, in the peak at 1230 cm^{-1} which is characteristic of syringyl nuclei [61]. This indicates that the degradation of lignin also occurs during heat treatment.

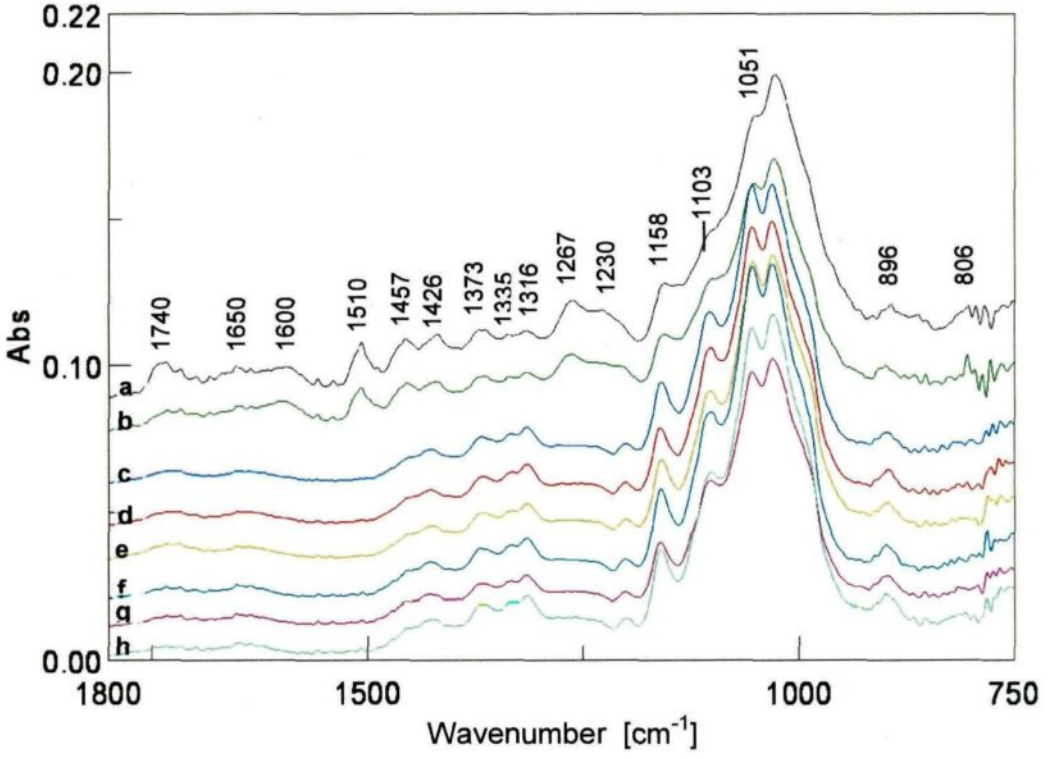

Figure 4. 62 FTIR spectra of jack pine heat-treated without water spray during artificial weathering: (a) untreated before weathering, (b-h) heat-treated samples weathered for : (b) 0 h, (c) 72 h, (d) 168 h, (e) 336 h, (f) 672 h, (g) 1008 h, (h) 1500 h

It is clearly apparent from the results of IR analysis that irradiation has a significant effect on the functional groups found on the heat-treated wood surfaces. Absorption intensities of certain absorption bands change after irradiation for 72 h. A general observation that can be made from the results is that the effect of irradiation on untreated and heat-treated samples might be very similar in the long term. Light irradiation degradation of heat-treated wood samples cause mainly changes in the absorption intensity at the peaks shown in Figure 4.62. The changes in these bands are related to changes in the chemical composition of functional groups and the chemical structure of wood components

listed in Table 4.6 (Section 4.2). All the bands at 1600 cm^{-1}, 1510 cm^{-1}, 1457 cm^{-1}, 1426 cm^{-1}, 1267 cm^{-1}, 1103 cm^{-1}, and 806 cm^{-1} represent lignin characteristics. As shown in Figure 4.62, all these characteristic bands of lignin decrease to different extents as a result of artificial sunlight irradiation of heat-treated jack pine sample. As shown in Table 4.6, the peak at 1510 cm^{-1} is mainly the characteristic absorption of C=C in an aromatic ring that originated from lignin in wood. It can be observed that the peak at 1510 cm^{-1} disappeared after irradiation for 72 h. This is in agreement with previous study on untreated wood reported by Pandey [118]. The intensities of peaks at 1373 and 896 cm^{-1} which are mainly due to carbohydrates (cellulose and hemicelluloses) and had no significant contribution from lignin are not affected significantly by irradiation. Moreover, the intensity of 1158 cm^{-1} band increases upon prolonged weathering indicating that lignin is the component of heat-treated wood which was most degraded during irradiation. As a result of this significant photochemical degradation of lignin by irradiation, Erin et al. [57] reported that the new bands at 1730 and 1650 cm^{-1}, which may be due to the formation of unconjugated free carbonyl groups, quinines, and quinine methides (responsible for yellowing of wood surface), were generated and changed under different artificial weathering conditions. However, as Figure 4.62 shows, the new bands at 1730 $cm^{-1}$and 1650 cm^{-1} are not detected in the present study on heat-treated wood surface during irradiation.

In order to determine the rate of lignin degradation and non-conjugated carbonyl groups content, the intensities of the carbonyl absorption band at 1740 cm^{-1}, lignin reference band at 1510 cm^{-1}, and carbohydrate reference bands at 1375 cm^{-1} were measured as suggested in literature [44]. The relative change in the ratio of lignin/carbohydrate peaks

at different irradiation times was calculated by determining the ratio of lignin reference band at 1510 cm^{-1} against carbohydrate reference bands. As stated above, irradiation has no significant effect on the intensity of bands at 1375 cm^{-1}, this carbohydrate band was used as an internal reference for calculating lignin loss due to light irradiation. The relative changes in the lignin/carbohydrate ratio (I_{1510}/I_{1375}) at different irradiation periods for both heat-treated and untreated samples are plotted in Figure 4.63 (a). The lignin/carbohydrate ratio decreases rapidly with increasing irradiation time. Lignin of both heat-treated and untreated jack pine samples decreases faster in the beginning of the irradiation test. The relative intensity of lignin aromatic band at 1510 cm^{-1}decreased to 65% of its original value after irradiation of 72 h for heat-treated sample whereas it became 84% of its original value for untreated wood for same irradiation time (see Figure 4.63 (a)). The rate of change of lignin/carbohydrate ratio of heat-treated wood is very high at short irradiation times up to 72 h. A significantly large decrease in the intensity ratio of lignin/carbohydrate peak shows rapid lignin degradation even at the beginning of irradiation for heat-treated wood. The slope of the curve changed significantly after 72 h irradiation weathering and the rate of change of lignin/carbohydrate ratio become very small at intermediate irradiation times. Then, its degradation rate increased at longer irradiation times. The lignin/carbohydrate ratios of heat-treated samples are higher than those of untreated ones after irradiation of same periods during all the tests. Lignin of heat-treated jack pine samples degrades at a faster rate than untreated samples. After 1500 h of irradiation, lignin/carbohydrate ratios of both woods are relatively close. This indicates that a long period of sunlight irradiation

decreases the differences in chemical characteristics of heat-treated and untreated wood surfaces, which supports the micro-structural and wettability findings stated above.

The proportion of carbonyl groups during irradiation was calculated by taking the ratio of intensity of carbonyl band at 1740 cm^{-1} to that of carbohydrates peaks at 1375 cm^{-1}. The ratio of intensity of C=O band at 1740 cm^{-1} to that of 1375 cm^{-1} band represents the relative changes of carbonyl groups due to light irradiation. The relative changes in the ratio of carbonyl peak at 1740 cm^{-1} ($I_{carbonyl}$) to carbohydrates peaks at 1375 cm^{-1} ($I_{carbohydrates}$) for heat-treated and untreated jack pine as a function of irradiation time were plotted in Figure 4.63 (b). The ratio I_{1740}/I_{1375} of both woods decreases during irradiation test. Thus, the above results indicate that the unconjugated carbonyl group at 1740 cm^{-1} decreases. This is in agreement with the finding reported by Masanori and Tokato [192]. They found that the unconjugated carbonyl group at 1740 cm^{-1} decreased with an weathering of more than 50 h for untreated tropical wood. However, Pandey [44] observed that the relative concentration of carbonyl groups increased with irradiation time for chir pine and rubber wood. These different findings might be due to the different wood species.

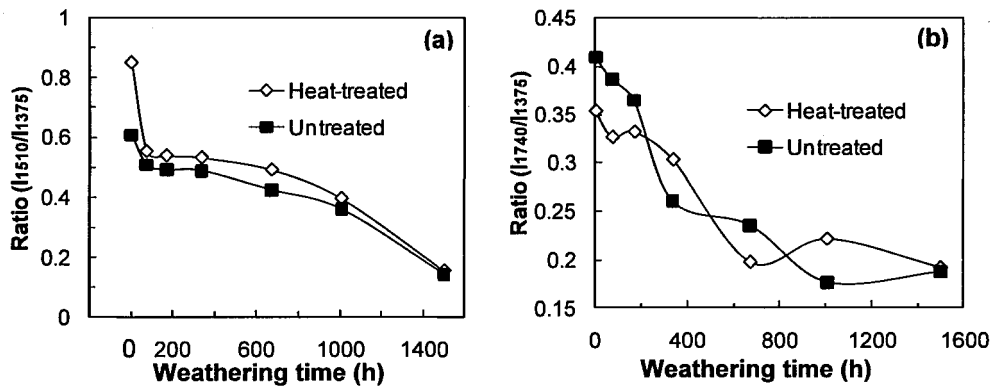

Figure 4. 63 (a) Variation of lignin ratio at 1510 cm^{-1} to carbohydrate at 1375 cm^{-1} as a function of weathering time, (b) behavior of band at 1740 cm^{-1} to carbohydrate at 1375 cm^{-1} plotted as a function of irradiation time for jack pine untreated and heat-treated without water spray

Pandey [44] reported that the color changes on wood surfaces were mainly due to the formation of C=O groups as a result of the photodegradation of lignin. Figure 4.64 shows the relationship of the color changes (L*, ΔE, and b*) of heat-treated and untreated wood surfaces with the lignin decay and relative intensity of carbonyl absorption peak at 1740 cm^{-1}. As can be seen from Figure 4.64 (a), the lightness of heat-treated samples increases linearly with the degradation of lignin whereas, for untreated samples, the lightness also increases when irradiated for more than 168 h, but is not in a linear relation to the lignin decay. This might be explained with the increasing amount of extractives coming from the interior of untreated wood substance to the wood surface during the first period of irradiation, consequently, reducing the surface lightness. The dependence of total color changes to loss of lignin on heat-treated wood surfaces is more than that of untreated wood (see Figure 4.64 (b)). In the view of these findings, the jack pine heat-treated wood color

changes are related to combination of changes in lignin and extractives contents during light irradiation. Pandey [44] also reported that for irradiation of chir pin and rubber wood, color differences correlated linearly with the formation of the non-conjugated carbonyl functional group (I_{1735}/I_{1375}) increasing as a function of irradiation time. The results of Masanori and Tokato [192] suggested that the formation of non-conjugated carbonyl functional group played an important role in the color change in woods for which Δb^* increased but not for woods for which Δb^* decreased. However, it can be observed from the color results shown in Figure 4.59 (b) and Figure 4.64 (c) that the b* and the non-conjugated carbonyl functional group (I_{1740}/I_{1375}) of both heat-treated and untreated jack pine surfaces decrease due to irradiation. b* seems to increase with the non-conjugated carbonyl function (I_{1740}/I_{1375}) decreases (Figure 4.64 (c)). Thus, it is possible to obtain a correlation of b* and carbonyl groups content (I_{1740}/I_{1375}) (see Figure 4.64 (c)).

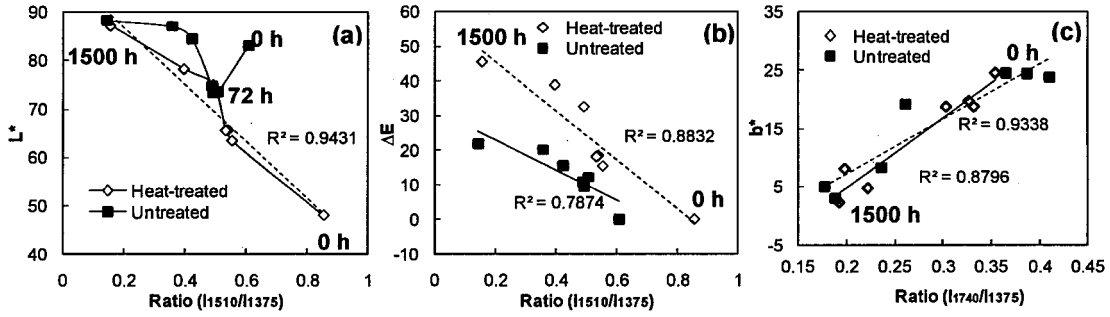

Figure 4. 64 Relationship of color changes with functional groups of jack pine untreated and heat-treated without water spray during weathering: (a) lightness vs. decay of lignin, (b) total color changes vs. decay of lignin, (c) b* vs. carbonyl groups content

As stated in Section 4.5, the degradation of lignin by weathering can increase the content of other components on wood surface and consequently make the surface more

hydrophilic. The ratio of peak heights at 1429 and 897 cm^{-1} (H_{1429}/H_{896}) of FTIR spectra of wood samples was used for the determination of crystallinity of cellulose in wood samples [196]. In this study, higher H_{1429}/H_{896} ratio for heat-treated wood samples was found compared to that of untreated wood samples. It is observed that the H_{1429}/H_{896} ratios decrease for both heat-treated and untreated samples during light irradiation as shown in Figure 4.65 (a). The results indicate that crystalline cellulose is degraded which caused a decrease in the crystallinity of all specimens, and the degradation occurs to different extents depending on the heat treatment.

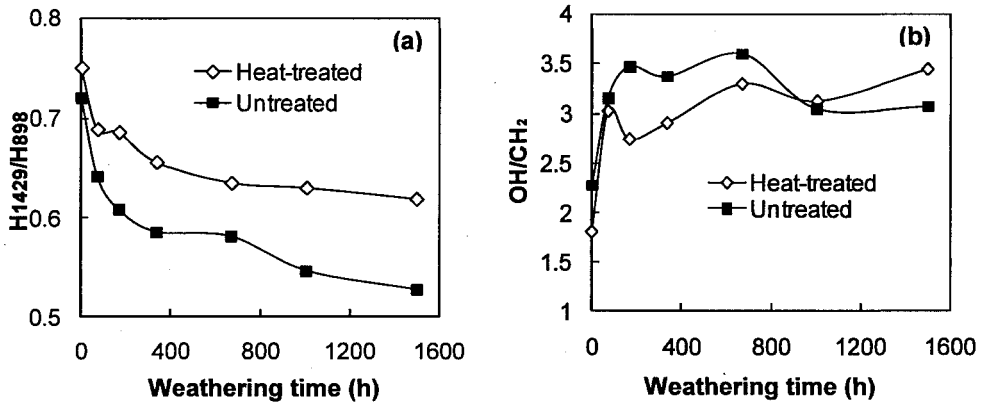

Figure 4. 65 (a) Evolution of crystallinity (H_{1429}/H_{898}) as a function of time during weathering, (b) intensity ratios of bands at 3500 cm^{-1} (OH/CH_2 ratio) to band at 2900 cm^{-1} in FTIR spectra

Figure 4.65 (b) shows the OH/CH_2 ratio of heat-treated and untreated jack pine as a function of different light irradiation time. The OH/CH_2 ratios of all samples increase as irradiation time increased up to 72 h and then change relatively slightly or stayed almost constant up to 1500 h as shown in Figure 4.65 (b). Before irradiation, there are more

hydroxyl groups on untreated wood surfaces than those of heat-treated wood; however, after weathering for 1008 h, the opposite occurred. This might result in increase in wettability of heat-treated woods by water compared to that of untreated woods after irradiation. However, the present study exhibits the contrary dynamic contact angle results after irradiation for 72 h as shown in Figure 4.61. It might be demonstrated that the different contents of extractives during heat-treated and untreated woods had a significant effect on the wettability of wood surface by water after irradiation for 72 h (see detailed explanation in Section 4.5). The results show that the contact angles of both heat-treated and untreated jack pine samples decrease with increasing irradiation time while OH/CH_2 ratios do not change after the irradiation of 72 h (see Figure 4.65 (b)). This indicates that the contact angle is dependent on OH/CH_2 ratios to different extents depending on irradiation time for the specimens in weathering tests without water spray. However, the OH/CH_2 ratios for heat-treated woods during weathering with water spray is inversely proportional to their contact angles (see Figure 4.53). Thus, it is probable that water spray of artificial weathering affects the changes in OH/CH_2 ratios of the heat-treated wood.

b) XPS analysis

The typical XPS survey spectra of heat-treated and untreated jack pine wood samples before and after artificial sunlight irradiation for 1500 h are shown in Figure 4.66, respectively. Both the spectra of untreated (see Figure 4.66 (a) and (b)) and heat-treated samples (see Figure 4.66 (c) and (d)) reveal the presence of carbon, oxygen, and small amounts of nitrogen as expected. It can be seen from the comparison of the survey spectra

of samples before and after irradiation that the carbon C1s peak decrease and the oxygen O1s peak increase due to irradiation for both untreated and heat-treated samples.

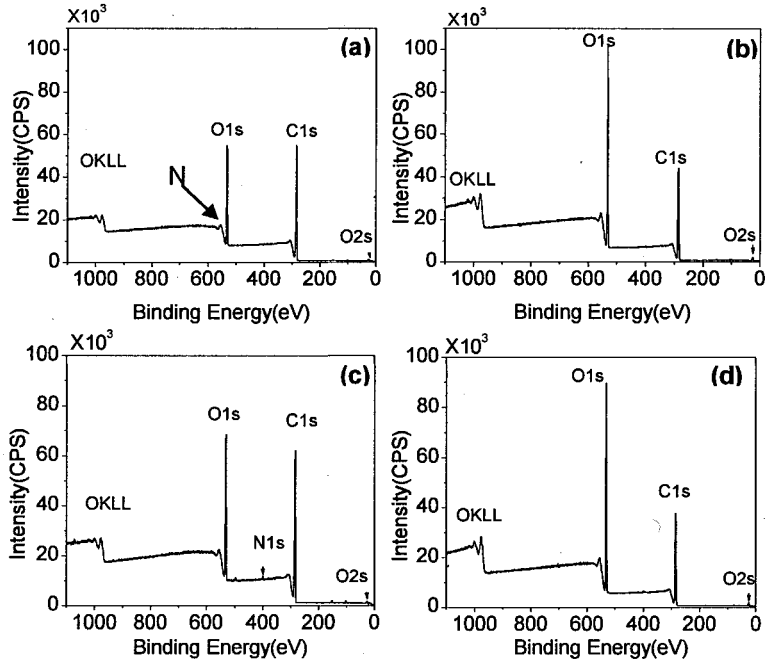

Figure 4. 66 XPS survey spectra of jack pine wood untreated and heat-treated without water spray before and after irradiation for 1500h: (a) untreated before irradiation, (b) untreated, irradiated for 1500h, (c) heat-treated before irradiation, (d) heat-treated, irradiated for 1500h

The relative distribution of composition of O and C atoms and the calculated oxygen to carbon (O/C) ratio for all samples (heat-treated and untreated) before and after irradiation for different times are presented in Figure 4.67. According to the chemical component analysis, untreated jack pine wood contains approximately 29% lignin, 60% holocellulose, and 6% extractives. As stated in Section 4.2, a high oxygen carbon atomic ratio (O/C) indicates high cellulose and hemicelluloses contents, while a low O/C ratio

reflects higher lignin content on wood surface. The O/C ratios of both heat-treated and untreated samples increase considerably at the initial irradiation time of 72 h, and they keep increasing at a lower rate than the initial rate up to 1500 h (see Figure 4.67). This means that irradiation reduces lignin content, consequently, the carbohydrates content increases on both wood surfaces. O/C ratios of both untreated and heat-treated wood after irradiation for 1500 h are much higher than O/C value of lignin (0.33) and relatively close to the ESCA experimental value of 0.62 of cellulose. This implies that irradiation results in wood surfaces richer in cellulose and poorer in lignin. O/C ratio gives a direct measurement of the surface oxygen content, and a high oxygen content normally points to the oxidation of the surface. The results are similar to those obtained during weathering with water spray (see section 4.2).

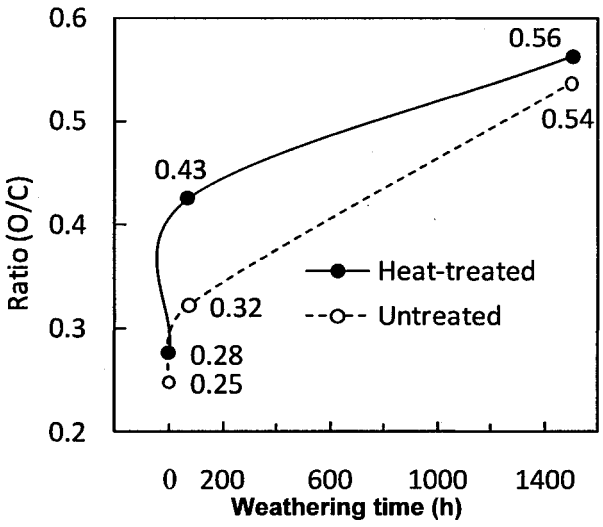

Figure 4. 67 O/C ratio of jack pine wood surface untreated and heat-treated without water spray during irradiation

The changes provoked in wood composition by heat treatment are less compared to those induced by light irradiation on wood surface. Figure 4.67 shows that O/C ratio increased slightly (from 0.25 to 0.28) after heat treatment for samples before irradiation. This is not in agreement with the result of study of Sernek [135] who showed that wood drying at high temperature (160°C <T< 180°C) decreased the oxygen to carbon ratio (O/C) of wood. Nguila and Petrissans also reported that the oxygen to carbon ratio (O/C) decreased after the high temperature treatment of beech wood (from 0.55 to 0.44), and this decrease in O/C ratio appeared to be closely related to carbohydrates (cellulose and hemicelluloses) degradation leading to the formation of volatile by-products with a lower oxygen content resulting from dehydration of polymers initially present in wood[140]. O/C ratio of all heat-treated samples are slight higher than those of untreated samples in this study during irradiation duration, however, this is not enough to suggest that irradiation has a less oxidizing and degrading influence on the lignin of the heat-treated sample surface. The high carbon content in wood samples has been reported as an indication of the presence of lignin and extractives on the wood surface [158]. Untreated jack pine wood is rich in carbon-rich extractives (about 6%): waxes, fats and terpenes, and lignin guaiacyl units [137]. This can be confirmed by the lower oxygen to carbon ratio (0.25) of untreated jack pine comparing to that of other species such as beach wood given in the literature (0.55) [140].The increase in O/C ratio is probably due to the partial removal of the abundant carbon-rich extractives in jack pine such as fatty acids, terpenes, and phenolics during the high temperature heat treatment.

Table 4. 9 XPS C1s peaks analysis of jack pine untreated and heat-treated without water spray and weathered for different times

Sample	Binding Energy				FWHM				Component (%)			
	C1	C2	C3	C4	C1	C2	C3	C4	C1	C2	C3	C_4
UT(0 h)	284.6	286.24	288.85	287.8	1.119	1.284	0.987	1.008	64.064	28.177	2.95	4.809
UT(72 h)	284.6	286.23	287.7	288.78	1.117	1.181	0.988	1.27	38.49	46.345	9.742	5.422
UT(1500 h)	284.6	286.18	287.61	288.91	1.182	1.095	1.171	0.965	26.47	55.791	14.813	2.926
HT(0 h)	284.6	286.17	287.73	288.88	1.051	1.323	0.963	0.823	65.393	27.596	3.241	3.769
HT(72 h)	284.6	286.18	287.65	288.73	1.187	1.654	0.75	1.387	52.294	35.598	2.435	9.673
HT(1500 h)	284.6	286.23	287.68	288.95	1.18	1.11	1.173	0.971	30.407	52.588	13.816	3.19

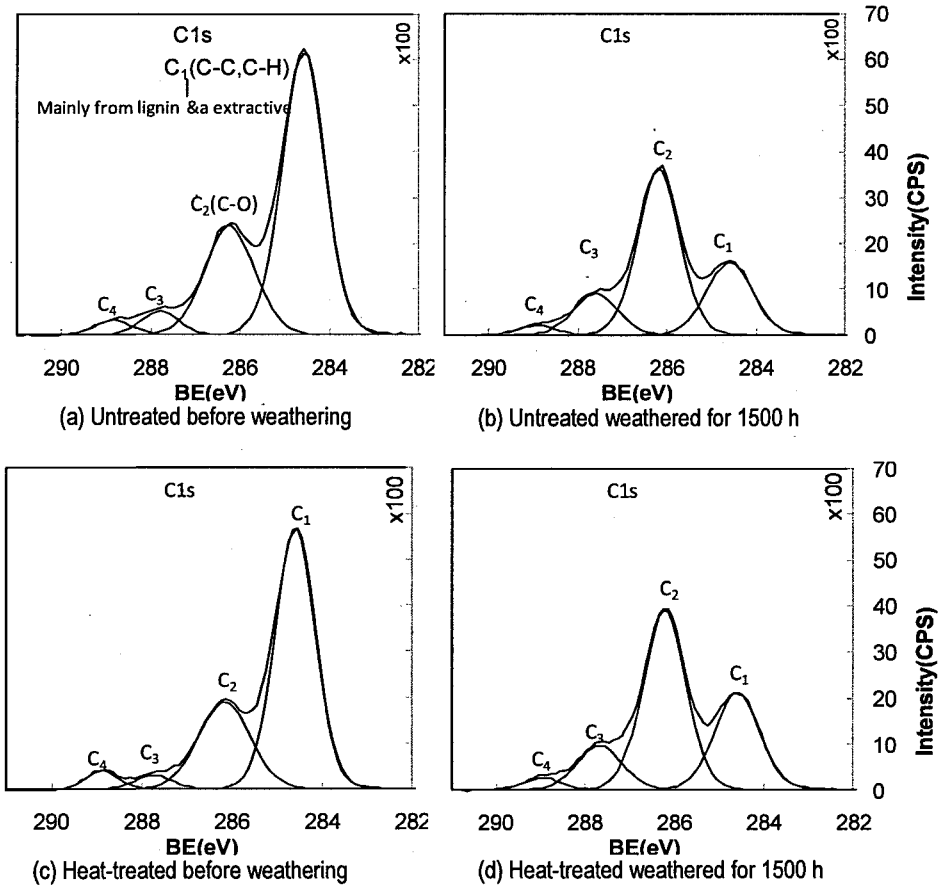

Figure 4. 68 C1s spectra of jack pine untreated and heat-treated without water spray before and after irradiation for 1500 h

Similar to Section 4.2, the high-resolution of C1s and O1s were also fitted with their decomposition into four and two components (see Table 3.3), respectively. Table 4.9 shows the chemical shifts and binding energies of C1s peaks. The high-resolution of the XPS spectra of C1s of untreated and heat-treated sample surfaces before and after irradiation for 1500 h were detected and shown in Figure 4.68. Similar to birch wood (see Section 4.2), the XPS patterns of heat-treated and untreated jack pine wood surfaces are similar but change considerably after irradiation without water spray for 1500 h. The concentrations of contribution at C_1 and C_2 peaks are higher than C_3 and C_4 for all samples, and they are also modified by the irradiation process even without water spray. The most important contributions for heat-treated jack pine surfaces before irradiation come from the C_1 class which corresponds to C–C and C-H groups present in lignin, hemicelluloses and extractives However, the contributions from the C_2 class, corresponds to OCH groups of lignin and C–O–C linkages of extractives and polysaccharides of wood [140], become more important for surfaces after irradiation(see Figure 4.68 (d)). This indicates the irradiation increases contribution of polysaccharides (hemicelluloses and celluloses) for heat-treated jack pine. As discussed previously, the weathering with water spray shows similar effects on the changes in component contributions for heat-treated jack pine, birch, and aspen (see Section 4.2).

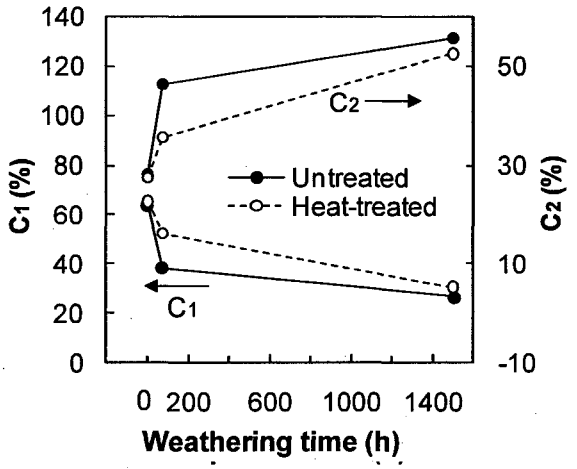

Figure 4. 69 Effect of irradiation on the C1 and C2 component on jack pine untreated and heat-treated without water spray

The variations in peak area contributions of C_1 and C_2 components as a function of irradiation time for both untreated and heat-treated jack pine are shown in Figure 4.69. As stated in Section 4.2, the C_1 is associated with the presence of lignin, and the C_2 mainly originates from cellulose and hemicelluloses on wood surface. The C_1 contribution decreases while the C_2 contribution increases with irradiation time increasing for both untreated and heat-treated jack pine samples (Figure 4.69). This indicates that the lignin is more sensitive than cellulose against sunlight irradiation and is degraded more; consequently, the lignin content becomes less important after irradiation weathering. In other words, the increase in the cellulose content (C_2) is attributed to preferential degradation of lignin (C_1) by irradiation. The results show that the irradiated heat-treated jack pine surface is rich in cellulose and poor in lignin. The increase in C_3 contribution (see Table 4.9), associated to the O-C-O linkages in cellulose and hemicelluloses and to carbonyl groups (C=O) to a less extent, confirms that cellulose and hemicelluloses go up

during irradiation. The insignificant contribution of C_4 peak in all six samples (< 9.7% see Table 4.9) implies low content of carboxylic groups on the wood surfaces. The analysis of the effect of high temperature treatment on the C1s spectra of jack pine wood surface shows no significant variation. C_1 contribution enhances slightly from 64.1% to 65.4%, and C_2 contribution is reduced slightly from 28.17 % to 27.6 %. However, the differences in contributions due to irradiation increase up to 72 h and then decrease afterwards. C_1 and C_2 contributions of heat-treated wood surfaces change less compared to that of untreated wood, implying that irradiation has less influence on the C1s component change of heat-treated wood surface than untreated wood.

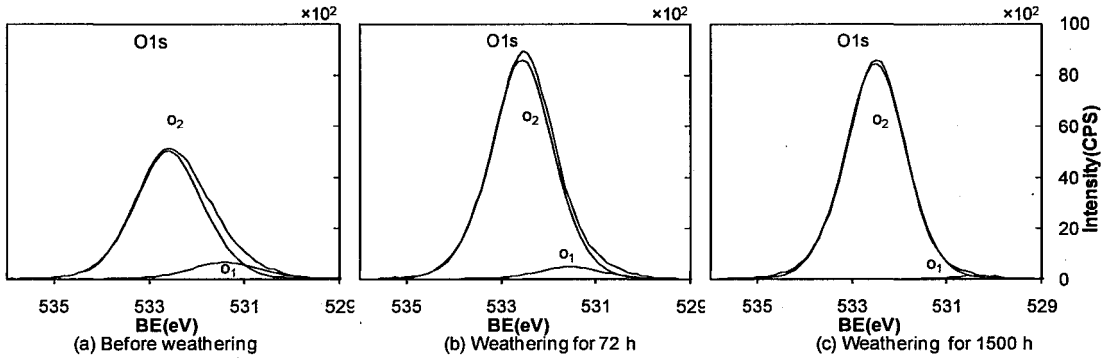

Figure 4.70 O1s peaks of jack pine wood heat-treated without water spray during different irradiation times

Figure 4.70 shows the O1s spectra of heat-treated jack pine sample studied during irradiation. These illustrations show only two components: O_1 and O_2. The spectra analyses give O_1 and O_2 binding energies of 531.6 ± 0.4eV and 532.6 ± 0.1eV, respectively (Table 4.10). The binding energies of O_1 are in excellent agreement with those reported in the literature [127, 140]. The binding energy of O_2 component value is somewhat lower than

that reported for birch and spruce chemicothermomechanical pulps [127]. Its binding energy is similar to that reported by Nguila et al.[140].

Table 4.10 XPS O1s peaks analysis of jack pine untreated and heat-treated without water spray and irradiated for different times

Sample	Binding Energy		FWHM		Component (%)	
	O_1	O_2	O_1	O_2	O_1	O_2
UT(0 h)	532.00	532.57	0.888	1.795	6.691	93.309
UT(72 h)	531.8	532.49	0.838	1.985	3.264	96.736
UT(1500 h)	531.32	532.58	0.979	1.577	0.636	99.364
HT(0 h)	531.41	532.59	1.659	1.659	11.503	88.497
HT(72 h)	531.55	532.56	1.546	1.546	5.34	94.66
HT(1500 h)	531.43	532.51	0.959	1.503	0.851	99.149

O_1 is associated with lignin and O_2 with carbohydrate (see Table 3.3 and Section 4.2). The contribution of the O_1 components increases while that of O_2 decreases due to heat treatment (Table 4.10), which is in agreement with the results presented in Section 4.2. However, the fractional areas of the O_1 components decrease whereas those of O_2 increase due to irradiation for both untreated and heat-treated samples (see Figure 4.71). Therefore, the O1s spectra results confirm that irradiation decreases the lignin content and increases the carbohydrate content on heat-treated jack pine surface. The degradation occurs during the initial period of irradiation (72 h) for both woods. After irradiation for 1500 h, the characteristics of O1s become similar between heat-treated and untreated samples. The results support that irradiation degrades wood surfaces and their properties become similar.

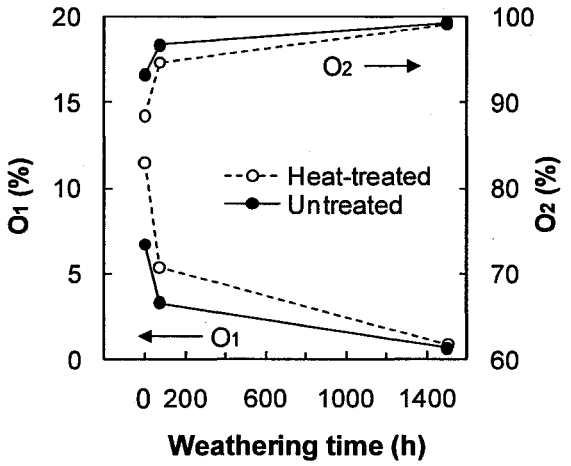

Figure 4. 71 Effect of irradiation on O_1 and O_2 components of jack pine surface untreated and heat-treated without water spray

The increase of C1 and O1 after heat treatment suggests that there are differences in the migration of the wood components. Any material should reach a temperature of 60-70°C higher than its glass transition temperature to migrate. The glass transition temperature of lignin was reported to be 90-110°C [127]. Consequently, lignin migration occurred when wood was heat-treated to 210°C and passed from a glass state to a rubber state in the presence of moisture. Thus, lignin presence on heat-treated wood surface is abundant. Lignin protects the hydrogen bonds that link adjacent fibers of cellulose from water and moist conditions by its hydrophobic nature. Decrease in wettability of heat-treated wood supported this affirmation (see Figure 4.71). Lignin may freeze between other components of wood (cellulose and hemicelluloses) and act as thermoplastic glue after cooling. However, the degradation of heat-treated wood due to irradiation suggests that this phenomenon is not likely to have an effect on lignin protection during long term irradiation.

Lignin is more sensitive to sunlight irradiation compared to other wood components; therefore, the heat-treated jack pine surface becomes richer in cellulose and poorer in lignin after irradiation. The results show that the lignin of heat-treated jack pine is degraded due to exposure to artificial sunlight. Based on the experimental and characterization results, as discussed previously, the following lignin photodegradation mechanism is proposed. Lignin is degraded by the cleavage of C-C bonds, leading to a reduction or elimination of side-chains as confirmed by the reduction of C_1 class in XPS spectra. The γ-C might split from quinone intermediates releasing formaldehyde. The α-carbonyl group of lignin absorbs the radiation energy and reaches an excited state [48], and this initiates the cleavage of the b-arylether linkage. After several electron migration steps, quinoid compounds are probably formed, which might be accompanied by a color change [57]. While this happens during the initial period up to 72 h of weathering with water spray (see Sections 4.3-4.5), it happens after 168 h of irradiation without water spray, which are confirmed by the color results. This indicates the degradation of lignin takes place earlier in the weathering process with water spray.

4.6.4. Conclusions

a) Degradation of middle lamellar, checking of cell wall, and destruction of bordered pits occurred due to irradiation on wood surface heat-treated without water spray. Photo-degradation occurred preferentially in the middle lamella of wood surface where the lignin concentration was the highest in the cell wall. There was not any notable difference in surface structure degradation of untreated and heat-treated wood after long term irradiation.

b) Discoloration of wood was due to combination of the photo-degradation of lignin and extractives on wood surface during irradiation. Further color changes occurring during irradiation of heat-treated jack pine were estimated to be due to the increasing of lignin condensation and decreasing extractives content on wood surfaces caused by heat treatment.

c) The irradiation increased the wettability of both heat-treated and untreated jack pine woods by water. Heat-treated and untreated wood exhibited different wetting behavior during artificial irradiation due to the differences in contents of extractives and other polymer components resulted from heat treatment. Changes in wettability during irradiation of heat-treated wood were induced by the combination of structural changes in surfaces and chemical changes. Cracks occurred during irradiation, and this degradation resulted in easier entrance of water into cell wall of heat-treated wood which consequently increased wood wettability. Lignin was more sensitive to irradiation than other components; therefore, heat-treated jack pine surface became richer in cellulose and poorer in lignin after irradiation. The cellulose-rich layer on wood surface and increasing amorphous cellulose transformed from crystallized cellulose caused the increase in free hydroxyl groups.

d) The comparison of the changes of heat-treated jack pine weathered with and without water spray indicates either the water spray has no obvious effect on the structural degradation of heat-treated wood or the presence of humidity (50% relative humidity) during artificial weathering without water spray plays a similar role, yielding similar results. The degradation of lignin takes place earlier in weathering process with water spray than in that without water spray.

4.7. Aging calculations

4.7.1. General

Sunlight is an important cause of damage to wood materials. Ultraviolet light has long been recognized as being responsible for most of this damage. Accelerated weathering testers are widely used for research and development, quality control, and material certification. There is a variety of light sources to simulate sunlight and the damage caused by sunlight. Comparative spectroradiometric measurements suggest that the xenon arc lamp gives the best correspondence with the natural atmospheric exposure.

4.7.2. Weathering chamber

The Q-sun Xenon Test chamber use full-spectrum xenon arc lamps to reproduce the damage encountered in numerous environments. It can be used to both simulate and accelerate these service conditions for quality control applications for different materials including wood. In this section, the heat transfer in Q-sun Xenon Test Chamber (model Xe-1-B/S) will be presented (see Figure 4.72).

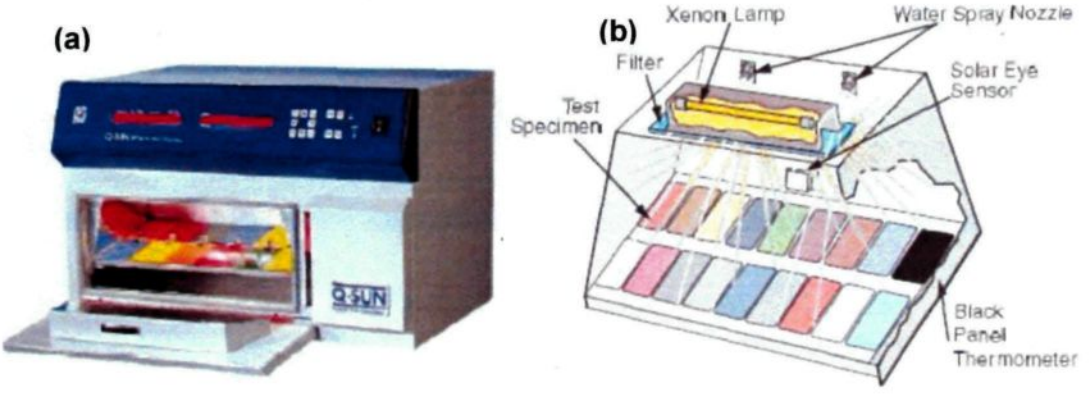

Figure 4. 72 (a) Picture and (b) Schematic of Q-sun xenon test chamber (model Xe-1-B/S) [197]

Light emitted by xenon arcs require a combination of filters to eliminate unwanted radiation. Xenon is considered to be the most realistic simulation of full spectrum sunlight, which includes UV, visible, and infrared wavelengths. There are two filters for Q-sun xenon arc test chamber model Xe-1-B/S: daylight filter and window-glass filter. Figure 4.73 (a, b) show the spectral irradiance distribution with these two different filters, respectively. The irradiance setting has an effect on the spectra. The most common irradiance settings are 0.35 or 0.55 W/m^2 nm at 340nm. A report from the Q-sun company suggests that 0.35 is more like winter sunlight while 0.55 compares better with summer sunlight [197].

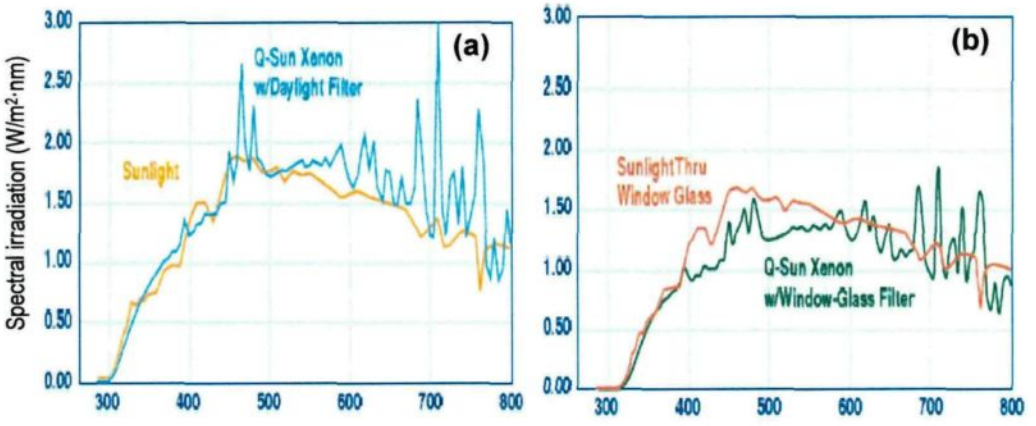

Figure 4. 73 (a) Q-sun Daylight Filter vs. Sunlight, (b) Q-Sun Window glass Filter vs. Sunlight through Window Glass [197]

The sun can be approximately considered a black body radiating at 5800 K. Due to the distance between the sun and the earth, the irradiation reduces to about 1373 W/m^2 outside the earth's atmosphere. Additional attenuation in the atmosphere (depending on the climatic conditions) as well as the position and orientation of a surface on earth with respect to the sun result in the decrease of this value even further.

The fraction of the total blackbody emission, f, in a spectral band is as a function of λT. The fraction for the 300 and 800 nm band can be calculated using Table 12.1 in reference [198]:

$$\lambda_1 = 0.3\mu m, T = 5800\ K: \quad \lambda_1 T = 1740\ \mu m \cdot K, f_{(0\to\lambda 1)} = 0.035$$

$$\lambda_2 = 0.8\mu m, T = 5800\ K: \quad \lambda_2 T = 4640\ \mu m \cdot K, f_{(0\to\lambda 2)} = 0.59$$

$$f_{(\lambda 1\to\lambda 2)} = 0.555$$

According to the data [199], the measured irradiance of xenon lamp used between 300 and 800 nm is 590.8 W/m^2. Since the shape of the E_λ vs. λ is similar for both the solar irradiation and the xenon lamp with the filter, the same fraction can be assumed to hold for the lamp-filter system. Hence the total irradiation can be estimated as:

$$q''_{B,rad,estimated} = \frac{590.8}{0.555} = 1075 W/m^2$$

Figure 4. 74 shows a schematic view of the test chamber with its dimensions. Surface 1 is the surface of the filter covering the xenon lamp, B is the surface of the total surface of the samples, surface 4 is the total side surfaces (lateral surfaces), and surface 5 is the sum of all surfaces except surfaces 1 and B inside the chamber. The heated air flows through the test chamber at a temperature lower than that of the sample surfaces; surfaces 1 (A_1 at temperature T_1 with an emissivity ε_1) and B (A_B at temperature T_B with an emissivity ε_B) were taken as gray surfaces, and surface 5 (A_5 at temperature T_5) as a reradiating surface. The chamber was assumed to be well insulated, thus the heat loss was taken as zero. The surfaces of the wood samples were measured using thermocouples inserted into the samples. The surface temperature was found to be about 45°C. The convection heat transfer between the air and the sample surfaces was estimated to be less than 5% of the radiative heat transfer and, thus, was neglected.

The xenon arc lamp is not an incandescent source. The emission from this lamp resembles that of a solar source after it is filtered through a special filter. Thus the lamp and filter system can be replaced by an equivalent surface (surface 1) with an effective emissivity ε_1 radiating at a certain temperature T_1. Also, the irradiation on the sample

surfaces should be equal to the above estimated value. Thus, T_1 and ε_1 were determined using the equations (4.10-4.11) and ensuring that the calculated irradiation is similar to the estimated one.

The dimensions for various lengths are given as: a=116 mm, b=15 mm, c=450 mm, d=247 mm, and L=230 mm. It is necessary to determine the view factors F_{1B}, F_{15}, and F_{B5} for the inside surfaces of the test chamber. Diffuse surfaces with uniform radiosities were assumed. As shown in Figure 4.74, the surface of the sample plate can be divided into three components (1', 2', and 3'). The desired view factor F_{15} and F_{1B} may be obtained, as seen upon inspection, using the reciprocity rule and the summation rule.

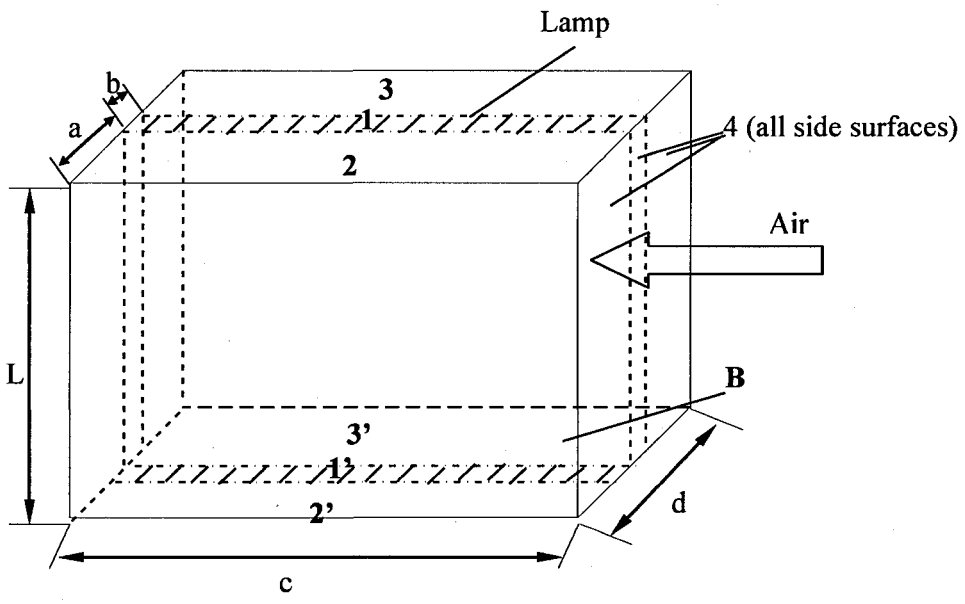

Figure 4. 74 A schematic view of the test chamber with dimension

With the summation rule:

$$F_{1B} = F_{11'} + F_{12'} + F_{13'} = F_{11'} + 2F_{12'} \qquad (4.2)$$

The view factor $F_{12'}$ can be expressed as:

$$F_{12'} = \frac{1}{2A_1}\left[A_{(1+2)}F_{(1+2)(1'+2')} - A_1F_{11'} - A_2F_{22'}\right] \tag{4.3}$$

where A is the area of different surfaces shown in Figure 4.74. Hence,

$$F_{1B} = F_{11'} + 2\times\frac{1}{2A_1}\left[A_{(1+2)}F_{(1+2)(1'+2')} - A_1F_{11'} - A_2F_{22'}\right] \tag{4.4}$$

$$F_{15} = 1 - F_{1B} \tag{4.5}$$

$$F_{B5} = 1 - F_{B1} = 1 - \frac{A_1}{A_2}F_{1B} \tag{4.6}$$

where all the view factors, $F_{11'}$, $F_{22'}$, $F_{(1'+2')(1+2)}$, in the above equations can be determined from Figure 13.4 of the reference [198] for aligned parallel rectangles:

F11'= 0.022, F22'=0.16, F (1+2) (1'+2') =0.17

A1=6450, A2=49880, A (1+2) =56330, AB=111150

A4=320620 mm2, A5= A4+ A2+ A3

F1B=0.247, F15=0.753, FB5=0.985

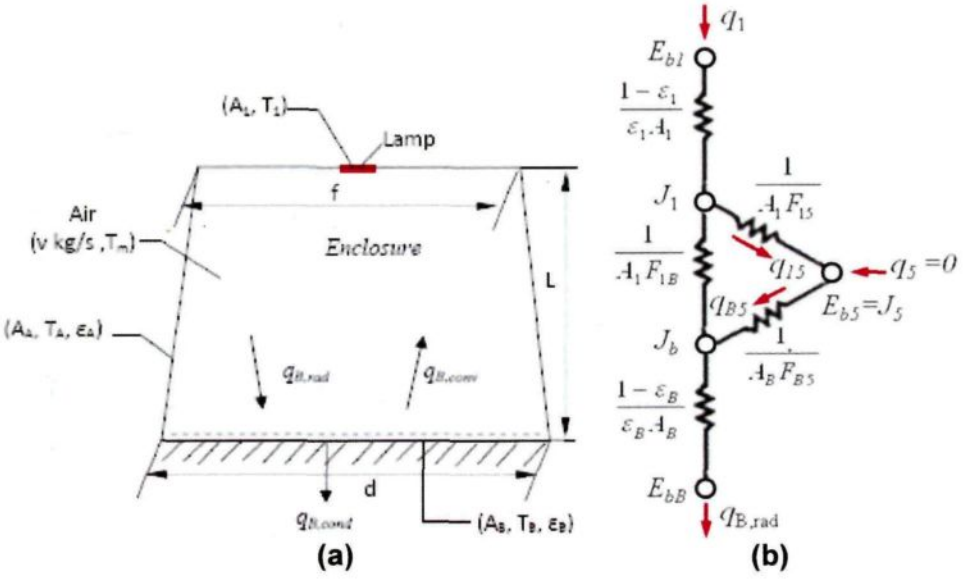

Figure 4. 75 Three-surface enclosure of the xenon test chamber with one surface reradiating (a) schematic, (b) network representation

The calculation is carried out assuming steady-state conditions. In view of the assumptions above, the test chamber is a three-surface enclosure in which surface 1 is a radiative heat source, surface B is a radiative heat sink, and surface 5 (see Figure 4.74) is a reradiating surface (q_5=0). A schematic view is shown in Figure 4.75 (a), and the corresponding radiative thermal network is shown in Figure 4.75 (b).

Since the chamber consists of two gray surfaces (1 and B) and one reradiating surface (5), the net radiation transfer to surface B may be evaluated as follow:

$$q_{B,rad,calculated} = \frac{E_1 - E_B}{R_{1B}} = \frac{\sigma(T_1^4 - T_B^4)}{R_{1B}} \tag{4.7}$$

where E is the total blackbody emissive power, σ is the Stefan-Boltzmann constant, $\sigma = 5.67 \times 10^{-8} W/m^2 \cdot K^4$, T_1 is the temperature of the filter surface (representing the

effective temperature of the filter-lamp system), and T_B is the sample surface temperature. The black panel temperature, which was set to 63°C, is the maximum temperature that the sample surfaces could attain; however, the sample surface temperature is lower (about 45°C) due to the lower wood surface emissivity, and the convective cooling by air.

The total resistance is given by:

$$R_{1B} = \frac{1-\varepsilon_1}{\varepsilon_1 A_1} + \frac{1}{\left[(1/A_1 F_{15}) + (1/A_B F_{B5})\right]^{-1} + A_1 F_{1B}} + \frac{1-\varepsilon_B}{\varepsilon_B A_B} \tag{4.8}$$

or

$$R_{1B} = \frac{1-\varepsilon_1}{\varepsilon_1 A_1} + 160.4 + \frac{1-\varepsilon_B}{A_B \varepsilon_B} \tag{4.9}$$

where ε_1 and ε_B are emissivities of filter and wood sample surfaces, respectively. A_1 and A_B represent the areas for the filter surface and the wood sample surface, respectively.

The gray spectral emissive power of surface 1 can expressed as:

$$E_1 = \int_{\lambda_1}^{\lambda_2} \frac{C_1 \varepsilon_1}{\lambda^5 \left[\exp\left(\frac{C_2}{\lambda T_1}\right) - 1\right]} d\lambda \tag{4.10}$$

Then, at a given wavelength, the temperature of the gray surface can be calculated from:

$$T_1 = \frac{C_2}{\lambda_1 \times \ln\left[1 + \frac{\varepsilon_1 \times C_1}{E_{1\lambda_1} \times \lambda_1^{\,5}}\right]} \tag{4.11}$$

where the first and second radiation constants are $C_1 = 3.742 \times 10^8 W \cdot \mu m^4 / m^2$ and $C_2 = 1.439 \times 10^4 \mu m \cdot K$.

In the weathering tests, the irradiance was set to 0.55 watts per square meter at 340 nm. Due to the porous structure of the surface, the surface emissivity of wood samples, ε_B, is around 0.9. Although it is expected that this value is affected by changing color and structure of wood surface during weathering, it was taken as constant. When the effective emissivity of surface 1, ε_1, was taken as 0.024, the calculated irradiation on sample surfaces was found to be similar to the estimated value above:

$$T_1 = \frac{1.439 \times 10^4}{0.34 \times \ln\left[1 + \frac{0.024 \times 3.742 \times 10^8}{0.55 \times 0.34^5}\right]} = 1923.5K$$

and,

$$R_{1B} = \frac{1 - 0.024}{0.024 \times 6480 \times 10^{-6}} + 160.4 + \frac{1 - 0.9}{0.9 \times 0.106210} = 6446 m^{-2}$$

Hence,

$$q_{B,rad,calculated} = \frac{5.670 \times 10^{-8} \times (1923.5^4 - (45 + 273)^4)}{6446} = 120.3W$$

then, the irradiation transferred from xenon lamp in the UV test chamber to wood sample surface can be calculated as:

$$q''_{B,rad,calculated} = \frac{q_{B,rad,calculted}}{A_B} = \frac{120.3W}{0.11115\ m^2} = 1082\ W/m^2$$

Thus, the lamp-filter system can be represented by an equivalent surface at a temperature of 1923.5K with an effective emissivity of 0.024.

Artificial and natural weathering tests can be correlated by comparing the calculated irradiation value of artificial weathering ($1082 W/m^2$) and that of natural weathering.

4.7.3. Comparison of natural and artificial weathering

Natural weathering is a long process. It can be accelerated using artificial weathering in test chambers where the samples are subjected to irradiation continuously. Even though it is difficult to simulate the natural weather conditions exactly, the artificial weathering tests can provide a basis for comparison for the aging of different materials. The artificial weathering tests in this study were carried out for a period of 1500 hours. Depending on the position of a surface on earth and climate conditions, this will correspond to different periods of time under natural conditions. The following is an example for Florida, USA, where the average yearly irradiance is 186 W/m^2 [200].

Assuming that wood has a surface of emissivity of ε_B= 0.9, a solar absorptivity of α_s=0.90, an average temperature of T_s= 15°C, and the average effective sky temperature is T_{sky}= -10°C, the net radiative heat flux on the surface q'' (W/m^2) can be estimated as follows (see Figure 4.76).

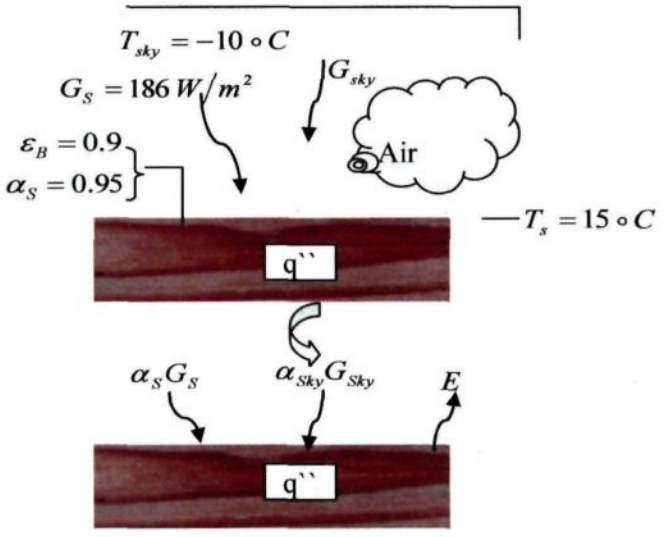

Figure 4. 76 A schematic representation of solar irradiation on a wood surface

Under steady-state conditions for a diffuse surface, the energy balance can be written as:

$$Energy_{in} - Energy_{out} = 0 \tag{4.12}$$

or, per unit surface area,

$$\alpha_S G_S + \alpha_{sky} G_{sky} - E - q'' = 0 \tag{4.13}$$

where,

$$G_{sky} = \sigma T_{sky}^4 \tag{4.14}$$

Since the sky radiation is concentrated in approximately the same spectral region as that of surface emission, it is reasonable to assume that

$$\alpha_{sky} \approx \varepsilon_B = 0.9$$

Then,

$$q'' = \alpha_S G_S + \alpha_{sky} G_{sky} - E \tag{4.15}$$

$$q'' = \alpha_S G_S + \varepsilon_B \sigma (T_{sky}^4 - T_S^4) \tag{4.17}$$

Inserting the numerical values,

$$q'' = 0.90 \times 186 W/m^2 + 0.9 \times 5.67 \times 10^{-8} W/m^2 \cdot K^4 \, (263^4 - 288^4) K^4$$

the average net heat flux on a wood surface is obtained as:

$$q'' = 167.4 W/m^2 - 106.9 W/m^2 = 60.5 W/m^2$$

The artificial and natural weathering tests are correlated by:

$$t_{nat} = t_{art} \times \frac{q''_{rad}}{q''} \tag{4.18}$$

where t_{art} is the period of time for artificial weathering, t_{nat} is the period of time for natural weathering.

For a sample was tested in the UV chamber for 1500 h, the corresponding time for natural weathering in Florida will be:

$$t_{nat} = t_{art} \times \frac{q''_{rad}}{q''} h = 1500h \times \frac{1082 W/m^2}{60.5 W/m^2} / 24 / 365 = 3 years \, 1 \, month$$

This is the average value. Depending on the orientation of the surface (its position with respect to the direction of sunlight), this period could be somewhat shorter or longer. The same analysis for Canada where the average irradiation is 133 W/m^2 (for an average wood surface temperature of T_s= 0°C, and the average effective sky temperature of T_{sky}= -25°C) gives 6 years and 4 months.

4.7.4. Conclusion

The aging calculations were carried out to determine the net radiative heat transfer to the wood sample surfaces. The artificial weathering time corresponds to different natural

weathering times depending on the location. For example, 1500 h of artificial weathering corresponds to about 3 years in Florida and 5 years in Quebec.

CHAPTER 5

CONCLUSIONS AND RECOMMENDATIONS

5.1. Conclusions

In this thesis, the effect of artificial weathering on the wood surface property modifications of three North American species (jack pine, aspen, and birch) heat-treated under different temperatures was studied by different methods. From the experimental results obtained and their analyses, the following conclusions were drawn.

1. Due to heat treatment, wood color becomes darker, wettability decreases, structure changes slightly, and hemicellulose decomposes most.
2. The weathering reduces lignin content (aromatic rings) on the surface of heat-treated wood, consequently, the carbohydrate content increases. This results in surfaces richer in cellulose and poorer in lignin. Heat-treated wood surfaces become acidic due to weathering, and the acidity increases as the weathering time increases. Three possible reasons are given to account for the increase of acidity during weathering. The lignin content increases whereas the hemicelluloses content decrease due to heat treatment. Heat-treated woods have lower acidity to basicity ratios than the corresponding untreated woods for all three species because of the decrease in carboxylic acid functions mainly present in hemicelluloses. The changes in wood composition induced by weathering are more significant compared to those induced by heat treatment on the wood surface. Exposure to higher temperatures causes more degradation of hemicelluloses, and this characteristic is maintained during weathering. However, the

wood direction has greater effect on the changes in chemical composition during weathering compared to that of heat treatment temperature. The heat-treated jack pine is affected most by weathering followed by heat-treated aspen and birch. This is related to differences in content and structure of lignin in softwood and hardwood.

3. Lignin is an amorphous three-dimensional natural polymer in which the building units are connected with ether and C–C bonds in a helical structure. In this study, the results showed that the lignin of heat-treated wood is degraded due to exposure to artificial weathering. Lignin is degraded by cleavage of C-C bonds, leading to a reduction or elimination of side-chains as confirmed by the reduction of C_1 class in XPS spectra. The γ-C might split from quinone intermediates, releasing formaldehyde. The α-carbonyl group of lignin absorbs the radiation energy and is transferred into an excited state, which initiates the cleavage of the β-arylether linkage. After several electron migration steps, quinoid compounds are probably formed, which might be accompanied by a color change. While this happens to untreated wood during the initial irradiation period up to 72 h, it happens to heat-treated wood after 168 h of irradiation.
4. A general understanding of the color behavior of heat-treated wood under artificial weathering is acquired using spectrocolorimetry. The findings from the analysis using CIE-L*a*b* system are in agreement with results of reflectance and K-M spectra. There is a major increase in yellow and red with corresponding decreases in the reflectance for all three species during heat treatment. Heat-treated woods have better color stability during the early times of weathering while the colors of heat-treated woods and untreated woods are very similar after the specimens have been subjected to long term

artificial weathering. Analysis of chemical components shows that the lignin percent of jack pine, aspen, and birch increases after heat treatment which might be due to smaller influence of heat treatment on lignin content than on hemicelluloses. This improves the resistance of heat-treated wood to photo-degradation. However, the lignin percent of heat-treated woods reduces to less than or equal to 2.5% after the artificial weathering of 1512 h. This suggests that the weathering degrades mostly the lignin matrix; consequently, both the colors of heat-treated woods and untreated woods are lighter and very similar after a long period of artificial weathering.

5. Effect of artificial weathering on the wettability of three heat-treated North American species was studied from the point of view of the structural and chemical changes taking place on the wood surface. Weathering increases wettability of all three heat-treated woods by water. Changes in wettability during artificial weathering differ according to heat treatment procedure and wood species, and are likely due to a combination of structural and chemical changes on the surfaces. The SEM analysis indicates that cracks form due to degradation taking place during weathering. As a result, water has easier entry into the cell wall, which consequently increases wettability. FTIR spectra suggest that the OH/CH_2 ratio for heat-treated specimens is inversely proportional to the contact angle regardless of the type of wood species. The presence of a cellulose-rich layer on wood surface and the increasing amount of amorphous cellulose transformed from crystallized cellulose due to weathering result in the increase of hydroxyl groups; consequently, heat-treated wood wettability increases.

6. The combined action of sunlight and humidity (water spray or simulated high humidity) results in lightening of the surface during the weathering of heat-treated wood surface and leads to the formation of macroscopic and microscopic cracks or checks. Cells lose bond strength with adjacent cells near the wood surface because of the degradation of lignin deposited in the cell corners and middle lamella. As weathering continues, humidity washes out degradation by-products present on the wood surface and the exposed surface goes through further degradation. Thus, a cyclic damage of heat-treated wood surface occurs during the weathering process. Discoloration and checking of heat-treated and untreated wood surfaces differ in intensity; however, both wood surfaces become increasingly uneven. Macro-cracks and micro-cracks form during weathering. This degradation results in easier entrance of water into cell wall of heat-treated wood, which consequently increases wood wettability. Lignin is more sensitive to irradiation compared to other wood components; therefore, the heat-treated wood surface becomes richer in cellulose and poorer in lignin after weathering. The cellulose-rich layer on wood surface and the increasing amorphous cellulose content which is transformed from crystallized cellulose result in the increase of free hydroxyl groups, and consequently enhance the wettability on heat-treated wood surfaces by water.
7. The aging calculations were carried out to determine the net radiative heat transfer to the wood sample surfaces and the corresponding natural weathering times.

5.2. Recommendations

The following is a brief summary of possible work that may be carried out with a view to acquire a greater understanding of the fundamental properties of heat-treated wood, which play an important role in the degradation mechanism during weathering.

1. In this research, the three wood species (jack pine, aspen, and birch) were studied during artificial weathering with and without water spray. The artificial weathering tests do not include the factor of snow. However, there is a lot of snow in winter in Quebec. It will be interesting and important to investigate the effect of snow on the degradation of heat-treated wood surface. In addition, the real outdoor weathering should be carried out to compare with the results of artificial weathering test.
2. To gain a better understanding of reactions on heat-treated wood surfaces during weathering, other analysis methods can be used. UV microscopic and UV spectroscopic studies of wood can show the lignin content in different cell wall layers as well as in the compound middle lamellae. They can be used to investigate the changes of lignin distribution in cell wall during weathering. TEM micrograph analysis of ultra-thin section can be used to analyze the breakdown of fibrils of wood due to heat treatment and weathering. The electron spin resonance spectrometry (ESR) analysis can be used to verify the generation of free radicals caused by the absorption of radiation energy by wood and its components. Changes in the degree of polymerization of cellulose after weathering for different periods can be determined to study the chemical changes in cellulose.

3. Different light sources with different narrow-wavelength ranges of UV radiation can be used to study the chemical changes occurring on heat-treated wood surface to determine which range has more influence.
4. The relation between the loss of components and the loss of weight of wood can be carried out to understand better the changes in different components of heat-treated wood due to weathering.
5. It is important to find good alternative solutions for protecting heat-treated wood surfaces. Since the substrate degradation may result in different coating-failure mechanisms, the future research should include the reaction of the substrate-coating interface to acid rain.
6. Degree of polymerisation of cellulose during weathering can be determined.
7. Effect of air humidity on degradation can be studied as well.
8. The aging calculations can be modified to include the effects of water spray (water vapor in the air) and dependence of emissivity on changing wood color and structure.

REFERENCES

[1] M. Nuopponen, H. Wikberg, T. Vuorinen, S.L. Maunu, S. Jämsä, P. Viitaniemi, Heat-treated softwood exposed to weathering, Journal of Applied Polymer Science, 91 (2004) 2128-2134.

[2] H. Sivonen, S.L. Maunu, F. Sundholm, S. Jämsä, P. Viitaniemi, Magnetic resonance studies of thermally modified wood, Holzforschung, 56 (2002) 648-654.

[3] R. Kotilainen, R. Alén, V. Arpiainen, Changes in the chemical composition of Norway spruce (Picea abies) at 160-260°C under nitrogen and air atmospheres, Paperi ja Puu/Paper and Timber, 81 (1999) 384-388.

[4] W.C. Feist, R.M. Rowell, R.J. Barbour, Outdoor wood weathering and protection, Archaeological Wood: Properties, Chemistry, and Preservation, (1990) 263-298.

[5] D.N.S. Hon, Photochemistry of wood, Wood and Cellulosic Chemistry, (1991) 525-555.

[6] W.C. Feist, WEATHERING CHARACTERISTICS OF FINISHED WOOD-BASED PANEL PRODUCTS, Journal of Coatings Technology, 54 (1982) 43-50.

[7] S.Y. Lin, K.P. Kringstad, Photosensitive groups in lignin and lignin model compounds, Tappi, 53 (1970) 658-663.

[8] D.N.S. Hon, S.-T. Chang, SURFACE DEGRADATION OF WOOD BY ULTRAVIOLET LIGHT, Journal of polymer science. Part A-1, Polymer chemistry, 22 (1984) 2227-2241.

[9] T. Syrjänen, E. Kangas, Heat treated timber in Finland, The International Research Group on Wood Preservation, IRG/WP 00-40158, IRG Secretariat, SE-100 (2000) 44.

[10] A. Ahajji, P.N. Diouf, F. Aloui, I. Elbakali, D. Perrin, A. Merlin, B. George, Influence of heat treatment on antioxidant properties and colour stability of beech and spruce wood and their extractives, Wood Science and Technology, 43 (2009) 69-83.

[11] M.K. Dubey, S. Pang, J. Walker, Color and dimensional stability of oil heat-treated radiata pinewood after accelerated UV weathering, Forest Products Journal, 60 (2010) 453-459.

[12] D. Mayes, O. Oksanen, Thermo Wood® Handbook, (2002) 52.

[13] Q. Shi, J.H. Jiang, Color stability of heat-treated okan sapwood during artificial weathering, in, Guilin, 2011, pp. 13-16.

[14] C.H.S. Del Menezzi, R.Q. de Souza, R.M. Thompson, D.E. Teixeira, E.Y.A. Okino, A.F. da Costa, Properties after weathering and decay resistance of a thermally modified wood structural board, International Biodeterioration and Biodegradation, 62 (2008) 448-454.

[15] N. Ayadi, F. Lejeune, F. Charrier, B. Charrier, A. Merlin, Color stability of heat-treated wood during artificial weathering, Holz als Roh - und Werkstoff, 61 (2003) 221-226.

[16] S. Jämsä, P. Ahola, P. Viitaniemi, Long-term natural weathering of coated ThermoWood, Pigment and Resin Technology, 29 (2000) 68-74.

[17] A. Temiz, N. Terziev, B. Jacobsen, M. Eikenes, Weathering, water absorption, and durability of silicon, acetylated, and heat-treated wood, Journal of Applied Polymer Science, 102 (2006) 4506-4513.

[18] M. Deka, M. Humar, G. Rep, B. Kričej, M. Šentjurc, M. Petrič, Effects of UV light irradiation on colour stability of thermally modified, copper ethanolamine treated and non-modified wood: EPR and DRIFT spectroscopic studies, Wood Science and Technology, 42 (2008) 5-20.
[19] K. Mitsui, Changes in the properties of light-irradiated wood with heat treatment: Part 2. Effect of light-irradiation time and wavelength, Holz als Roh - und Werkstoff, 62 (2004) 23-30.
[20] D. Letourneau, M. Irmoulr, C. Krause, C. Belloncle, Colour stability of three different heat treated wood species during artificial weathering, Proceedings of the Second European Conference on Wood Modification, (2005) 57-60.
[21] B. Mazela, R. Zakrzewski, W. GrzesÌ• kowiak, G. Cofta, M. Bartkowiak, Resistance of thermally modified wood to basidiomycetes, Wood Technology, 7 (2004) 253-262.
[22] S. Poncsak, D. Kocaefe, R. Younsi, Y. Kocaefe, L. Gastonguay, Thermal treatment of electrical poles, Wood Science and Technology, 43 (2009) 471-486.
[23] M.J. Boonstra, B. Tjeerdsma, Chemical analysis of heat treated softwoods, Holz als Roh - und Werkstoff, 64 (2006) 204-211.
[24] M. Nuopponen, T. Vuorinen, S. Jämsä, P. Viitaniemi, Thermal modifications in softwood studied by FT-IR and UV resonance Raman spectroscopies, Journal of Wood Chemistry and Technology, 24 (2004) 13-26.
[25] R.A. Kotilainen, T.J. Toivanen, R.J. Alén, FTIR monitoring of chemical changes in softwood during heating, Journal of Wood Chemistry and Technology, 20 (2000) 307-320.
[26] B.F. Tjeerdsma, H. Militz, Chemical changes in hydrothermal treated wood: FTIR analysis of combined hydrothermal and dry heat-treated wood, Holz als Roh - und Werkstoff, 63 (2005) 102-111.
[27] D. Kocaefe, B. Chaudhry, S. Poncsak, M. Bouazara, A. Pichette, Thermogravimetric study of high temperature treatment of aspen: Effect of treatment parameters on weight loss and mechanical properties, Journal of Materials Science, 42 (2007) 854-866.
[28] D. Kocaefe, S. Poncsak, Y. Boluk, Effect of thermal treatment on the chemical composition and mechanical properties of birch and aspen, BioResources, 3 (2008) 517-537.
[29] D. Kocaefe, J.L. Shi, D.Q. Yang, M. Bouazara, Mechanical properties, dimensional stability, and mold resistance of heat-treated jack pine and aspen, Forest Products Journal, 58 (2008) 88-93.
[30] J.L. Shi, D. Kocaefe, T. Amburgey, J. Zhang, A comparative study on brown-rot fungus decay and subterranean termite resistance of thermally-modified and ACQ-C-treated wood, Holz als Roh - und Werkstoff, 65 (2007) 353-358.
[31] J.L. Shi, D. Kocaefe, J. Zhang, Mechanical behaviour of QueÌ• bec wood species heat-treated using ThermoWood process, Holz als Roh - und Werkstoff, 65 (2007) 255-259.
[32] L. Yixing, L. Jian, W. Jinman, Y. Jinsong, M. Yanhua, The effect of heat treatment on different species wood colour, Journal of Northeast Forestry University, 5 (1994) 73-78.

[33] P. Bekhta, P. Niemz, Effect of high temperature on the change in color, dimensional stability and mechanical properties of spruce wood, Holzforschung, 57 (2003) 539-546.
[34] I. Aydin, G. Colakoglu, Effects of surface inactivation, high temperature drying and preservative treatment on surface roughness and colour of alder and beech wood, Applied Surface Science, 252 (2005) 430-440.
[35] M.J. Boonstra, J.F. Rijsdijk, C. Sander, E. Kegel, B. Tjeerdsma, H. Militz, J. Van Acker, M. Stevens, Microstructural and physical aspects of heat treated wood. Part 1. Softwoods, Maderas: Ciencia y Tecnologia, 8 (2006) 193-208.
[36] b. Francis Mburu a, Stephane Dumarcay a, Francoise Huber a, Mathieu Petrissans a,, Philippe Gerardin a, Evaluation of thermally modified Grevillea robusta heartwood as an alternative to shortage of wood resource in Kenya: Characterisation of physicochemical properties and improvement of bio-resistance, Bioresource Technology, (2007).
[37] M. Petrissans, P. Gerardin, I. El Bakali, M. Serraj, Wettability of heat-treated wood, Holzforschung, 57 (2003) 301-307.
[38] M. Hakkou, M. Petrissans, A. Zoulalian, P. Gerardin, Investigation of wood wettability changes during heat treatment on the basis of chemical analysis, Polymer Degradation and Stability, 89 (2005) 1-5.
[39] M. Hakkou, M. Pétrissans, I. El Bakali, P. Gérardin, A. Zoulalian, Wettability changes and mass loss during heat treatment of wood, Holzforschung, 59 (2005) 35-37.
[40] R.M. Rowell, Weathering of wood, Handbook of Wood Chemistry and Wood Composites, (2005).
[41] W.C. Feist, Weathering perormance of finished southern pine plywood siding, Forest Products Journal, 38 (1988) 22-28.
[42] D.N.S. Hon, Weathering and photochemistry of wood, Wood and Cellulosic Chemistry, (2001) 512-546.
[43] A. Davis, The weathering of polymers in development in polymer degradation - 1, (1977).
[44] K.K. Pandey, Study of the effect of photo-irradiation on the surface chemistry of wood, Polymer Degradation and Stability, 90 (2005) 9-20.
[45] M. Kishino, T. Nakano, Artificial weathering of tropical woods. Part 1: Changes in wettability, Holzforschung, 58 (2004) 552-557.
[46] U. Muller, M. Ratzsch, M. Schwanninger, M. Steiner, H. Zobl, Yellowing and IR-changes of spruce wood as result of UV-irradiation, Journal of Photochemistry and Photobiology B: Biology, 69 (2003) 97-105.
[47] D.N.S. Hon, Weathering of wood in structural use, in, Va Polytech Inst, Lab for the Study of Environ Degrad of Eng Mater, Blacksburg, Va, USA, 1981, pp. 519-529, 518.
[48] W.C. Feist, D.N.S. Hon, Chemistry of weathering and protection, The Chemistry of Solid Wood, (1984) 401-451.
[49] J.R. Tobiska, Space environment (natural and artificial) - Process for determining solar irradiances, (2002).
[50] history.nasa.gov/NP-119/ch6.htm.

[51] B. Ranby, J.F. Rabek, Photodegradation, Photooxidation and Photostabilization of Polymers, (1975) 236.
[52] H. Derbyshire, E.R. Miller, The photodegradation of wood during solar irradiation. Part 1. Effects on the structural integrity of thin wood strips, Holz Roh Werkst, 39 (1981) 341-350.
[53] D.N.S. Hon, G. Ifju, Measuring penetration of light into wood by detection of photo-induced free radicals, Wood Sci., 11 (1978) 118-127.
[54] C. Coupe, R.W. Watson, Fundamental aspects of weathering, Proc. Ann. Conv. Br. Wood Preservation Ass., (1967) 37-49.
[55] A.J. Stamm, Wood and Cellulose Science Ronald Press, New York, (1964).
[56] W.B. Banks, P.D. Evans, The Degradation of Wood Surfaces by Water, (1984).
[57] E.L.P. Anderson, Zenon1; Owen, Noel L.1; Feist, William C.2, Infrared Studies of Wood Weathering. Part I: Softwoods Society for Applied Spectroscopy, 45 (1991) 521-714 (May 1991) , pp. 1641-1647(1997).
[58] P. Brennan, C. Fedor, Accelerated weathering light sources compared to sunlight spectra, in, Publ by SPI, Cincinnati, OH, USA, 1988, pp. 23A.21-23A.23.
[59] P. Gróf, G. Rontó, E. Sage, A computational study of physical and biological characterization of common UV sources and filters, and their relevance for substituting sunlight, Journal of Photochemistry and Photobiology B: Biology, 68 (2002) 53-59.
[60] D.B. Brown, A.E. Peritz, D.L. Mitchell, S. Chiarello, J. Uitto, F.P. Gasparro, Common fluorescent sunlamps are an inappropriate substitute for sunlight, Photochemistry and Photobiology, 72 (2000) 340-344.
[61] X. Colom, F. Carrillo, F. Nogués, P. Garriga, Structural analysis of photodegraded wood by means of FTIR spectroscopy, Polymer Degradation and Stability, 80 (2003) 543-549.
[62] K.K. Pandey, A note on the influence of extractives on the photo-discoloration and photo-degradation of wood, Polymer Degradation and Stability, 87 (2005) 375-379.
[63] N.M. Stark, L.M. Matuana, Characterization of weathered wood-plastic composite surfaces using FTIR spectroscopy, contact angle, and XPS, Polymer Degradation and Stability, 92 (2007) 1883-1890.
[64] D.N.S. Hon, N. Minemura, Color and discoloration, Wood and Cellulosic Chemistry, (2001) 385-442.
[65] S.T. Chang, D.N.S. Hon, W.C. Feist, Photodegradation and photoprotection of wood surfaces, Wood Fiber, 14 (1982) 104-117.
[66] N. Minemura, K. Umehara, Color improvement of wood. I, Rep Hokkaido for Prod Res Inst, (1979).
[67] Y. Kataoka, M. Kiguchi, R.S. Williams, P.D. Evans, Violet light causes photodegradation of wood beyond the zone affected by ultraviolet radiation, Holzforschung, 61 (2007) 23-27.
[68] W. Sandermann, F. Schlumbom, On the effect of filtered ultraviolet light on wood. Part II. Kind and magnitude of color difference on wood surfaces, Holz Roh-Werkstoff, 20 (1962) 285-291.
[69] G.J. Leary, The Yellowing of Wood by Light, Tappi, 50 (1967) 17-19.

[70] L. Tolvaj, O. Faix, Artificial ageing of wood monitored by DRIFT spectroscopy and CIE L*a*b* color measurements, Holzforschung, 49 (1995) 397-404.
[71] N.M. Stark, L.M. Matuana, Influence of photostabilizers on wood flour-HDPE composites exposed to xenon-arc radiation with and without water spray, Polymer Degradation and Stability, 91 (2006) 3048-3056.
[72] K. Mitsui, L. Tolvaj, G. Papp, J. Bohus, S. SzatmÃ¡ri, O. Berkesi, Changes in the properties of light-irradiated wood with heat treatment - Application of laser, Wood Research, 50 (2005) 1-8.
[73] F. Kawamura, H. Ohashi, S. Kawai, F. Teratani, Y. Kai, Photodiscoloration of Western Hemlock (Tsuga heterophylla) sapwood II. Structures of constituents causing photodiscoloration, Mokuzai Gakkaishi/Journal of the Japan Wood Research Society, 42 (1996) 301-307.
[74] R.S. Williams, W.C. Feist, Application of ESCA to evaluate wood and cellulose surfaces modified by aqueous chromium trioxide treatment, Colloids and Surfaces, 9 (1984) 253-271.
[75] V.P. Miniutti, Microscale changes in cell structure at softwood surfaces during weathering, Forest Prod. J., 14 (1964) 571-576.
[76] L.P. Futo, Der photochemische Abbau des Holzes als Praî parations- and Analusenmethode, Holz Roh- Werkstoff, 32 (1974) 303-311.
[77] M.-L. Kuo, Hu, N., Ultrastructural changes of photodegradation of wood surfaces exposed to UV, Holzforschung, (1991) 45, pp. 347-353.
[78] P.D. Evans, Structural changes in Pinus radiata during weathering, J. Inst. Wood Sci., 11 (1989) 172-181.
[79] D.N.S. Hon, Cellulose: a random walk along its historical path, Cellulose, 1 (1994) 1-25.
[80] E.R. Miller, H. Derbyshire, PHOTODEGRADATION OF WOOD DURING SOLAR IRRADIATION, in, NBS, Gaitherburg, MD, USA, 1981, pp. 279-287.
[81] D.N.S. Hon, ESCA study of oxidized wood surfaces, Journal of Applied Polymer Science, 29 (1984) 2777-2784.
[82] P.D. Evans, A.J. Michell, K.J. Schmalzl, Studies of the degradation and protection of wood surfaces, Wood Science and Technology, 26 (1992) 151-163.
[83] P.D. Evans, P.D. Thay, K.J. Schmalzl, Degradation of wood surfaces during natural weathering. Effects on lignin and cellulose and on the adhesion of acrylic latex primers, Wood Science and Technology, 30 (1996) 411-422.
[84] K. Borgin, N. Parameswaran, W. Liese, The effect of aging on the ultrastructure of wood, Wood Science and Technology, 9 (1975) 87-98.
[85] D.N.S. Hon, W.C. Feist, Weathering characteristics of hardwood surfaces, Wood Science and Technology, 20 (1986) 169-183.
[86] J.A. Owen, N.L. Owen, W.C. Feist, Scanning electron microscope and infrared studies of weathering in Southern pine, Journal of Molecular Structure, 300 (1993) 105-114.
[87] L.M. Paajanen, Structural changes in primed Scots pine and Norway spruce during weathering, Materiaux et constructions, 27 (1994) 237-244.
[88] P.D. Evans, N.L. Owen, S. Schmid, R.D. Webster, Weathering and photostability of benzoylated wood, Polymer Degradation and Stability, 76 (2002) 291-303.

[89] K.K. Pandey, A.J. Pitman, Weathering characteristics of modified rubberwood (hevea brasiliensis), Journal of Applied Polymer Science, 85 (2002) 622-631.
[90] K.J. Schmalzl, P.D. Evans, Wood surface protection with some titanium, zirconium and manganese compounds, Polymer Degradation and Stability, 82 (2003) 409-419.
[91] H.W. Fox, W.A. Zisman, The spreading of liquids on low energy surfaces. I. Polytetrafluoroethylene J. Colloid Sci., 7 (1950) 515-531.
[92] B.M. Collett, A review of surface and interfacial adhesion in wood science and related fields, Wood Science and Technology, 6 (1972) 1-42.
[93] T. Nguyen, W.E. Johns, The effects of aging and extraction on the surface free energy of Douglas fir and redwood, Wood Science and Technology, 13 (1979) 29-40.
[94] M.A. Kalnins, W.C. Feist, Increase in wettability of wood with weathering, Forest Prod J, 43 (1993) 55-57.
[95] R.M. Nussbaum, The critical time limit to avoid natural inactivation of spruce surfaces (Piceo abies) intended for painting or gluing, Holz als Roh - und Werkstoff, 54 (1996) 26.
[96] C.M. Chen, Effects of extractive removal on adhesion and wettability of some tropical woods, Forest Products Journal, 20 (1970) 36-41.
[97] D.J. Gardner, N.C. Generalla, D.W. Gunnells, M.P. Wolcott, Dynamic wettability of wood, Langmuir, 7 (1991) 2498-2502.
[98] J. Nylund, K. Sundberg, Q. Shen, J.B. Rosenholm, Determination of surface energy and wettability of wood resins, Colloids and Surfaces A: Physicochemical and Engineering Aspects, 133 (1998) 261-268.
[99] M.E.P. Walinder, I. Johansson, Measurement of wood wettability by the Wilhelmy method. Part 1. Contamination of probe liquids by extractives, Holzforschung, 55 (2001) 21-32.
[100] M. Gindl, A. Reiterer, G. Sinn, S.E. Stanzl-Tschegg, Effects of surface ageing on wettability, surface chemistry, and adhesion of wood, Holz als Roh - und Werkstoff, 62 (2004) 273-280.
[101] M. Kishino, T. Nakano, Artificial weathering effects on wettability of tropical woods for outdoor purposes, Artificial weathering effects on wettability of tropical woods for outdoor purposes, 19 (2005) 7-12.
[102] T.N. Kleinert, Photochemical changes of wood surfaces in the open atmosphere, Holzforsch Holzverwert, 22 (1970) 21.
[103] N. Hartler, H. Norrstrom, LIGHT-ABSORBING PROPERTIES OF PULP AND PULP COMPONENTS- 3, Tappi, 52 (1969) 1712-1715.
[104] D.N.S. Hon, W. Glasser, On possible chromophoric structures in wood and oulps - A survey of the present state of knowledge, Polym. Plast. Technol. Eng., 12 (1979) 159-179.
[105] R.L. Desai, J.A. Shields, Photochemical degradation of Cellulose material, Makromol. Chem, 122 (1969) 134-144.
[106] D.N.S. Hon, PHOTOOXIDATIVE DEGRADATION OF CELLULOSE: REACTIONS OF THE CELLULOSIC FREE RADICALS WITH OXYGEN, in: J Polym Sci Polym Chem Ed, 1979, pp. 441-454.

[107] K.M. Torr, B.S.W. Dawson, R.M. Ede, J. Singh, Surface changes on acetylation and exposure to ultraviolet radiation of Pinus radiata using X-ray photo-electron spectroscopy, Holzforschung, 50 (1996) 449-456.
[108] N.M. Stark, L.M. Matuana, Surface chemistry changes of weathered HDPE/wood-flour composites studied by XPS and FTIR spectroscopy, Polymer Degradation and Stability, 86 (2004) 1-9.
[109] N. Minemura, K. Umehara, Color improvement of wood, I. Rept. Hokkaido For. Res. Inst., 68 (1979) 92-145.
[110] R.W.G. Hunt, The Reproduction of Color, (1995).
[111] D.M. Hembree Jr, H.R. Smyrl, Anomalous dispersion effects in diffuse reflectance infrared Fourier transform spectroscopy: A study of optical geometries, Applied Spectroscopy, 43 (1989) 267-274.
[112] T.C.M. Pastore, K.O. Santos, J.C. Rubim, A spectrocolorimetric study on the effect of ultraviolet irradiation of four tropical hardwoods, Bioresource Technology, 93 (2004) 37-42.
[113] L.F. de Moura, R.E. Hernández, Evaluation of varnish coating performance for two surfacing methods on sugar maple wood, Wood and Fiber Science, 37 (2005) 355-366.
[114] L.F. De Moura, R.E. Hernández, Effects of abrasive mineral, grit size and feed speed on the quality of sanded surfaces of sugar maple wood, Wood Science and Technology, 40 (2006) 517-530.
[115] H. Resch, Microwave for the drying of wood products, Holz Roh- Werkstoff, 26 (1968) 317-324.
[116] R.R. Exley, B.G. Butterfield, B.A. Meylan, Preparation of wood specimens for the scanning electron microscope, Journal of Microscopy, 101 (1974) 21-30.
[117] T.P. Schultz, Rapid determination of lignocellulose by diffuse reflectance fourier transform infrared spectrometry, Analytical Chemistry, 57 (1985) 2867-2869.
[118] K.K. Pandey, A Study of Chemical Structure of Soft and Hardwood and Wood Polymers by FTIR Spectroscopy, Journal of Applied Polymer Science, 71 (1999) 1969-1975.
[119] A. Ferraz, J. Baeza, J. Rodriguez, J. Freer, Estimating the chemical composition of biodegraded pine and eucalyptus wood by DRIFT spectroscopy and multivariate analysis, Bioresource Technology, 74 (2000) 201-212.
[120] M. Ohkoshi, FTIR-PAS study of light-induced changes in the surface of acetylated or polyethylene glycol-impregnated wood, Journal of Wood Science, 48 (2002) 394-401.
[121] M. Nuopponen, H. Wikberg, T. Vuorinen, S.L. Maunu, S. Ja?msa, P. Viitaniemi, Heat-treated softwood exposed to weathering, Journal of Applied Polymer Science, 91 (2004) 2128-2134.
[122] B.F. Tjeerdsma, H. Militz, Chemical changes in hydrothermal treated wood: FTIR analysis of combined hydrothermal and dry heat-treated wood, Holz als Roh- und Werkstoff, 63 (2005) 102-111.
[123] G. Nguila Inari, M. Petrissans, P. Gerardin, Chemical reactivity of heat-treated wood, Wood Science and Technology, 41 (2007) 157-168.

[124] K.K. Pandey, T. Vuorinen, Comparative study of photodegradation of wood by a UV laser and a xenon light source, Polymer Degradation and Stability, 93 (2008) 2138-2146.
[125] G. Sinn, A. Reiterer, S.E. Stanzl-Tschegg, Surface analysis of different wood species using X-ray photoelectron spectroscopy (XPS), Journal of Materials Science, 36 (2001) 4673-4680.
[126] G. Nguila Inari, M. Petrissans, J. Lambert, J.J. Ehrhardt, P. Geì• rardin, XPS characterization of wood chemical composition after heat-treatment, Surface and Interface Analysis, 38 (2006) 1336-1342.
[127] A. Koubaa, B. Riedl, Z. Koran, Surface analysis of press dried-CTMP paper samples by electron spectroscopy for chemical analysis, Journal of Applied Polymer Science, 61 (1996) 545-552.
[128] A.G. McDonald, A.B. Clare, B. Dawson, Surface characterization of radiata pine high-temperature TMP fibres by X-ray photo-electron spectroscopy, APPITA Annual General Conference, 1 (1999) 51-57.
[129] L.S. Johansson, J.M. Campbell, K. Koljonen, P. Stenius, Evaluation of surface lignin on cellulose fibers with XPS, Applied Surface Science, 144-145 (1999) 92-95.
[130] L.M. Matuana, D.P. Kamdem, Accelerated ultraviolet weathering of PVC/wood-flour composites, Polymer Engineering and Science, 42 (2002) 1657-1666.
[131] G.N. Salaita, F.M.S. Ma, T.C. Parker, G.B. Hoflund, Weathering properties of treated southern yellow pine wood examined by X-ray photoelectron spectroscopy, scanning electron microscopy and physical characterization, Applied Surface Science, 254 (2008) 3925-3934.
[132] A. Tóth, O. Faix, G. Rachor, I. Bertóti, T. Székely, ESCA (XPS) study on light-induced yellowing of thermomechanical and chemothermomechanical pulps, Applied Surface Science, 72 (1993) 209-213.
[133] M. Kiguchi, Photo-deterioration of chemically modified wood surfaces: Acetylated wood and alkylated wood, Japan Agricultural Research Quarterly, 31 (1997) 147-154.
[134] F.P. Liu, T.G. Rials, J. Simonsen, Relationship of wood surface energy to surface composition, Langmuir, 14 (1998) 536-541.
[135] M. Sernek, F.A. Kamke, W.G. Glasser, Comparative analysis of inactivated wood surface, Holzforschung, 58 (2004) 22-31.
[136] G. Sinn, M. Gindl, A. Reiterer, S. Stanzl-Tschegg, Changes in the surface properties of wood due to sanding, Holzforschung, 58 (2004) 246-251.
[137] P. Geìrardin, M. PetricìŒ, M. Petrissans, J. Lambert, J.J. Ehrhrardt, Evolution of wood surface free energy after heat treatment, Polymer Degradation and Stability, 92 (2007) 653-657.
[138] Q. Shen, P. Mikkola, J.B. Rosenholm, Quantitative characterization of the subsurface acid-base properties of wood by XPS and Fowkes theory, Colloids and Surfaces A: Physicochemical and Engineering Aspects, 145 (1998) 235-241.
[139] I. Mohammed-Ziegler, Z. Holìrvoìˆlgyi, A. Toìth, W. Forsling, A. Holmgren, Wettability and spectroscopic characterization of silylated wood samples, Polymers for Advanced Technologies, 17 (2006) 932-939.

[140] G. Nguila Inari, M. Petrissans, J. Lambert, J.J. Ehrhardt, P. Gérardin, XPS characterization of wood chemical composition after heat-treatment, Surface and Interface Analysis, 38 (2006) 1336-1342.
[141] D.j.g. Sheldon Q. Shi Dynamic adhesive wettability of wood wood and fiber science 33(1),2001,pp58-68, (2001).
[142] S.Q. Shi, D.J. Gardner, Dynamic adhesive wettability of wood, Wood Fiber Sci, 33 (2001) 58-68.
[143] D. Kocaefe, S. Poncsak, G. Dore, R. Younsi, Effect of heat treatment on the wettability of white ash and soft maple by water, Holz Roh Werkst, 66 (2008) 355-361.
[144] R. Rowell, S. Lange, M. Davis, Steam stabilization of aspen fiberboards, Proc. of Fifth Pacific Rim Bio-based Composites Symp., (2000) 425-438.
[145] M. Scheikl, M. Dunky, Measurement of dynamic and static contact angles on wood for the determination of its surface tension and the penetration of liquids into the wood surface, Holzforschung, 52 (1998) 89-94.
[146] K. Richter, W.C. Feist, M.T. Knaebe, The Effect of Surface-Roughness on the Performance of Finishes .1. Roughness Characterization and Stain Performance, Forest Prod J, 45 (1995) 91-97.
[147] L.F. de Moura, R.E. Hernandez, Effects of abrasive mineral, grit size and feed speed on the quality of sanded surfaces of sugar maple wood, Wood Sci Technol, 40 (2006) 517-530.
[148] M. Stehr, D.J. Gardner, M.E.P. Walinder, Dynamic wettability of different machined wood surfaces, J Adhesion, 76 (2001) 185-200.
[149] G.I. Mantanis, R.A. Young, Wetting of wood, Wood Science and Technology, 31 (1997) 339-353.
[150] D. Fengel, G. Wegener, Chemical composition and analysis of wood, in: Wood Chemistry, Ultrastructures, Reactions, 1984, pp. 26-65.
[151] A.L.K. Bentum, W.A. CÃ´tÃ© Jr, A.C. Day, T.E. Timell, Distribution of lignin in normal and tension wood, Wood Science and Technology, 3 (1969) 218-231.
[152] S. Poncsak, D. Kocaefe, F. Simard, A. Pichette, Evolution of extractive composition during thermal treatment of Jack pine, Journal of Wood Chemistry and Technology, 29 (2009) 251-264.
[153] Y. Xie, P.M.A. Sherwood, X-ray photoelectron spectroscopic studies of carbon fiber surfaces. 13. Valence-band studies of oxidized fibers interpreted by XÎ± calculations, Chemistry of Materials, 3 (1991) 164-168.
[154] W.T.Y. Tze, G. Bernhardt, D.J. Gardner, A.W. Christiansen, X-ray photoelectron spectroscopy of wood treated with hydroxymethylated resorcinol, International Journal of Adhesion and Adhesives, 26 (2006) 550-554.
[155] F.M. Fowkes, Quantitative characterisation of the acid-base properties of solvents, polymers, and inorganic surfaces, J. Adhesion Sci. Technol., 4 (1990) 669-691.
[156] S.R. Holmes-Farley, G.M. Whitesides, Reactivity of carboxylic acid and ester groups in the functionalized interfacial region of "polyethylene carboxylic acid" (PE-CO2H) and its derivatives: Differentiation of the functional groups into shallow and deep subsets based on a comparison of contact angle and ATR-IR measurements, Langmuir, 3 (1987) 62-76.

[157] X. Huang, D. Kocaefe, Y. Kocaefe, Y. Bolukb, A. Pichette, A spectrocolorimetric and chemical study on color modification of heat-treated wood during artificial weathering, Applied Surface Science (revision), (2012).
[158] D.P. Kamdem, B. Riedl, A. Adnot, S. Kaliaguine, ESCA spectroscopy of poly (methyl methacrylate) grafted onto wood fibers, Journal of Applied Polymer Science, 43 (1991) 1901-1912.
[159] K. Nishimiya, Analysis of chemical structure of wood charcoal by X-ray photoelectron spectroscopy, Journal of Wood Science, 44 (1998) 56-61.
[160] X. Huang, D. Kocaefe, Y. Kocaefe, Y. Bolukb, A. Pichette, Changes in Wettability of Heat-Treated Wood due to Artificial Weathering, Wood Science and Technology (revision).
[161] P.A. Evans, Differentiating "hard" from "soft" woods using Fourier transform infrared and Fourier transform spectroscopy, Spectrochimica Acta Part A: Molecular Spectroscopy, 47 (1991) 1441-1447.
[162] A. Ahmed, A. Adnot, S. Kaliaguine, ESCA Study of the solid residues of supercritical extraction of populus tremuloides in methanol, Journal of Applied Polymer Science, 34 (1987) 359-375.
[163] X. Hua, S. Kaliaguine, B.V. Kokta, A. Adnot, Surface analysis of explosion pulps by ESCA Part 1. Carbon (1s) spectra and oxygen-to-carbon ratios, Wood Science and Technology, 27 (1993) 449-459.
[164] M. De Meijer, S. Haemers, W. Cobben, H. Militz, Surface energy determinations of wood: Comparison of methods and wood species, Langmuir, 16 (2000) 9352-9359.
[165] D. Fengel, G. Wegener, Lignin - Polysaccharide complexes, Wood: Chemistry, Ultrastructure, Reactions, (2003) 167-174.
[166] A. Temiz, N. Terziev, M. Eikenes, J. Hafren, Effect of accelerated weathering on surface chemistry of modified wood, Applied Surface Science, 253 (2007) 5355-5362.
[167] C. Skaar, Wood-water relationships, Chemistry of Solid Wood. Adv. Chem., 207 (1984) 127-172.
[168] H.-Y. Kang, S.-J. Park, Y.-S. Kim, Moisture sorption and ultrasonic velocity of artificially weathered spruce, Mokchae Konghak, 30 (2002) 18-24.
[169] M.L. Nelson, R.T. O'Connor, Relation of certain infrared bands to cellulose crystallinity and crystal lattice type. Part II. A new infrared ratio for estimation of crystallinity in cellulose I and II, J. Appl. Polym. Sci., 8 (1964) 1325-1341.
[170] D. Kocaefe, S. Poncsak, J. Tang, M. Bouazara, Effect of heat treatment on the mechanical properties of North American jack pine: Thermogravimetric study, Journal of Materials Science, 45 (2010) 681-687.
[171] S. Poncsák, D. Kocaefe, M. Bouazara, A. Pichette, Effect of high temperature treatment on the mechanical properties of birch (Betula papyrifera), Wood Science and Technology, 40 (2006) 647-663.
[172] S. Lekounougou, D. Kocaefe, N. Oumarou, Y. Kocaefe, Effect of Thermal modification on Mechanical Properties of Canadian White Birch (Betula papyrifera), International Wood Products Journal, (2011).
[173] F. Avat, Contribution à l'étude des traitements Thermiques du bois jusqu'à 300 °C: Transformations chimiques et caractérisations physico-chimiques, Contribution a

L'étude des Traitements Thermiques du Bois Jusqu'à 300 °C: Transformations Chimiques et Caracterizationsphysico-Chimiques, (1993).
[174] F. Kollmann, A. Schneider, Über das Sorptionsverhalten wärmebehandelter Hölzer, Holz Roh- Werkstoff, 21 (1963) 77-85.
[175] C.C. Brunner, G.B. Shaw, D.A. Butler, J.W. Funck, Using color in machine vision systems for wood processing, Wood Fiber Sci., 22 (1990) 413-428.
[176] S. Wang, Y. Zhang, C. Xing, Effect of drying method on the surface wettability of wood strands, Einfluss des Trocknungsverfahrens auf die Oberflächenbenetzbarkeit von OSB-spänen, 65 (2007) 437-442.
[177] M.A. Kalnins, W.C. Feist, Increase in wettability of wood with weathering, Forest Products Journal, 43 (1993) 55.
[178] M. Gindl, G. Sinn, S.E. Stanzl-Tschegg, The effects of ultraviolet light exposure on the wetting properties of wood, Journal of Adhesion Science and Technology, 20 (2006) 817-828.
[179] D. Kocaefe, S. Poncsak, G. Dore, R. Younsi, Effect of heat treatment on the wettability of white ash and soft maple by water, Einfluss der Wa?rmebehandlung auf die Benetzbarkeit von Weißesche und Rot-Ahorn mit Wasser, 66 (2008) 355-361.
[180] V.P. Miniutti, Microscopic observations of ultraviolet irradiated and weathered softwood surfaces and clear coatings, US Forest Service Research Paper FPL, 74 (1967) 1-32.
[181] V.P. Miniutti, Contraction in softwood surfaces during ultravilet irradiation and weathering, J Paint Technol, 45 (1973) 27-34.
[182] T.C. Patton, Simplified review of adhesion theory based on surface energetics, Tappi, 53 (1970) 421-429.
[183] Y. Kataoka, M. Kiguchi, Depth profiling of photo-induced degradation in wood by FT-IR microspectroscopy, Journal of Wood Science, 47 (2001) 325-327.
[184] B.A. Horn, J. Qiu, N.L. Owen, W.C. Feist, FT-IR studies of weathering effects in Western red cedar and Southern pine, Chemical Modification of Lignocellulosics, (1992).
[185] W.B. Banks, Water uptake by scots pine sapwood, and its restriction by the use of water repellents, Wood Science and Technology, 7 (1973) 271-284.
[186] D.F. Caulfield, The effect of cellulose on the structure of water, Fiber-water Interactions in Paper-making, (1978) 63.
[187] A.J. Stamm, Selective adsorption from solution, Wood and Cellulose Science, (1964) 175-185.
[188] Y. Sumi, R.R. Hale, J.A. Meyer, A.B. Leopold, B.G. Ranby, Accessibility of wood and wood carbohydrates measured with tritiated water, Tappi J, 47 (1964) 621-624.
[189] W.C. Feist, D.N.S. Hon, Chemistry of Weathering and Protection, The Chemistry of Solid Wood, Ed., (1984).
[190] A.J. Stamm, W.K. Loughborough, Variation in shrinking and swelling of wood, Trans. Amer. Soc. Mech. Eng, 64 (1942) 379–386.
[191] R.M. Rowell, R. Pettersen, J.S. Han, J.S. Rowell, M.A. Tshabalala, Cell wall chemistry, Handbook of Wood Chemistry and Wood Composites, (2005) 35-74.

[192] M. Kishino, T. Nakano, Artificial weathering of tropical woods. Part 2: Color change, Holzforschung, 58 (2004) 558-565.
[193] T. Yoshimoto, M. Samejima, Rengas wood extractives relating to light induced reddening, Mokuzai Gakkaishi, 23 (1977) 601-604.
[194] F. Kollmann, D. Fengel, Changes in the chemical composition of wood by thermal treatment, Änderungen der chemischen Zusammensetzung von Holz durch thermische Behandlung, 23 (1965) 461-468.
[195] F. Avat, Contribution a L'etude des traitements thermiques du bois jusqu'à 300 °C: Transformations Chimiques et Caracterizationsphysico-Chimiques, (1993).
[196] M. Åkerholm, B. Hinterstoisser, L. Salmén, Characterization of the crystalline structure of cellulose using static and dynamic FT-IR spectroscopy, Carbohydrate Research, 339 (2004) 569-578.
[197] http://www.q-lab.com/products/q-sun-xenon-arc-test-chambers/q-sun-xe-1, in.
[198] F.P.e.a. Incropera, Radiation:Processes and Properties, in: F.P. Incropera (Ed.) Fundamentals of Heat and Mass Transfer, John Wiley&Sons, New york, 2007.
[199] http://www.atlas-mts.com/, in.
[200] CABOT, UV weathering and related test methods, in: CABOT creating what matters.

APPENDIX 1

Visual appearance of heat-treated jack pine surface after weathering at different times (LT: longitudinal tangential surface, LR: longitudinal radial surface)

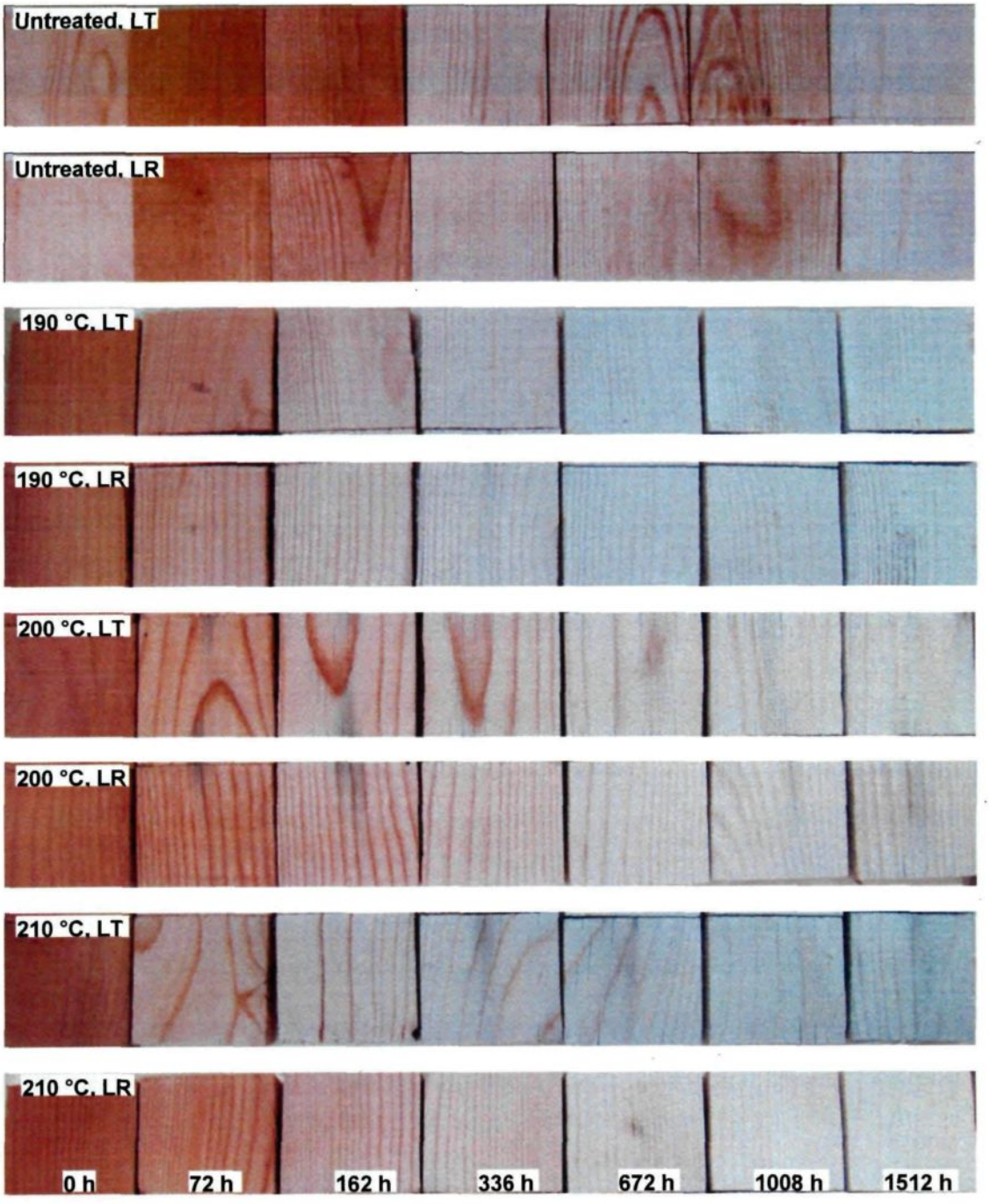

APPENDIX 2

Visual appearance of heat-treated aspen surface after weathering at different times
(LT: longitudinal tangential surface, LR: longitudinal radial surface)

APPENDIX 3

Visual appearance of heat-treated birch surface after weathering at different times
(LT: longitudinal tangential surface, LR: longitudinal radial surface)